

**ANALYSIS OF BIODYNAMIC RESPONSES ASSOCIATED WITH UPPER
LIMB REACHING MOVEMENTS UNDER WHOLE-BODY VIBRATION:
SUPPORT FOR AN ACTIVE BIODYNAMIC MODEL**

by

Heon-Jeong Kim

A dissertation submitted in partial fulfillment
of the requirements for the degree of
Doctor of Philosophy
(Mechanical Engineering)
in The University of Michigan
2010

Doctoral Committee:

Associate Professor Bernard J. Martin, Co-Chair
Associate Professor Brent Gillespie, Co-Chair
Professor Thomas J. Armstrong
Professor Noel C. Perkins

© Heon-Jeong Kim

All rights Reserved

2010

To God, Wife, Sons, and Parents

ACKNOWLEDGEMENTS

I am sincerely grateful for the support, collaboration, and encouragement that I have received from many people over past years. This dissertation would not have been possible by me alone without their professional and personal assistances.

Firstly, I wish to express my gratitude and appreciation to my advisor and chair, Professor Bernard J. Martin, for his mentoring, guidance, advice, patience, and humanity. His profession and personal mentorship have encouraged me to pursue my research interests and personal vision incessantly. I would also like to give my sincere appreciations to my co-chair, Professor Brent Gillespie for his expertise, suggestion, and encouragement. I would also like to thank my other committee members, Professor Thomas J. Armstrong and Professor Noel C. Perkins for making their advice and valuable comments for enhancing my dissertation.

I would like to thank Dr. Matthew Reed and Professor Don Chaffin for supporting my work in HUMOSIM with continuous interests and support.

I would also like to express my appreciation to the sponsors of this project, the Automotive Research Center at the University of Michigan and the Detroit Arsenal of the U.S. Army Tank Automotive and Armaments Command for financial support. Specially, I wish to give my sincere gratitude to Harry Zywiol, Victor Paul, AnnMarie Meldrum, Stacy Budzik, and Steve Patterson who greatly contributed to the process of performing experiments.

I would like to take the opportunity to thank the staffs of the HUMOSIM laboratory and the Center for Ergonomics who contributed to my work in numerous ways, Charles Woolley, Eyvind Claxtion, Mint rahaman, Christopher Konrad, Randy Rabourn, Richard Krause, Amy Warhaftr, and Tina Blay.

Many thanks go out to my colleagues, so-called HUMOSIMians, Shin-Yuan Yu, Divya Srinivasan, Monica Jones, Helen Fuller, and Wei Zhou for mutual support, collaboration, and encouragement.

Most importantly, I wish to express my deepest thank to my parents and family for the love, prayer, supports, patience, and encouragement. Especially, I would like to express to my loving appreciation to my wife and two sons, Jee-hyun Park, David Tae-ho Kim, Joseph Tae-in Kim. They are the most precious persons who will remain motivation, driving force, encouragement, and award in my life forever.

Lastly, I sincerely hope that this study very difficult, complicated, and time-consuming analysis of the empirical data will be of value to human vibration studies and not only a burden.

TABLE OF CONTENTS

DEDICATION	ii
ACKNOWLEDGEMENTS	iii
LIST OF FIGURES	ix
LIST OF TABLES	xvi
LIST OF APPENDICES.....	xviii
NOMENCLATURE	xix
ABSTRACT.....	xxi
CHAPTER 1 INTRODUCTION	1
1.1 Problem Statement & Motivation	2
1.2 Objectives & Hypotheses.....	4
1.2.1 Experimental Approach.....	5
1.2.2 Specific Aims & Hypotheses	6
1.3 Potential Impacts	7
1.4 Thesis Organization	8
CHAPTER 2 BACKGROUND LITERATURE	11
2.1 Introduction	11
2.2 Human Response to Vibration	11
2.3 Human Movements & Reach Kinematics in a Static Environment	15
2.4 Reach Kinematics or Performance in Dynamic Environments	20
2.5 Biomechanical Model of the Seated Human under Whole-Body Vibration	21
CHAPTER 3 VIBRATION TRANSMISSION OF UPPER BODY SEGMENTS UNDER SINUSOIDAL WHOLE-BODY VIBRATION EXPOSURE.....	25
3.1 Introduction	25

3.2 Methods	28
3.2.1 Biodynamic Reach Experiment I	28
3.2.2 Data Analysis	36
3.2.2.1 Movement Phase Analysis	36
3.2.2.2 Frequency Analysis	37
3.3 Results	41
3.3.1 Displacements of Upper Body Segments in Time and Frequency Domains	41
3.3.2 Vibration Transmission through the Upper Limb	44
3.3.2.1 Effects of Vibration Conditions.....	44
Vertical Sinusoidal WBV Exposure	44
Horizontal Sinusoidal WBV Exposure	46
3.3.2.2 Effects of Target Location.....	46
3.3.3 Propagated Transmission through each body segment (Inter-segment Transmission)	49
3.4 Discussion	52
3.5 Conclusions.....	54
CHAPTER 4 VIBRATION-INDUCED CHANGES IN UPPER LIMB REACH KINEMATICS	55
4.1 Introduction	55
4.2 Method	59
4.2.1 Experiment Data Selection for Kinematic Analysis.....	59
4.2.2 Movement Phase Analysis.....	62
4.2.3 Joint Kinematic Analysis	63
4.3 Results	64
4.3.1 Reach Trajectory and Kinematics in the Static Environment	64
4.3.1.1 Joint Trajectory and Linear Velocity.....	64
4.3.1.2 Joint Angular Kinematics	69
4.3.2 Reach Trajectory and Kinematics under Vibration Condition.....	72

4.3.2.1 Vibration-Induced Joint Trajectory and Linear Velocity.....	72
4.3.2.2 Vibration-Induced Alteration in Joint Angular Kinematics.....	76
4.4 Discussion	81
4.5 Conclusions	82
CHAPTER 5 EFFECTS OF POSTURE AND MOVEMENT ON VIBRATION	
TRANSMISSION THROUGH THE UPPER LIMBS	83
5.1 Introduction	83
5.2 Methods	86
5.2.1 Biodynamic Reach Experiment II.....	86
5.2.1.1 Subject.....	86
5.2.1.2 Experimental Setup	87
5.2.1.3 Data Acquisition.....	88
Human Body Segment Motion Capture	88
Vibration Acceleration Measurement	90
5.2.1.4 Vibration Condition	91
5.2.1.5 Target Directions and Intermediate Stops	92
5.2.1.6 Movement Constraints in Reaching Task	95
Session I: Intermediate Reach without Visual Compensation	95
Session II: Intermediate Reach with Visual Compensation	96
Session III: End Reach with Different Elbow Flexion	97
5.2.2 Vibration Analysis.....	98
5.2.2.1 Joint Position Deviation and Angle Perturbation	98
5.2.2.2 Frequency Response and Vibration Transmission.....	98
5.3 Results	99
5.3.1 Variation of WBV transmission along the Fingertip Trajectory	99
5.3.1.1 Upper Body Displacement and Joint Angle	99
5.3.1.2 Frequency Response and Vibration Transmission of the Upper Limbs	100

5.3.2 Effects of Visual Compensation on WBV-induced Transmission.....	111
5.3.2.1 Upper Body Displacement and Joint Angles with Visual Compensation	111
5.3.2.2 Frequency Response and Vibration Transmission with Visual Compensation.....	112
5.3.3 Effects of Elbow Extension or Flexion on Vibration Transmission.....	116
5.3.3.1. Joint Displacements and Angles with Elbow Extended or Flexed Posture.....	116
5.3.3.2. Frequency Response and Vibration Transmission through Body Segments.....	118
5.4 Discussion	124
5.5 Conclusions.....	126
CHAPTER 6 EMPIRICAL SUPPORT FOR A MODEL REPRESENTING THE BIODYNAMIC RESPONSE TO WHOLE-BODY VIBRATION DURING UPPER LIMB MOVEMENTS IN THE SEATED POSTURE.....	127
6.1 Introduction	127
6.2 Groundwork for a Biodynamic Response Model	129
CHAPTER 7 CONCLUSIONS	145
7.1 Summary of Findings.....	145
7.2 Limitations and Future Research Opportunities	152
APPENDICES	157
Appendix A. Transmission propagated through the upper limbs in three- dimension.....	157
Appendix B. The Percentage Distribution of Total Body Weight.....	167
Appendix C. The Effect of Total Body Weight on Fingertip Transmission....	168
BIBLIOGRAPHY.....	169

LIST OF FIGURES

Figure 1.1: Research approach and procedure:.....	10
Figure 3.1: Experimental Setup and RMS cab:.....	29
Figure 3.2: Ride Motion Simulator (RMS): compressed (left) and extended (right) configurations.....	29
Figure 3.3: Reach difficulty rating by ride-motion frequency and target location (Rider et al, 2003)	31
Figure 3.4: RMS cab and target locations:.....	33
Figure 3.5: Retro-reflective markers placed on a subject. Twenty-six markers were placed on body landmarks.....	34
Figure 3.6: Retro-reflective marker set placed on body landmarks: R=right, L=left, FHD=front-head, BHD=back-head, CLAV=Clavicle, MIDSTRN=mid-sternum, STRN=sternum, SHO=shoulder, UPA=upper-arm, ELB=elbow, FRA=fore-arm, WR=wrisk, NCK=knuckle, FIN=finger	35
Figure 3.7: T-pose for anthropometric and range of motion calibration.....	35
Figure 3.8: Movement phases in a reach trial: [1] resting phase, [2] aiming phase, [3] pointing phase, and [4] returning phase. The pointing phase [3] was used to compute the vibration transmissibility of body segments.	36
Figure 3.9: Frequency analysis of input and body link displacement outputs - The frequency bandwidth of interest is in the 0.2 - 15 Hz frequency range.....	39
Figure 3.10: Transmission at the forcing frequency.	40
Figure 3.11: Time responses of upper body joint perturbations under vertical whole-body vibration.	42
Figure 3.12: Time responses of upper body joint perturbations under horizontal whole-body vibration.	42
Figure 3.13: Frequency responses of upper body joints perturbation under WBV exposures: 2Hz (1 st row), 4Hz (2 nd row), and 6Hz (3 rd row) & vertical direction (left column) and fore-and-aft direction (right column).	43

Figure 3.14: Transmission through the body segment at forcing frequency as a function of WBV frequency and direction under vertical WBV exposures: S = shoulder, E = elbow, and F = fingertip.....	45
Figure 3.15: Transmission through the body segment at forcing frequency as a function of WBV frequency and direction under horizontal WBV exposures: S = shoulder, E = elbow, and F = fingertip.....	45
Figure 3.16: Transmission (body segment) as a function of target location: 2Hz (1 st row), 4Hz (2 nd row), and 6Hz (3 rd row) & vertical direction (left column) and fore-and-aft direction (right column).	47
Figure 3.17: Propagated transmission through each body segment as a function of WBV frequency and direction: Right Shoulder (1 st row), Elbow (2 nd row), and Fingertip (3 rd row) & Vertical WBV (1 st column) and Horizontal WBV (2 nd column)	50
Figure 4.1: RMS cab and target directions: Four targets are distributed in the right hemisphere of the seated operator: Upward (TG1), Forward (TG2), Diagonal (TG5), and Lateral (TG 8).....	61
Figure 4.2: Movement phases in a reach trial: One reach consists of four movement phase: (1) resting phase, (2) aiming transition phase, (3) pointing phase, and (4) returning phase.	62
Figure 4.3: Joint angles of the upper body segments for kinematic analysis: Three joint angles were used in the analysis: right shoulder (θ_s), right elbow (θ_E), and right wrist (θ_w) angles.	63
Figure 4.4: Three-dimensional joint trajectories of the upper right extremity and head motion for upward reach in a static environment.	65
Figure 4.5: Three-dimensional joint trajectories of the upper right extremity and head motion for forward reach in a static environment.....	65
Figure 4.6: Three-dimensional joint trajectories of the upper right extremity and head motion for diagonal reach in a static environment.....	66
Figure 4.7: Three-dimensional joint trajectories of the upper right extremity and head motion for lateral reach in a static environment.	66
Figure 4.8: Joint trajectories and linear/tangential velocities of upper body joints for upward reach movement in a static environment: lSHO (left shoulder joint), rSHO (right shoulder joint), rELB (right elbow joint), rWRT (right wrist joint), and rFIN (right index fingertip).....	67
Figure 4.9: Joint trajectories and linear/tangential velocities of upper body joints for forward reach movement in a static environment: lSHO (left shoulder joint),	

rSHO (right shoulder joint), rELB (right elbow joint), rWRT (right wrist joint), and rFIN (right index fingertip).....	68
Figure 4.10: Joint trajectories and linear/tangential velocities of upper body joints for diagonal reach movement in a static environment: lSHO (left shoulder joint), rSHO (right shoulder joint), rELB (right elbow joint), rWRT (right wrist joint), and rFIN (right index fingertip).....	68
Figure 4.11: Joint trajectories and linear/tangential velocities of upper body joints for lateral reach movement in a static environment: lSHO (left shoulder joint), rSHO (right shoulder joint), rELB (right elbow joint), rWRT (right wrist joint), and rFIN (right index fingertip).....	69
Figure 4.12: Joint angular kinematics in the static environment: Angle (1 st row), Angular velocity (2 nd row), and Angular acceleration (3 rd row) & Upward reach (left column) and Forward reach (right column): rSHO (right shoulder joint), rELB (right elbow joint), and rWRT (right wrist joint).....	70
Figure 4.13: Joint angular kinematics in the static environment: Angle (1 st row), Angular velocity (2 nd row), and Angular acceleration (3 rd row) & Diagonal reach (left column) and Lateral reach (right column): rSHO (right shoulder joint), rELB (right elbow joint), and rWRT (right wrist joint).....	71
Figure 4.14: Example of joint trajectory and linear/tangential velocity of the upper extremity for the diagonal reach under the 2 Hz whole-body vibration: lSHO (left shoulder joint), rSHO (right shoulder joint), rELB (right elbow joint), rWRT (right wrist joint), and rFIN (right index fingertip).....	73
Figure 4.15: Example of joint trajectory and linear/tangential velocity of the upper extremity for the diagonal reach under the 4 Hz whole-body vibration: lSHO (left shoulder joint), rSHO (right shoulder joint), rELB (right elbow joint), rWRT (right wrist joint), and rFIN (right index fingertip).....	74
Figure 4.16: Example of joint trajectory and linear/tangential velocity of the upper extremity for the diagonal reach under the 6 Hz whole-body vibration: lSHO (left shoulder joint), rSHO (right shoulder joint), rELB (right elbow joint), rWRT (right wrist joint), and rFIN (right index fingertip).....	75
Figure 4.17: Example of shoulder and elbow joint angular kinematics for the diagonal reach under the 2 Hz whole-body vibration. Subscript f indicates filtered data	77
Figure 4.18: Example of shoulder and elbow joint angular kinematics for the diagonal reach under the 4 Hz whole-body vibration. Subscript f indicates filtered data	78

Figure 4.19: Example of shoulder and elbow joint angular kinematics for the diagonal reach under the 6 Hz whole-body vibration. Subscript f indicates filtered data	79
Figure 5.1: Reach Experiment on the Ride Motion Simulator.....	87
Figure 5.2: Diagram of the Experimental Setup.....	88
Figure 5.3: Marker definition on a human body: R=right, L=left, FHD=front-head, BHD=back-head, CLAV=Clavicle, MIDSTRN=mid-sternum, STRN=sternum, SHO=shoulder, UPA=upper-arm, ELB=elbow, FRA=fore-arm, WR=wrist, FIN=finger	89
Figure 5.4: T-pose for anthropometric measure and calibration	90
Figure 5.5: Tri-axial accelerometer attached to cab/seat/hip interface.....	90
Figure 5.6: Target Directions and Cartesian Coordinate.....	93
Figure 5.7: Session I - Pointing posture w/o visual compensation.....	96
Figure 5.8: Session II - Pointing posture w/ visual compensation.....	96
Figure 5.9: Session III – Pointing postures with different elbow flexion.....	97
Figure 5.10: 3-Dimensional displacements of upper limbs in diagonal and upward reach [TG5] for the 4 Hz vertical vibration	100
Figure 5.11: Joint angles of the right shoulder and elbow in diagonal and upward reach [TG5] for the 4 Hz vertical vibration	100
Figure 5.12: Frequency responses of upper limbs in diagonal and upward reach [TG5] for the 4 Hz vertical vibration: lSHO (1 st row), rSHO (2 nd row), rELB (3 rd row), and rFIN (4 th row) & intermediate stop1 (1 st column), intermediate stop 2 (2 nd column), and final target (3 rd column).....	101
Figure 5.13: Vibration transmission through upper body segments for diagonal reach [TG4] under the 2Hz vertical WBV	108
Figure 5.14: Vibration transmission through upper body segments for diagonal reach [TG4] under the 4Hz vertical WBV	108
Figure 5.15: Vibration transmission through upper body segments for diagonal reach [TG4] under the 6Hz vertical WBV	108
Figure 5.16: Vibration transmission through upper body segments for diagonal-upward reach [TG5] under the 2Hz vertical WBV	109
Figure 5.17: Vibration transmission through upper body segments for diagonal-upward reach [TG5] under the 4Hz vertical WBV	109

Figure 5.18: Vibration transmission through upper body segments for diagonal-upward reach [TG5] under the 6Hz vertical WBV	109
Figure 5.19: Vibration transmission through upper body segments for lateral-far reach [TG7] under the 2Hz vertical WBV	110
Figure 5.20: Vibration transmission through upper body segments for lateral-far reach [TG7] under the 4Hz vertical WBV	110
Figure 5.21: Vibration transmission through upper body segments for lateral-far reach [TG7] under the 6Hz vertical WBV	110
Figure 5.22 3-Dimensional displacements of upper limbs in diagonal and upward reach [TG5] for the 4 Hz vertical vibration	111
Figure 5.23 Joint angles of the right shoulder and elbow in diagonal and upward reach [TG5] for the 4 Hz vertical vibration	112
Figure 5.24: Frequency responses of upper limbs in diagonal and upward reach [TG5] for the 4 Hz vertical vibration: lSHO (1 st row), rSHO (2 nd row), rELB (3 rd row), and rFIN (4 th row) & without visual compensation (left), with visual compensation (right).....	113
Figure 5.25: Vibration transmission through upper body segments for diagonal-upward reach [TG5] under the 2Hz vertical WBV	115
Figure 5.26: Peak of vibration transmission through upper body segments for diagonal-upward reach [TG5] under the 4Hz vertical WBV	115
Figure 5.27: Peak of vibration transmission through upper body segments for diagonal-upward reach [TG5] under the 6Hz vertical WBV	115
Figure 5.28 3-dimensional displacements of upper limbs in diagonal reach [TG4] for the 4 Hz vertical vibration	116
Figure 5.29 Joint angles of the right shoulder and elbow in diagonal reach [TG4] for the 4 Hz vertical vibration	116
Figure 5.30 3-dimensional displacements of upper limbs in diagonal-upward reach [TG5] for the 4 Hz vertical vibration	117
Figure 5.31 Joint angles of the right shoulder and elbow in diagonal and upward reach [TG5] for the 4 Hz vertical vibration	117
Figure 5.32: Frequency responses of upper limbs in diagonal reach [TG4] for the 4 Hz vertical vibration: lSHO (1 st row), rSHO (2 nd row), rELB (3 rd row), and rFIN (4 th row) & elbow extended posture (left) and elbow flexed posture (right)..	119
Figure 5.33: Frequency responses of upper limbs in diagonal-upward reach [TG5] for the 4 Hz vertical vibration: lSHO (1 st row), rSHO (2 nd row), rELB (3 rd row),	

and rFIN (4 th row) & elbow extended posture (left) and elbow flexed posture (right).....	120
Figure 5.34: Vibration transmission of upper body segments in two pointing postures for lateral reach [TG4]: 2Hz (1 st row), 4Hz (2 nd row), and 6Hz (3 rd row) & elbow extended posture (left) and elbow flexed posture (right)	122
Figure 5.35: Vibration transmission of upper body segments in two pointing postures for diagonal and upward reach [TG5]: 2Hz (1 st row), 4Hz (2 nd row), and 6Hz (3 rd row) & elbow extended posture (left) and elbow flexed posture (right).....	123
Figure 6.1: Vibration input and human body segment responses through the biodynamic system.....	130
Figure 6.2: The simple biomechanical model to represent the upper body segments with equivalent parallel/series elements. The control of joints or segment stiffness is not represented.	131
Figure 6.3: Reach posture, joint trajectories in task space, frequency responses, and transmission through upper right joints under 4 Hz vertical vibration exposure [TG4]	134
Figure 6.4: Reach posture, joint trajectories in task space, frequency responses, and transmission through upper right joints under 4 Hz vertical vibration exposure [TG5]	135
Figure 6.5: Reach posture, joint trajectories in task space, frequency responses, and transmission through upper right joints under 4 Hz vertical vibration exposure [TG7]	136
Figure 7.1: The example reach model of the seated human with six degrees-of-freedom	153
Figure 7.2: Information flow and vibration influence on human activity	154
Figure A.1: Transmission propagated through the upper limbs [SS1 – 2 Hz Vertical WBV Exposure]	158
Figure A.2: Transmission propagated through the upper limbs[SS1 – 4 Hz Vertical WBV Exposure]	159
Figure A.3: Transmission propagated through the upper limbs[SS1 – 6 Hz Vertical WBV Exposure]	160
Figure A.4 Transmission propagated through the upper limbs [SS2 – 2 Hz Vertical WBV Exposure]	161
Figure A.5: Transmission propagated through the upper limbs [SS2 – 4 Hz Vertical WBV Exposure]	162

Figure A.6: Transmission propagated through the upper limbs [SS2 – 6 Hz Vertical WBV Exposure]	163
Figure A.7: Transmission propagated through the upper limbs [SS3 – 2 Hz Vertical WBV Exposure]	164
Figure A.8 Transmission propagated through the upper limbs [SS3 – 4 Hz Vertical WBV Exposure]	165
Figure A.9: Transmission propagated through the upper limbs [SS3 – 6 Hz Vertical WBV Exposure]	166

LIST OF TABLES

Table 3.1: Anthropometry Data	28
Table 3.2: Vibration input conditions	30
Table 3.3: Task conditions (target locations) The origin of the coordinate system is at the right top of the steering handle.....	33
Table 3.4: Analysis Matrix associated with the selected levels of each variable.	37
Table 3.5: Analysis of Variance for vertical WBV transmission (thru-)	48
Table 3.6: Analysis of Variance for horizontal WBV transmission (thru-).....	48
Table 3.7: Analysis of Variance for vertical WBV transmission (inter-)	51
Table 3.8: Analysis of Variance for horizontal WBV transmission (inter-).....	51
Table 4.1: Vibration Input Conditions for Reach Kinematic Study.....	59
Table 4.2: Reach task (reach direction) The origin of the coordinate system is at the right top of a steering handle.	61
Table 4.3: Joint angular kinematics peak values of upper body joints in static and vibratory environments: rSHO (right shoulder), rELB (right elbow), rWRT (right wrist): ANG (joint angle [deg]), ANG_VEL (joint angular velocity [deg/s]), and ANG_ACC (joint angular acceleration [deg/s ²]).....	80
Table 5.1: Anthropometry Data	86
Table 5.2: Marker Definition	89
Table 5.3: Tri-axial Accelerometers on a Cab and Seat.....	91
Table 5.4: RMS inputs.....	92
Table 5.5: Reach Target Directions and Locations	94
Table 5.6: 3-way ANOVA [Inter-Pose, Target location, and Vibration Freq.].....	103
Table 5.7: 2-way ANOVA for diagonal reach [TG4]	104
Table 5.8: 2-way ANOVA for diagonal-upward reach [TG5].....	105

Table 5.9: 2-way ANOVA for lateral far reach [TG7].....	106
Table 5.10: 3-way ANOVA for Vision, Target location, and Vibration Frequency	114
Table 5.11: 3-way ANOVA for Elbow, Target location, and Vibration Frequency	121
Table 6.1: Shoulder and elbow joint angles during reaching three representative target locations, [TG4], [TG5], and [TG7].....	133
Table 6.2: Vibration transmission for each body segment (Mean \pm SD) [Session I – under the 2Hz vertical vibration exposure].....	137
Table 6.3: Vibration transmission for each body segment (Mean \pm SD) [Session I – under the 4Hz vertical vibration exposure].....	138
Table 6.4: Vibration transmission for each body segment (Mean \pm SD) [Session I – under the 6Hz vertical vibration exposure].....	139
Table 6.5 Vibration transmission for each body segment (Mean \pm SD) [Session II – under the 2Hz vertical vibration exposure].....	140
Table 6.6 Vibration transmission for each body segment (Mean \pm SD) [Session II – under the 4Hz vertical vibration exposure].....	141
Table 6.7 Vibration transmission for each body segment (Mean \pm SD) [Session II – under the 6Hz vertical vibration exposure].....	142
Table 6.8 Vibration transmission for each body segment (Mean \pm SD) [Session III – elbow fully extended posture]	143
Table 6.9 Vibration transmission for each body segment (Mean \pm SD) [Session III – elbow flexed posture].....	144
Table B.1: The Percentage Distribution of Total Body Weight According to Different Segmentation Plans (Chaffin, 1999, from Webb Associates, 1978)	167
Table C.1: 3-way ANOVA for Subject Weight, Target Location, and Vibration Frequency.....	168

LIST OF APPENDICES

Appendix A. Transmission propagated through the upper limbs in three-dimension	157
Appendix B. The Percentage Distribution of Total Body Weight.....	167
Appendix C. The Effect of Total Body Weight on Fingertip Transmission	168

NOMENCLATURE

ANG: Angle

ANG_ACC: Angular Acceleration

ANG_VEL: Angular Velocity

CAE: Computer-Aided engineering

DHM: Digital Human Model

DOF: Degree of Freedom

DMU: Digital Mock-Up

EASHW: European Agency for Safety and Health at Work

E/F: Elbow Flexion

E/X: Elbow Extension

FFT: Fast Fourier Transform

HUMOSIM: Human Motion Simulation Laboratory

RMS: Ride Motion Simulator

MADYMO: Mathematical Dynamic Models

TACOM: Tank-automotive and Armaments Command

WBV: Whole-Body Vibration

CLAV: clavicle

LBHD: left behind head

IELB/LELB: left elbow joint

LFHD: left front head

IFRA/LFRA: left fore-arm

ISHO/LSHO: left shoulder joint
IUPA/LUPA: left upper-arm
IWRA/LWRA: left wrist A
IWRB/LWRB: left wrist B
RBHD: right behind head
rELB/RELB: right elbow joint
RFHD: right front head
rFIN/RFIN: right index finger tip
rFRA/RFRA: right fore-arm
rNCK/RNCK: right knuckle
rSHO/RSHO: right shoulder joint
rUPA/RUPA: right upper-arm
rWRA/RWRA: right wrist A
rWRB/RWRB: right wrist B
rWRT: right wrist joint

ABSTRACT

ANALYSIS OF BIODYNAMIC RESPONSES ASSOCIATED WITH UPPER LIMB REACHING MOVEMENTS UNDER WHOLE-BODY VIBRATION: SUPPORT FOR AN ACTIVE BIODYNAMIC MODEL

by

Heon-Jeong Kim

Co-Chairs: Bernard J. Martin and Brent Gillespie

Vehicle vibration is a well-recognized environmental stressor inducing discomfort, health risks, and performance degradation of the operator on board. More specifically, vibration transmitted by heavy transportation, construction, or military vehicles to the whole body of a seated occupant interferes with manual activities, which in turn may significantly compromise performance. Numerous approaches have attempted to understand the effects of vibration on the seated human for developing biomechanical models or to identify human reaching behaviors for developing human movement models. However, all these studies were limited to biomechanical models of the torso excluding the upper limbs, or to reach models based only on static conditions with no consideration of the interaction

between environmental conditions of vibration and biodynamic characteristics of arm movements.

The ultimate goal of this work is to provide a framework for an active biodynamic model of operators in vehicles based on empirical analyses of biodynamic responses of seated humans performing reaching movements under simplified whole-body vibration conditions. Hence, the present work investigates vibration transmission through multi-body segments as a function of vibration frequency and direction, identifies vibration-induced changes in reach kinematics of upper arm movements, analyzes the mechanisms of vibration transmission through a multi-body system as a function of posture and movement coordination, and proposes the integration of these empirical results for developing a biodynamic model. Five major results characterize our findings: a) vibration frequency is the dominant factor determining transmission characteristics through upper body segments, b) reach directions in three-dimensional space may be divided into three groups corresponding to transmission propagated through the upper limbs, c) visual compensation contributes to hand stabilization but does not modify significantly propagated transmission, d) elbow flexion contributes to the enhancement of hand stabilization by dissipating vibration energy, and e) biodynamic responses must be considered as three-dimensional tensors including the auto-axial and cross-axial transmissions. Furthermore, movement coordination and joint movement kinematics of reach movements are consistent between static and vibratory environments. The integration of these results may be used to support the structure of an active biodynamic model of the seated human.

CHAPTER 1

Introduction

Whole-body vibration (WBV) exposure is often cited as an environmental stressor causing discomfort, musculoskeletal disorders, motor performance degradations and physiological reactions. For the proper assessment of WBV effects on human performance or safety, a biomechanical model capable of simulating realistic human motor behaviors must be developed.

The work aims at characterizing vibration transmission associated with upper limb reaching movements under specific WBV conditions in the frequency range corresponding to high sensitivity of human motor performances. Ultimately this analysis will provide the empirical basis for the development of an active biomechanical model that can predict and simulate realistically the behavior of body segments in reaching and pointing tasks performed in a vibratory environment.

To achieve this aim, empirical studies were performed to analyze biodynamic responses through the human multi-body system during arm movements under selected sinusoidal WBV conditions. The results from this work are expected to enable us to anticipate performance degradation induced by WBV, thus contributing to the development of a model, the design of controls-and-displays interface and suspension system, and guidelines for movement strategies in this environment.

1.1 Problem Statement & Motivation

Mechanical vibration generated by the operation of vehicles has been shown to be an environmental stressor that can contribute to discomfort and health problems, and can interfere with motor performance of the operator in any given workspace (Lewis and Griffin, 1976; Martin et al. 1980; Martin 1981; Gauthier et al. 1981; Gauthier et al. 1983; Bovenzi and Zadini, 1992; Wilder and Pope, 1996; Pope et al, 1999; Palmer et al, 2000; EuFritz et al, 2005; Bovenzi, 2006; Burton et al, 2006; Okunribido et al, 2007; Seidel et al, 2008). More specifically, when vibration is applied to the whole body of the seated human, it can produce abdominal or back pains, musculoskeletal injuries, and body part resonances, and it can contribute as well to an increase in muscle tone and the degradation of motor performance (Griffin, 1990; Linder, 2004). Generally, exposure to high vibration frequencies leads to poor vision, numbness, or degradation of sensory motor functions, while exposure to low frequency vibration is associated with motion sickness or nausea.

In vehicles, vibration transmitted from rough terrain to occupants interferes with manual activities including the operation of controls and other interfaces (Rider, 2003; Rider, 2004; Oullier et al. 2009). Especially in heavy construction and military vehicles driven off-road, unpredictable vibration exposure over severely rough terrain disturbs rapid and accurate accomplishment of tasks such as identification and manipulation of vehicle controls that are critical for the successful conduct of work tasks or missions. Furthermore, according to a report from the European Agency for Safety and Health at Work (EASHW), lateral and longitudinal movements of the cab and operator could so significantly degrade manual performance that they might be a factor resulting in rollover accidents. These types of accidents are responsible for nearly 20% of all deaths associated with construction vehicles (EASHW, 2006).

Also, the advancement of technology in communication, navigation, and control systems has contributed to an increase in complexity and high density of controls and displays in vehicles. As a consequence, control interfaces may be downsized and placed further away from the operator seat, which in turn contributes to increased difficulty in reach performance, as formulated by Fitts' law (Fitts, 1954; Fitts and Peterson 1964).

Optimal design of controls and displays is of significant interest for occupational health and safety, as a driver's operation associated with secondary tasks is one of the most common causes of inattention-induced crashes (Wang et al, 1996). It is estimated that 55% of inattention crashes resulted from interaction with objects, a passenger, and/or instrumentation in a vehicle (Wierwille and Tijerina, 1996).

In addition, to improve workplace and product design with concurrent consideration of various parameters, digital human models (DHM) capable of simulating WBV effects on the seated human have been proposed (Amirouche, 1987a; Amirouche, 1987b; Li et al, 1995; Fritz, 1997; Fritz, 1998; Fritz, 2000). These models may be used to evaluate and improve designs in a virtual computer-aided engineering (CAE) environment. Human motion simulation technology can not only reduce design time and cost, but also allow an increase in the number of design parameters or options, thus enhancing the quality of design optimization (Chaffin, 2002). These earlier studies about human response to environmental vibration have been limited to static seated postures without any dynamic movements (see Griffin 1990 for review). However, since most activities in seated task include dynamic reach movements, a biomechanical model considering multi-body dynamics is necessary for the realistic simulation of human behaviors, the proper evaluation of human performances, and the better design of control interfaces placed in vibratory operation environments.

As stated above, vibration constitutes an environmental stressor, which interferes with human activities, thus leading to the degradation of performance, the increase of health risks, and even death of vehicle occupants in accidents caused by operation failure. For improving safety and performances under WBV exposure, it is of significant importance to enhance precision, accuracy, reliability, and robustness in vehicle operation, which can be achieved by optimizing the design of vehicle suspensions and controls-and-displays to minimize the influence of vibration-induced perturbations. Therefore, this work was proposed to identify biodynamic characteristics of the human body and WBV transmission through multi-body segments. The results may consequently provide the framework for an active DHM as well as assistance for appropriate design of vehicle control interface and the revision of safety guidelines.

1.2 Objectives & Hypotheses

The long term goal of this work is to support for the development of an active biodynamic model capable of representing seated human behaviors in vibratory environments. In order to obtain realistic simulations of human responses under WBV exposure, empirical studies are necessary to characterize biodynamic responses associated with movements performed in vibratory environmental conditions.

Thus, the main objective of this work is to investigate biodynamic responses through multi-body segments in individuals performing reaching and pointing tasks under specific WBV conditions as functions of vibration characteristics and movement directions. This main objective is based primarily on the hypotheses that WBV response of the end-effector may be derived from vibration-induced responses of body segments along the transmission path and that segmental responses are functions of vibration characteristics and upper body posture.

1.2.1 Experimental Approach

Simplification of WBV conditions in this work are necessary to focus on the empirical analyses of vibration transmission through the complex and non-stationary system constituted by the human body during movements, provide insights on vibration-induced perturbation of reach kinematics of the upper limbs, and understand harmonic distortion phenomena in human responses to WBV due to the nonlinearity of the system

As time variations of the mechanical properties of the system are expected, the associated non-stationary and non-linear features in regard to the low frequency range of vehicle vibration require a discrete approach to vibration stimulation. Indeed, human movements are relatively slow and their duration is either equivalent or slightly longer than the cycle of frequencies in the 2-10 Hz range. Furthermore, movement directions are associated with significant differences in posture, which also affect significantly the mechanical properties of the system. Hence, this first approach of the effects of vibration on discrete movements was based on selected sinusoidal vibration frequencies. The frequencies were chosen to reflect the component of vehicle vibration spectra and the range of frequencies corresponding to the high sensitivity of the seated human. The vertical direction of the vibratory stimuli was selected to reflect a major characteristic of vehicle vibration.

This discrete approach with sinusoidal inputs also allows us to determine more specifically the superposition of vibration-induced oscillation on movement kinematics and then to analyze the organization/reorganization of movements under vibration exposure. This approach also facilitates the analysis of vibration transmission along cross axes induced by the forcing stimulation along the vertical axis. The cross axis transmission is expected to reflect the interaction between the

vibration direction and the relative orientation of joint axes associated with different postures or changes with movement.

Furthermore, this approach may also enable the identification of mechanical properties, such as resonance of the system through a phase analysis.

1.2.2 Specific Aims & Hypotheses

To achieve our main objective, six specific aims and their corresponding hypotheses were defined as follows

Aim 1: to estimate vibration transmission through upper body segments in different pointing postures under selected vibratory environments, and to determine the feasibility of the main idea and hypothesis of this work.

Hypothesis 1: WBV characteristics can be derived from multi-body segment vibration characteristics. That is, the vibration response of the end-effector such as the fingertip can be predicted by synthesizing vibration characteristics of body segments along the transmission path.

Aim 2: to identify qualitative characteristics of upper limb joint kinematics in reaching activities common to vehicle operations, to investigate vibration-induced changes in reach kinematics and upper body coordination, to differentiate kinematic features in static and vibratory environments, and to understand associated motor control issues.

Hypothesis 2: The core paths of upper body joints are not significantly different in static and dynamic environmental conditions. They may differ only by the superimposed perturbation generated by the transmission of vibration.

Aim 3: to analyze variation of WBV transmission through upper body segments along reach movement trajectories. Perturbations of upper body joints are quantified for postures corresponding to intermediate stops along the fingertip trajectories to a predetermined final target location.

Hypothesis 3: Vibration transmission through body segments is a function of reach direction and instantaneous postures along the reach trajectory, which may be associated with changes in biomechanical properties of body segments.

Aim 4: to investigate the efficiency of visual compensation on the adjustment of vibration-induced reaching and pointing errors under WBV exposure.

Hypothesis 4: Reach performance in a vibratory environment may be compensated by visual control. However, specific task and vibration conditions determined by frequency and direction may not allow visual feedback to compensate effectively performance degradation.

Aim 5: to investigate the contribution of elbow extension/flexion constraints to WBV transmission at the end of a reach.

Hypothesis 5: The elbow joint contributes significantly to reach dynamic characteristics of the upper body. Hence, changes in degree of elbow flexion may significantly influence WBV-induced pointing errors at the fingertip while performing arm reaching movements,

Aim 6: to analyze the characteristics of vibration transmission through upper body segments in reaching movements of various directions under vertical WBV.

Hypothesis 6: Understanding the characteristics of WBV transmission along the transmission path of the upper limbs may provide information supporting the development of a biodynamic model of the seated human.

1.3 Potential Impacts

This study provides new findings concerning reaching movement characteristics in dynamic environments and vibration transmission through a multi-body system of the human body under WBV exposure. Vibration transmission through upper body segments is described as a function of vibration variables, spatial target locations, postures, and movements.

Based on these findings, this empirical study may support a promising framework for the elaboration of an active biodynamic model of the seated human, the simulation of manual performance, and biomechanical behaviors of the upper body under WBV exposure. The simulations will allow the proper ergonomic analysis of interactive tasks to be performed in a moving vehicle, which may significantly contribute to curtailment of costs associated with design, engineering, and manufacturing, as well as to reduction of the time spent in product development.

In addition, the findings of this work may be applicable to the improvement of the design of control interfaces to be used in vibratory environment and the design of vehicle suspensions.

Movement and posture strategies in reaching and pointing tasks may be suggested to reduce WBV interference with motor activities. Furthermore, this work may be expanded to evaluate the severity of vibration exposure and the associated health risks.

1.4 Thesis Organization

This dissertation is organized following the flow of complementary studies designed to investigate vibration transmission through body segments and to identify kinematics of reach movements under WBV exposure, as illustrated in Figure 1.1.

The first two chapters include the introduction and the literature review. The following three chapters present the three steps necessary to build the empirical database supporting the development of the model. Chapter 6 integrates empirical results obtained from biodynamic analysis to support for the framework of a model development. Chapter 7 summarizes the findings and achievements and discusses the limitations and possible future research opportunities.

Chapter 1 presents an overview of the research topic, including the problem definition, the motivation, the objectives and hypotheses, the potential impacts, and the research approach and procedure.

Chapter 2 summarizes the background literature classified into four subsections pertaining to human response to whole-body vibration, reach movements in the static environment, reach performance in dynamic environments, and recent biomechanical models of the seated human under vibration exposure.

Chapter 3 presents the estimation of vibration transmission through upper body segments under exposure to simplified WBV conditions. The corresponding study was designed to evaluate the core ideas and hypotheses of the proposed research. WBV responses and transmission through multi-body segments are estimated as a function of vibration frequency and direction.

Chapter 4 describes the kinematic analysis of upper body joints in reach movements under static and dynamic environments. Movement patterns observed in static and dynamic environments are compared.

Chapter 5 concerns the investigation of three-dimensional WBV transmission through multi-body segments along the upper body path as function of environmental conditions, reaching postures associated with the locations of targets to be reached, and movement constraints in a reaching and pointing task. Specifically, this chapter analyzes the effects of reaching postures and movements on WBV transmission through upper body path and the influence of visual feedback on reach performance under selected WBV conditions. The results constitute the empirical database supporting the model to be developed.

Chapter 6 illustrates an empirical support for an active biodynamic model based on statistical and empirical analyses of biodynamic responses through upper limb during reaching movements under selected WBV conditions.

Chapter 7 states conclusions and proposes directions for future work on the basis of the limitations and contributions of this work.

Appendix A presents the database concerning WBV transmissions obtained in the context of our experiments and an example reference about the percentage distribution of total body weight.

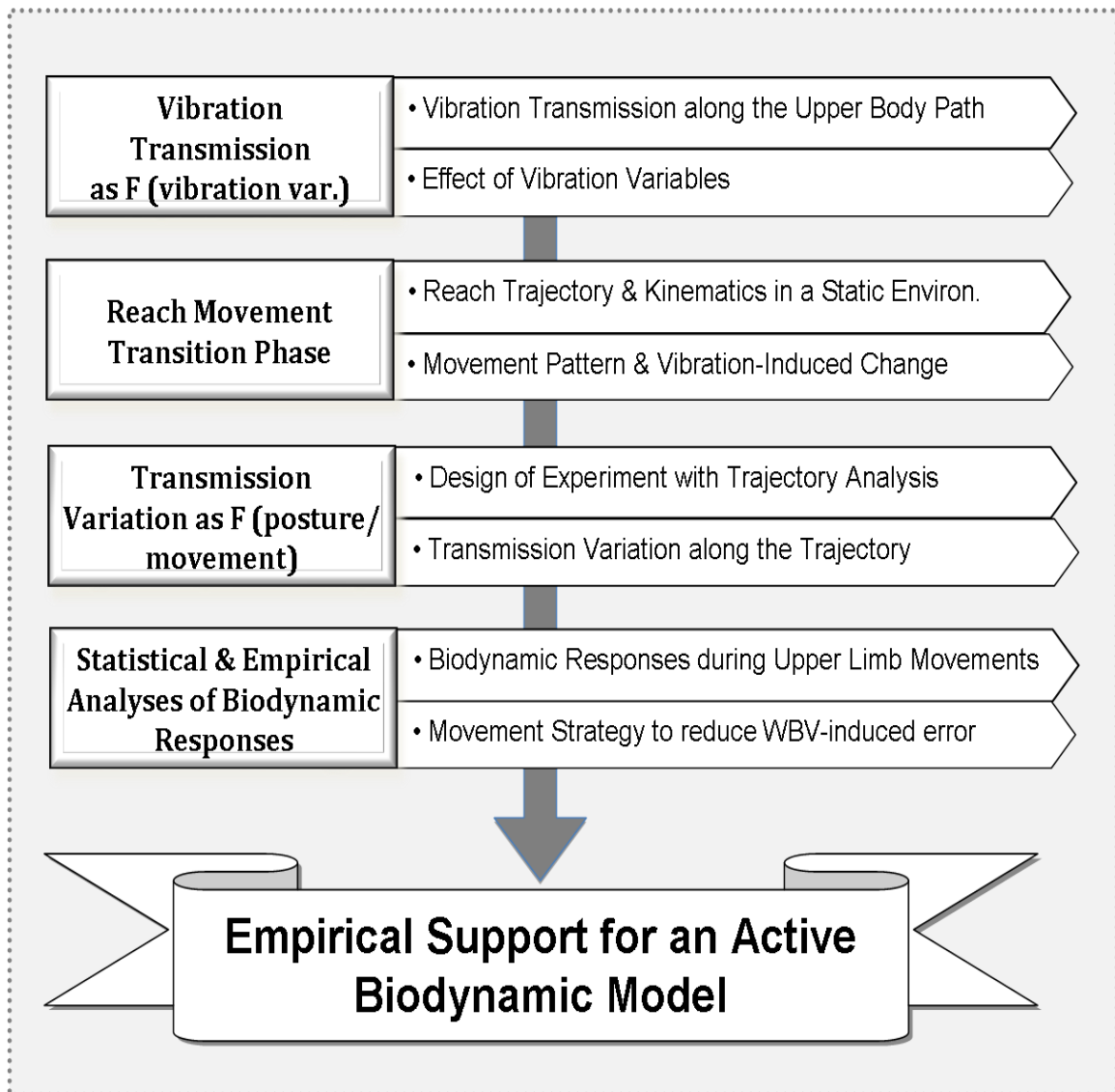


Figure 1.1: Research approach and procedure: Four complementary studies are used to characterize human biodynamic response to whole-body vibration. The last stage of the diagram corresponds to the future outcome of the results.

CHAPTER 2

Background Literature

2.1 Introduction

A number of approaches have attempted to identify how vibration affects humans in the workplace. These studies have emphasized the necessity of biomechanical models for the proper assessment of health risk and motor performance of the seated human under whole-body vibration exposure. However, the majority of the studies on human vibration responses focused on the torso and spinal system in static postures. The studies on reach performance under vibration examined the end point response of a fingertip without considering multi-body dynamics, and reach kinematic models developed in earlier studies cannot be modified to represent reach movements in vibratory environments.

2.2 Human Response to Vibration

Numerous studies have quantified human response to whole-body vibration in terms of apparent mass, driving point mechanical impedance, transfer function, transmissibility, absorbed power, etc., in order to evaluate whole-body vibration effects on the human health and performance (Lee and Pradko, 1968; Gurdjian et al, 1970; Martin et al, 1980; Roll et al, 1980a; Gauthier et al, 1981; Gauthier et al, 1983; Ribot et al, 1986; Boileau and Scory, 1990; Fritz, 1997; Fritz, 1998; Fritz, 2000; Hinz et al, 2001; Ljungberg et al, 2004; Fritz et al, 2005; Mansfield, 2005; Gillespie and

Sövényi, 2006; Rahmatalla et al, 2006; Abercromby et al, 2007; Rahmatalla et al, 2007; Sövényi and Gillespie, 2007; Seidel et al, 2008; Oullier et al, 2009). Some studies have investigated vibration effects on sensory motor performance. Martin et al (1980) estimated the extent of alterations in postural and movement control during exposure to WBV and immediately after exposure and showed a shift in mean resting posture and an increase in sway amplitude despite no participants' awareness of alterations. Gauthier et al (1981) evaluated the performance of sensory motor system performance under WBV by quantifying the increase in tracking position errors and torque reproduction variations. Ribot et al (1986) also assessed the performance of a compensatory targeting task conducted under both natural and vibration conditions. Oullier et al (2009) investigated postural post-effects induced by WBV. The latter study reported that the perturbation on the postural system remained even after prolonged exposure to WBV, and that postural instability induced by WBV could decrease by the special motor treatment after exposure, so-called 'sensorimotor recalibration'. Gillespie and Sövényi (2006 and 2007) estimated the tracking performance of vehicle operators using a force-reflecting joystick on a single-axis motion platform. These authors proposed a model-based cancellation controller to reduce biodynamic feedthrough and reported that the tracking performance was improved using this controller by forty-five percentages reduction in the RMS tracking error and that spectral energy of joystick movements significantly decreased in the 1-7 Hz frequency range. Hence this study demonstrated that the effects of WBV on a manual performance could be partially compensated by an adaptive control.

Some research has investigated vibration response through the torso and spinal system with specific interest in low back pain injuries of vehicle operators. Fritz (1997, 1998, 2000) computed the forces transmitted in the lumbar spine using the transfer functions and suggested that the spinal forces could be the crucial

component in the pathogenesis of the vibration-induced injury of the lumbar spine. Seidel et al (2008) evaluated intraspinal forces and health risks caused by WBV and predicted intraspinal compressive and vibration-induced shear forces at the seat, backrest, feet, and hands.

Other studies have investigated multi-stressor effects on human performance. Ljungberg et al (2004) examined the effects of noise and vibration, individually and combined, on cognitive performance and subjective experience. According to their investigation, compared to individual effects, combination of two stressors did not alter significantly reaction times, but extremely influence subjective ratings.

Many studies have reported that the response of the seated human could be affected by vibration variables such as vibration frequency, magnitude, direction axis, exposure duration, and system dynamics (Fairley and Griffin, 1989; McLeod and Griffin, 1989; Fairley and Griffin, 1990; Griffin, 1990; Kitazaki and Griffin, 1998; Mansfield and Griffin, 1998; Mansfield, 2005; Mansfield et al, 2006; Kim et al, 2007). Fairley and Griffin (1989) found that the body resonance frequency decreased as the vibration magnitude increased, and Griffin (1998) also found that the frequency at which the peak of absorbed power occurred decreased as the vibration magnitude increased. Fairley and Griffin (1990) also observed by measuring the apparent mass in the fore-and-aft and lateral direction that there exist two modes of in-phase motion at 0.7Hz and out-of-phase motion between the torso and the shoulder at 1.5-3Hz. Matsumoto and Griffin (2002) investigated the effects of the phase between two frequency components on the vibration dose value (VDV), and found that there was no significant effect except when the ratio of the two frequencies was three, i.e. 3Hz and 9Hz. Matsumoto and Griffin (2005) also studied the relationship between subjective responses and dynamic responses, and found a high correlation between the relative discomfort rate and the normalized mechanical impedance in the 3.15 - 8.0Hz frequency range.

More recent studies have focused on the effects of multi-axis vibration exposure on the apparent mass or mechanical impedance of the seated human (Holmlund and Lundström, 2001; Hinz et al, 2006; Mansfield and Maeda, 2006; Mansfield et al, 2006; Matsumoto et al, 2006; Mansfield and Maeda, 2007). They showed that vibration applied to the human body in one direction also caused motion and dynamic forces in other directions. Mansfield et al (2006) investigated the apparent mass and cross-axis transfer functions as functions of vibration magnitude, vibration spectrum, and posture. According to their evaluation, as vibration magnitude increased, the frequency of the primary peak in the apparent mass decreased for a relaxed posture while the magnitude in cross-axis transfer functions decreased for a tense posture. Matsumoto et al (2006) investigated the effects of the phase between the vertical and fore-and-aft sinusoidal vibration on discomfort, reporting that both discomfort and biodynamic responses were significantly influenced by the relative phase but could not be predicted simply by the superposition of individual responses to each single-axis perturbation. Mansfield and Maeda (2006, 2007) compared the apparent mass and cross-axis apparent masses of the seated human under single-axis and dual-axis vibration conditions. These authors reported that apparent masses were almost identical for the single-axis and dual-axis vibrations; however, the peaks of responses occurred at a lower frequency for the dual-axis than for the single-axis vibration.

In contrast to studies concerning the influence of vibration variables, other studies have investigated the biodynamic responses of the seated individuals as a function of the seat, sitting posture, hand position and back support conditions (Fairley and Griffin, 1989; Kitazaki and Griffin, 1998; Matsumoto and Griffin, 2002; Paddan and Griffin, 2002; Rakheja et al, 2002; Wang et al, 2004; Huang and Griffin, 2006). Fairley and Griffin (1989) found that the resonance frequency of the body increased with a backrest or in the erect posture. Matsumoto and Griffin (2002)

investigated the effect of muscle tension on the non-linearity in apparent mass, and found that muscle tension in the abdomen or buttocks did not affect significantly their nonlinear characteristics. Rakheja et al (2002) showed that hand position and body mass had a significant influence on the apparent mass of the seated body under vibration exposure whereas the influence of foot position was relatively negligible. Wang et al (2004) found that seat height affected the peak magnitude, and that the combined effects of hand position and back support conditions strongly influenced the primary resonant frequency and bandwidth of the biodynamic responses while the hand position influenced the apparent mass only with an inclined backrest. Huang and Griffin (2006) reported that voluntary periodic muscular activity of the upper body influenced biodynamic responses to vibration since voluntary muscular activity might alter the equivalent stiffness of a body segment.

As presented above, the influences of various factors on the responses of the seated human in static postures have been investigated to evaluate whole-body vibration effects on humans. However, WBV transmission through the multi-body system of the upper limbs when performing dynamic arm movements has not been investigated.

2.3 Human Movements & Reach Kinematics in a Static Environment

Reach movements are the primary activity of operators in any workplace, and therefore the simulation of human reach motions is an essential component for proactive ergonomic analysis and biomechanical models (Chaffin et al. 1999; Wang, 1999; Zhang and Chaffin, 2000; Chaffin, 2002; Chaffin, 2005; Park et al, 2005). To predict human reach movements and postures for the design and evaluation of ergonomic workspaces, seated reach movements have been studied from various perspectives.

Mathematical models were developed using optimization technique or statistics methodologies (Flash and Hogan, 1985; Haken et al, 1985; Schöner et al, 1986; Faraway, 2000; Faraway and Hu, 2001; Faraway, 2003). Flash and Hogan (1985) developed a reach model including an objective function for the square of the magnitude of 'jerk (rate of change of acceleration)' of the hand over the entire movement, in order to reduce the dimensionality problem in describing movement kinematics. Schöner et al (1986) proposed a time-dependent stochastic differential equation determined by stationary points for the transition region of hand movement. Faraway (2000, 2001 and 2003) described a functional regression model with endpoint constraints and the use of Bezier curves for predicting time-varying angles as well as trajectories as a function of the target to be reached and the anthropometry of the individual.

Kinematic features of arm movements and upper-body reach postures have been extensively analyzed in static environments (Prablanc et al, 1979; Morraso, 1981; Jeannerod, 1981; Soechting and Lacquaniti, 1981; Jeannerod, 1984; Atkeson and Hollerbach, 1985; Prablanc et al, 1986; Jeannerod, 1986; Jeannerod, 1988; Jeannerod and Marteniuk, 1992; Wang, 1991; Soechting et al, 1995; Desmurget et al, 1995; Haggard et al., 1995; Jeannerod et al, 1995; Jung et al, 1995; Zhang and Chaffin, 1996; Desmurget and Prablanc, 1997; Gielen et al, 1997; Gottlieb et al, 1997; Jeannerod et al, 1998; Wang, 1999; Zhang and Chaffin, 2000; Barreca and Guenther, 2001; Faraway, 2003; Admirral et al, 2004; Kim, et al; 2004). Soechting and Lacquaniti (1981) identified invariant features in pointing movements. The invariant characteristics are that the trajectory is independent of movement speed, that the ratio of the peak velocities at the elbow and the shoulder is equal to the ratio of the angular excursion at the two joints, that the two angular velocities reach a peak at the same time, and that their slopes are independent of target location. Many reach studies have pointed out invariance in reach kinematics such as the

hand or wrist path and its bell-shaped tangential velocity profile (Morrasso, 1981; Haggard et al., 1995). Through investigation of unrestrained human arm trajectories, Atkeson and Hollerbach (1985) also found that either curved or straight movements showed invariance in the tangential velocity profile when normalized for speed and distance. Some studies argued that hand movements are characterized by two phases consisting of feed-forward for hand transition and feedback for accurate landing of the hand (Soechting and Lacquaniti, 1981; Wang, 1991). Soechting et al (1995) examined Donders' law for arm movements and found dependency of arm posture at a given hand location upon the starting location of the movement. Gielen et al (1997) investigated pointing movements with the fully extended arm reducing rotational degrees of freedom in the shoulder and elbow during pointing movements to targets in various directions and at various distances. Barreca and Guenther (2001) suggested that consistent posture-dependent curvature of the spatial paths in the kinematic transformation might result in a systematic curvature of movements initially planned as straight-line trajectories toward the target. Admirral et al (2004) investigated kinematics and dynamics of human arm movements, and their finding that arm postures for a particular target depended on previous arm postures contradicted Donders' law. They suggest that both kinematics and dynamics affect postures depending on instruction and task complexity.

The temporal coordination of the upper body during multi-joint arm movements has also been investigated (Wadman et al, 1980; Atkeson and Hollerbach, 1985; Kaminski and Gentile, 1986, Karst and Hasan, 1991; Kaminski et al., 1995; Gottlieb et al, 1997; Wang, 1999a; Lim et al, 2004; Park et al, 2005). Many studies on movement coordination have found that shoulder and elbow joint reach movements in the horizontal plane differ in movement timing (Atkeson and Hollerbach, 1985; Kaminski and Gentile, 1986, Kaminski et al., 1995; Wang, 1999a).

In addition, EMG data showed that the shoulder movement is usually activated earlier than the elbow movement and that muscle activation time varies with movement direction (Wadman et al, 1980; Karst and Hasan, 1991). Gottlieb et al (1997) found that for most directions of reaching movements in the sagittal plane, the dynamic components of the muscle torques at the elbow and shoulder were related linearly to each other and that both were biphasic, almost synchronous, and symmetrical pulses. Lim et al (2004) investigated the effects of target location on temporal coordination of the upper body in three-dimensional reaching movements over an extensive range of motion. They found that movements of the upper body were differently initiated and completed and that movement coordination strongly depended on the geometry and representation of the target. Park et al (2005) suggested a joint contribution vector for representing arm movements using individual joint contributions to the achievement of the task.

Many investigations have attempted to build a movement prediction model to represent postures and joint kinematics for seated reach in static environments. (Hoff and Arbib, 1993; Rosenbaum et al, 1995; Jung et al, 1994; Jung et al, 1995; Jung et al, 1996; Zhang and Chaffin, 1996; Wang, 1998; Zhang et al, 1998; Chaffin et al, 1999; Wang, 1999; Zhang and Chaffin, 2000; Park et al, 2002; Jax et al, 2003; Kang et al, 2005; Park et al, 2006; Park et al, 2008). Hoff and Arbib (1993) developed a model describing the kinematics of hand movements in reaching and grasping tasks. Rosenbaum et al (1995) proposed a theory that movement coordination patterns in reaching movements were selected from stored postures. Jung et al (1994, 1995, and 1996) developed an optimization model showing that reach posture prediction was more accurate when using a psychophysical cost function of joint discomfort than when using a biomechanical cost function of joint torque. Wang (1998 and 1999) proposed a behavior-based inverse kinematic algorithm capable of handling the non-linearity of joint limits in a straightforward

way. Zhang and Chaffin (1996) examined two generic task factors such as hand movement direction and completion time in reaching movements, and suggested that hand movement direction was a significant factor determining instantaneous posture while movement completion time did not show any distinctive effects. Zhang et al (1998) proposed an optimization-based differential inverse kinematics approach for efficiently solving the kinematic redundancy in the velocity domain, and assigned weighting parameters to individual segments for quantifying their relative contributions to a change in the instantaneous posture. Based on these investigations, Zhang and Chaffin (2000) developed a three-dimensional dynamic posture prediction model with seven degrees-of-freedom of a four-segment linkage system representing the torso, clavicle, and right upper extremity and simulating in-vehicle seated reaching movements.

Chaffin et al (1999) examined two approaches for developing human reach models: one was an optimization based inverse kinematics to minimize the weighted sum of the instantaneous velocities of body segments, and the other was a new functional regression technique to fit polynomial equations to the angular displacements of body segments. They then proposed a combination of both approaches for representing actual movements performed in a variety of circumstances. Based on a review of motor control principles, Jax et al (2003) proposed that postures should be internally specified before motion activation, that tasks should be defined with flexible hierarchical constraints, and that movements could be shaped based on task demands. Kang et al (2005) presented an algorithm to predict the joint angles of a four degrees of freedom arm model based on the wrist location along the trajectory of reaching movements. Park et al (2002) proposed a memory-based model for realistic simulation of human motions using a motion modification algorithm, and later extended the 2-dimensional, 5 degree-of-

freedom, saggital-plane human model to simulate human obstruction avoidance during target reaching in a task space partitioned into small cells (2006, 2008).

From the musculoskeletal, biomechanical, and neurophysiological aspect, numerous studies have investigated multi-joint posture and movement control with focus on arm stiffness and equilibrium-point trajectory during multi-joint movements (Abend et al, 1982; Hogan, 1985; Flash and Mussa-Ivaldi, 1990; Gomi and Kawato, 1996; Gomi and Kawato, 1997; Gomi and Osu, 1998; Osu and Gomi, 1999; Burdet et al, 2000; Franklin et al, 2003; zehr et al, 2003; Darainy et al, 2006; Darainy et al, 2007; Kistemaker et al, 2007). Abend et al (1982) investigated the CNS control of multi-joint movements in terms of trajectory formation. Gomi et al (1996, 1997, 1998, 1999) estimated joint stiffness from EMG levels and investigated the relationship between effective muscle stiffness and joint stiffness.

As this review indicates, innumerable studies have identified kinematic features or motor aspects and/or proposed human reach models, providing some basic principles of reach movements. However, the majority of reach studies have been limited to the analysis within a two-dimensional space, and most investigations of three-dimensional reaches have been limited to small ranges of motion (Soechting et al, 1995; Wang, 1999a; Zhang and Chaffin, 2000). Furthermore, none of the analyses and models of reach kinematics can be extended to represent reach movements under whole-body vibration exposure.

2.4 Reach Kinematics or Performance in Dynamic Environments

To understand human movements in vehicle vibration environments, reach kinematics and/or performance in ride motion were investigated in terms of upper body coordination (Park et al, 2004; Yoon, 2004; Lee, 2006). Some have characterized upper body coordination under vibration exposure, in terms of the joints angle-angle relationships and body segment movement timings (Yoon, 2004;

Lee, 2006: not published). Others have identified reach strategies by quantifying the contribution of each joint to the displacement of the end-effector using new indicators such as the joint change vector and joint contribution vector (Yoon, 2004; Park et al, 2004). All these studies showed that movement sequences and joint angles were affected by vibration variables, but they did not provide the mathematical foundation that could be implemented in a biodynamic reach model.

In addition, some studies evaluated reach performance, focusing on the trade-offs between accuracy and speed under vibration exposure (Rider et al, 2003; Rider et al, 2004). Rider et al (2003) found that vibration exposure led to an increase in the duration of the adjustment phase near the destination and fingertip excursions during that phase and that the fingertip deviation from a static trajectory varied with reach direction and vibration frequency. The overhead upward reach showed larger fingertip excursion and higher reach difficulty than other directional reaches. For the assessment of the deviation of the fingertip, Rider et al (2004) also developed a 'trajectory index' that was calculated from two metrics: one was the largest deviation from the Frechet distance and the other was the integral of infinitesimal deviation of fingertip trajectory from a straight line. Their results showed that the peak deviation of the fingertip trajectory increased as the reach distance increased. In addition, they suggested an 'effective target size' determined on the basis of 95% confidence ellipses of finger accuracy. However, all these studies focused solely on fingertip oscillation without considering biodynamic characteristics of vibration transmissibility through multi-body dynamics and influence of posture change on reach performance.

2.5 Biomechanical Model of the Seated Human under Whole-Body Vibration

To evaluate and predict the effect of the whole-body vibration for improving comfort, safety, and manual performance, a number of investigations aimed at the

development of biomechanical models to represent the human response to vibration environment inputs (Amirouche, 1987a; Amirouche, 1987b; Fritz, 1991; Li et al, 1995; Fritz, 1997; Kitazaki and Griffin, 1997; Fritz, 1997; Fritz, 1998; Wei and Griffin, 1998; Fritz, 2000; Harrison et al, 2000; Hinz et al, 2001; Holmlund and Lundstrom, 2001; Griffin, 2001; Matsumoto and Griffin, 2001; Seidel and Griffin, 2001; Seidel et al, 2001; Paddan and Griffin, 2002; Rosen and Arcan, 2003; Yu and Luo, 2004; Kim et al, 2005; Yoshimura et al, 2005; Liang and Chiang, 2006; Mansfield et al, 2006; Rider et al, 2006; Mansfield et al, 2007; Okunribido et al, 2007; Oullier et al, 2009). Wei and Griffin (1998) compared biomechanical models of single- and multi-degree-of-freedom under vertical vibration, and suggested that a two-degree-of-freedom model provided a better fit than a one-degree-of-freedom model for the phase of the apparent mass at frequencies greater than 5Hz and the modulus of the apparent mass at frequencies around 8Hz. Li et al (1995) used a standard linear solid model for qualitatively simulating the influence of disc level and degradation of the disc durability for prolonged loading and low-frequency vibration; however, their model underestimated the stress relaxation, dynamic modulus, and hysteresis of thoracic and lumbar discs subjected to low-frequency vibration. Fritz (1998) developed a biomechanical model consisting of sixteen rigid bodies and visco-elastic joint elements and fifty-six force elements for the human trunk, neck, head, and arms. The model was validated by comparing the forces with the compressive strength of the spine, but the relationship between the spine forces and damage/pain is not clearly defined. Yoshimura et al (2005) evaluated the vibration effects on the spinal column of the seated human body through multi-body dynamics model with ten degrees of freedom for cervical, thoracic, and lumbar vertebrae. The model succeeded in estimating the relative displacements between vertebrae. However, an expansion of the degrees of freedom of the multi-body model is necessary to improve the model accuracy.

Other studies considered biomechanical models consisting of multiple lumped mass-spring-damper subsystems, for evaluating the vibration transmissibility from the seat to the head, by means of an optimization algorithm (Amirouche, 1987; Matsumoto and Griffin, 2001; Rosen and Arcan, 2003; Kim et al, 2005; Yoshimura et al 2005; Liang and Chiang, 2006; Stein et al, 2007). Amirouche (1987) investigated the dynamic response of the human body by modeling connective tissues, muscles, ligaments, and disks vertebra with linear and nonlinear springs and damping forces. Rosen and Arcan (2003) developed a multi degrees-of-freedom lumped parameter model simulating dynamics of human responses that varied with posture, backrest, muscle tension, vibration direction, and cushioning interface. Yu and Luo (2004) investigated response and stability of a human body to the periodic impact input by linearly modeling vehicle and passenger system with a lumped mass and a massless bar, assuming that vehicle motion is quite small compared to the passenger's motion due to large mass and moment of inertia of the vehicle system. Kim et al (2005) examined models consisting of several lumped masses connected by linear translational and rotational springs and dampers, and proposed two four-body-segment models. The finite element method was also used to develop a two-dimensional model of human biomechanical responses to vertical WBV (Kitazaki and Griffin, 1997). They modeled the spine, viscera, head, pelvis, and buttocks using beam, spring, and mass elements, and suggested that posture change from erect to slouched might decrease the axial stiffness and increase shear deformation of tissue below the pelvis.

For the validation of models, Griffin (2001) proposed the checklists corresponding to model categories such as 'mechanistic', 'quantitative', and 'effects' models. Liang et al (2005) simulated transmissibility through the seated human using the BIODYN-II model, the biodynamic part of the AVB-DYN software package that is an integrated software package combining anthropometric, vehicle dynamics,

biodynamic, and system analysis tools. Their simulation suggested that the force between hip and seat, the torque at the waist, the torque at the shoulder, and the force at the hand/grip interface were major factors in driving posture affecting the biodynamic response; however, their model failed in predicting empirical results. Rider et al (2006) proposed a trajectory planning and feedback controller in the model, on the basis of hypothesis that movement alterations and adjustments were predictable by visual and/or proprioceptive information. However, the model did not integrate joint stiffness parameters.

As reviewed above, numerous approaches have attempted to develop biomechanical or biodynamic models representing WBV responses through the seated human body. However, most of the developed models have been limited to the upper torso or spinal system of the human in static sitting postures or to the end effector motion without considering transmission through multi-joints. None of these models has addressed the vibration transmission issue through a multi-segmental human body performing dynamic activities. Because of these limitations, I initiated empirical studies to analyze vibration transmission through multi-body system performing upper limb reaching movements under exposure to selected WBV conditions corresponding to specific frequency sinusoidal excitations.

CHAPTER 3

Vibration Transmission of Upper Body Segments under Sinusoidal Whole-Body Vibration Exposure

Vehicle vibration is transmitted to the whole body of the seated driver and operators, thus causing discomfort and interfering with the driver's movements in this dynamic environment. Several studies have examined the effects of vibration on human performance such as the speed and accuracy of the seated reach, or have investigated biodynamic responses of the upper torso in static postures. The present study investigates vibration transmission through multi-body segments along the upper body path by analyzing displacements of upper body joints in the frequency domain. This study shows that transmission through upper body segments is affected by vibration frequency, direction, and location of the target to be reached.

3.1 Introduction

Vibration perturbation is one environmental stressor causing discomfort and degradation of human activities. In a vehicle, the vibratory environment may affect the motion of an operator through whole body transmission and disturb the manual ability of vehicle operator, thus limiting the performance of the entire system.

Whole-body vibration response of the seated human has been investigated as a function of vibration frequency, magnitude, direction axis, and exposure duration (Fairley and Griffin, 1989; McLeod and Griffin, 1989; Fairley and Griffin, 1990; Griffin, 1990; Griffin and Hayward, 1994; Kitazaki and Griffin, 1998; Mansfield and Griffin, 1998; Mansfield, 2005; Mansfield et al, 2006; Kim et al, 2007). These studies reported that manual tasks were the most sensitively affected by vertical vibration in the 3 to 8 Hz frequency range. Similarly, tasks performed under horizontal vibration were most disruptive at frequencies below about 3 Hz, and the degradation effect decreased as the vibration frequency increased up to 12 Hz. For both vertical and horizontal vibration, vibration transmission to the shoulders and head was maximal in the frequency range corresponding to the highest discomfort sensitivity. These studies also indicated that whole-body vibration response increased with vibration magnitude. Although these investigations described some vibration characteristics of the human body, they were limited to the vibration response through the torso or spinal system of the upper body in static postures or to the description of the hand behavior without consideration of active movements.

Vibration-induced alterations in reach kinematics and performance have been investigated in terms of the fingertip trajectory and excursion (Rider et al 2003 and 2004). These studies evaluated the level of task difficulty using the concept of effective target size and confidence ellipses of finger excursions and indicated that the highest level of task difficulty corresponded to the principal resonant frequency of the trunk between 4 and 6 Hz under vertical vibration exposure. In addition, the role of visual feedback in hand movement guidance was also investigated by means of movement time and peak tangential velocity (Rider et al, 2006). According to their study, movement time is longer in the vision condition than in the occluded vision condition, as visual feedback provides additional information capable of increasing the accuracy of task but requiring additional time for corrective sub-

movements. Peak tangential velocities of the fingertip movements were higher in the occluded vision condition, corresponding to shorter movement times. These studies provided an ergonomic evaluation of vibration-induced reach performance; however, the contribution of each body segment perturbation to fingertip deviation was neither identified nor included in a model for systematic assessment of vibration effects.

Biomechanical modeling of the human body has been attempted by investigating the biodynamic characteristics of human body transmission (Amirouche, 1987; Fairley and Griffin 1990; Wei and Griffin, 1998; Matsumoto and Griffin, 2001; Paddan and Griffin, 2002; Rosen and Arcan, 2003; Yoshimura et al, 2005; Liang and Chiang, 2006). Some studies tried to develop a biomechanical model of the upper torso using a finite element method. Other models consisted of multiple lumped mass-spring-damper systems in different static postures; however, no attempt in human vibration analysis or biomechanical modeling has been made to describe changes in the WBV response through the upper limbs during dynamic activities requiring changes in posture as a function of time and space thus changes in biodynamic properties of the human body during reach movements.

In order to provide a framework supporting an active biodynamic model, this work aims at analyzing biodynamic responses of seated human operators under exposure to simplified WBV conditions. As the first step of this research, this chapter estimates the vibration transmission through the right shoulder, elbow, and fingertip in pointing postures at the end of a reach along the selected directions under exposure to vertical and horizontal sinusoidal vibration conditions.

3.2 Methods

3.2.1 Biodynamic Reach Experiment I

Subjects

Thirteen right-handed young adults participated in the experiment voluntarily. All participants were in good health and had no known musculoskeletal or neurological disorders, chronic back pain, nor acute back pain. The average values (\pm SD) of age and anthropometry dimensions (stature, torso length, right upper arm and forearm lengths, and hand length) are listed in Table 3.1.

Table 3.1: Anthropometry Data

	Age (years)	Stature (cm)	Torso length (cm)	Upper arm length (cm)	Forearm length (cm)	Hand (wrist-fingertip) length (cm)
Mean	32 \pm 6.5	177.6 \pm 5.4	46.9 \pm 1.6	34.5 \pm 1.0	28.6 \pm 1.8	17.2 \pm 1.8

Experimental Setup

The experiment was conducted on the Ride Motion Simulator (RMS) of the U.S Army at TACOM (Figure 3.1). The RMS is controlled by six linear hydraulic actuators that can generate the six degrees-of-freedom of vehicle vibration (Figure 3.2). Six cameras of a VICON™ motion capture system were rigidly fixed on the RMS cab to record the relative displacements of upper body segments of individuals performing reach movements.



Figure 3.1: Experimental Setup and RMS cab:

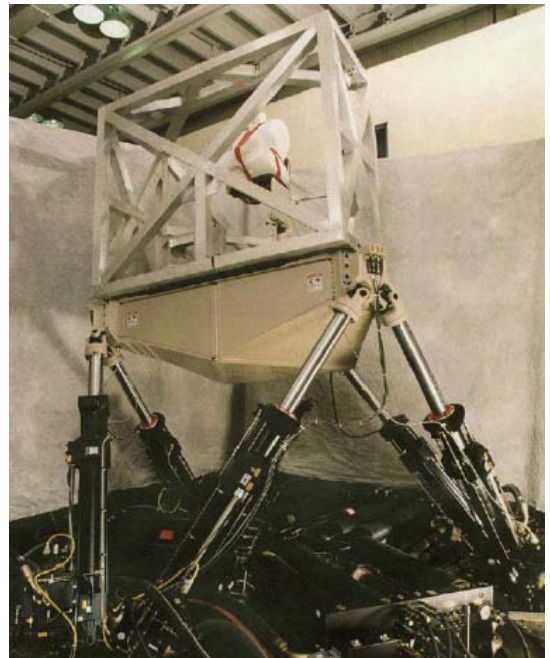
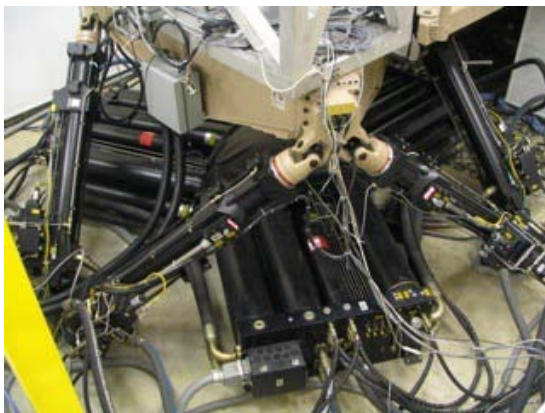


Figure 3.2: Ride Motion Simulator (RMS): compressed (left) and extended (right) configurations

Vibration Condition

Reach trials were performed under seven simplified vibration conditions generated by the RMS. The reference condition was a static condition in which no vibration was applied. Six vibration conditions were generated by the combination of three discrete sinusoidal vibration frequencies (2, 4, or 6 Hz) and two vibration directions (vertical or fore-and-aft), as summarized in Table 3.2. These sinusoidal vibration conditions were selected to estimate vibration transmission for the simplified excitation conditions corresponding to specific vibration frequencies in which reaching performance is highly sensitive (Figure 3.3; Rider et al, 2003) and the frequency range of major vehicle vibrations (Lee and Pradko, 1968; McLeod and Griffin, 1989; Fairley and Griffin, 1990; Griffin, 1990). The peak acceleration magnitudes for the vertical and fore-and-aft vibration directions were 0.5G and 0.4G respectively, and the constant magnitude was applied for all frequencies vibration to avoid the effects of interaction between vibration frequency and magnitude (McLeod and Griffin, 1989).

Table 3.2: Vibration input conditions

Direction	Vibration Frequency, Magnitude		
No Vibration	-		
Vertical Vibration (up-and-down)	2Hz, 0.5G	4Hz, 0.5G	6Hz, 0.5G
Horizontal Vibration (fore-and-aft)	2Hz, 0.3G	4Hz, 0.3G	6Hz, 0.3G

Surface Map of Difficulty

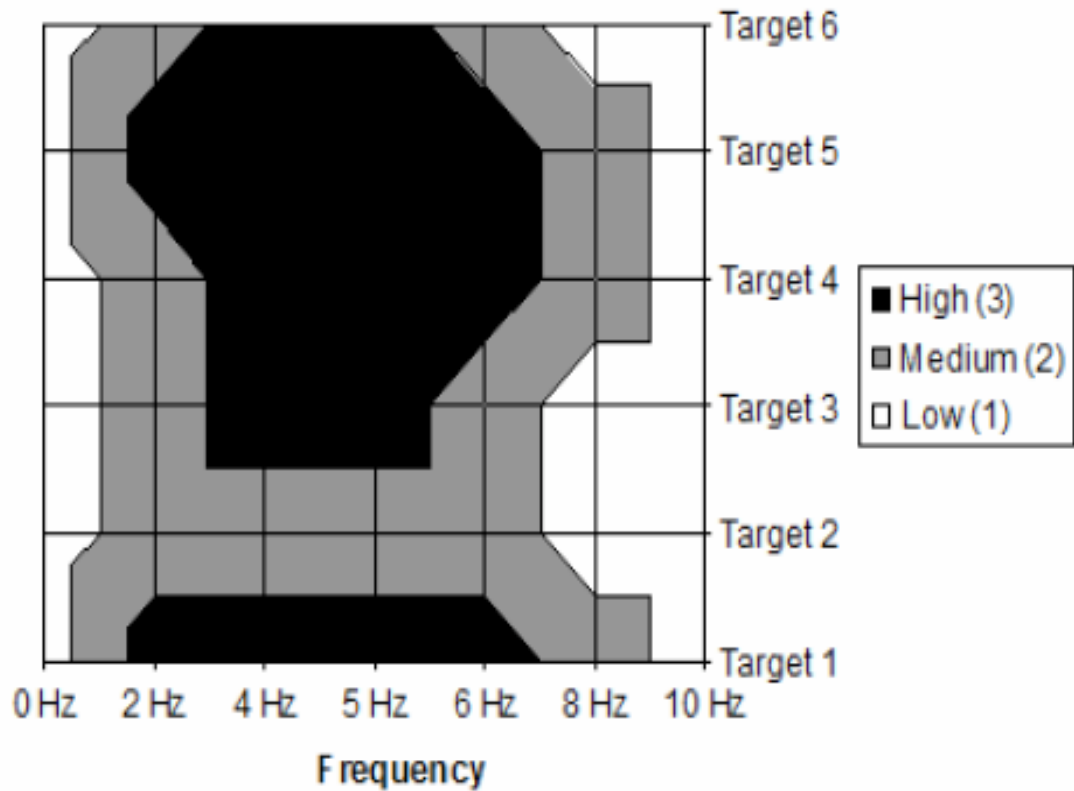


Figure 3.3: Reach difficulty rating by ride-motion frequency and target location (Rider et al, 2003)

Target Location & Reach Task

The participants were required to perform reaches from an initial location to eight targets distributed in the right hemisphere of the operator seat (Figure 3.3). These eight targets represent the overall reach space for in-vehicle operation: upward [TG1], forward & upward [TG2], forward [TG3], forward & lateral [TG4], diagonal & upward [TG5], lateral & upward [TG6], lateral near [TG7], and lateral far [TG8]. The locations of the targets were designed with respect to the coordinate system whose origin was located at the right top of a steering handle (Table 3.2). All participants were required to reach every target in a random order. Each target was reached twice.

Minor constraints were applied for data collection and safety. A lap seat belt must be fastened tightly enough to prevent relative slip between the seat and the hip. The location of foot placement was not specified but both feet must rest on the cab floor during the experiment. Participants were requested to hold a steering handle with both hands and to fixate their gaze on a front monitor, which corresponded to the initial posture prior to any reaching movement. While reaching the target with the right hand, the left hand must remain on the steering handle to avoid large variation in posture and boundary condition of the body system between reach trials.

Participants were requested to perform all reaches at the self-determined speed. When reaching the target, participants were required to point to the center of the target for three seconds without contact. This constraint was imposed to estimate the real amount of vibration response transmitted through the arm. In addition, to eliminate vision-induced movement adjustments, participants were allowed to look at a target at the beginning of each reach trial, but they must redirect their gaze to the saggital plane immediately after reaching a target.

For the safety purposes, a lightweight helmet was used by all participants and the task was performed with the seat belt fastened. Emergency safety buttons that were placed in several locations around the RMS for easy accesses allowed the participant or the experimenters to stop the motion of the RMS at any time. To monitor symptoms of simulation sickness, participants were asked to answer orally a short survey before and after each session on the RMS.

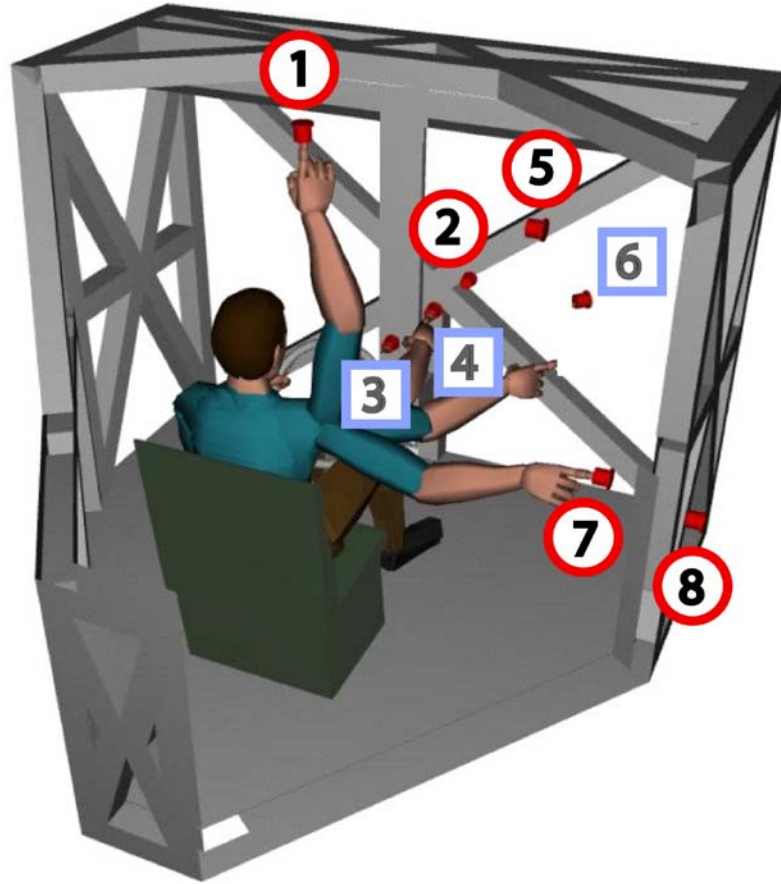


Figure 3.4: RMS cab and target locations:
The targets selected for this analysis are identified by the circled numbers.

Table 3.3: Task conditions (target locations)
The origin of the coordinate system is at the right top of the steering handle.

No.	Target Direction	Target	Location (x, y, z) [mm]
1	Upward	TG 1	(143, -357, 678)
2	Forward & Upward	TG 2	(132, 133, 269)
3	Forward	TG 3	(206, 139, -171)
4	Forward & Lateral	TG 4	(426, 44, -66)
5	Diagonal & Upward	TG 5	(564, -274, 420)
6	Lateral & Upward	TG 6	(563, -293, 420)
7	Lateral Near	TG 7	(578, -271, -114)
8	Lateral Far	TG 8	(870, -295, -114)

Motion Capture

For the recording of body segment movements, retro-reflective markers were placed on twenty-six body landmarks including four markers for head position and orientation, ten markers for torso movements, seven for the right arm and hand movements, and five for the left arm (Figure 3.5 and 3.6). Dynamic movements of the upper body were recorded by a VICON™ optical motion tracking system using six cameras, with a sampling rate of 100Hz. For anthropometric measures and subject calibration, a static T-pose and the range of motion were also recorded at the same rate for each participant (Figure 3.7).



(a) frontview



(b) rearview

Figure 3.5: Retro-reflective markers placed on a subject. Twenty-six markers were placed on body landmarks

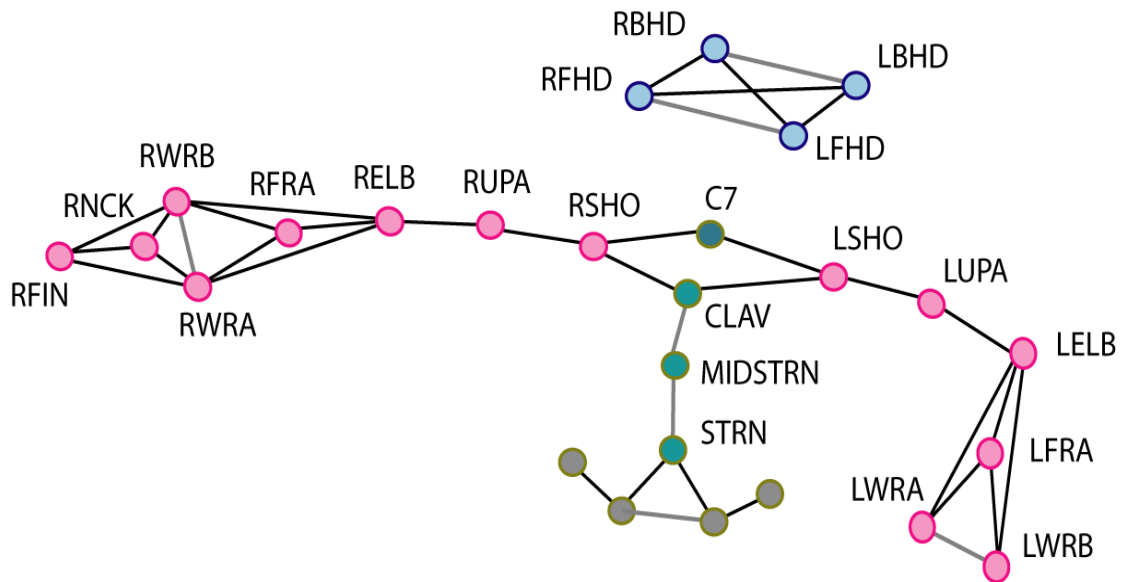


Figure 3.6: Retro-reflective marker set placed on body landmarks: R=right, L=left, FHD=front-head, BHD=back-head, CLAV=Clavicle, MIDSTRN=mid-sternum, STRN=sternum, SHO=shoulder, UPA=upper-arm, ELB=elbow, FRA=fore-arm, WR=wrist, NCK=knuckle, FIN=finger



Figure 3.7: T-pose for anthropometric and range of motion calibration

3.2.2 Data Analysis

3.2.2.1 Movement Phase Analysis

A reach trial consists of four movement phases: [1] the initial resting posture while holding the steering handle at home position, [2] the aiming transition phase to reach a target, [3] the quasi-static posture while pointing to the target for three seconds, and [4] the returning phase of hand transition back to the initial position, as illustrated in Figure 3.8. This study analyzes specifically the perturbation of the upper body segments induced by the selected sinusoidal vibration conditions during the pointing phase.

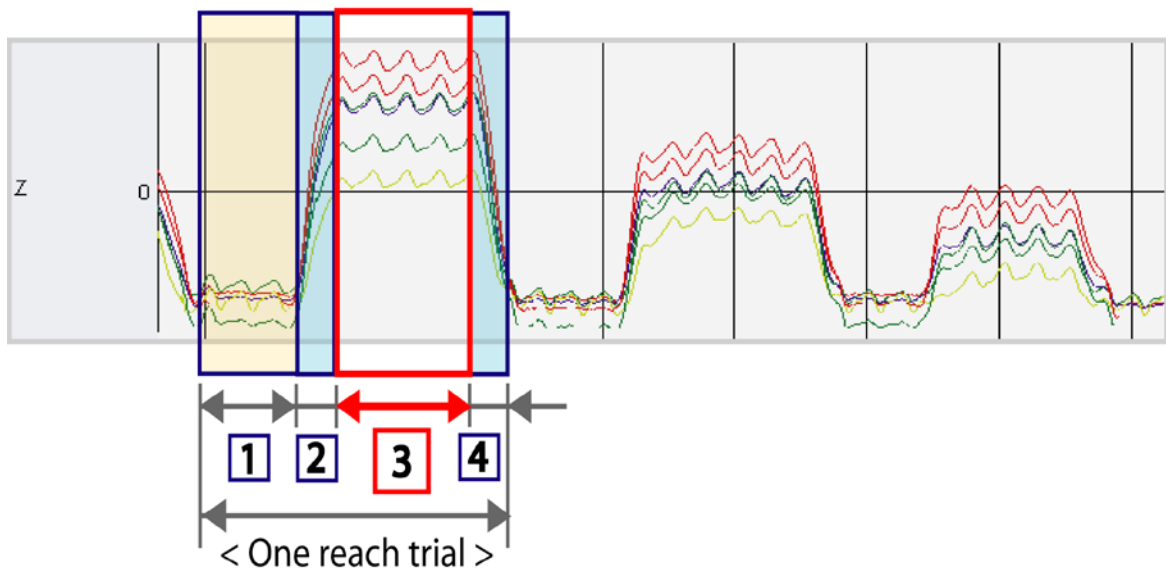


Figure 3.8: Movement phases in a reach trial: [1] resting phase, [2] aiming phase, [3] pointing phase, and [4] returning phase. The pointing phase [3] was used to compute the vibration transmissibility of body segments.

Among all of reach trials, only movements to five target locations in four directions were selected for this study; TG1 = upward, TG2 = forward, TG5 =

diagonal, and TG7 & TG8 = lateral. This selection was based on data quality. The inclusion criteria for this analysis were: all link markers could be tracked without errors or interpolation of missing data was acceptable (less than six consecutive frames drop out and/or less than four drop out sequences in time data). The analysis matrix consisted of three vibration frequencies and five target locations for each vibration direction as displayed in Table 3.4.

Table 3.4: Analysis Matrix associated with the selected levels of each variable.

		Upward	Forward	Diagonal & Upward	Lateral Near	Lateral Far
		TG 1	TG 2	TG 5	TG 7	TG 8
Vertical Vibration (up-and-down)	2 Hz					
	4 Hz					
	6 Hz					
Fore-Aft Vibration	2 Hz					
	4 Hz					
	6 Hz					

3.2.2.2 Frequency Analysis

The present analysis focused specifically on the motion of the torso, upper arm, lower arm-hand, which corresponded to the links delineated by three markers placed on the shoulder, the elbow and the right index finger along the transmission path. It was assumed that the hip translational and rotational movements relative to the seat were negligible.

To estimate vibration transmission along the upper body path, the sinusoidal input and body segment displacement outputs in the time domain were transformed into the frequency domain by the Fast Fourier Transform (FFT), as shown in Figure

3.9. The FFT is an efficient algorithm to compute the Discrete Fourier Transform (DFT), as represented by (Eq. 3.1).

$$X(k) = \sum_{j=1}^N x(j) \omega_N^{(j-1)(k-1)} \dots\dots\dots (Eq. 3.1)$$

where $\omega_N = e^{(-2\pi i)/N}$

In Eq. 3.1, $x = x(t)$ is a signal in the time domain and $X = X(\omega)$ is the signal transformed in the frequency domain.

No windowing was applied to the FFT. The frequency bandwidth of interest was in the range of 0.2 – 15 Hz. For identifying the contribution of each body segment perturbation along the transmission path to the fingertip’s deviation from a target, the frequency responses of three body segments were analyzed and the vibration transmission through three segments were estimated by the ratio of peak magnitudes in an input and responses at the forcing frequency in the excitation direction (Figure 3.10 and Eq.3.2). This term of vibration transmission is an analytical index borrowed from linear system theory for empirical evaluation on a highly nonlinear human body system.

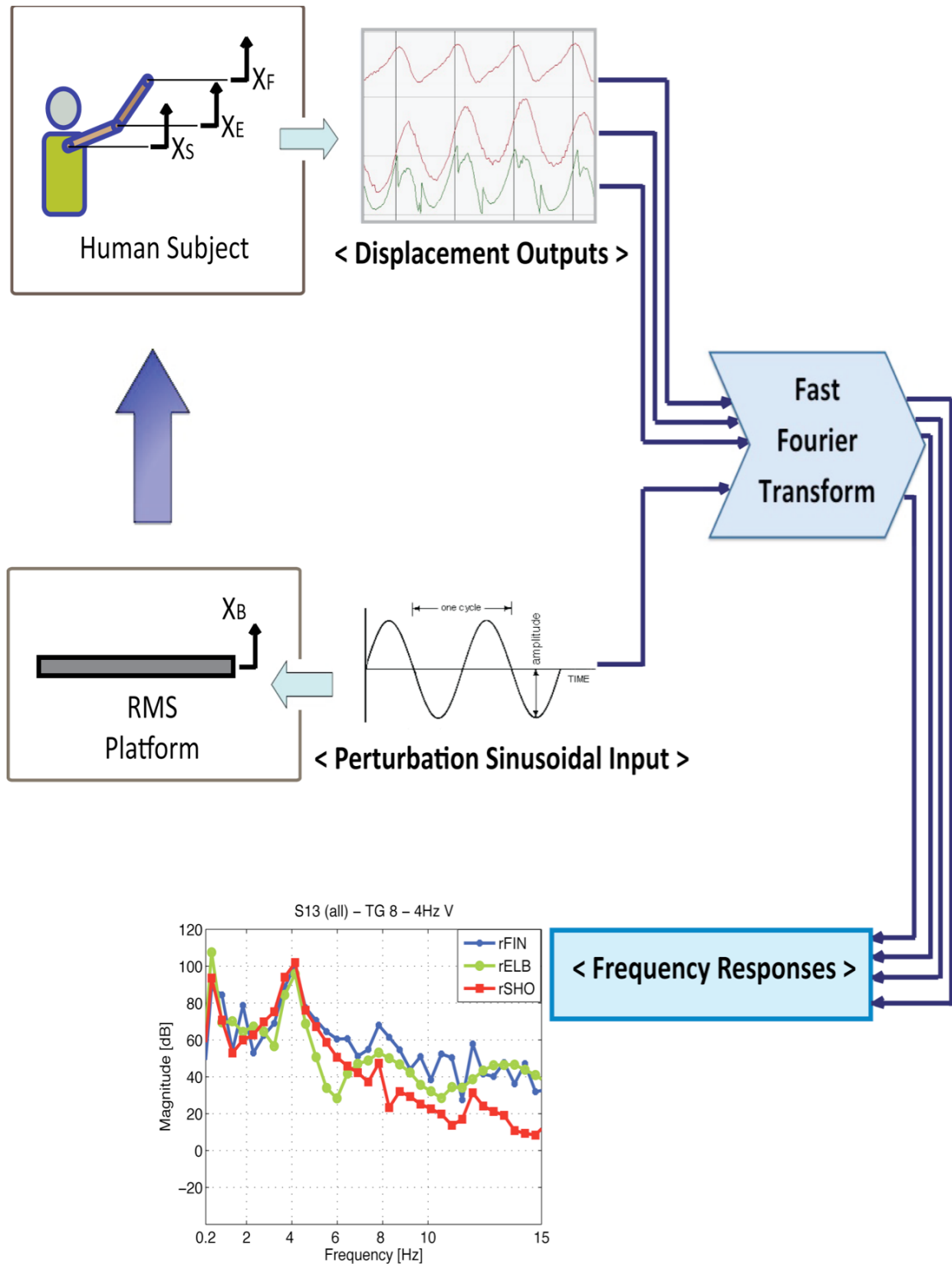


Figure 3.9: Frequency analysis of input and body link displacement outputs – The frequency bandwidth of interest is in the 0.2 - 15 Hz frequency range.

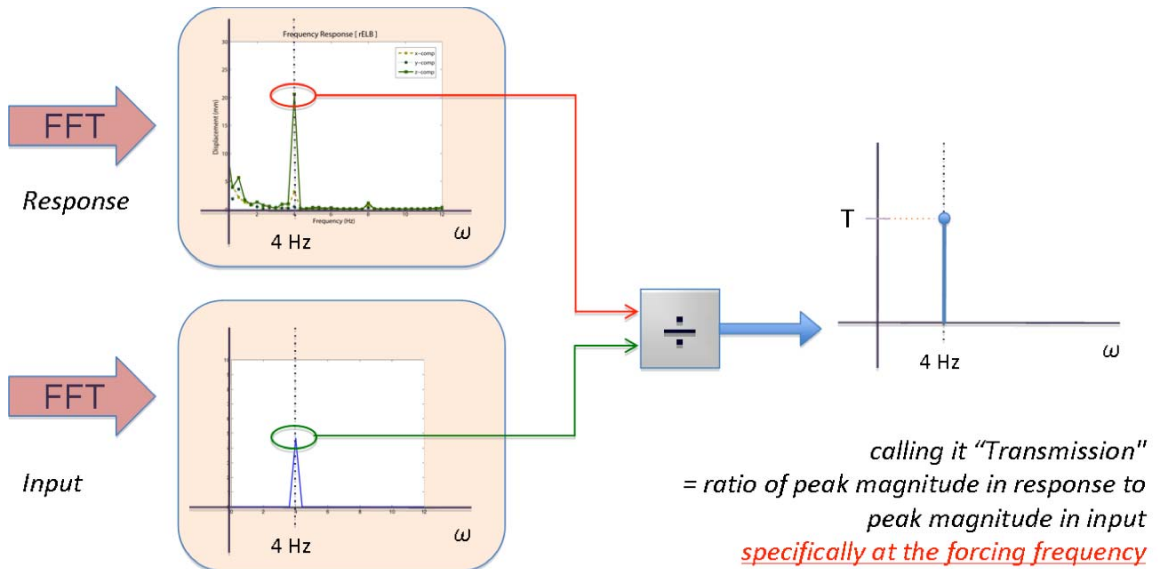


Figure 3.10: Transmission at the forcing frequency.

$$H_B^S(\omega_f) = \frac{X_S(\omega_f)}{X_B(\omega_f)} \quad \dots\dots\dots \text{(Eq. 3.2)}$$

$$H_B^E(\omega_f) = \frac{X_E(\omega_f)}{X_B(\omega_f)}$$

$$H_B^F(\omega_f) = \frac{X_F(\omega_f)}{X_B(\omega_f)}$$

Vibration transmission $H_i^o(\omega_f)$ is equal to the ratio of the peak magnitude in the response displacement output $X_o(\omega_f)$ to the peak magnitude in the excitation displacement input $X_i(\omega_f)$ specifically at the forcing frequency (ω_f), and superscript or subscript B , S , E , and F denote the cab base, the right shoulder, elbow, and fingertip respectively. Relative transmission through individual body segment can be easily calculated from two vibration transmissions through distal and proximal end joints of body segments, e.g. relative transmission through the upper arm can be calculated from transmission at the shoulder and elbow as shown in Eq. 3.3. Comparisons of the relative transmissions through each body segment can provide

information on how vibration is transmitted through each segment independently, which may be useful for modeling vibration characteristics of each body segment in a multi-body structure.

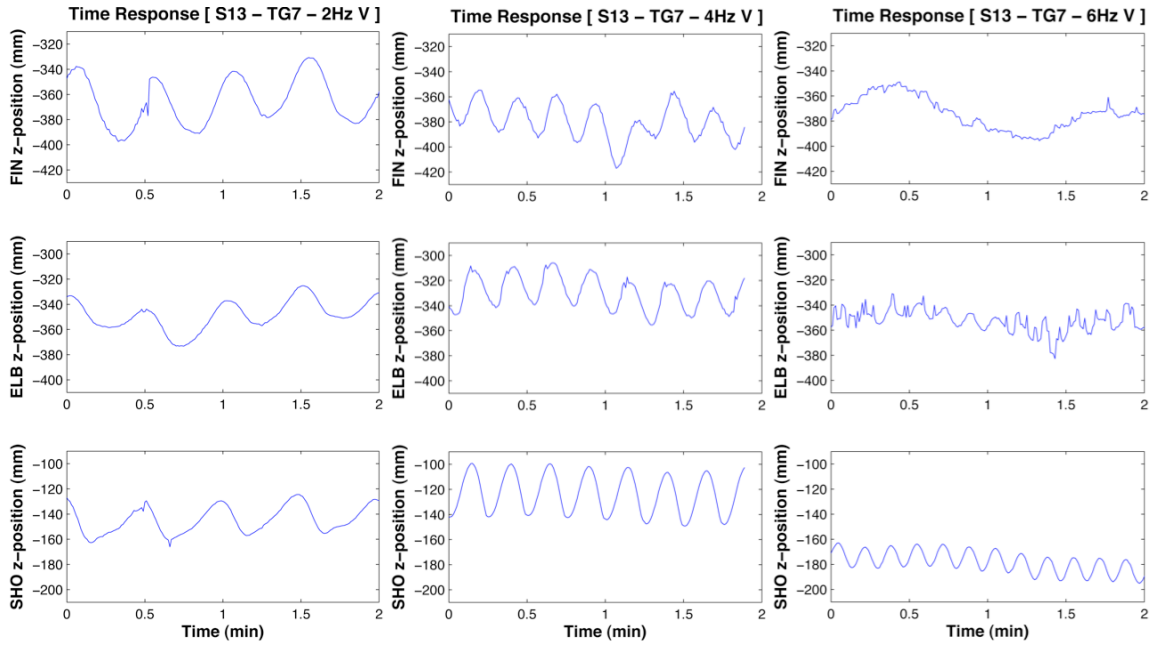
$$H_S^E(\omega_f) = \frac{X_E(\omega_f)}{X_S(\omega_f)} = \frac{X_E(\omega_f)}{X_B(\omega_f)} \bigg/ \frac{X_S(\omega_f)}{X_B(\omega_f)} = \frac{H_B^E(\omega_f)}{H_B^S(\omega_f)} \dots\dots\dots \text{(Eq. 3.3)}$$

3.3 Results

3.3.1 Displacements of Upper Body Segments in Time and Frequency Domains

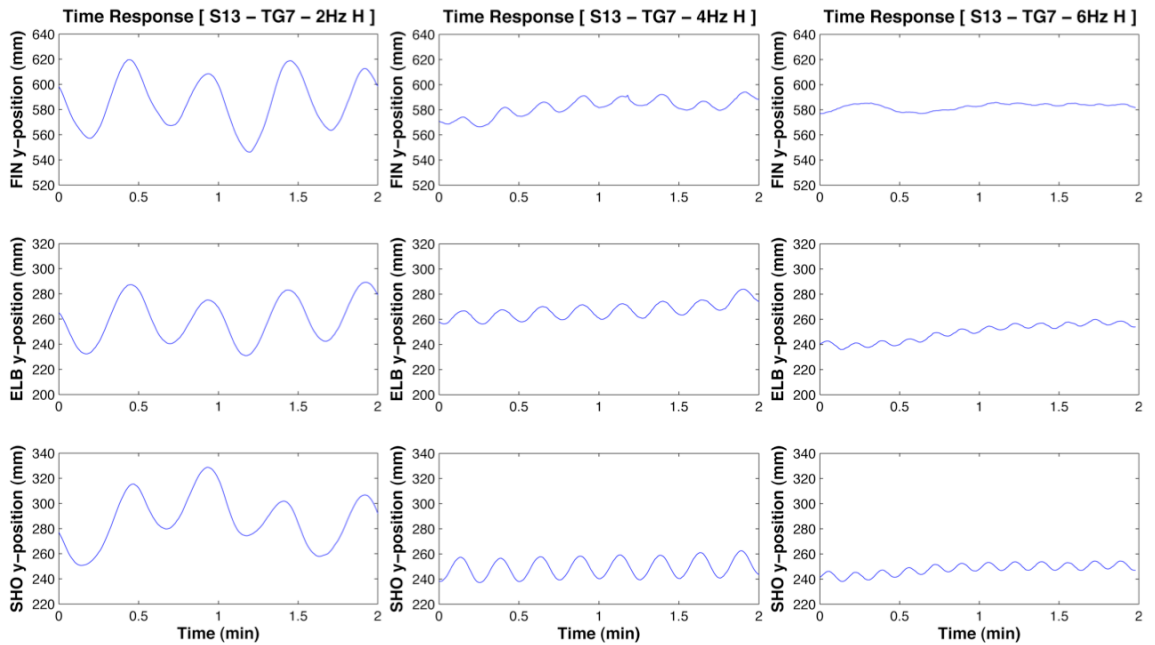
Typical displacement samples of the right shoulder, the elbow, and the fingertip while pointing to target 7 (lateral near) are represented in Figure 3.11 and 3.12 for vertical and horizontal WBV exposure, respectively. Vibration responses through the right arm conspicuously decrease at the fingertip specifically under the 6Hz WBV exposure in both vertical and horizontal directions.

To compare vibration characteristics of these three body segments as a function of vibration conditions, displacement responses are analyzed in the frequency domain. The frequency responses of body segments in the pointing posture are presented in Figure 3.13 for each vibration frequency in the vertical and horizontal WBV directions. For both vibration directions, vibration responses at the fingertip are the largest among the three joints under 2Hz perturbation while responses at the shoulder are the largest for 4Hz and 6Hz perturbations. When compared to the shoulder, perturbation at the fingertip decreases noticeably for both 6 Hz vibrations. For 4Hz and 6Hz exposures, responses at all three joints are larger for the vertical than for the horizontal vibration; however, this comparison with time responses is not conclusive in the present context, since the magnitude of stimulation was different for each direction.



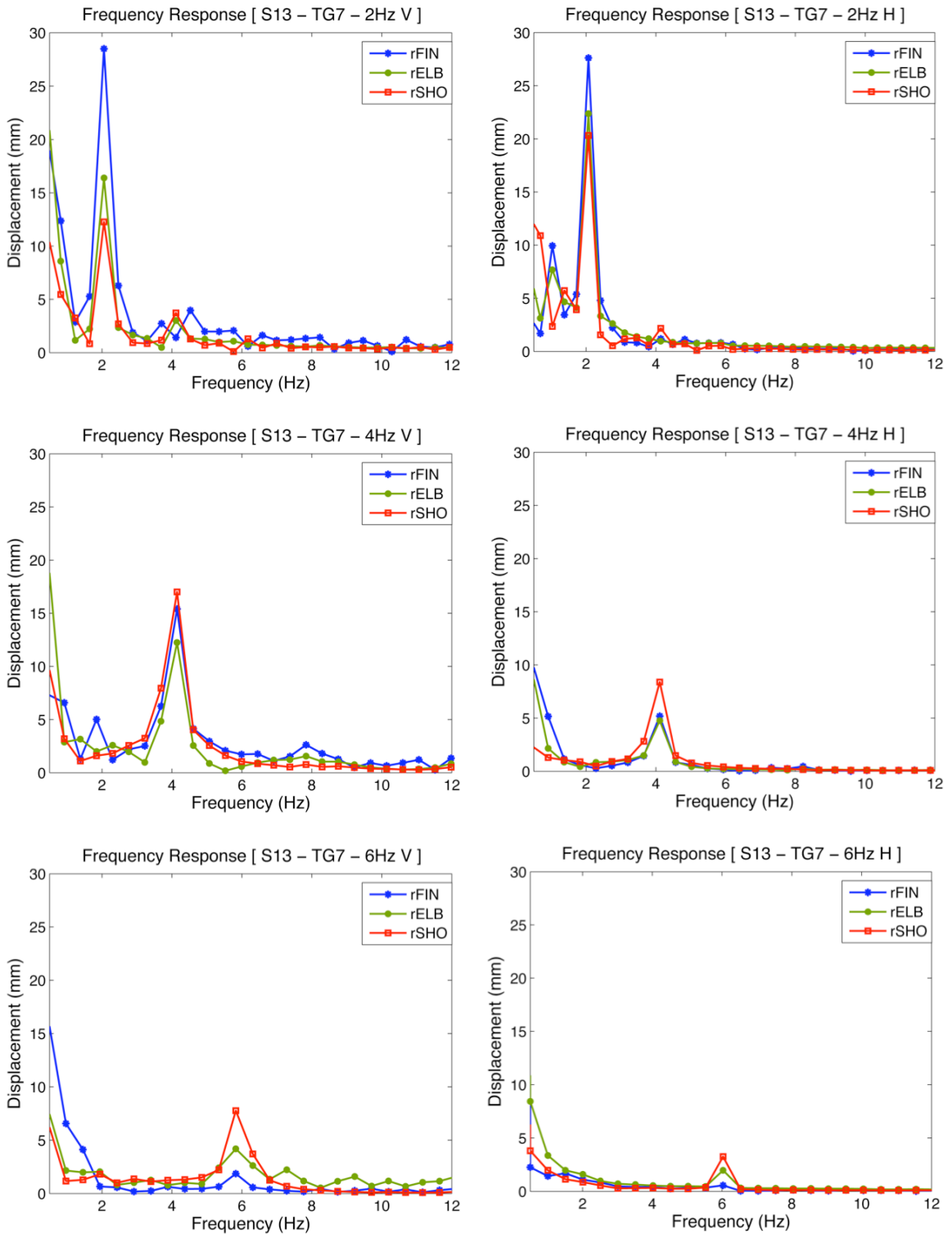
(a) 2Hz WBV exposure (b) 4Hz WBV exposure (c) 6Hz WBV exposure

Figure 3.11: Time responses of upper body joint perturbations under vertical whole-body vibration.



(a) 2Hz WBV exposure (b) 4Hz WBV exposure (c) 6Hz WBV exposure

Figure 3.12: Time responses of upper body joint perturbations under horizontal whole-body vibration.



(a) under vertical WBV exposures (b) under horizontal WBV exposures
Figure 3.13: Frequency responses of upper body joints perturbation under WBV exposures: 2Hz (1st row), 4Hz (2nd row), and 6Hz (3rd row) & vertical direction (left column) and fore-and-aft direction (right column).

3.3.2 Vibration Transmission through the Upper Limb

3.3.2.1 Effects of Vibration Conditions

Vibration transmission through the right arm under vertical and horizontal WBV exposures is illustrated in Figure. 3.14 and 3.15. Note that in this study, vibration transmission specifically means the ratio of peak magnitude in the response to peak magnitude in the input at the forcing frequency.

Vertical Sinusoidal WBV Exposure

Vibration transmission through upper body segments varies with the vibration frequency, as illustrated in Figure 3.14. According to statistical analysis using ANOVA, the influence of vibration frequency for the vertical vibration on the transmission through each body segment is significant for all body segments such as the shoulder ($p \approx 0 \ll 0.01$), the elbow ($p \approx 0 \ll 0.01$), and the finger ($p \approx 0 \ll 0.01$), since p-values for all are extremely small, as indicated in Table 3.5.

Vibration transmission along the upper body path is amplified from the shoulder to the finger along the right arm for all reaches to the five targets - target 1 (upward), 2 (forward & upward), 5 (diagonal & upward), 7 (lateral near), and 8 (lateral far) under the 2Hz vibration condition, whereas it is attenuated for all reaches for the 6Hz frequency vibration. However, under the 4Hz vibration, vibration transmission through the upper body segments shows different characteristics depending on target location. In this vibration condition, transmission through the elbow is lower than through the shoulder and the finger for lateral reaches to target 7 (lateral near) and 8 (lateral far). However, transmission monotonously decreases along the arm path for other reaches to target 1 (upward), 2 (forward & upward), and 5 (diagonal & upward). In addition,

for these targets, the decrease in transmission from the shoulder to the finger is larger at 6 Hz than at 4 Hz.

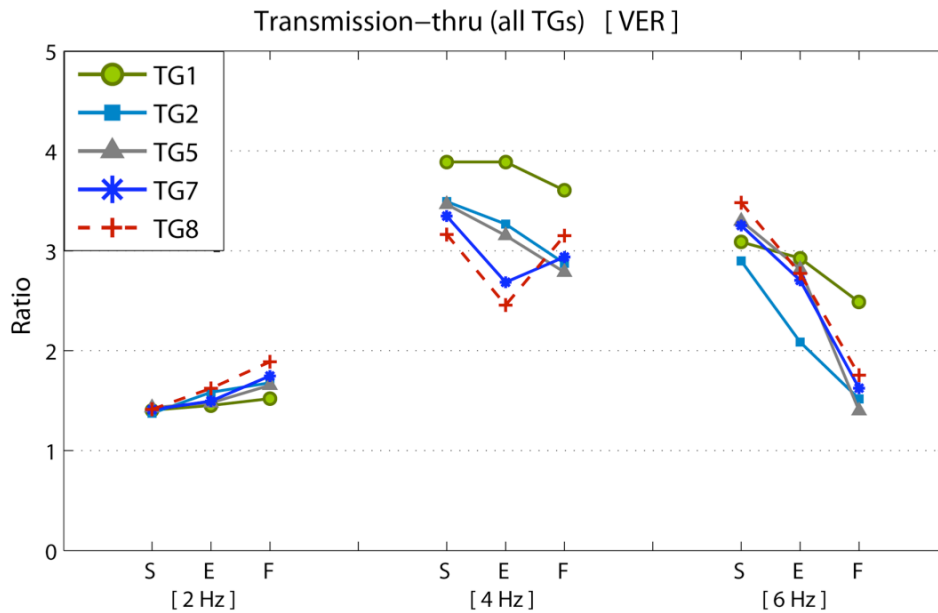


Figure 3.14: Transmission through the body segment at forcing frequency as a function of WBV frequency and direction under vertical WBV exposures: S = shoulder, E = elbow, and F = fingertip

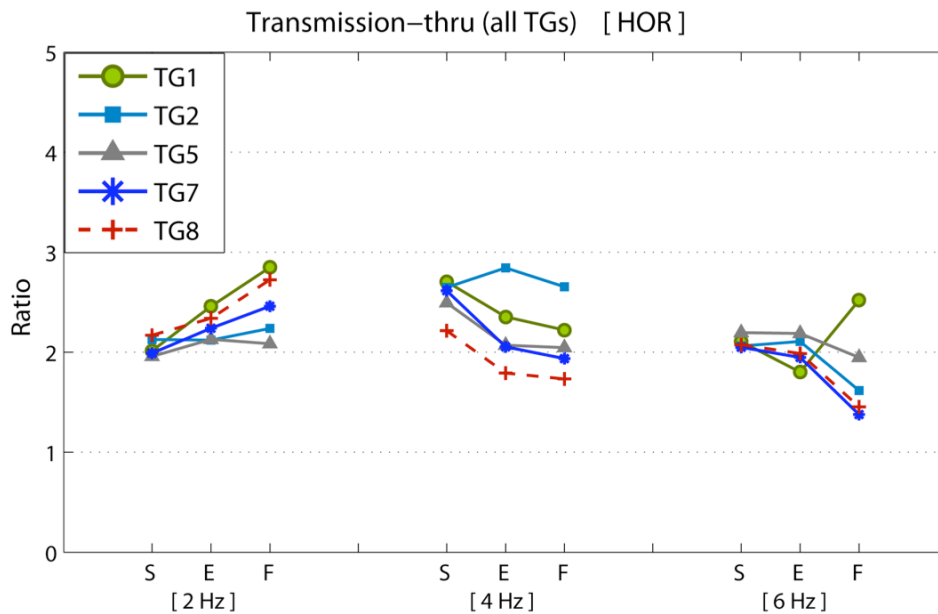


Figure 3.15: Transmission through the body segment at forcing frequency as a function of WBV frequency and direction under horizontal WBV exposures: S = shoulder, E = elbow, and F = fingertip

Horizontal Sinusoidal WBV Exposure

The ANOVA analysis explains that transmissions at all body segments are also influenced by vibration frequency for the horizontal perturbation the same as for the vertical vibration since p-values for the shoulder, elbow, and finger are almost 0, 0.0001, and 5.664e-009 respectively ($p \ll 0.01$ for all body segments), as shown in Table 3.6. Vibration transmission through upper body segments also varies with the frequency of the horizontal vibration, as shown in Figure 3.15. Transmission is amplified along the right arm for all reaches under the 2Hz vibration. Under 4 and 6Hz vibration, transmission decreases along the arm similarly as observed for the vertical vibration conditions except for reaches to target 2 (forward & upward) under 4Hz and to target 1 (upward) under 6Hz vibration.

3.3.2.2 Effects of Target Location

As presented in Figure 3.14 and 3.15, transmission through the upper body segments is as a function of perturbation characteristics such as vibration frequency and direction. In addition, transmission is also affected by target location. However, the individual effect of target location on transmission through body segments cannot be easily interpreted due to a complex interaction between perturbation characteristics and motion direction as shown in Figure 3.16, thus showing a complex interaction between perturbation characteristics and motion direction.

Statistical analysis results from two-way ANOVA for vibration frequency and target location were illustrated in Table 3.5 and 3.6. For the vertical vibration, target location significantly influence transmission for the elbow and the finger ($p = 2.016e-004 < 0.01$ and $2.4e-010 \ll 0.01$, respectively), but it does not significantly affect transmission through the shoulder ($p = 0.3713 > 0.01$). However, in this

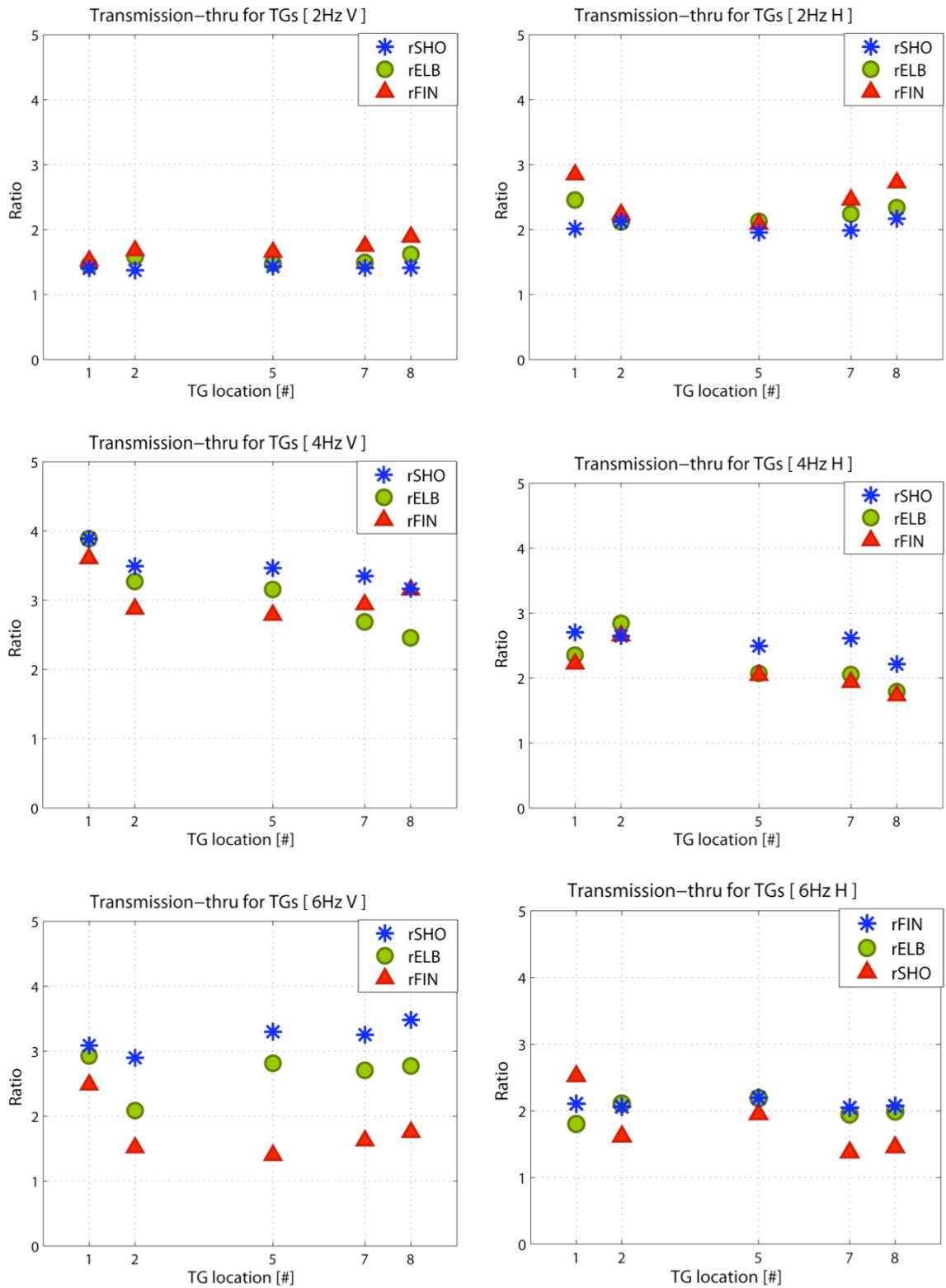


Figure 3.16: Transmission (body segment) as a function of target location: 2Hz (1st row), 4Hz (2nd row), and 6Hz (3rd row) & vertical direction (left column) and fore-and-aft direction (right column).

Table 3.5: Analysis of Variance for vertical WBV transmission (thru-)

	Transmission (rSHO)		
	DoF	F	p
Vibration frequency (VF)	2	337.34	< 0.01
Target location (TG)	4	1.08	0.3713
VF × TG	8	3.28	< 0.01
	Transmission (rELB)		
	DoF	F	P
Vibration frequency (VF)	2	201.18	< 0.01
Target location (TG)	4	7.76	< 0.01
VF × TG	8	9.31	< 0.01
	Transmission (rFIN)		
	DoF	F	p
Vibration frequency (VF)	2	316.88	< 0.01
Target location (TG)	4	17.36	< 0.01
VF × TG	8	7.77	< 0.01

Table 3.6: Analysis of Variance for horizontal WBV transmission (thru-)

	Transmission (rSHO)		
	DoF	F	p
Vibration frequency (VF)	2	17.25	< 0.01
Target location (TG)	4	0.29	0.8865
VF × TG	8	1.06	0.4004
	Transmission (rELB)		
	DoF	F	P
Vibration frequency (VF)	2	9.77	< 0.01
Target location (TG)	4	4.64	< 0.01
VF × TG	8	8.94	< 0.01
	Transmission (rFIN)		
	DoF	F	p
Vibration frequency (VF)	2	23.62	< 0.01
Target location (TG)	4	7.51	< 0.01
VF × TG	8	5.19	< 0.01

environmental condition, interaction between target location and vibration frequency influences transmission through all body segments significantly ($p = 0.0025$, 0 , and $7.072e-008$ for the shoulder, elbow, and finger respectively).

For the horizontal vibration, transmission of the elbow and the fingertip is significantly affected by target location ($p = 0.0001$ and $5.664e-009$) and by strong interaction between target location and vibration frequency ($p = 0$ and $2.411e-005$). However, transmission of the shoulder is not significantly affected by target location ($p = 0.8865 > 0.01$) or by interaction between vibration frequency and target location ($p = 0.4004 > 0.01$). Transmission of the shoulder is affected only by vibration frequency ($p \approx 0$).

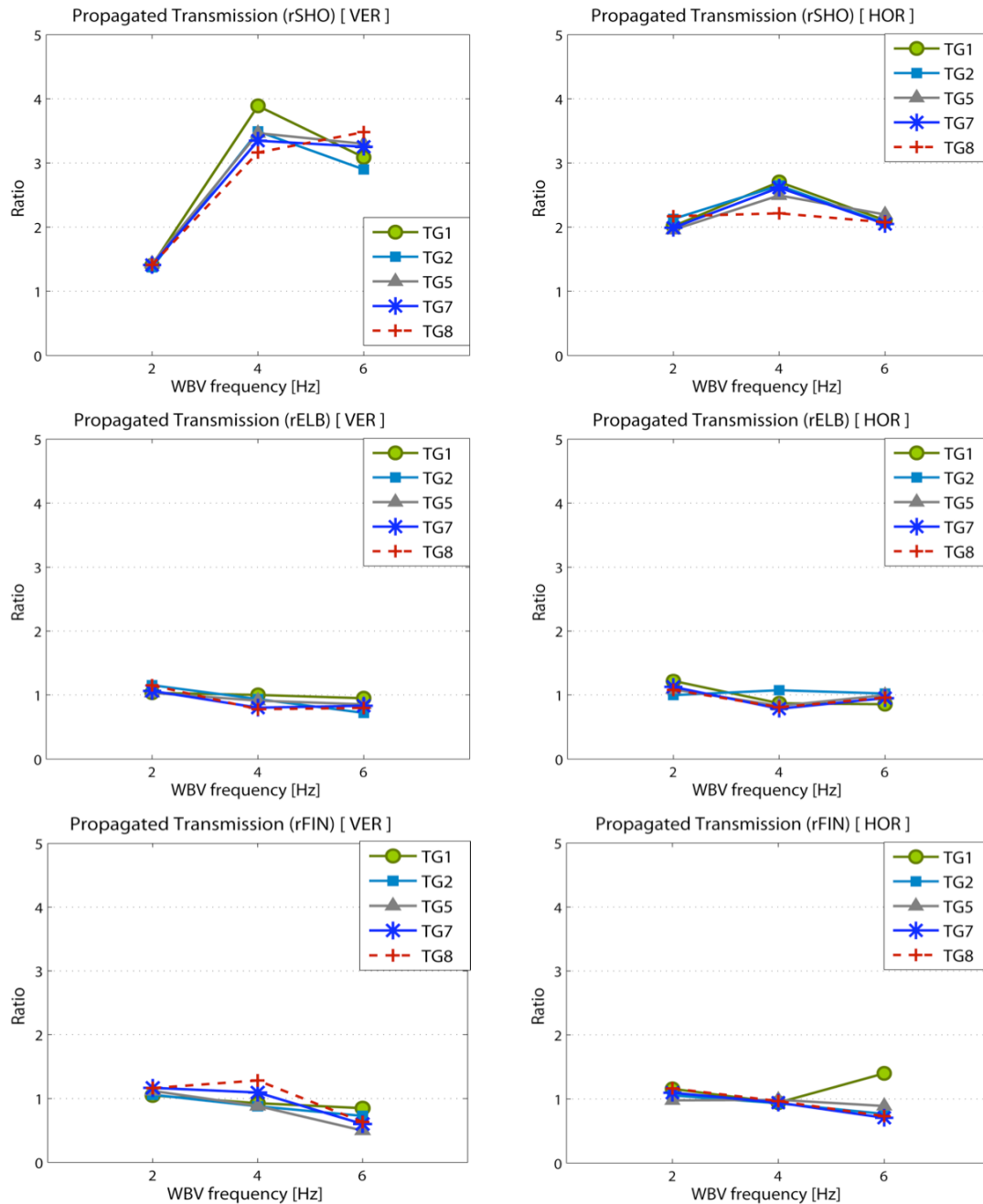
3.3.3 Propagated Transmission through each body segment

(Inter-segment Transmission)

According to two-way ANOVA about the propagated transmission through individual segments (Table 3.7 and 3.8), vibration frequency influences all the propagated transmission through the torso, the upper arm, and the forearm for both the vertical and horizontal perturbation. Target location does not influence vertical and horizontal propagated transmission of the torso ($p = 0.3713 > 0.01$ and $0.8865 > 0.01$) and horizontal propagated transmission through the upper arm ($p = 0.4439$). In addition, interaction between target location and vibration frequency does not affect the horizontal propagated transmission of the torso ($p = 0.4004 > 0.01$).

The propagated transmission of each body segment that is computed from Eq. 3.3 is illustrated in Figure 3.17. Relative propagated transmission through individual segment showed that there is no significant amplification in vibration response through the upper-arm and the forearm for all vibration frequencies, 2, 4, and 6 Hz. However, through the upper torso, input vibration can increase up to three or four times at the shoulder under vertical 4 and 6Hz WBV exposures, and

vibration is amplified twice at the shoulder under all frequencies of horizontal WBV exposures



(a) under vertical WBV exposure (b) under horizontal WBV exposure

Figure 3.17: Propagated transmission through each body segment as a function of WBV frequency and direction: Right Shoulder (1st row), Elbow (2nd row), and Fingertip (3rd row) & Vertical WBV (1st column) and Horizontal WBV (2nd column)

Table 3.7: Analysis of Variance for vertical WBV transmission (inter-)

	Propagated Transmission (rSHO)		
	DoF	F	p
Vibration frequency (VF)	2	337.34	< 0.01
Target location (TG)	4	1.08	0.3713
VF × TG	8	3.28	< 0.01
	Propagated Transmission (rELB)		
	DoF	F	P
Vibration frequency (VF)	2	68.16	< 0.01
Target location (TG)	4	3.89	< 0.01
VF × TG	8	5.83	< 0.01
	Propagated Transmission (rFIN)		
	DoF	F	P
Vibration frequency (VF)	2	137.52	< 0.01
Target location (TG)	4	8.78	< 0.01
VF × TG	8	10.17	< 0.01

Table 3.8: Analysis of Variance for horizontal WBV transmission (inter-)

	Propagated Transmission (rSHO)		
	DoF	F	p
Vibration frequency (VF)	2	17.25	< 0.01
Target location (TG)	4	0.29	0.8865
VF × TG	8	1.06	0.4004
	Propagated Transmission (rELB)		
	DoF	F	p
Vibration frequency (VF)	2	24.9	< 0.01
Target location (TG)	4	0.94	0.4439
VF × TG	8	3.42	< 0.01
	Propagated Transmission (rFIN)		
	DoF	F	p
Vibration frequency (VF)	2	8.43	< 0.01
Target location (TG)	4	6.89	< 0.01
VF × TG	8	4.15	< 0.01

3.4 Discussion

This study investigates biomechanical responses at the right shoulder, elbow, and fingertip to whole-body vibration applied vertically or horizontally when human operators perform reach movements to five targets distributed in the operation space of a vehicle. The results show that peak transmission through upper body segments is a function of vibration characteristics, target location, and their interaction. That is to say, characteristics of whole-body vibration can be affected by environmental conditions and task variables.

Among these variables, the vibration frequency is the dominant factor affecting WBV transmission. Results from statistical analysis with two-way ANOVA also show the dominance of vibration frequency on WBV responses, since p-values of vibration frequency influence are almost zero for all body segments. Regardless of the vibration direction, the trend of an increase or decrease in transmission through the upper limb from the shoulder to the finger is similar for all the 2 Hz, 4 Hz, and 6 Hz vibration.

Nevertheless, the vibration direction also affects transmission. For 4 and 6Hz vibrations, transmission through all body segments is larger for the vertical vibration than for the horizontal vibration. It is assumed that although the magnitude of the stimulation was lower for the horizontal than for the vertical direction, upper torso resonance occurring around 4 to 5 Hz for vertical vibrations while no body resonance is induced by the horizontal vibration (see Griffin, 1990 for review). For the 2Hz vibration, transmission through all body segments under horizontal exposure is higher than under vertical exposure. This phenomenon seems to reflect the motion of the inverse pendulum created by the anchoring of the torso on the seat and free to move above the hip under the horizontal vibration.

Target location also affects the vibration characteristics of body segments, especially for reaches to target 7 (lateral near) and 8 (lateral far) under the 4 Hz vertical vibration. In these situations, inter-segment transmission decreases from the shoulder to the elbow and increases from the elbow to the fingertip. This phenomenon may be caused by an increase of instability in seated balance with full extension of the elbow and abduction of the shoulder in the lateral direction.

In addition, transmission is also affected by strong and complex interaction between vibration condition and target location. Thus, all factors must be considered simultaneously for the design of vehicle interfaces and other application of human vibration analysis.

As stated above, transmission through the body multi-linkage system is function of vibration characteristics, task condition, and interaction between those. Reach movements to different target locations are associated with posture changes which in turn modify biomechanical properties such as inertia, stiffness, and damping of upper body segments, as would be predicted by the equilibrium point hypothesis (Feldman, 1986; Gomi and Kawato, 1997) stating that a posture can be viewed as the result of a mechanical equilibrium.

Information about body segment transmission may be useful to identify biomechanical properties and resonance characteristics of each segment, and may be necessary for developing a biomechanical model of multi-degrees-of-freedom system. These results imply that reach performance and WBV characteristics can be expressed by synthesizing peak transmission of body segments along the path, which represent the core idea of this research.

3.5 Conclusions

In this study, a reach trial was divided into four movement phases, and estimation of the peak value of vibration transmission through body segments was carried out for the pointing phase of a reach trial while the operator maintained the pointing posture for a target without contact between the finger and the target. A strong and complex interaction was found between vibration characteristics and target location.

CHAPTER 4

Vibration-Induced Changes in Upper Limb Reach Kinematics

Simulation of human reach movements is an essential component for proactive ergonomic analysis and computer-aided engineering of biomechanical models. Most studies on reach kinematics described human movements in a static environment, however the models derived from these studies cannot be applied to the analysis of human reach movements in vibratory environments such as in-vehicle operations. Earlier studies on reach performance under vibration exposure focused mainly on fingertip end-point accuracy. This study analyzes three-dimensional joint kinematics of the upper extremity in reach movements performed in static and specific vibratory conditions. Thirteen seated subjects performed reach movements to four target directions distributed in the right hemisphere. The results show differences and similarities in the characteristics of movement patterns of upper body segments for static and dynamic environments. Identification of movement patterns in terms of joint kinematics can be used to determine some biodynamic principles of upper body segment coordination in reach movements.

4.1 Introduction

Reaching to controls is the primary activity of operators in vehicles. To evaluate and predict human movements and postures in a workspace, reaching

movements have been studied from various perspectives with the goals of improving comfort, safety, and manual performance of operators.

Mathematical models of reach movements have been developed using optimization (Flash and Hogan, 1985; Schönér et al, 1986) or statistical methods such as functional regression, Bezier Curve, etc (Faraway, 2000; Faraway and Hu, 2001; Faraway, 2003). Their model reduced the dimensionality of the problem for describing movement kinematics, and succeeded in describing hand trajectory with endpoint constraints. However, all the developed models were limited to simulate only two-dimensional reach in static environments with no obstacle.

Kinematic features of reach movements or postures have been extensively analyzed in the static environment (Soechting and Lacquaniti, 1981; Atkeson and Hollerbach, 1985; Prablanc et al, 1986; Jeannerod and Marteniuk, 1992; Haggard et al., 1995; Jung et al, 1995; Soechting et al, 1995; Gottlieb et al, 1997; Jeannerod et al, 1998; Wang, 1999; Zhang and Chaffin, 2000; Barreca and Guenther, 2001; Faraway, 2003; Admirral et al, 2004; Kim, et al; 2004; Lim et al, 2004; Park et al, 2005). These studies reported that the trajectory in space is independent of movement speed and that the tangential velocity profiles of the arm and hand are bell shaped profiles consisting of feed-forward control phase and feedback control phase for accurate landing. Gottlieb et al (1997) also found that for most movement directions, the dynamic components of the muscle torques at both the elbow and shoulder were related linearly to each other and both were biphasic, almost synchronous and symmetrical pulses. In addition, Soechting et al (1995) and Admirral et al (2004) found that arm posture at a given hand location was dependent on the starting location of the movement. Park et al (2005) suggested a quantitative index termed joint contribution vector to represent a motion in terms of individual joint contribution to the achievement of the task goal. All these studies suggested that

both kinematics and dynamics affected postures and their relative contribution depended on instruction and complexity of the task.

Baaed on the analysis of reach kinematics, reach models have been developed to predict the trajectory of reaching and pointing movements (Hoff and Arbib, 1993; Rosenbaum et al, 1995; Jung et al, 1996; Chaffin et al, 1999; Wang, 1999; Zhang and Chaffin, 2000; Park et al, 2002; Jax et al, 2003; Kang et al, 2005; Park et al, 2006; Park et al, 2008). Some models employed an optimization method based on inverse kinematic structure to minimize the weighted sum of body segment velocity (Jung et al, Wang, Zhang and Chaffin) while others used functional regression fitting polynomial equations to the joint angular kinematics (Kang et al). The optimization-based model developed by Jung et al (1996) indicated that reach posture prediction was more accurate when using a psychophysical cost function of joint discomfort than using a biomechanical cost function of joint torque. Rosenbaum et al (1995) and Jax et al (2003) suggested that postures stored in the motor memory were used to select reaching movements and that costs of possible postures and postural transitions were taken into account in the selection process. Based on this assumption, Park et al (2002) proposed a memory-based model for realistic simulation of human reach motions and extended the model to simulate reaching with obstacle avoidance in two-dimensional task spaces (2006, 2008). However, all these models based on reach kinematics in static conditions cannot be applicable to simulate reach movements in vehicle vibratory environments.

Reach kinematics or performance during vibration exposure has been investigated in terms of upper body coordination or speed-accuracy tradeoff (Rider et al 2003; Park et al, 2004; Rider et al, 2004; Yoon, unpublished). Some studies (Park et al, 2004; Yoon, unpublished) proposed a joint contribution vector to characterize movement coordination and determine changes in coordination as a function of the environmental condition; however, this analytic index may not be

suitable for movement prediction. Other studies reported that ride motion produced an increase in the duration of the adjustment phase near the aimed target and an increase in fingertip excursions during that phase and that the fingertip deviation from a trajectory obtained from a static environment is a function of reach direction and vibration frequency (Rider et al, 2004). These authors also suggested an 'effective target size' for the measure of the accuracy in fingertip reaching/pointing tasks. However, all these studies did not analyze the influence of vibration transmission through the multi-linkage system consisting of the body segments to predict segment movements and their contribution to the movement of the end effector.

For further in-depth understanding of biodynamic responses associated with upper limb reaching movement under exposure to vibration, this study investigates the effects of vibration on reach kinematics and movements patterns of the upper extremity. In the previous chapter, vibration transmission through the upper body segments was estimated as a function of vibration frequency and direction for sinusoidal WBV conditions (Kim and Martin, 2007). In addition, since transmission was affected by target location and interaction between target location and vibration condition, it was anticipated that vibration transmission varies with postures associated with target locations. In order to examine the effects of posture or movement on biodynamic responses to WBV inputs, the kinematic characteristics of upper body segments during the aiming movement phase (transition phase) need to be investigated since upper body movement coordination contributes to posture definition.

The specific aims of this study are to identify the characteristics of upper body movement patterns during the aiming movement phase using a joint kinematic analysis, and to investigate vibration-induced changes in joint kinematics of the arm.

4.2 Method

4.2.1 Experiment Data Selection for Kinematic Analysis

A subset of the data that were collected in the experiment described in the previous chapter was selected for the analysis of reach kinematics.

Subjects

Thirteen right-handed young adults participated in the experiment. They were free from any known musculoskeletal disorders, neuromuscular disorders, chronic back pain, or acute back pain. Their anthropometric dimensions are listed in Table 3.1.

Experimental Setup

The experiment was conducted on the RMS at the U.S Army RDECOM TARDEC to produce the dynamics of a military ground vehicle. A VICON™ motion capture system equipped with six cameras was used to record movements of the upper body segments.

Vibration Condition

Seven vibration conditions were generated by the RMS as illustrated in Table 3.1. However, only the data collected in four environmental conditions including a static condition and the vertical 2, 4, and 6 Hz sinusoidal vibrations were analyzed in this study (Table 4.1).

Table 4.1: Vibration Input Conditions for Reach Kinematic Study

Direction	Vibration Frequency, Magnitude		
No Vibration	-		
Vertical Vibration	2Hz, 0.5G	4Hz, 0.5G	6Hz, 0.5G

Reach Direction

Four target locations were selected as representative directions: upward [TG1], forward [TG2], diagonal [TG5], and lateral [TG8] (Figure 4.1 and Table 4.2). The origin of the coordinate system for target positions was located at the right top of the steering handle, where the right hand rested in the initial posture. All four targets were reached twice in a random order.

To maintain the initial posture constantly prior to any reach, all participants were requested to hold the steering wheel with both hands in a standardized location and to look at the center of a front monitor. During every reaching task, the left hand kept holding the handle for the constant boundary condition of human upper body system, the feet were resting on the cab floor, and the seat belt was fastened tightly enough to prevent a relative slip motion between the seat and the hip. Each reach task was performed at a self-determined speed.

Motion Capture

Twenty-six retro-reflective markers were placed on body landmarks (Figure 4.3). Reach movements of the upper body segments were sampled at 100Hz by an optical motion track system (VICON™). For anthropometric measures and subject model calibration, a T-pose and the range of motion were also captured at 100Hz for each subject.

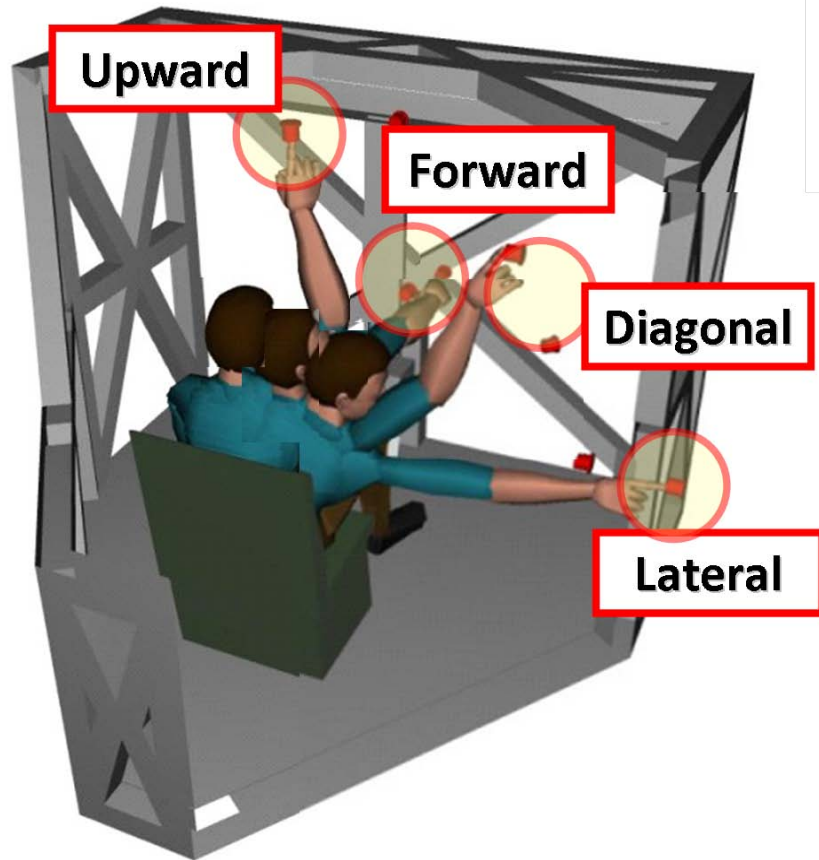


Figure 4.1: RMS cab and target directions: Four targets are distributed in the right hemisphere of the seated operator: Upward (TG1), Forward (TG2), Diagonal (TG5), and Lateral (TG 8).

Table 4.2: Reach task (reach direction)

The origin of the coordinate system is at the right top of a steering handle.

No.	Reach Direction	Target	Location (x, y, z) [mm]
1	Upward	TG 1	(143, -357, 678)
2	Forward	TG 2	(132, 133, 269)
3	Diagonal	TG 5	(564, -274, 420)
4	Lateral	TG 8	(870, -295, -114)

4.2.2 Movement Phase Analysis

Figure 4.2 shows that reach movements to a target consist of four movement phases: (1) the initial phase corresponding to a resting posture at the home position, (2) the aiming transition phase showing the dynamic change in joint kinematics of upper extremity, (3) the pointing phase in which the participant is required to maintain the posture for a few seconds without contact with the target, and (4) the returning phase. This study analyzes the right arm-hand movements during the aiming phase, which was defined by the time interval starting with the head rotation to identify the location of a target and ending when the right hand arrives at the steady-state position near the target location.

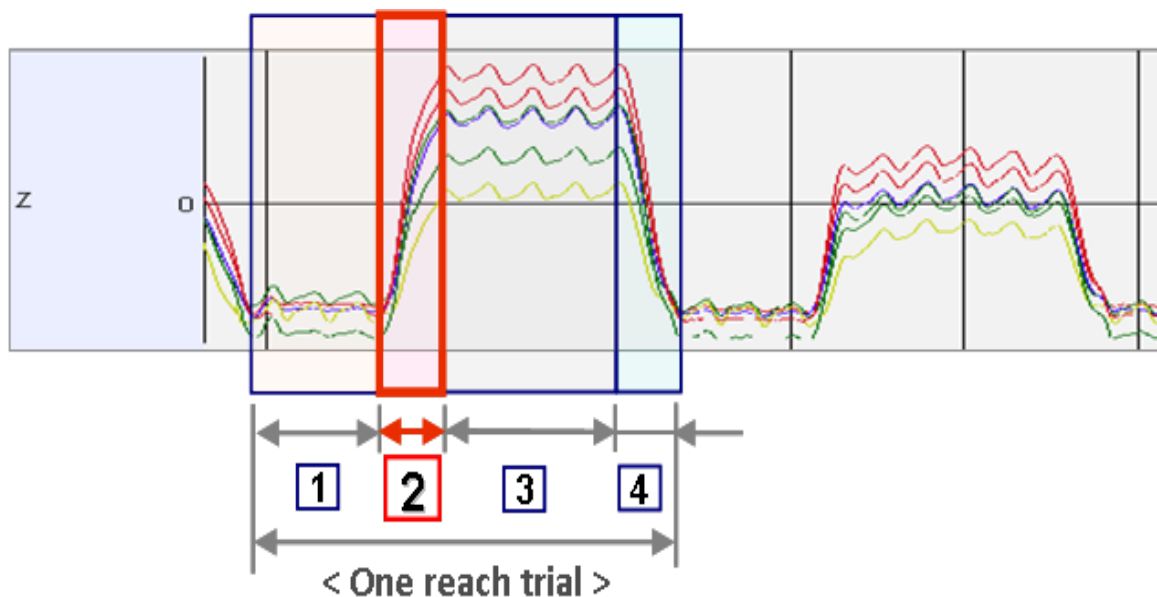


Figure 4.2: Movement phases in a reach trial: One reach consists of four movement phase: (1) resting phase, (2) aiming transition phase, (3) pointing phase, and (4) returning phase.

4.2.3 Joint Kinematic Analysis

Seated reach movements can be described by movement coordination of the torso, right upper-arm, right lower-arm, and right hand. The present analysis focused specifically on the kinematics of upper body joints such as the right shoulder, elbow, and wrist joints (Figure 4.3). It was assumed that hip movements and the relative motion at the hip–seat interface were negligible. Variations of these joint angles in the time domain were analyzed to describe the movement patterns for each target directions. Since all subjects performed self-paced reaches, a normalized time was used for the kinematic analysis. Joint angular kinematics such as joint angle (θ_j), angular velocity ($\dot{\theta}_j$), and acceleration ($\ddot{\theta}_j$) were computed using a vector analysis with the definition of a body segment as a vector, based on the assumption that the upper limb is a rigid and linear linkage system (Eq. 4.1). Shoulder rotation about the vertical axis, elbow flexion/extension, and wrist flexion/extension were considered (Figure 4.3).

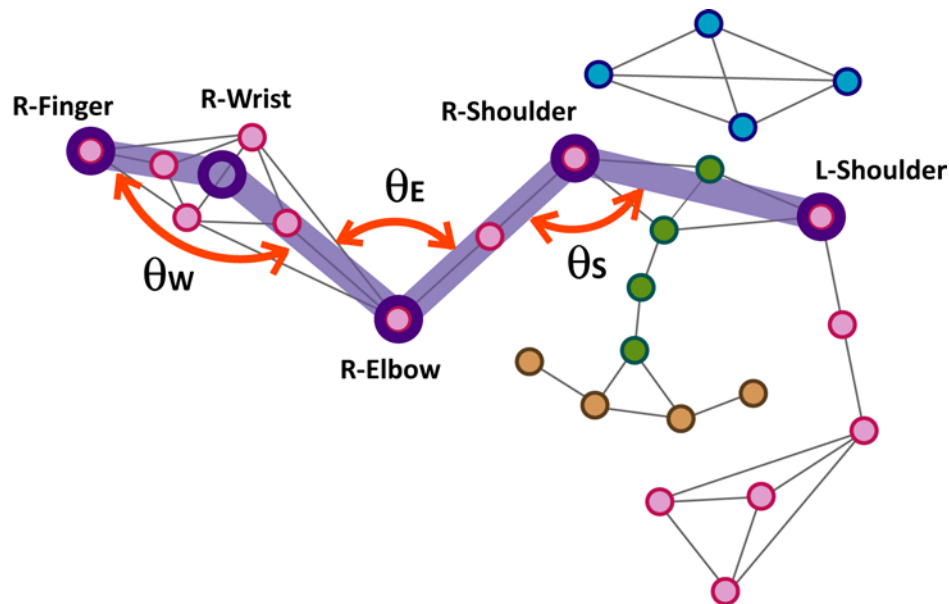
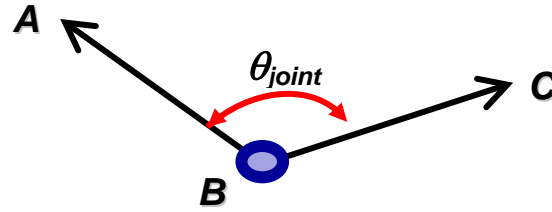


Figure 4.3: Joint angles of the upper body segments for kinematic analysis: Three joint angles were used in the analysis: right shoulder (θ_s), right elbow (θ_E), and right wrist (θ_w) angles.



$$\theta_j = \cos^{-1} \left(\frac{\overline{BA} \cdot \overline{BC}}{\|\overline{BA}\| \times \|\overline{BC}\|} \right) \dots\dots\dots \text{(Eq. 4.1)}$$

$$\dot{\theta}_j = \frac{d\theta_j}{dt} \quad , \quad \ddot{\theta}_j = \frac{d\dot{\theta}_j}{dt}$$

4.3 Results

4.3.1 Reach Trajectory and Kinematics in the Static Environment

4.3.1.1 Joint Trajectory and Linear Velocity

Typical examples of three-dimensional joint trajectories of the left shoulder, and the right shoulder, the right elbow, the right index finger-tip, and the head are illustrated in Figure 4.4, 4.5, 4.6 and 4.7, for upward, forward, diagonal, and lateral reaches, respectively. For each reach, the representation includes six instantaneous postures, which are sampled at one-sixth of normalized time.

As shown in these figures, the hand movement is activated for the forward reach at the second frame, while the hand movements are not activated yet for the upward, diagonal, and lateral reaches.

For every reach, a head rotation occurs prior to a hand movement in order to identify the location of a target before initiating the hand movement. The head orientation is then maintained in the direction of the target without seeing the arm or hand movement. As for movement time, the right hand almost arrives at

destination within the fifth frame, which suggested that the fine adjustment of the hand position takes one-sixth of the aiming transition time after the arm transition is usually achieved for four-sixth to five-sixth of normalized time for the aiming

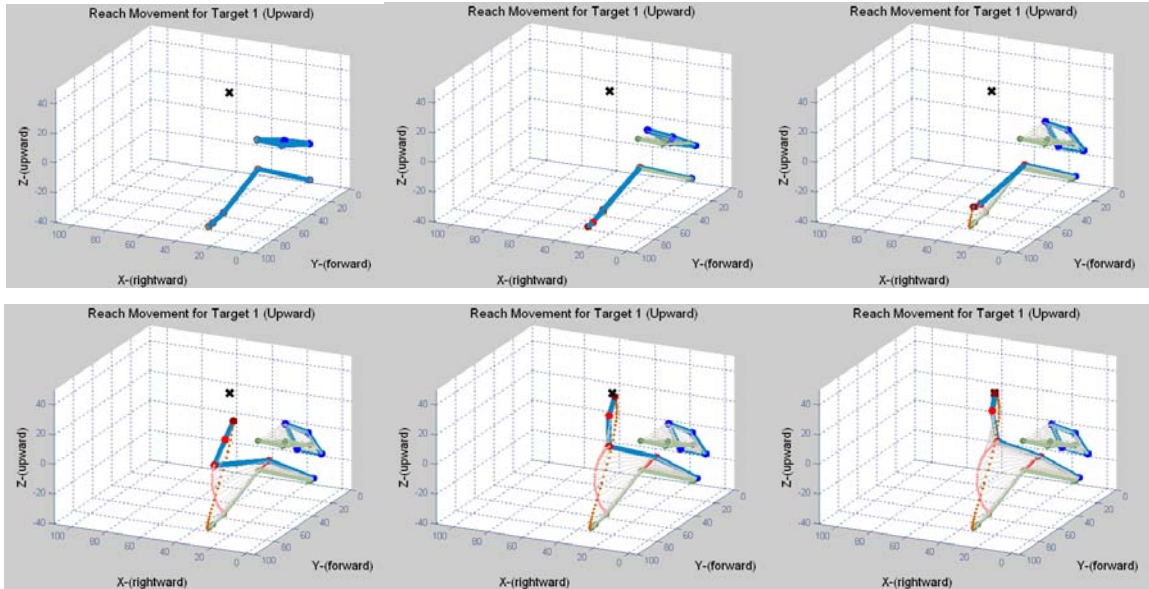


Figure 4.4: Three-dimensional joint trajectories of the upper right extremity and head motion for upward reach in a static environment.

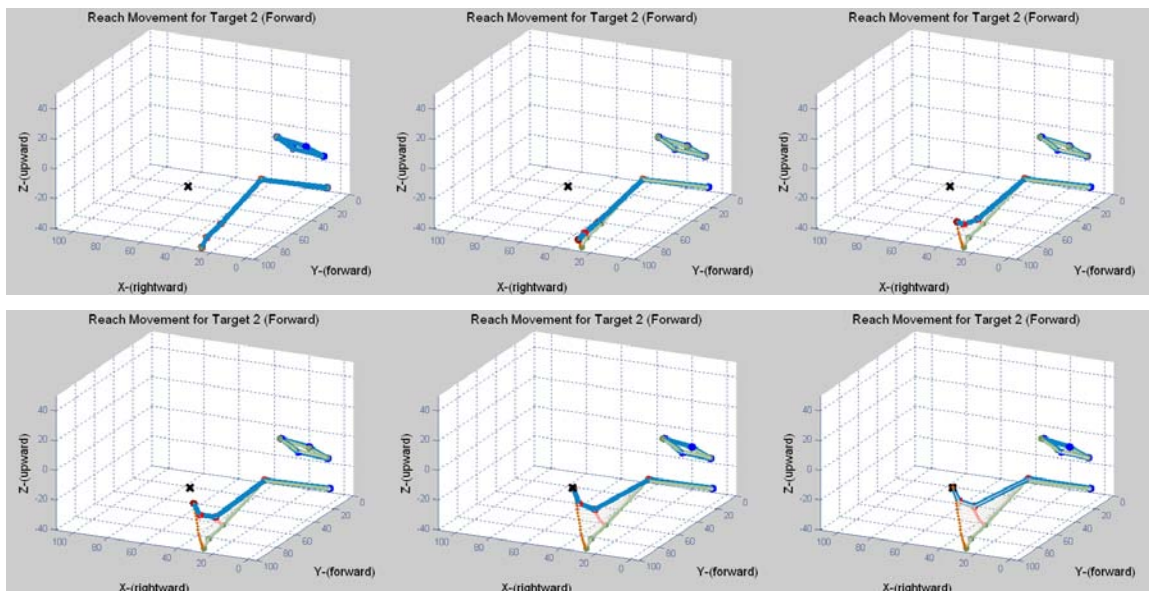


Figure 4.5: Three-dimensional joint trajectories of the upper right extremity and head motion for forward reach in a static environment.

movement phase. In addition, the fingertip trajectory shows relatively longer and straighter line from the home position than the elbow trajectory.

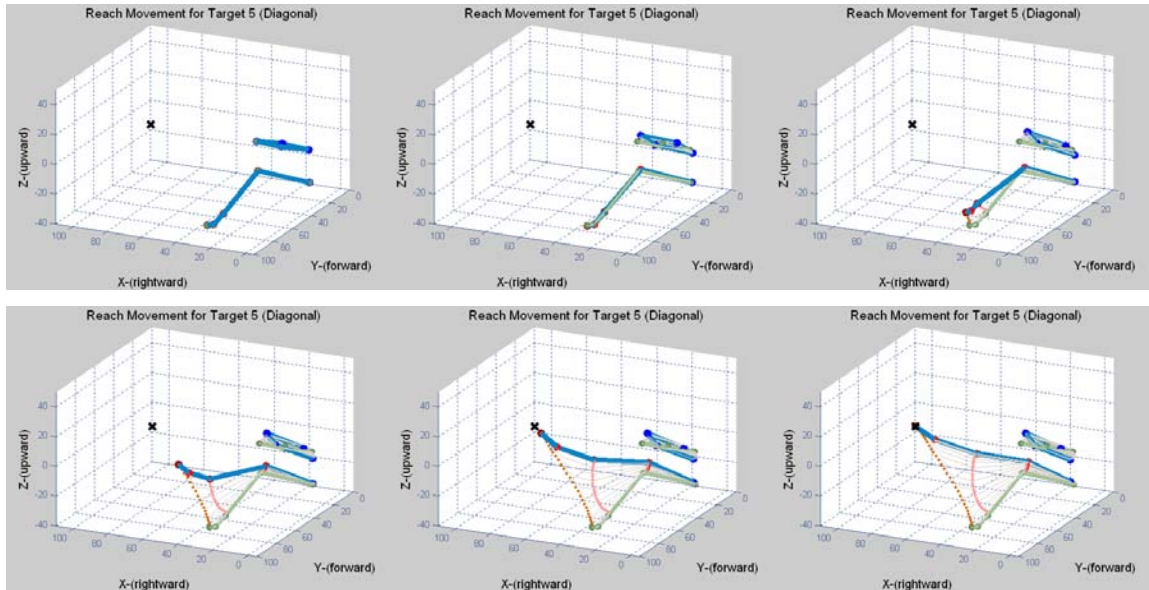


Figure 4.6: Three-dimensional joint trajectories of the upper right extremity and head motion for diagonal reach in a static environment.

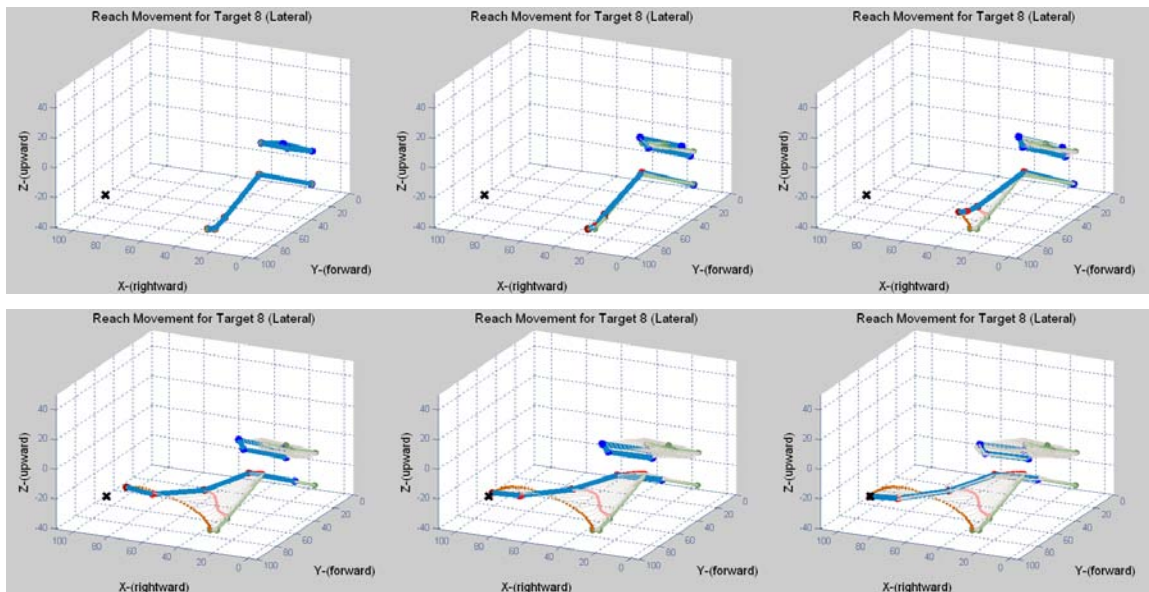


Figure 4.7: Three-dimensional joint trajectories of the upper right extremity and head motion for lateral reach in a static environment.

Figure 4.8a, 4.9a, 4.10a, and 4.11a illustrate joint trajectories of all upper body joints for the four directional reach movements in the static environment. All joint trajectories vary with target location or direction. However, regardless of these variations, all joint trajectories show smooth profiles along the three axes of the Cartesian coordinate system of reference, as illustrated in the respective figures.

Figure 4.8b, 4.9b, 4.10b, and 4.11b show the linear velocities in x-, y-, and z- directions and velocities in tangent to the trajectories path of all upper body joints for all four reaches in the static environment. All joint tangential velocities present bell-shaped profiles, as stated in the relevant literature (Morrasso, 1981; Soetiching and Lacquaniti, 1981; Atkeson and Hollerbach, 1985; Haggard et al., 1995; Jung et al, 1995; Wang, 1999; Faraway, 2003; Rider et al, 2003; Lim et al, 2004). However, the maximum velocities of the respective joints do not occur simultaneously.

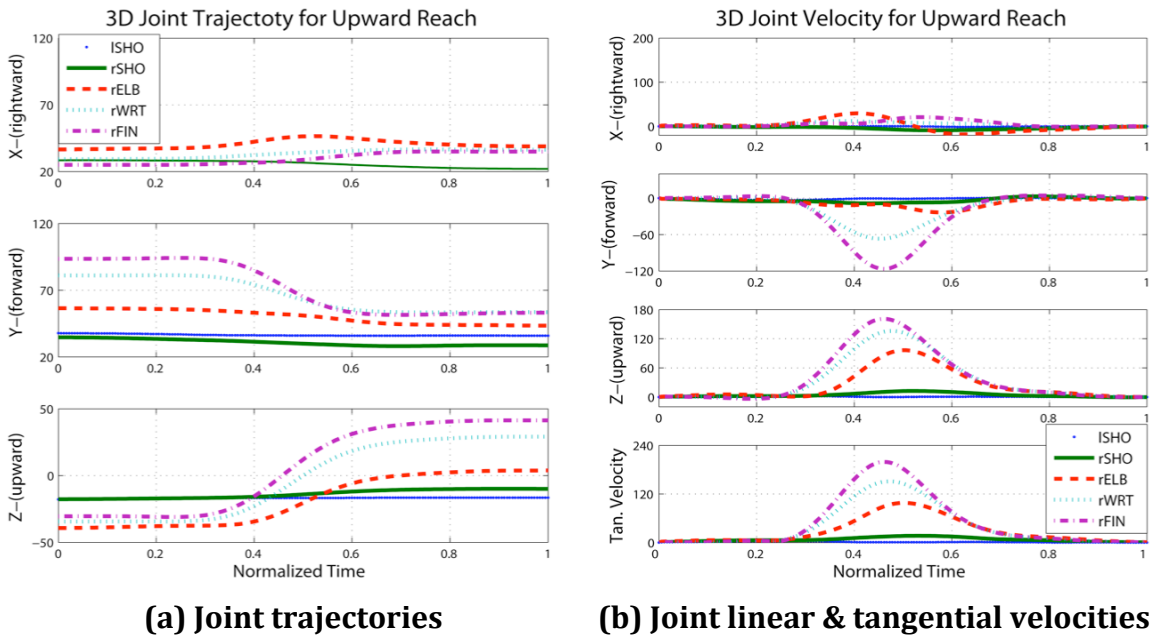
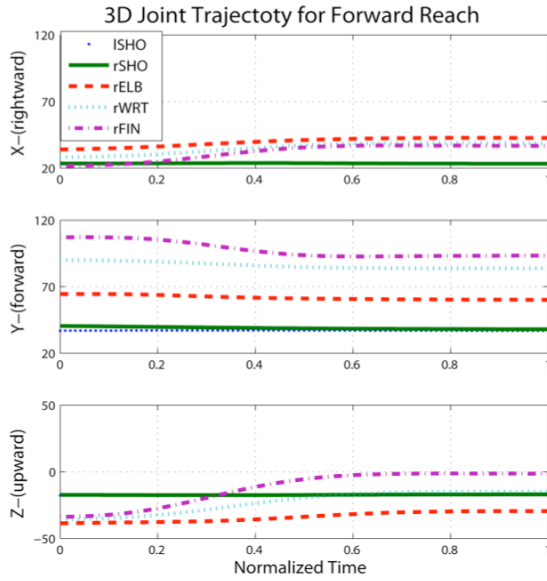
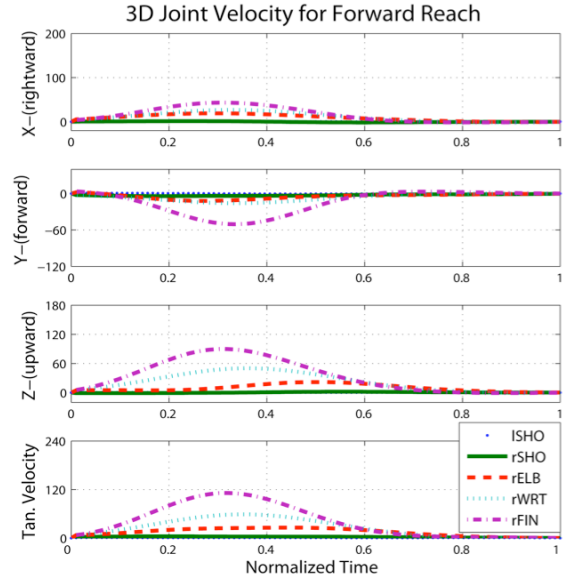


Figure 4.8: Joint trajectories and linear/tangential velocities of upper body joints for upward reach movement in a static environment: ISHO (left shoulder joint), rSHO (right shoulder joint), rELB (right elbow joint), rWRT (right wrist joint), and rFIN (right index fingertip).

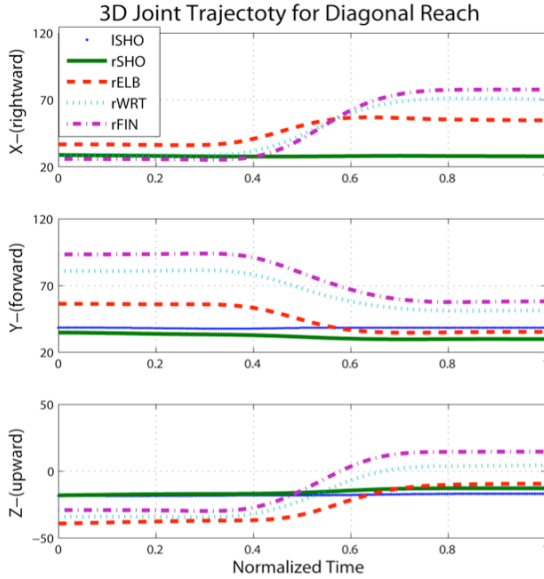


(a) Joint trajectories

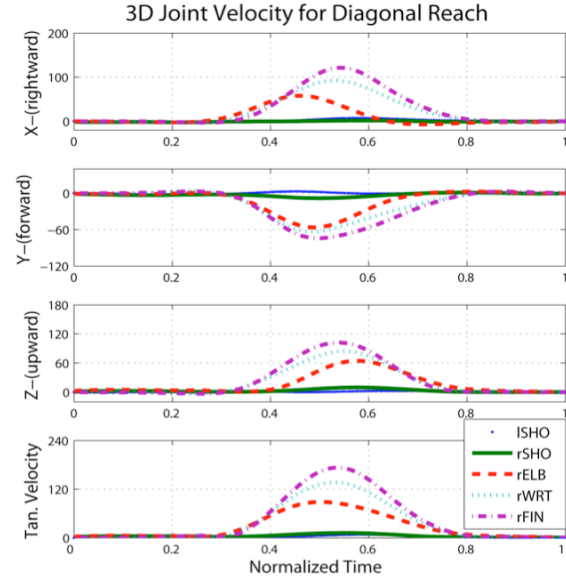


(b) Joint linear & tangential velocities

Figure 4.9: Joint trajectories and linear/tangential velocities of upper body joints for forward reach movement in a static environment: ISHO (left shoulder joint), rSHO (right shoulder joint), rELB (right elbow joint), rWRT (right wrist joint), and rFIN (right index fingertip).

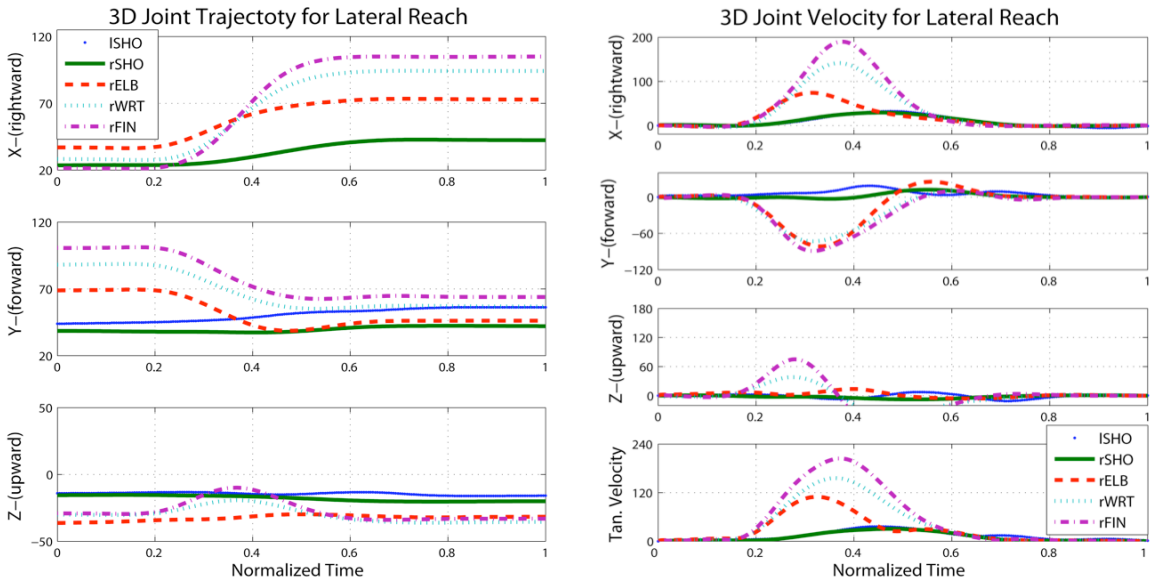


(a) Joint trajectories



(b) Joint linear & tangential velocities

Figure 4.10: Joint trajectories and linear/tangential velocities of upper body joints for diagonal reach movement in a static environment: ISHO (left shoulder joint), rSHO (right shoulder joint), rELB (right elbow joint), rWRT (right wrist joint), and rFIN (right index fingertip).



(a) Joint trajectories

(b) Joint linear & tangential velocities

Figure 4.11: Joint trajectories and linear/tangential velocities of upper body joints for lateral reach movement in a static environment: ISHO (left shoulder joint), rSHO (right shoulder joint), rELB (right elbow joint), rWRT (right wrist joint), and rFIN (right index fingertip).

4.3.1.2 Joint Angular Kinematics

The Joint angular kinematic analysis shows that all joint angular movements were influenced by the direction of reach (Figure 4.12 and 4.13). However, regardless of this influence, all directional reaches show a qualitative similarity in joint angular movement patterns. The angular velocity profile of the elbow joint is bi-phasic, while the angular velocity of the shoulder joint presents a mono-phasic profile. In addition, the elbow joint moved with higher peak velocity and acceleration than the shoulder joint, for all directional reaches (3rd row in Figure 4.12 and 4.13, and Table 4.3). The wrist joint movement shows large variation in the shape and order of its angular kinematic profile. This variation does not present any consistent pattern between subjects or target directions, which suggests a loose control of wrist movements in the present context.

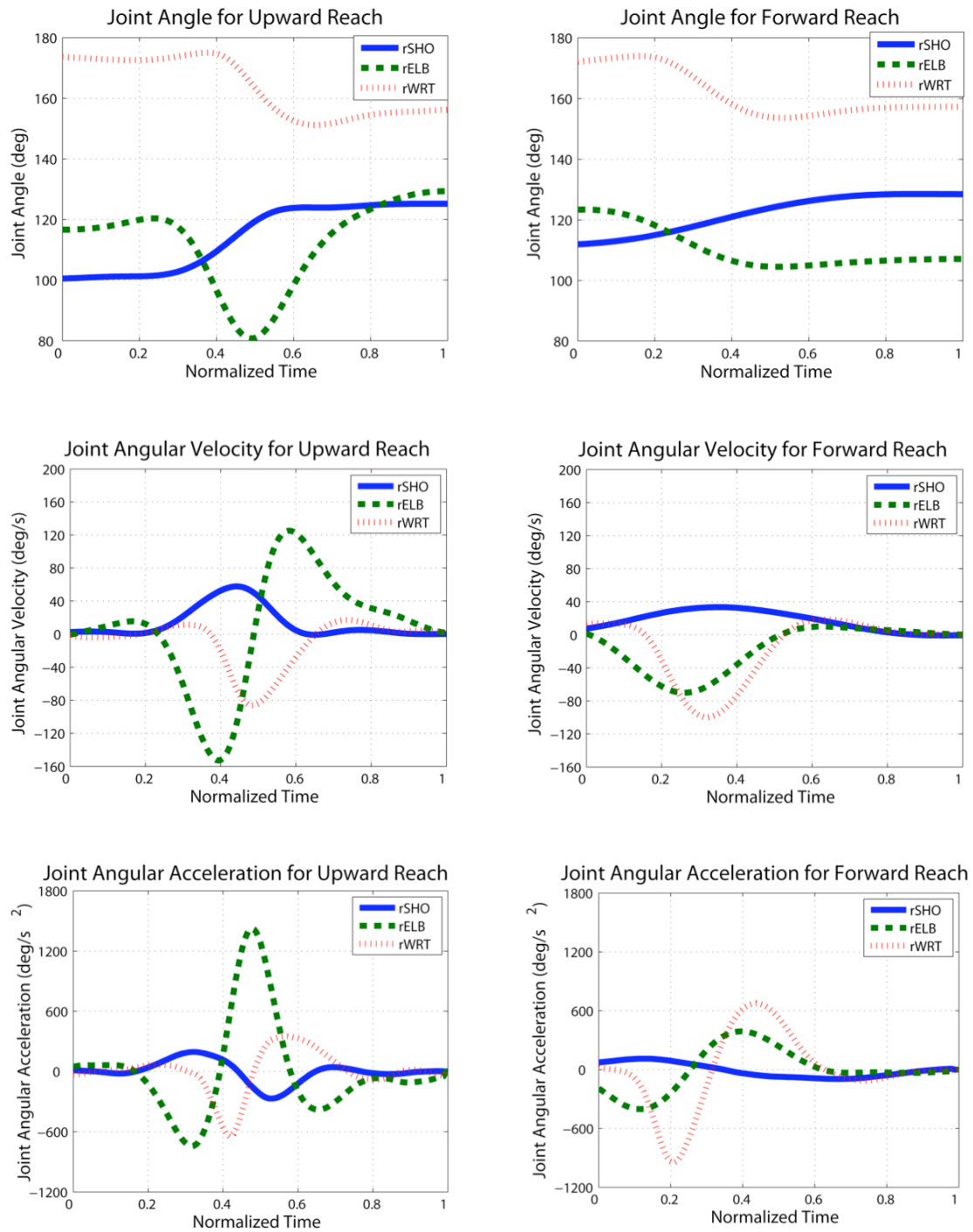


Figure 4.12: Joint angular kinematics in the static environment: Angle (1st row), Angular velocity (2nd row), and Angular acceleration (3rd row) & Upward reach (left column) and Forward reach (right column): rSHO (right shoulder joint), rELB (right elbow joint), and rWRT (right wrist joint)

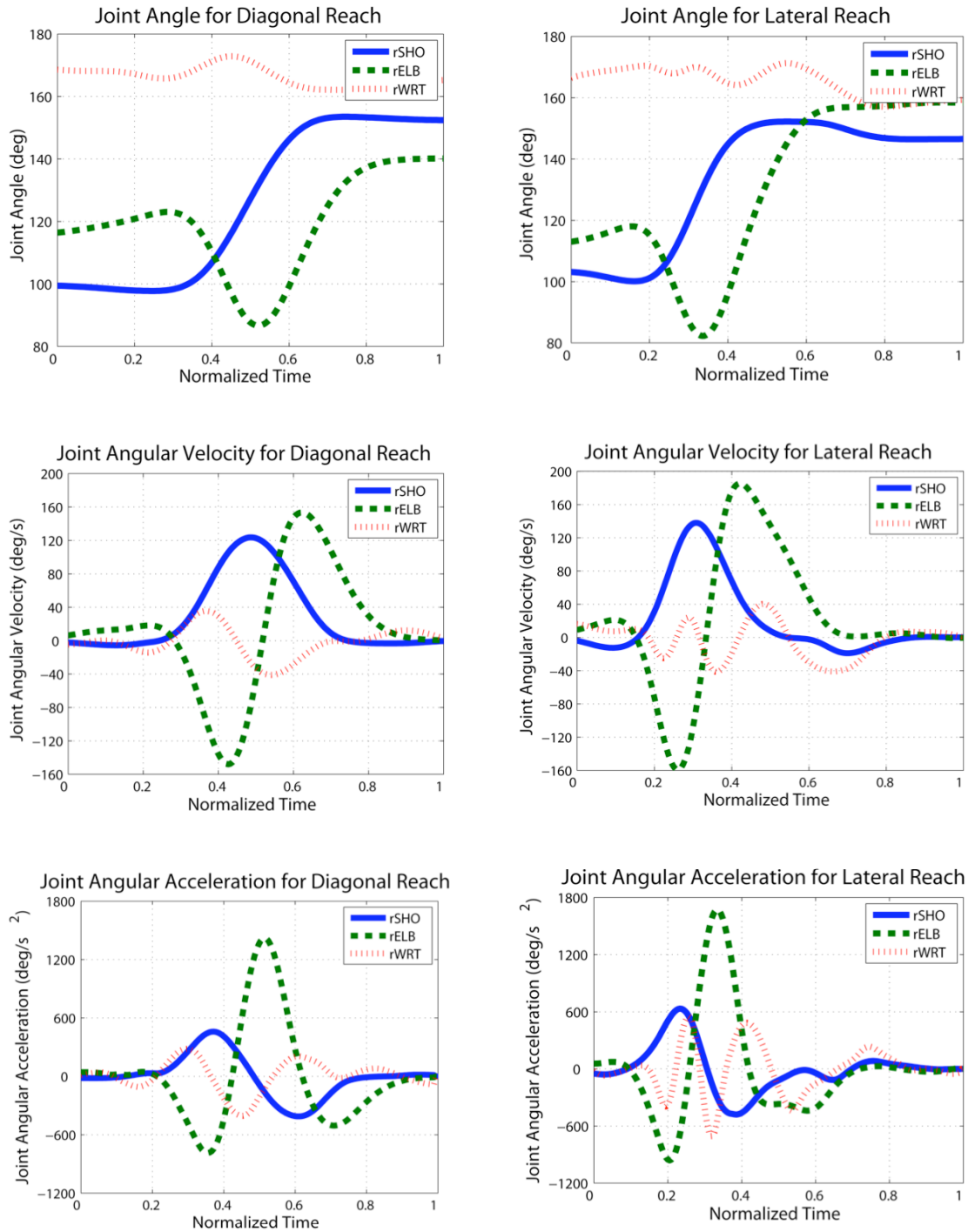


Figure 4.13: Joint angular kinematics in the static environment: Angle (1st row), Angular velocity (2nd row), and Angular acceleration (3rd row) & Diagonal reach (left column) and Lateral reach (right column): rSHO (right shoulder joint), rELB (right elbow joint), and rWRT (right wrist joint)

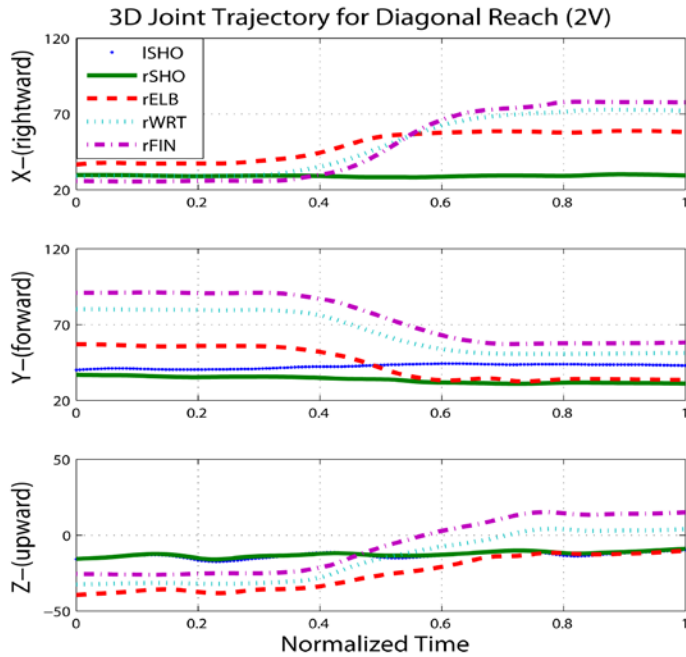
4.3.2 Reach Trajectory and Kinematics under Vibration Condition

This section illustrates the features of vibration-induced kinematics only for a diagonal reach movement, since reach kinematics are more influenced by vibration characteristics than by reach direction and vibration-induced reach kinematics are qualitatively similar for all directional reaches.

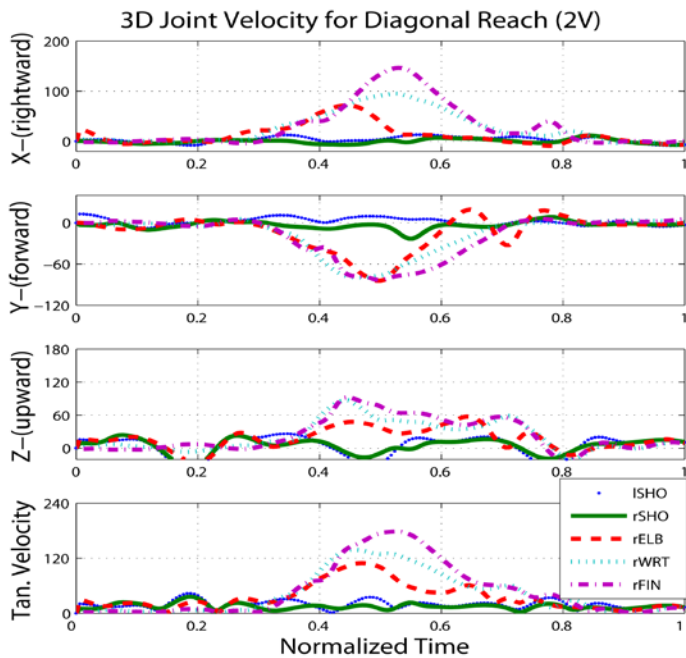
4.3.2.1 Vibration-Induced Joint Trajectory and Linear Velocity

Joint trajectories and linear kinematics of reach movements under vertical whole-body vibration are shown in Figure 4.14, 4.15, and 4.16. Both trajectories and linear/tangential velocities are affected by the vertical vibration inputs. However, these vibration influences are easier observed in the joint velocity profiles than in the joint trajectories.

One-dimensional vertical vibration induced alterations of the joint kinematics in the other orthogonal directions (x- and y-axes) as well as in the same direction (z-axis), although the vertical vibration predominantly affects on the z-components of joint kinematics for all vibration frequency inputs (Figure 4.14b, 4.15b, and 4.16b). Especially under 4 and 6 Hz vibration exposure, periodic alterations that are induced by vibration are more prominent for the right shoulder joint than for the elbow and the finger.

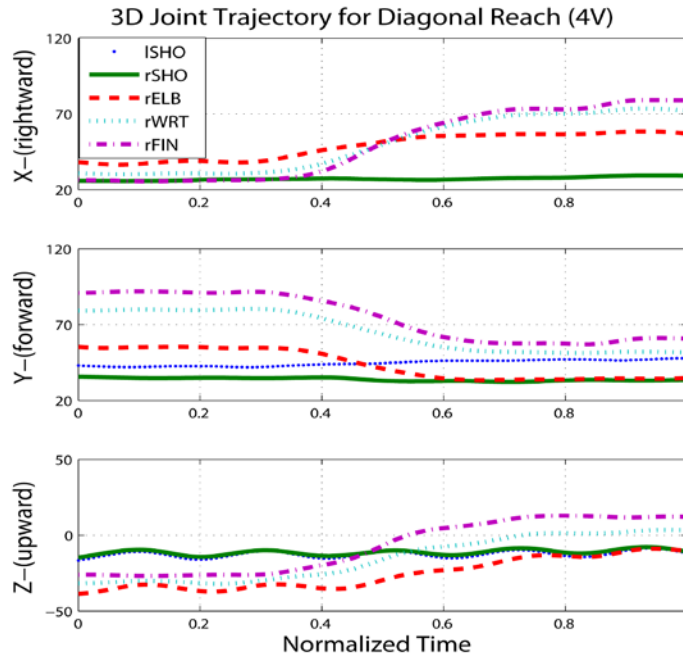


(a) Joint trajectory

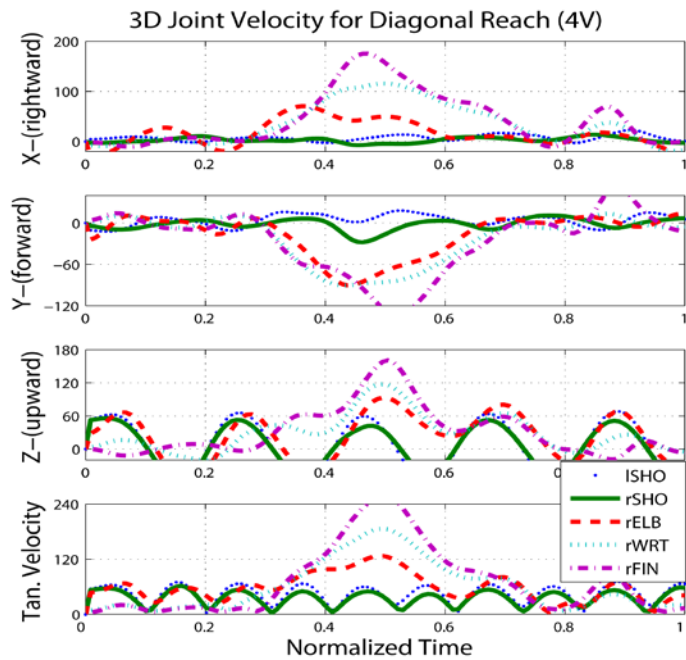


(b) Joint linear and tangential velocities

Figure 4.14: Example of joint trajectory and linear/tangential velocity of the upper extremity for the diagonal reach under the 2 Hz whole-body vibration: ISHO (left shoulder joint), rSHO (right shoulder joint), rELB (right elbow joint), rWRT (right wrist joint), and rFIN (right index fingertip).

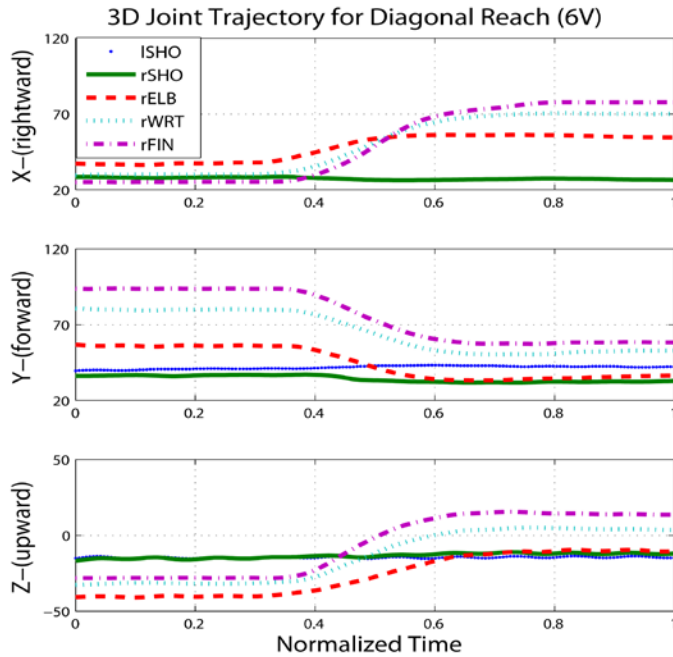


(a) Joint trajectory

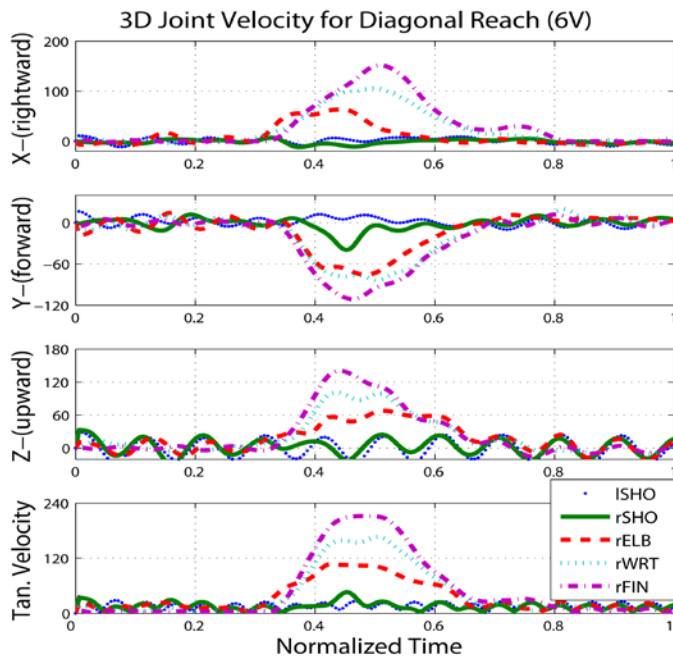


(b) Joint linear and tangential velocities

Figure 4.15: Example of joint trajectory and linear/tangential velocity of the upper extremity for the diagonal reach under the 4 Hz whole-body vibration: ISHO (left shoulder joint), rSHO (right shoulder joint), rELB (right elbow joint), rWRT (right wrist joint), and rFIN (right index fingertip).



(a) Joint trajectory



(b) Joint linear and tangential velocities

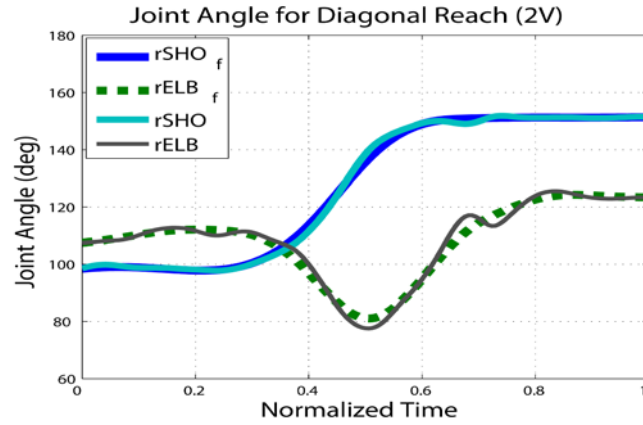
Figure 4.16: Example of joint trajectory and linear/tangential velocity of the upper extremity for the diagonal reach under the 6 Hz whole-body vibration: ISHO (left shoulder joint), rSHO (right shoulder joint), rELB (right elbow joint), rWRT (right wrist joint), and rFIN (right index fingertip).

4.3.2.2 Vibration-Induced Alteration in Joint Angular Kinematics

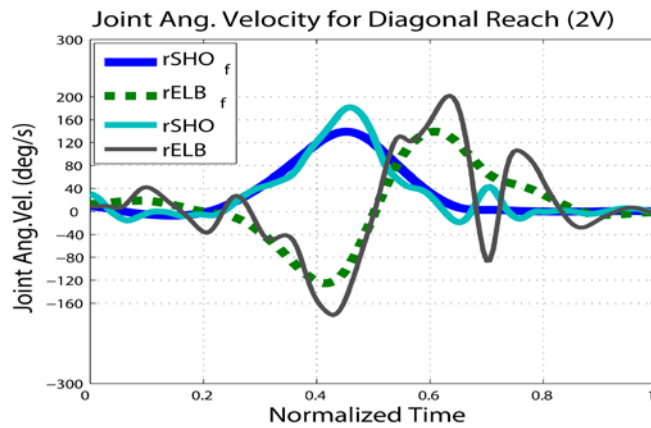
Vibration exposure alters angular kinematics of the arm joints as shown in Figure 4.17, 4.18, and 4.19. Figure 4.17 presents the angular kinematics of the right shoulder and elbow under 2Hz vertical whole-body vibration exposure, while Figure 4.18 and 4.19 illustrate the joint angular kinematics under the 4 Hz and 6 Hz vibration exposure respectively. Since inter-subject variation in angular kinematics is quite large for the wrist joint, this study focuses on angular kinematics of the shoulder and the elbow joints, which show consistent patterns for all directional reaches.

Whole-body vibrations increase the difficulty in controlling upper body movement as indicated by the superimposed oscillation (see Figure 4.7, 4.8 and 4.9). The joint angular kinematics of the right shoulder and elbow joints presents the vibration-induced periodic oscillations, which contribute to an increase in the peak values of joint angular kinematics (Table 4.3).

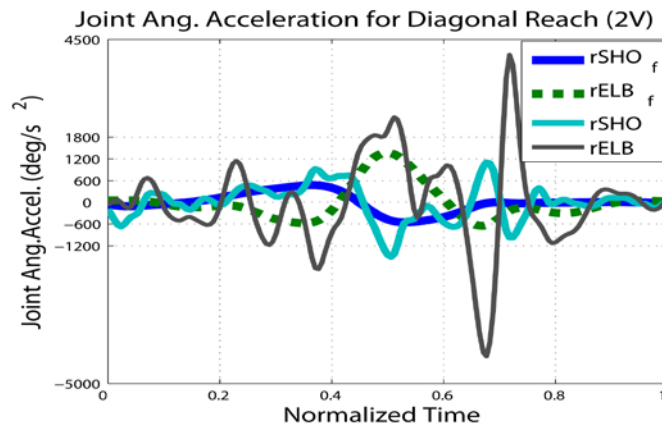
To examine how movement patterns of joint angular kinematics are affected by vibration, all joint angular kinematics were filtered by a low pass filter with a cut-off frequency of 7Hz (see Figure 4.17, 4.18, and 4.19). Table 4.3 describes the maximum values in angular kinematics of upper body joints with variation of vibration condition. Filtered angular kinematics shows qualitatively quite similar movement patterns and maximum value of angular kinematics for the static and vibratory conditions. The filtered kinematics of the elbow joint shows the bi-phasic angular velocity profile. The peak velocity and acceleration are higher for the elbow than for the shoulder joint under all vibration frequency exposure as well as in a static condition (Table 4.3).



(a) Joint angle

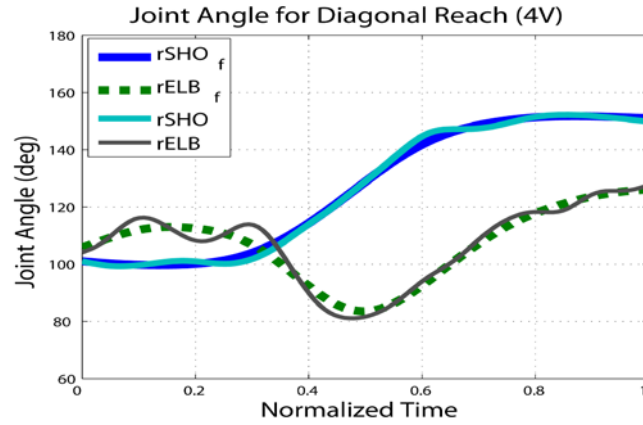


(b) Joint angular velocity

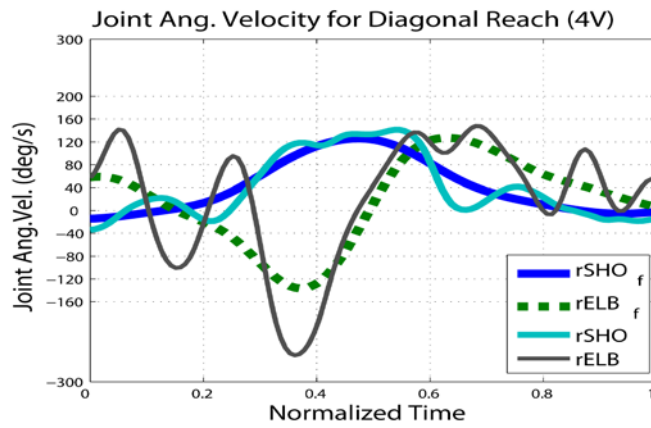


(c) Joint angular acceleration

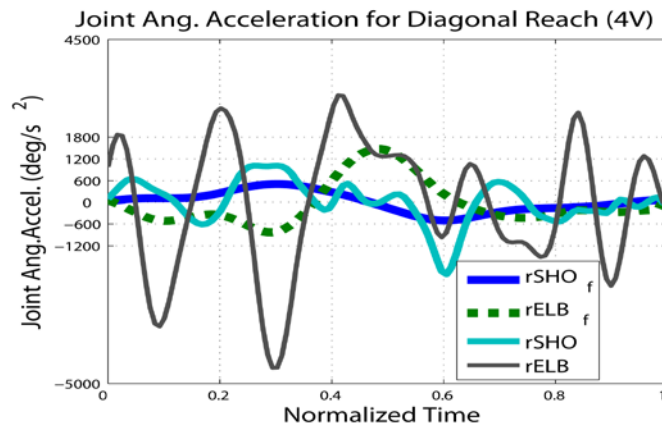
Figure 4.17: Example of shoulder and elbow joint angular kinematics for the diagonal reach under the 2 Hz whole-body vibration. Subscript f indicates filtered data



(a) Joint angle

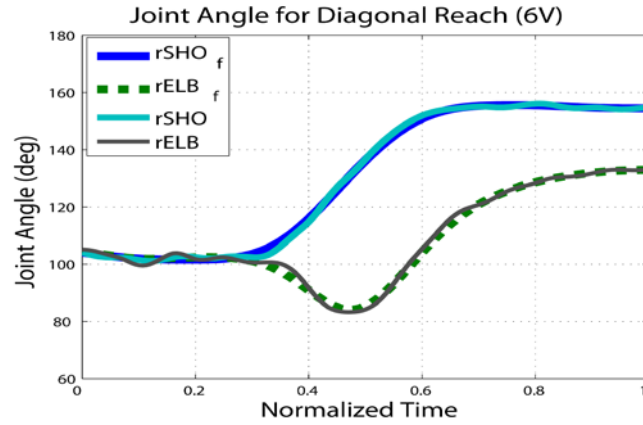


(b) Joint angular velocity

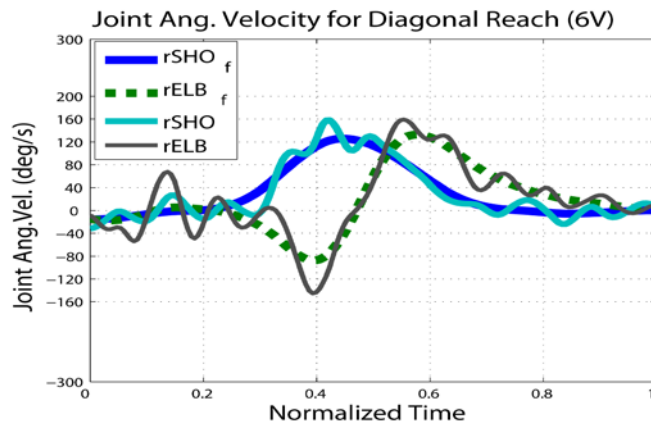


(c) Joint angular acceleration

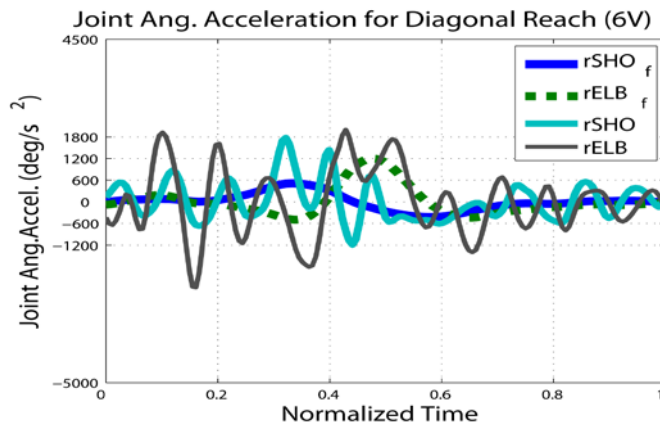
Figure 4.18: Example of shoulder and elbow joint angular kinematics for the diagonal reach under the 4 Hz whole-body vibration. Subscript f indicates filtered data



(a) Joint angle



(b) Joint angular velocity



(c) Joint angular acceleration

Figure 4.19: Example of shoulder and elbow joint angular kinematics for the diagonal reach under the 6 Hz whole-body vibration. Subscript f indicates filtered data

Table 4.3: Joint angular kinematics peak values of upper body joints in static and vibratory environments: rSHO (right shoulder), rELB (right elbow), rWRT (right wrist): ANG (joint angle [deg]), ANG_VEL (joint angular velocity [deg/s]), and ANG_ACC (joint angular acceleration [deg/s²]).

		rSHO	rELB	rWRT
No VIB.	ANG	153.5	140.2	172.9
	ANG_VEL	123.6	153.4	41.1
	ANG_ACC	459.0	1420.9	406.7
2 Hz pure	ANG	151.8	125.5	176.9
	ANG_VEL	181.5	201.9	184.2
	ANG_ACC	1507.3	4248.3	4644.3
4 Hz pure	ANG	154.5	131.6	176.7
	ANG_VEL	141.7	253.9	164.0
	ANG_ACC	1983.7	4570.3	5389.4
6 Hz pure	ANG	156.1	133.0	178.7
	ANG_VEL	157.8	159.0	134.4
	ANG_ACC	1777.4	2366.7	3331.7
2 Hz filtered	ANG	151.3	124.3	172.9
	ANG_VEL	139.1	139.2	54.1
	ANG_ACC	550.5	1369.1	708.3
4 Hz filtered	ANG	151.7	126.1	172.1
	ANG_VEL	126.5	134.1	74.9
	ANG_ACC	531.0	1463.7	691.0
6 Hz filtered	ANG	155.6	133.0	177.9
	ANG_VEL	126.0	133.1	67.0
	ANG_ACC	513.6	1197.8	1013.3

4.4 Discussion

Reach kinematics in the static environment suggests that angular kinematics of the right shoulder and elbow joint are qualitatively similar for all target directions although coordination characteristics of upper body segments vary as a function of target direction. When compared to other joints, the higher angular velocity and acceleration of the elbow indicate that this joint movement may contribute more significantly to the dynamic characteristics of upper body movements in reaching tasks. In addition, the “U-shaped” profile of the elbow joint angle indicates a flexion followed by an extension. In this two-phasic angular movement, elbow flexion may contribute to decrease the moment of inertia of the right arm, which reduces the arm resistance to rotation, thus making the arm transition shorter and more controllable.

In addition, movement initiation differs between the joints and arm movements are not initiated before visual identification of the target location. After visual identification, arm transition to the region near the target is achieved and fine adjustment of the fingertip position at destination occurs with deceleration of arm movements. It explains the bell-shaped profile in the joint velocities during the aiming phase, thus corresponding to the differentiation of movement in the respective feed-forward and feedback control phases.

Vibration induces significant alterations of joint trajectory and linear velocity predominantly along the vibration direction (z-axis). However, vibration in one direction generates body perturbation in other directions as well. This cross transmission may result from the nonlinearity in biomechanical properties of the upper body and from the difficulty in maintaining the balance while performing a reach task. This cross-effect may also be caused by the eccentricity of the mass

moment of inertia for multi-body segments, and the cross transmission may be more affected by biomechanical property variation associated with arm transition.

Vibration may also influence all joint angular movements, and contribute to an increase in the peak velocity and acceleration for all joint movements. However, the consistency in the pattern of angular kinematics may not be altered by vibration, which suggests that movement coordination may not be fundamentally different in the static and vibratory conditions, despite the fact that the timing of joint movements and relative contribution of each joint may be altered during vibration (Yoon and Martin, unpublished data).

4.5 Conclusions

This study qualitatively characterized movement pattern and joint kinematics of reach movements in static and dynamic environments. The qualitative analysis reveals that movement trajectories in the vibratory environment may be described by their properties in a static environment to which an oscillation driven by the vibration input is superimposed. This qualitative analysis of reach trajectories serves as the basis of the next study, in which variation of vibration transmission along reach trajectory is investigated.

CHAPTER 5

Effects of Posture and Movement on Vibration Transmission through the Upper Limbs

Vibration transmission to the human body is a function of both vehicle vibration characteristics and reach movement and posture. The majority of earlier studies investigating biomechanical responses to WBV have considered only a static posture excluding dynamic limb movements. A few recent studies have reported the effect of vehicle vibration on arm reaching movements by describing fingertip deviation from a desired trajectory. The present work investigates the variation of vibration transmission to upper extremities with changes in posture and movement along the intended reach trajectory under selected sinusoidal WBV conditions. Twenty-one subjects performed hand reach movements to a series of targets that consist of the final targets distributed in the right hemisphere and intermediate targets placed along the movement trajectories to the final target. Biodynamic responses of the upper body are analyzed as a function of posture, with-/without-visual control, and elbow flexion/extension. This study establishes the empirical database necessary to support a biodynamic model and may provide a promising groundwork for model development.

5.1 Introduction

The main objectives of this work are to investigate the biodynamic characteristics of vibration transmission through the upper limbs while performing

a reaching task in selected vibration conditions for various posture/movement constraints and to provide an empirical support for the development of a biodynamic model.

To achieve the objectives of this work, the first two studies (Chapter 3 - 4) investigated the characteristics of vibration transmission through upper body segments and reach kinematics of upper body joint under vibration exposure, as illustrated in Figure 1.1. It was first observed that vibration transmission through multi-body segments (the right shoulder, elbow and fingertip) vary as functions of vibration frequency and direction axis. This result was in agreement with earlier studies concerning the characteristics of transmissibility through the trunk of the seated human (Fairley and Griffin, 1989; McLeod and Griffin, 1989; Fairley and Griffin, 1990; Griffin, 1990; Kitazaki and Griffin, 1998; Mansfield and Griffin, 1998; Mansfield, 2005; Mansfield et al, 2006). The second study showed that vibration influences the trajectories of joint angular movements and their linear velocities; however, the pattern of joint angular kinematics remains consistent, as it is not qualitatively altered by vibration. On the basis of these analyses, an in-depth investigation of the vibration transmission through upper body segments as a function of reach posture and movements was pursued to determine more specifically biodynamic changes as a function of postural change associated with upper limb movements and of visual control for compensating WBV-induced pointing error at the fingertip.

Several studies considering posture as an independent variable, have indicated that response of the seated human to vibration is as a function of fixed hand position and back support conditions (Fairley and Griffin, 1989; Kitazaki and Griffin, 1998; Matsumoto and Griffin, 2002; Paddan and Griffin, 2002; Rakheja et al, 2002; Wang et al, 2004; Huang and Griffin, 2006; Mansfield et al, 2006).

Studies concerning the role of visual feedback in movement control have reported that upper limb movements were continuously controlled by visual feedback to smoothly modify the motor program by comparing the locations of the hand and the target (Prablanc et al, 1979a; Prablanc et al, 1979b; Prablanc et al, 1986a; Péllisson et al, 1986b; Desmurget and Prablanc, 1997; Wallis et al, 2002; Hondzinski and Kwon, 2009). According to their results, gaze direction may be considered as an input signal for upper limb control, and the eye and hand movements are controlled in parallel rather than in series (Prablanc et al, 1979a; Hondzinski and Kwon, 2009). Interestingly, the durations of hand movements are not significantly different with or without visual information of the hand position (Prablanc et al, 1986a; Péllisson et al, 1986b). In addition, Desmurget and Prablanc (1997), suggested that despite joint redundancy in three-dimensional movements, the target posture was invariant when the movement context remained stable in a static environment.

Therefore, this study analyzed variation in three-dimensional biodynamic responses through the upper limbs as a function of vibration frequency, reach direction, and posture/movement constraints. The specific objectives of this study are to investigate the effects of dynamic posture change along the reach direction, visually induced compensation, and elbow extension constraint at the end of a reach on vibration transmission through upper body segments. The design of this experiment and the analysis are based on the following hypotheses.

- Changes in biomechanical properties of body segments associated with movement direction affect vibration transmission.
- Performance degradation induced by vibration varies with target location corresponding to reach direction.

- Constraints on elbow flexion induce significant differences in vibration transmission to the end effector.

The results provide empirical support for understanding vibration-induced biodynamic alterations, which may contribute to the development of a biodynamic model, to the enhancement of workplace design, to the better design of control interfaces used in vibratory environments, and to the determination of movement strategies to reduce WBV interference.

5.2 Methods

5.2.1 Biodynamic Reach Experiment II

5.2.1.1 Subject

Twenty-one right-handed young adults participated in the experiment voluntarily. All were in good health and had no known history of injuries such as musculoskeletal or neurological disorders, chronic back pain, or acute back pain. The average and standard deviation values (AVG \pm SD) of age and anthropometric data including stature, weight, torso length, right upper arm and forearm lengths, and hand length are listed in Table 5.1.

Table 5.1: Anthropometry Data

	Age (years)	Weight (kg)	Stature (cm)	Torso length (cm)	Upper- arm length (cm)	Forearm length (cm)	Hand (wrist- fingertip) length (cm)
AVG \pm SD	29 \pm 5.1	79.2 \pm 10.9	177.9 \pm 8.0	46.6 \pm 2.4	34.1 \pm 1.9	27.6 \pm 1.7	17.6 \pm 1.3

5.2.1.2 Experimental Setup

The experiment designed on the basis of the preceding analyses was conducted on the RMS at the U.S Army TARDEC (Figure 5.1). Six infrared cameras were positioned to capture the volume encompassing the right arm-hand reach space for in-vehicle operation. Two-way data acquisitions were used for recording the relative displacements of upper body segments of individuals performing reach movements and measuring the accelerations of vibration transmitted to the upper body through the seat.



Figure 5.1: Reach Experiment on the Ride Motion Simulator

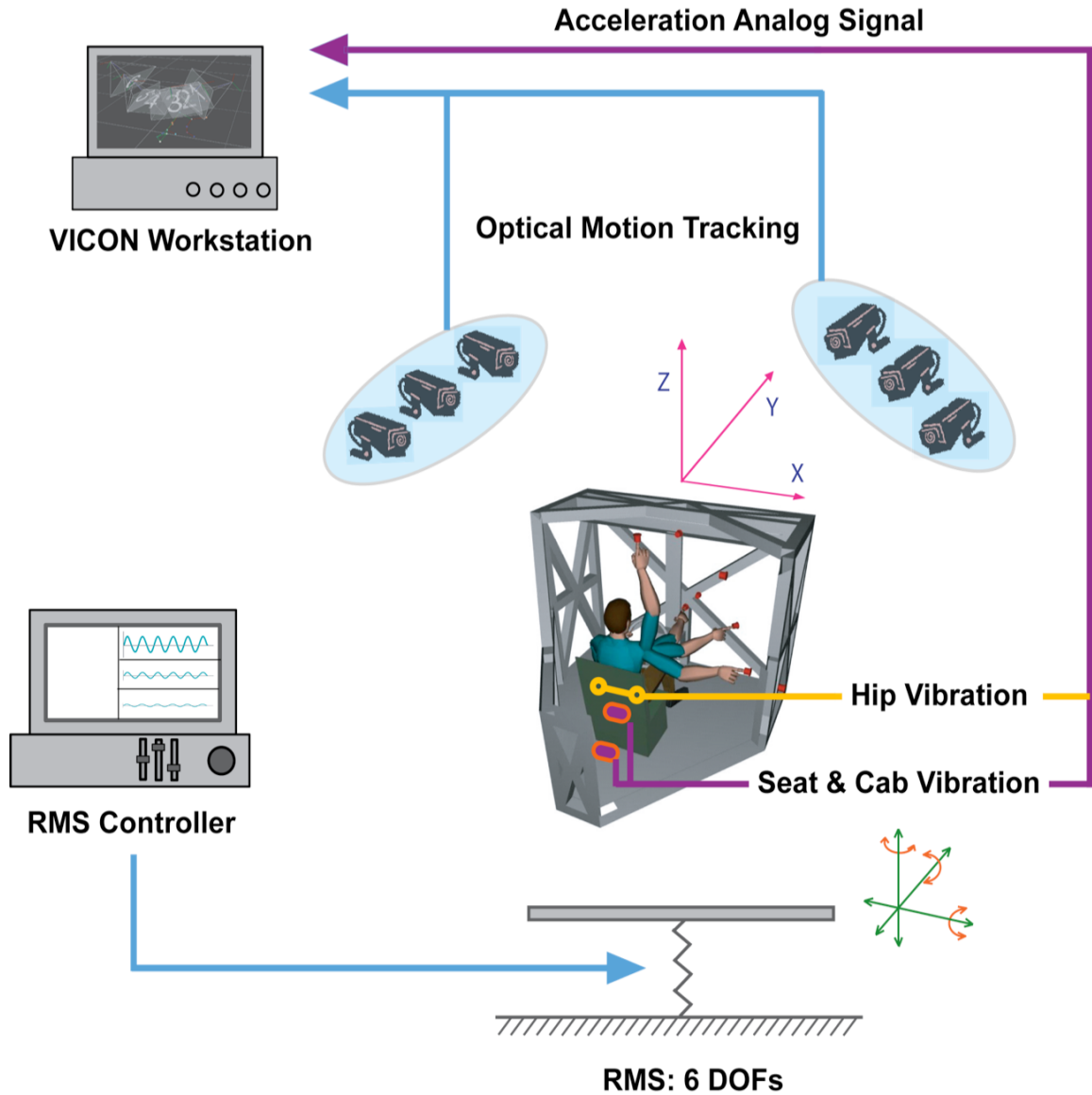


Figure 5.2: Diagram of the Experimental Setup

5.2.1.3 Data Acquisition

Human Body Segment Motion Capture

Twenty-three retro-reflective markers were placed on body landmarks (Table 5.2 and Figure 5.3). Specifically, four markers were attached for head orientation and rotation and seven markers were used for the right arm-hand

movements. For anthropometric measures and system calibration, a T-pose and the range of motion were recorded for each subject (Figure 5.4). The static reference posture, the range of motion and reach movements were sampled at 150Hz by the motion analysis system.

Table 5.2: Marker Definition

Body Segment	# of Markers	Marker Name
Head (on a soft helmet)	4	RFHD, RBHD, LFHD, LBHD
Centerline of a torso	4	C7, CLAV, MIDSTRN, STRN
Hip	2	LASI, RASI
Right Arm-hand	7	RSHO, RUPA, RELB, RFRA, RWRA, RWRB, RFIN
Left Arm-hand	6	LSHO, LUPA, LELB, LFRA, LRWA, LRWB
Total	23	

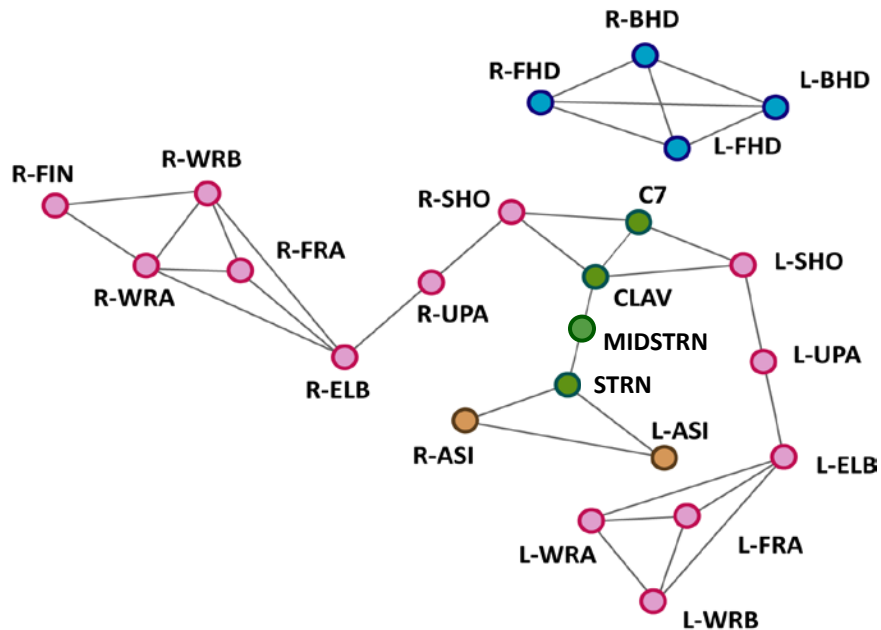


Figure 5.3: Marker definition on a human body: R=right, L=left, FHD=front-head, BHD=back-head, CLAV=Clavicle, MIDSTRN=mid-sternum, STRN=sternum, SHO=shoulder, UPA=upper-arm, ELB=elbow, FRA=fore-arm, WR=wrisk, FIN=finger



Figure 5.4: T-pose for anthropometric measure and calibration

Vibration Acceleration Measurement

To determine vibration transmission from the cab floor through the seat, four tri-axial accelerometers were used to record cab, seat, and hip joints vibration (Figure 5.5). Hence, 12-channel accelerometer signals were recorded by a VICON Workstation, which synchronized the analog signals with the motion capture data (Table 5.3 and Figure 5.2).



(a) for cab floor & seat



(b) for hip joints

Figure 5.5: Tri-axial accelerometer attached to cab/seat/hip interface

Table 5.3: Tri-axial Accelerometers on a Cab and Seat

Channel No.	Analogue Signal	Tri-axial Accelerometer
1	Cab floor – X	Tri-axial Accelerometer #1
2	Cab floor – Y	
3	Cab floor – Z	
4	Seat – X	Tri-axial Accelerometer #2
5	Seat – Y	
6	Seat – Z	
7	Left Hip – X	Tri-axial Accelerometer #3
8	Left Hip – Y	
9	Left Hip – Z	
10	Right Hip – X	Tri-axial Accelerometer #4
11	Right Hip – Y	
12	Right Hip – Z	

5.2.1.4 Vibration Condition

The RMS generated eleven vibration conditions selected to characterize vibration transmission through the upper limbs at discrete vibration conditions similar to vehicle vibrations (Table 5.4). In the reference condition, no vibration was applied. Nine one-dimensional vibration conditions were generated by the combination of three discrete sinusoidal vibration frequencies (2, 4, or 6 Hz) and three vibration directions (vertical, fore-and-aft, or lateral). The vibration frequencies were selected on the basis of the frequency range of high sensitivity of the human upper body and the spectra of vehicle vibrations as described in Chapter 3 (Lee and Pradko, 1968; McLeod and Griffin, 1989; Fairley and Griffin, 1990; Griffin, 1990). The peak acceleration magnitudes were 0.3 G for the vertical and were 0.2 G for the fore-and-aft and the lateral vibration directions respectively. The same magnitude was used for all frequencies in the same direction to prevent the interaction between vibration frequency and magnitude, since variation of vibration

magnitude may reflect the nonlinear features in human responses to vibration (McLeod and Griffin, 1989). An additional dynamic condition corresponding to a three-dimensional random vibration input was used to simulate a HMMWV vehicle driven over rough terrain. The biodynamic analysis of this work was limited to investigate the effects of three vertical sinusoidal vibrations on transmission through the upper limbs and their influence on transmission along transverse axes. Hence, three-dimensional transmissions along the auto-axis and the cross-axes are analyzed. The vertical vibration conditions were selected as the dominant component that seated operators commonly are experienced in most vehicles.

Table 5.4: RMS inputs

No.	Frequency	Direction	Magnitude
1	No Vibration		
2	2 Hz	Vertical	0.3 G
3	2 Hz	Fore-and-Aft	0.2 G
4	2 Hz	Lateral	0.2 G
5	4 Hz	Vertical	0.3 G
6	4 Hz	Fore-and-Aft	0.2 G
7	4 Hz	Lateral	0.2 G
8	6 Hz	Vertical	0.3 G
9	6 Hz	Fore-and-Aft	0.2 G
10	6 Hz	Lateral	0.2 G
11	3D Random (HMMWV pitch)		

5.2.1.5 Target Directions and Intermediate Stops

The dynamic task consisted in reaching to seven target directions distributed in the right hemisphere of a vehicle operator seat; upward [TG1], forward and upward [TG2], forward [TG3], diagonal [TG4], diagonal and upward [TG5], lateral

near [TG6], and lateral far [TG7] (Figure 5.6). These seven directions represent the reach space of the right arm-hand. Along each target direction, two intermediate stops were assigned on the basis of fingertip reach trajectories derived from the previous analysis of reach trajectory to the same target directions (Table 5.5). These intermediate stops were designed to investigate variation of vibration transmission as a function of posture changed along the reach trajectory. The locations of all targets and stops were determined with respect to the coordinated system centered at the right top of the steering handle (see Table 5.5). All participants were asked to reach the targets in a random order, and the intermediate stops along the movement trajectory were reached in the natural near to far order.

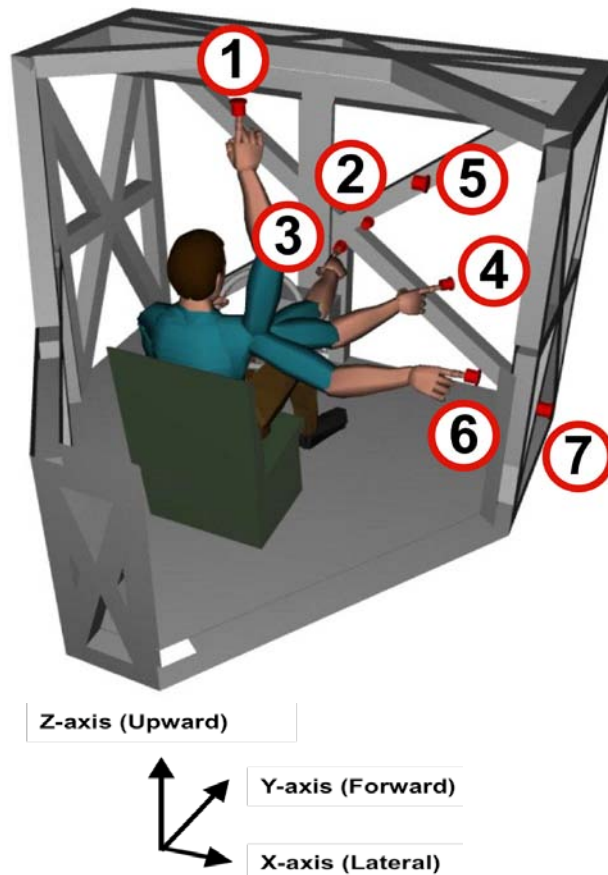





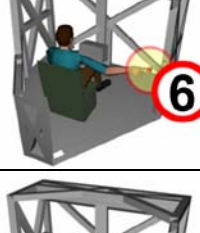



Figure 5.6: Target Directions and Cartesian Coordinate

Table 5.5: Reach Target Directions and Locations

No.	Target Direction		Sub-target	Location (x, y, z) [mm]
1	Upward		TG 1-1 TG 1-2 TG 1-3 TG 1-4	(0, 0, 0) (65, -45, 80) (139, -146, 413) (143, -357, 678)
2	Forward & Upward		TG 2-1 TG 2-2 TG 2-3 TG 2-4	(0, 0, 0) (65, -45, 80) (93, 8, 194) (132, 133, 269)
3	Forward		TG 3-1 TG 3-2 TG 3-3 TG 3-4	N/A N/A N/A (206, 139, -171)
4	Diagonal		TG 4-1 TG 4-2 TG 4-3 TG 4-4	(0, 0, 0) (65, -45, 80) (233, -26, 35) (426, 44, -66)
5	Diagonal & Upward		TG 5-1 TG 5-2 TG 5-3 TG 5-4	(0, 0, 0) (209, -7, 118) (298, -83, 242) (564, -274, 420)
6	Lateral Near		TG 6-1 TG 6-2 TG 6-3 TG 6-4	(0, 0, 0) (233, -26, 35) (468, -110, 3) (578, -271, -114)
7	Lateral Far		TG 7-1 TG 7-2 TG 7-3 TG 7-4	(0, 0, 0) (233, -26, 35) (544, -172, 17) (870, -295, -114)

5.2.1.6 Movement Constraints in Reaching Task

All participants performed the reaching task in three sessions following different movement constraints. All sessions included the eleven vibration conditions. Movement constraints were used to investigate the effects of posture change along the reach trajectory, to identify the effects of visual compensation, and to analyze the influence of elbow flexion on WBV transmissibility. All reaching tasks were performed at the self-determined speed, and were repeated in a random order.

Session I: Intermediate Reach without Visual Compensation

Session I concerned variation in transmissibility along reach trajectory when visual feedback is not allowed. Participants were required to point to a series of a target placed along the anticipated finger trajectory in six target directions: upward [TG1], forward and upward [TG2], diagonal [TG4], diagonal and upward [TG5], lateral near [TG6], and lateral far [TG7]. Forward reach [TG3] was excluded since the distance was too short to allocate additional intermediate stops.

Each target direction includes two intermediate stops between the initial and final positions of the finger along the reach trajectory derived from the analysis presented in Chapter 4. At the intermediate stop, the participant was requested to maintain the corresponding posture for three seconds. While maintaining the pointing posture, the participant must return the gaze to the initial fixation direction, which prevented the use of visual feedback to control the hand position (Figure 5.7). Then, the subject resumed the movement to the next stop or the final target.



Figure 5.7: Session I - Pointing posture w/o visual compensation

Session II: Intermediate Reach with Visual Compensation

As in Session I, participants were required to point to a series of targets along the anticipated finger trajectory for each reach direction. However, in this Session, continuous visual feedback of the right hand while pointing at the target was allowed to compensate the pointing errors induced by vibration (Figure 5.8).



Figure 5.8: Session II - Pointing posture w/ visual compensation

Session III: End Reach with Different Elbow Flexion

The participant was assigned to reach and point only to the final target for six reach directions, without stopping at intermediate targets. These six directions excluded the lateral far target [TG7], but included the forward target [TG3] instead, since [TG7] can be reached only when the elbow is fully extended while [TG3] can be reached with elbow extended or flexed. For all reaches, two final pointing postures were used; 1) elbow fully extended [EE] and 2) elbow flexed [EF] (Figure 5.9). Visual compensation by feedback control was not allowed while maintaining the final posture, as in Session I.



(a) Elbow fully extended postures



(b) Elbow flexed postures

Figure 5.9: Session III – Pointing postures with different elbow flexion

5.2.2 Vibration Analysis

Three-dimensional vibration transmissions through the upper body segments were analyzed since a one-dimensional vibration input can generate the cross-axis motions of body segments in other directions, as observed in Chapter 4.

5.2.2.1 Joint Position Deviation and Angle Perturbation

For analyzing WBV transmission through the upper limbs, position fluctuations of four upper body landmarks such as the left shoulder, the right shoulder, the right elbow, and the right index fingertip were quantified along x-, y-, and z-directions. Joint angles of the right shoulder and elbow were calculated for each pointing phase to present posture changes between reaching tasks in different conditions.

5.2.2.2 Frequency Response and Vibration Transmission

The frequency responses were calculated in three-dimensions using the FFT (Eq. 3.1). No windowing was applied and the frequency range of interest was in the 0.2 – 12Hz (see Chapter 3). WBV transmission through the body segment was also analyzed along the three-directions of space, which consisted of the auto-axis transmission and the two cross-axis transmissions (Eq. 5.1). The transmission at the excitation frequency was emphasized in this work. At this frequency, the vibration transmissions through three upper body segments were estimated by the ratio of the peak magnitude in the response to the peak magnitude in the input at the forcing frequency (Figure 3.10). Superscript B, LS, RS, RE, and RF denote the cab base, the left shoulder, right shoulder, right elbow, and right index fingertip, respectively. Subscript x, y, and z denote the axis of the vibration or the response. The total transmission integration T^* is estimated from magnitude of the transmission vector of the body landmark (Eq. 5.2).

$$\vec{T}^{RF} = \frac{\vec{X}^{RF}}{X_z^B} = T_x^{RF} + T_y^{RF} + T_z^{RF} \dots\dots\dots (\text{Eq. 5.1})$$

$$\text{where } T_x^{RF} = \frac{X_x^{RF}}{X_z^B}, \quad T_y^{RF} = \frac{X_y^{RF}}{X_z^B}, \quad T_z^{RF} = \frac{X_z^{RF}}{X_z^B}$$

$$T^* = \left| T_x + T_y + T_z \right| \dots\dots\dots (\text{Eq. 5.2})$$

5.3 Results

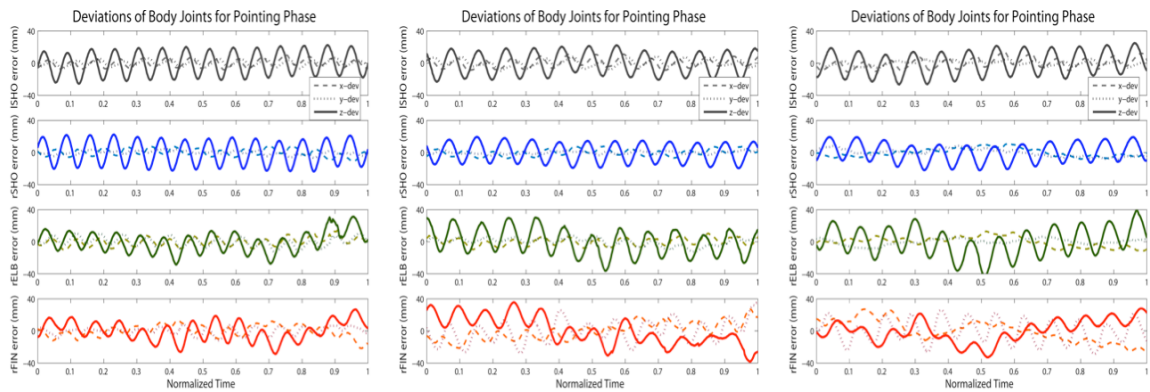
5.3.1 Variation of WBV transmission along the Fingertip Trajectory

From the reach movement data obtained from session I, variation of WBV transmission through upper body segments under the selected sinusoidal vibrations was quantified as a function of the reaching posture for six reach directions.

5.3.1.1 Upper Body Displacement and Joint Angle

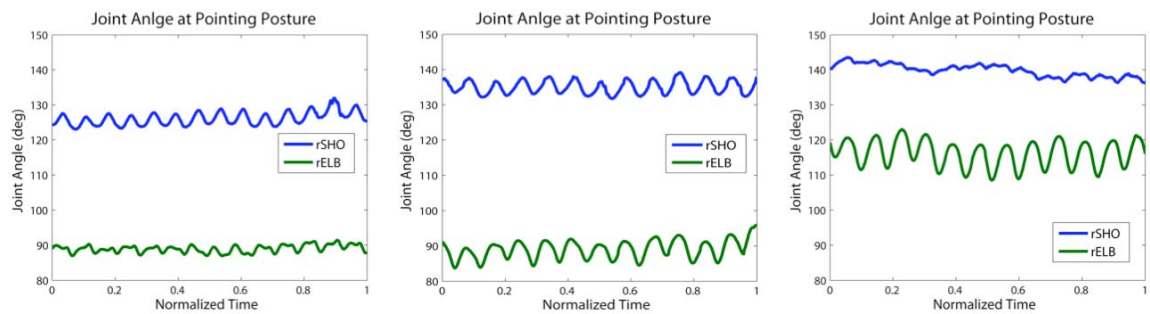
Typical three-dimensional displacement samples of the upper limbs at three digitalized stops along the fingertip trajectory when reaching to the diagonal and upward target [TG5] under the 4 Hz vertical sinusoidal vibration are presented in Figure 5.10. As the hand moves toward the final target, vertical perturbation of the elbow joint increases and the cross-axis perturbations of the finger remarkably increase. The finger movement indicates the presence of low frequency components as well.

Joint angles of the right shoulder and elbow are illustrated in Figure 5.11, corresponding to intermediate postures and final pointing posture along the trajectory. As the hand is closer to the final destination, both joint angles increase however, perturbation of the shoulder angle decreases while the perturbation of the elbow increases.



(a) at intermediate step 1 (b) at intermediate step 2 (c) at the final target

Figure 5.10: 3-Dimensional displacements of upper limbs in diagonal and upward reach [TG5] for the 4 Hz vertical vibration



(a) at intermediate step 1 (b) at intermediate step 2 (c) at the final target

Figure 5.11: Joint angles of the right shoulder and elbow in diagonal and upward reach [TG5] for the 4 Hz vertical vibration

5.3.1.2 Frequency Response and Vibration Transmission of the Upper Limbs

To identify frequency component features in upper body perturbation, displacements of the upper body joints are analyzed in the frequency domain. Figure 5.12 illustrates frequency responses of the left shoulder, the right shoulder, the right elbow, and the right index fingertip when performing diagonal and upward reach [TG5] under the 4 Hz vertical vibration exposure. As expected, when the hand arrives at the final target, the peak value of frequency response of the shoulder decreases and the peak response of the elbow increases. In addition, for all body

joints, low frequency perturbation components appear more conspicuous and are amplified at the fingertip.

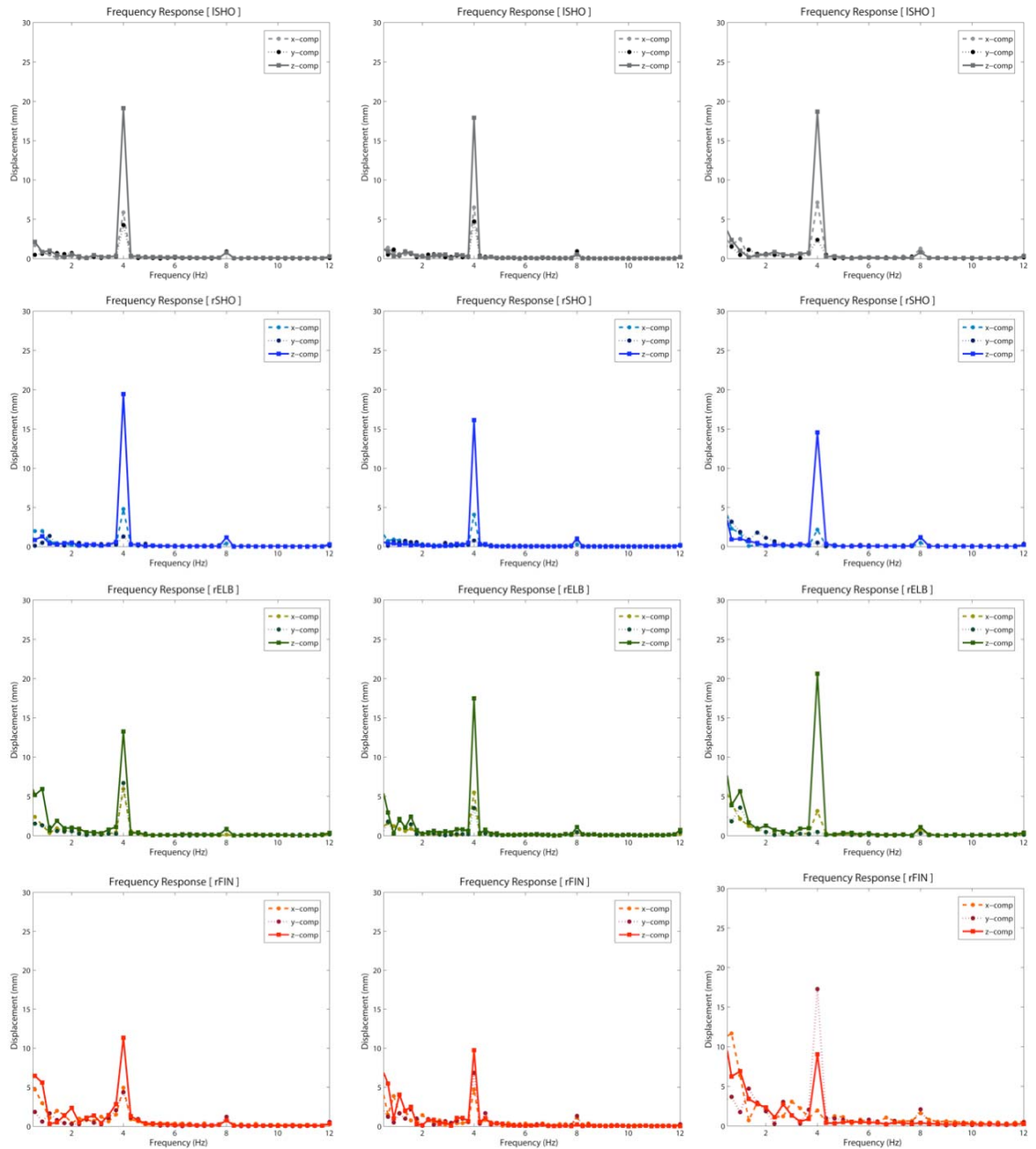


Figure 5.12: Frequency responses of upper limbs in diagonal and upward reach [TG5] for the 4 Hz vertical vibration: ISHO (1st row), rSHO (2nd row), rELB (3rd row), and rFIN (4th row) & intermediate stop1 (1st column), intermediate stop 2 (2nd column), and final target (3rd column)

Vibration transmission of the upper limbs is quantified by Eq. 5.1 and 5.2, for all directional reaches including intermediate stops under the vertical vibration exposure. To identify the significance of the effects of independent variables such as intermediate posture, target location, and vibration frequency, a three-way ANOVA was performed for all transmission information (x-, y-, and z-components and total transmission) obtained from session I (Table 5.6). Intermediate posture and target location as well as vibration frequency significantly affects the z-component of transmission and the total transmission to the shoulders and the finger. This influence is more pronounced for the cross-axis (x- and y- directions) than for the auto-axis to the elbow.

For a more detail analysis of vibration transmission, the six reach directions were divided into three groups: horizontal reaches (diagonal [TG4] and lateral near [TG6]), upward reaches requiring shoulder flexion (upward [TG1], forward-upward [TG2], and diagonal-upward [TG5]), and far reach requiring torso leaning (lateral far [TG7]). These three groups show similarity of WBV transmission through the upper body segments (see appendix A). A 2-way ANOVA was conducted for three target directions - [TG4], [TG5], and [TG7] - representing each reach group respectively (Table 5.7, 5.8, and 5.9).

Table 5.7 indicates that for diagonal reach [TG4], no significant change in transmission occurs through all body segments along the reach trajectory (All $p >> 0.1$). For diagonal-upward reaches [TG5], only the z-component through the elbow and total transmission through the finger are significantly affected and increase by changes in posture while transmission through two shoulders are not significantly influenced ($p >> 0.1$ for the left shoulder and $p > 0.05$ for the right shoulder, Table 5.8). For lateral far reach [TG7], both the z-component and the total transmission through the right shoulder and through the finger are significantly

Table 5.6: 3-way ANOVA [Inter-Pose, Target location, and Vibration Freq.]

	Transmission (ISHO)				
	DoF	p (T _X)	p (T _Y)	p (T _Z)	p (T _{TOTAL})
Pose (Intermediate)	2	0.0282	0.6309	0	0
Target-L	5	0.0001	0.2896	0.0026	0.0030
Vib-Freq	2	0	0	0	0
Pose × Target-L	10	0.0132	0.7740	0.1920	0.4589
Pose × Vib-Freq	4	0.0019	0.0022	0	0.0001
Target-L × Vib-Freq	10	0.0007	0.1257	0.0059	0.0058
	Transmission (rSHO)				
	DoF	p (T _X)	p (T _Y)	p (T _Z)	p (T _{TOTAL})
Pose (Intermediate)	2	0	0.2299	0	0
Target-L	5	0.0042	0.0238	0.0003	0.0003
Vib-Freq	2	0	0	0	0
Pose × Target-L	10	0.0943	0.1958	0.0413	0.0262
Pose × Vib-Freq	4	0.0002	0.0082	0.0039	0.0030
Target-L × Vib-Freq	10	0.0516	0.0218	0.0061	0.0085
	Transmission (rELB)				
	DoF	p (T _X)	p (T _Y)	p (T _Z)	p (T _{TOTAL})
Pose (Intermediate)	2	0.0004	0	0.0098	0.5652
Target-L	5	0.0009	0.0002	0.3357	0.1248
Vib-Freq	2	0	0	0	0
Pose × Target-L	10	0.0356	0.0122	0.5178	0.3613
Pose × Vib-Freq	4	0.0094	0	0.1661	0.5568
Target-L × Vib-Freq	10	0.0711	0.0704	0.0547	0.0908
	Transmission (rFIN)				
	DoF	p (T _X)	p (T _Y)	p (T _Z)	p (T _{TOTAL})
Pose (Intermediate)	2	0.1465	0.0017	0.0028	0
Target-L	5	0.6358	0.0021	0	0.0015
Vib-Freq	2	0	0	0	0
Pose × Target-L	10	0.1550	0.0266	0.0051	0.0063
Pose × Vib-Freq	4	0.0166	0.1541	0.0610	0.0436
Target-L × Vib-Freq	10	0.5642	0.0334	0.1036	0.5789

Table 5.7: 2-way ANOVA for diagonal reach [TG4]

	Transmission (ISHO)				
	DoF	p (T _X)	p (T _Y)	p (T _Z)	p (T _{TOTAL})
Pose (Intermediate)	2	0.9506	0.6959	0.2277	0.4086
Vib-Freq	2	0	0	0	0
Pose × Vib-Freq	4	0.9868	0.9325	0.5517	0.7121
	Transmission (rSHO)				
	DoF	p (T _X)	p (T _Y)	p (T _Z)	p (T _{TOTAL})
Pose (Intermediate)	2	0.6472	0.4782	0.9694	0.9867
Vib-Freq	2	0	0	0	0
Pose × Vib-Freq	4	0.7325	0.0542	0.9116	0.9418
	Transmission (rELB)				
	DoF	p (T _X)	p (T _Y)	p (T _Z)	p (T _{TOTAL})
Pose (Intermediate)	2	0.1178	0.0246	0.0682	0.6393
Vib-Freq	2	0	0	0	0
Pose × Vib-Freq	4	0.5933	0.0971	0.2033	0.7785
	Transmission (rFIN)				
	DoF	p (T _X)	p (T _Y)	p (T _Z)	p (T _{TOTAL})
Pose (Intermediate)	2	0.1582	0.0001	0.4839	0.5804
Vib-Freq	2	0	0	0	0
Pose × Vib-Freq	4	0.2386	0.0896	0.2938	0.2881

influenced and increase ($p \ll 0.01$ for the right shoulder and the finger, Table 5.9), however transmission through the left shoulder and the elbow are not significantly affected ($p > 0.05$ for the left shoulder and $p > 0.1$ for the elbow).

As indicated above, WBV transmission changes along the reach trajectory are dependent on the direction of reach (final target location). That is, in the horizontal reaches, there is no significant change in variation of WBV transmission. Furthermore, all components of auto-axial, cross-axial, and total transmissions are strongly influenced by vibration frequency ($p < 0.05$).

Table 5.8: 2-way ANOVA for diagonal-upward reach [TG5]

	Transmission (ISHO)				
	DoF	p (T _X)	p (T _Y)	p (T _Z)	p (T _{TOTAL})
Pose (Intermediate)	2	0.9418	0.1067	0.4606	0.7342
Vib-Freq	2	0	0	0	0
Pose × Vib-Freq	4	0.9506	0.0942	0.3741	0.6824
	Transmission (rSHO)				
	DoF	p (T _X)	p (T _Y)	p (T _Z)	p (T _{TOTAL})
Pose (Intermediate)	2	0.0338	0.1284	0.2196	0.0739
Vib-Freq	2	0	0	0	0
Pose × Vib-Freq	4	0.0121	0.1091	0.5687	0.2221
	Transmission (rELB)				
	DoF	p (T _X)	p (T _Y)	p (T _Z)	p (T _{TOTAL})
Pose (Intermediate)	2	0.0006	0.0005	0.0114	0.6888
Vib-Freq	2	0	0	0	0
Pose × Vib-Freq	4	0	0.0011	0.0431	0.1409
	Transmission (rFIN)				
	DoF	p (T _X)	p (T _Y)	p (T _Z)	p (T _{TOTAL})
Pose (Intermediate)	2	0.0319	0	0.6416	0.0072
Vib-Freq	2	0	0	0.0112	0.0163
Pose × Vib-Freq	4	0.0727	0.0062	0.3137	0.4010

Three-dimensional and total transmissions through the upper limbs are presented in Figure 5.13 – 5.21, for three representative reach directions respectively. The three components of transmission are demonstrated by bar plots, in which cross-axial transmissions are illustrated as thinner bar than auto-axial transmissibility is. Auto-transmission and total transmission are connected by a solid line and a dotted-line respectively.

Table 5.9: 2-way ANOVA for lateral far reach [TG7]

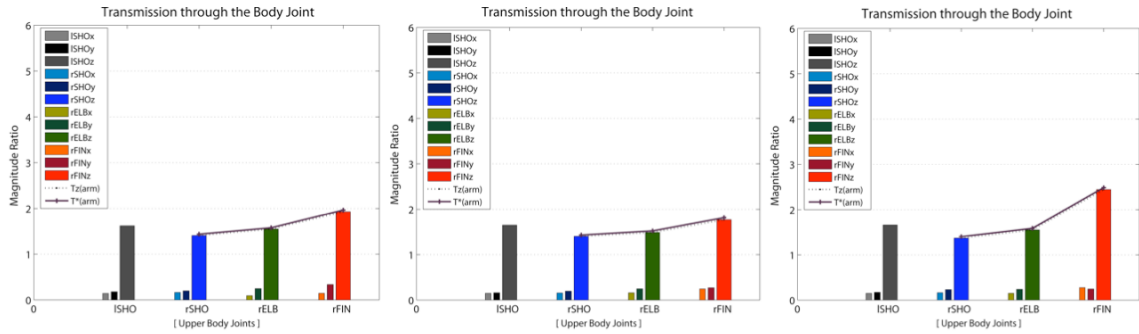
	Transmission (ISHO)				
	DoF	p (T _X)	p (T _Y)	p (T _Z)	p (T _{TOTAL})
Pose (Intermediate)	2	0.1831	0.4016	0.0469	0.0868
Vib-Freq	2	0	0	0	0
Pose × Vib-Freq	4	0.3379	0.3260	0.1354	0.1346
	Transmission (rSHO)				
	DoF	p (T _X)	p (T _Y)	p (T _Z)	p (T _{TOTAL})
Pose (Intermediate)	2	0.2150	0.1185	0	0.0001
Vib-Freq	2	0	0	0	0
Pose × Vib-Freq	4	0.0007	0.0542	0.0109	0.0133
	Transmission (rELB)				
	DoF	p (T _X)	p (T _Y)	p (T _Z)	p (T _{TOTAL})
Pose (Intermediate)	2	0	0	0.4117	0.2096
Vib-Freq	2	0	0	0	0
Pose × Vib-Freq	4	0	0	0.0965	0.0026
	Transmission (rFIN)				
	DoF	p (T _X)	p (T _Y)	p (T _Z)	p (T _{TOTAL})
Pose (Intermediate)	2	0.0013	0	0.0106	0
Vib-Freq	2	0	0	0.9178	0
Pose × Vib-Freq	4	0.0026	0	0.6649	0.1910

For diagonal reach [TG4], there is no significant change in vibration transmission, induced by posture changes along the reach trajectory (Figure 5.13, 5.14, and 5.15). The transmission trend through the upper limbs is almost the same for the intermediate or final postures in each vibration condition.

For diagonal-upward reach [TG5], under the 2Hz vertical vibration, perturbation of the elbow and finger increase monotonously as the hand is moving toward the target (Figure 5.16). Under the 4Hz vibration, as the arm is elevated to reach the final target, the auto-axis perturbation of the elbow significantly increases while the cross-axis perturbations decrease. However, the auto-axis perturbation of

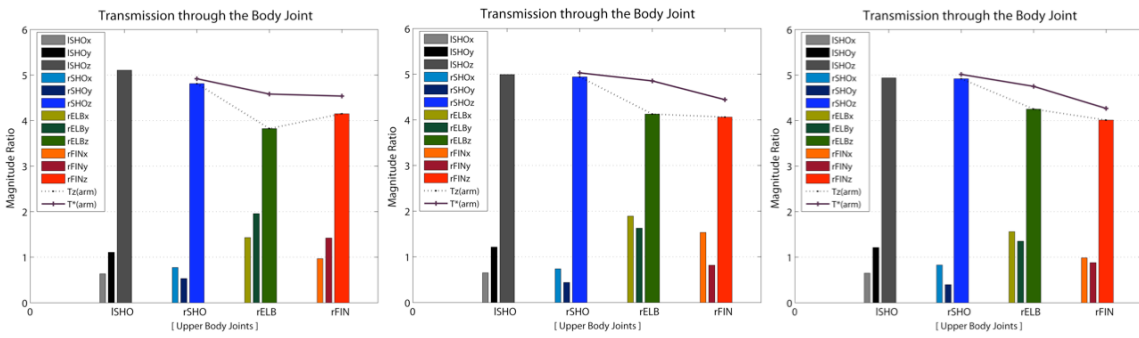
the finger decreases and the cross-axis perturbations increase. The total transmission to the finger increases as the hand is moving in direction of the target, since the amount of increase in cross-transmission is bigger than the amount of decrease in auto-transmission. In addition, the total transmission is larger for the elbow than the shoulder. Thus, the trend of vertical (z-axis) transmission through the upper limbs changes with the hand movements, but the trend of total transmission is not significantly altered. Interestingly, under the 6Hz vibration exposure, the total transmission through the finger largely increases when the hand arrives near the final target. For the final posture, auto-transmission remains small; however cross-transmissions of the finger are relatively larger.

For lateral-far reach [TG7], transmissibility through the upper limbs does not show significant change between intermediate postures. However, at the end of reach to the final target, the peak of vibration transmission of the finger increases remarkably. This characteristic is more pronounced for the 4Hz and 6Hz than for the 2Hz vibration exposure. Especially for the 6Hz vibration, cross-axis transmission of the fingertip is relatively high and the difference between auto-transmission and total transmission is the largest among all vibration and reach conditions.



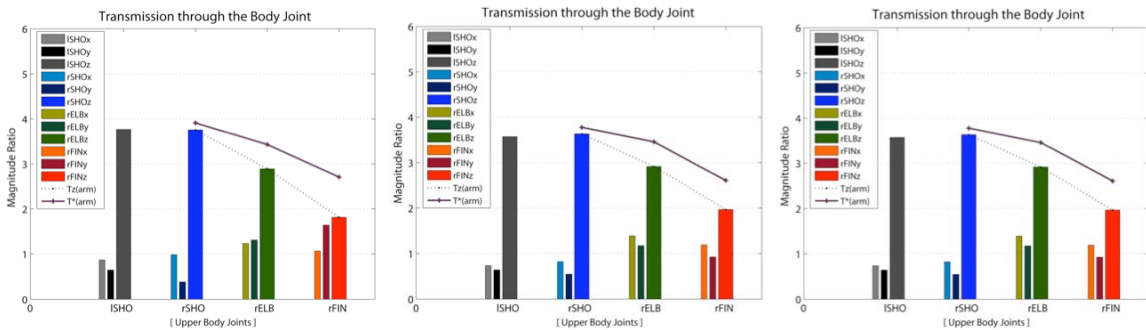
(a) at intermediate stop 1 (b) at intermediate stop 2 (c) at the final target

Figure 5.13: Vibration transmission through upper body segments for diagonal reach [TG4] under the 2Hz vertical WBV



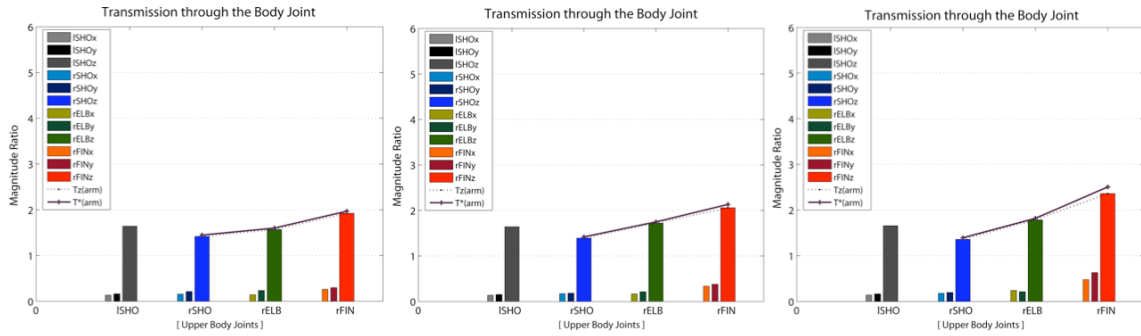
(a) at intermediate stop 1 (b) at intermediate stop 2 (c) at the final target

Figure 5.14: Vibration transmission through upper body segments for diagonal reach [TG4] under the 4Hz vertical WBV



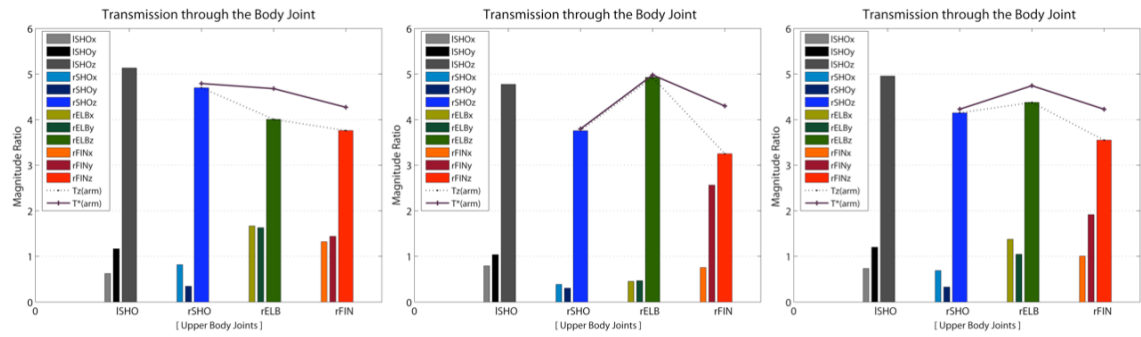
(a) at intermediate stop 1 (b) at intermediate stop 2 (c) at the final target

Figure 5.15: Vibration transmission through upper body segments for diagonal reach [TG4] under the 6Hz vertical WBV



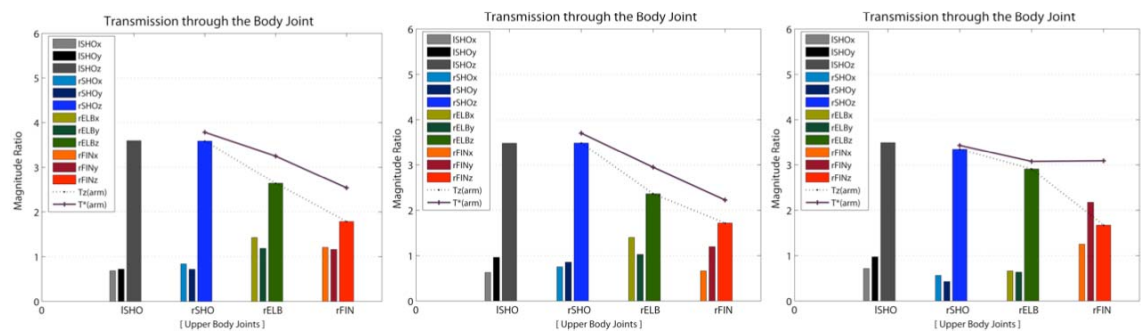
(a) at intermediate step 1 (b) at intermediate step 2 (c) at the final target

Figure 5.16: Vibration transmission through upper body segments for diagonal-upward reach [TG5] under the 2Hz vertical WBV



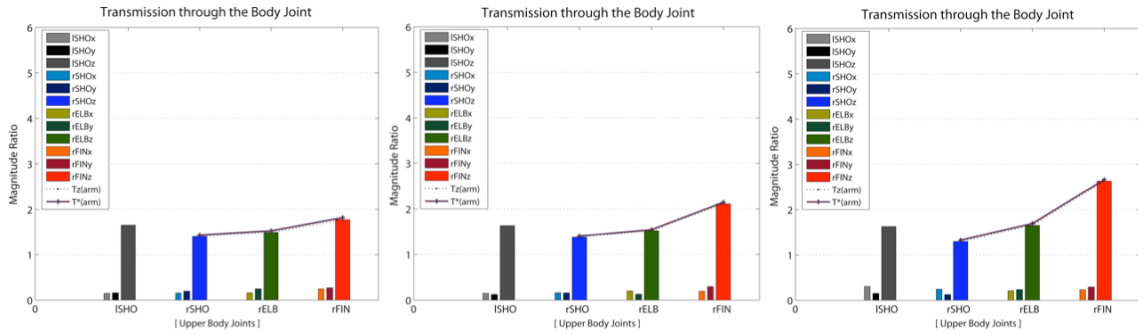
(a) at intermediate step 1 (b) at intermediate step 2 (c) at the final target

Figure 5.17: Vibration transmission through upper body segments for diagonal-upward reach [TG5] under the 4Hz vertical WBV

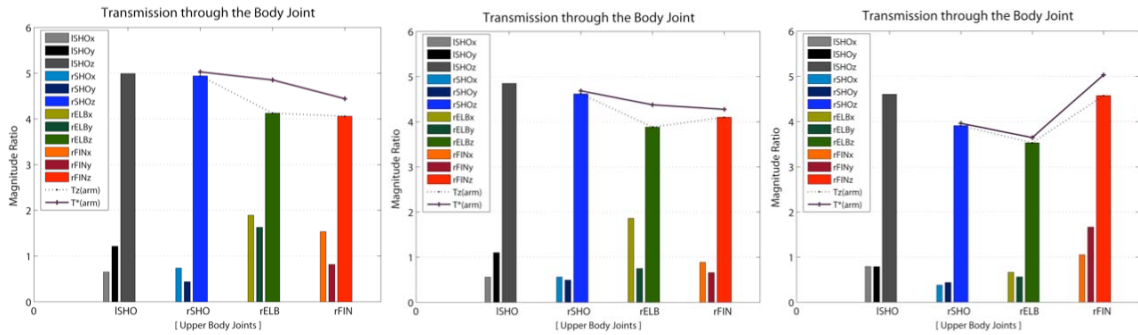


(a) at intermediate step 1 (b) at intermediate step 2 (c) at the final target

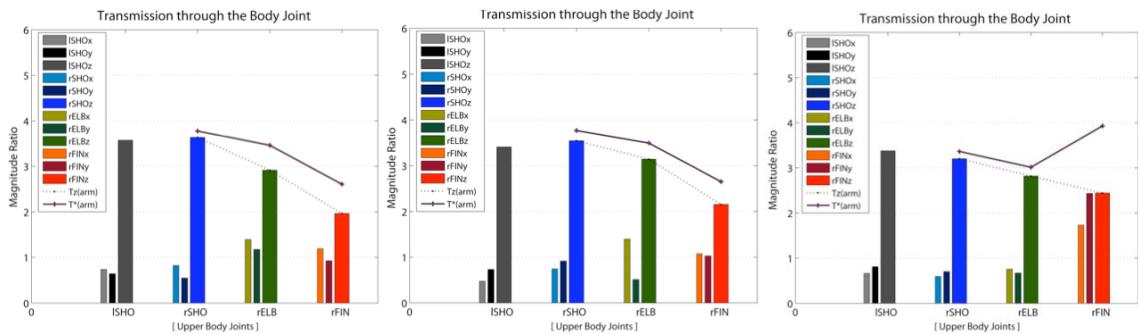
Figure 5.18: Vibration transmission through upper body segments for diagonal-upward reach [TG5] under the 6Hz vertical WBV



(a) at intermediate stop 1 (b) at intermediate stop 2 (c) at the final target
Figure 5.19: Vibration transmission through upper body segments for lateral-far reach [TG7] under the 2Hz vertical WBV



(a) at intermediate stop 1 (b) at intermediate stop 2 (c) at the final target
Figure 5.20: Vibration transmission through upper body segments for lateral-far reach [TG7] under the 4Hz vertical WBV



(a) at intermediate stop 1 (b) at intermediate stop 2 (c) at the final target
Figure 5.21: Vibration transmission through upper body segments for lateral-far reach [TG7] under the 6Hz vertical WBV

5.3.2 Effects of Visual Compensation on WBV-induced Transmission

5.3.2.1 Upper Body Displacement and Joint Angles with Visual Compensation

For the specific case of diagonal-upward reach [TG5] under the 4Hz vibration, upper body perturbation and joint angles under no visual feedback and visual compensation are shown in Figure 5.22 and 5.23 respectively. Displacements of body segment with no visual feedback show superposition of excitation frequency and lower frequency components. This phenomenon is more pronounced for the fingertip. Although displacement amplitudes of the shoulder and elbow joint do not change visibly, the mean value of the elbow joint angle is larger when visual compensation is allowed while pointing at the target (Figure 5.23).

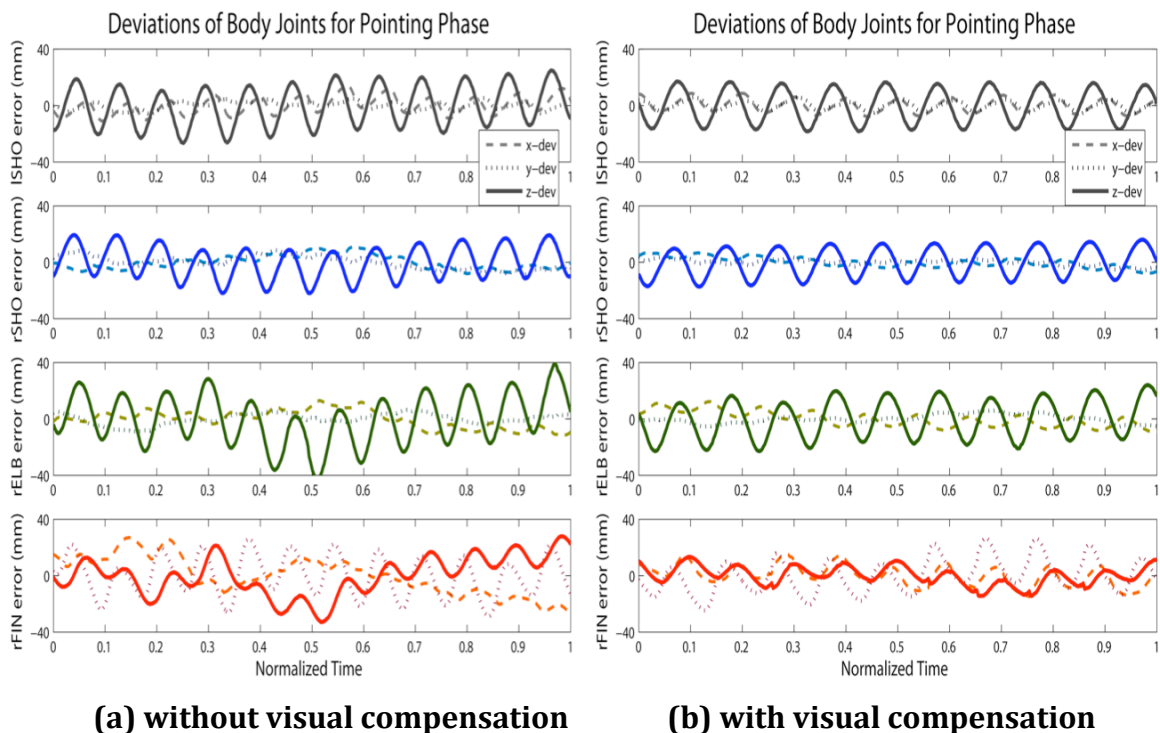
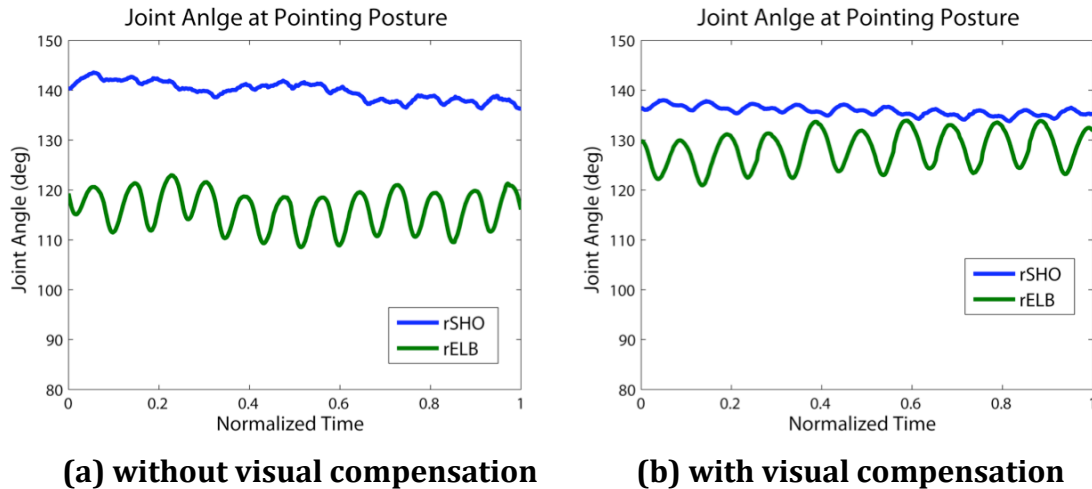


Figure 5.22 3-Dimensional displacements of upper limbs in diagonal and upward reach [TG5] for the 4 Hz vertical vibration



(a) without visual compensation (b) with visual compensation
Figure 5.23 Joint angles of the right shoulder and elbow in diagonal and upward reach [TG5] for the 4 Hz vertical vibration

5.3.2.2 Frequency Response and Vibration Transmission with Visual Compensation

As indicated in Figure 5.24, the peak values of vibration transmission through all body segments are reduced when performing reaching task with visual compensation. In addition, the low frequency perturbation of the body segment seems to be eliminated when vision of the hand and target is allowed during pointing.

The 3-way ANOVA including vision, target location, and vibration frequency as main factors indicates that visual compensation affects the z-component and total WBV transmission of the elbow and finger (Table 5.10). Interactions between these factors were not significant.

Three-dimensional and total transmissions are presented in Figure 5.21, 5.22, and 5.23 for the 2Hz, 4Hz, and 6Hz vertical vibration respectively. As indicated by the ANOVA, there is no significant change in the propagated transmission through the upper body, although perturbation of the joints is reduced by vision-induced feedback control.

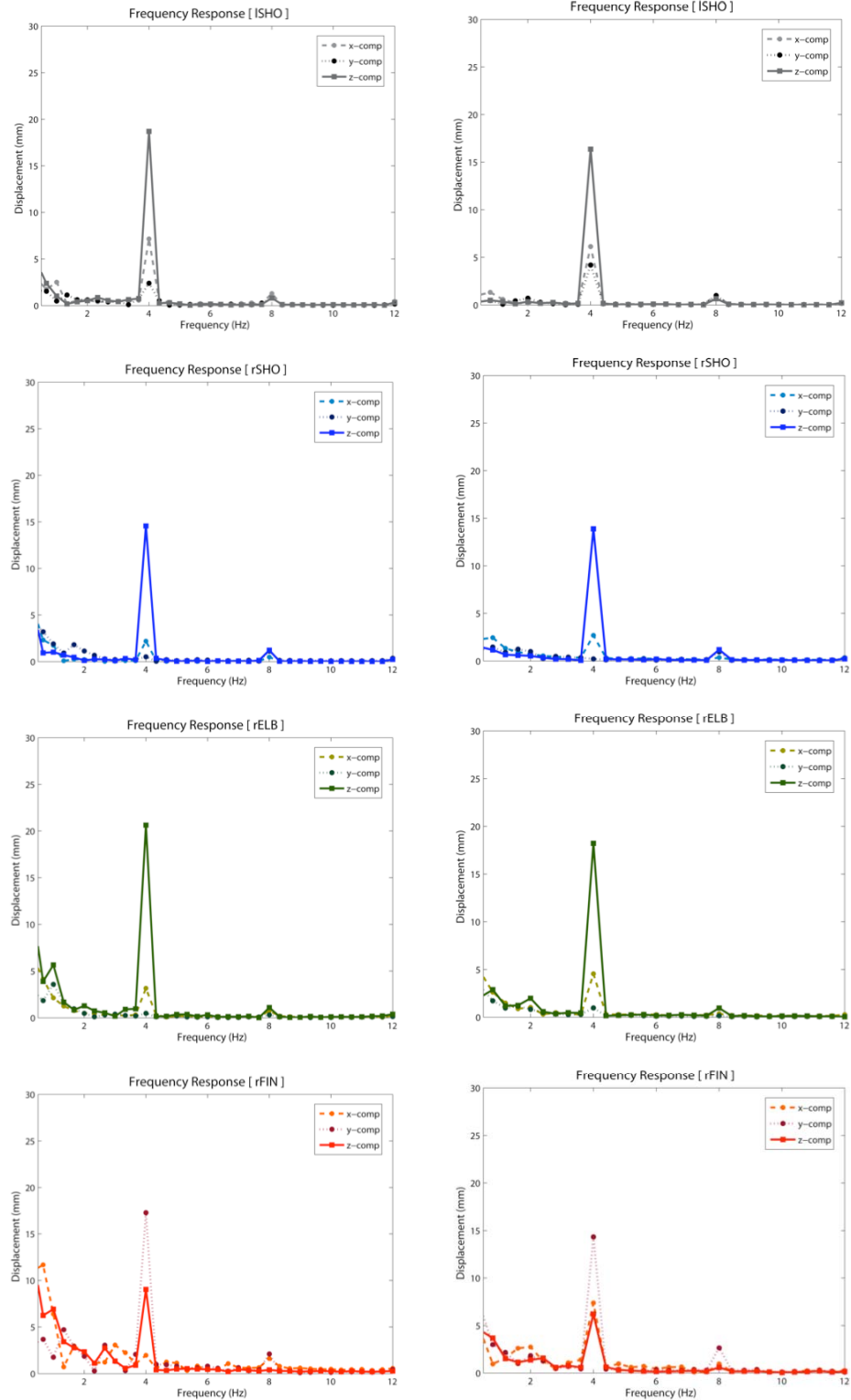
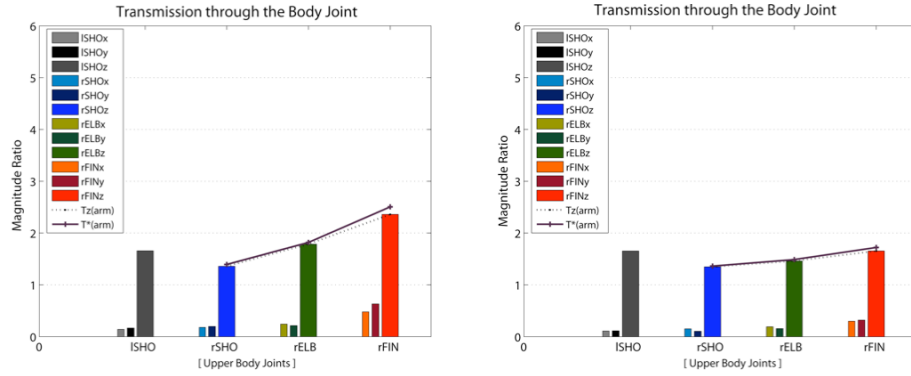


Figure 5.24: Frequency responses of upper limbs in diagonal and upward reach [TG5] for the 4 Hz vertical vibration: ISHO (1st row), rSHO (2nd row), rELB (3rd row), and rFIN (4th row) & without visual compensation (left), with visual compensation (right)

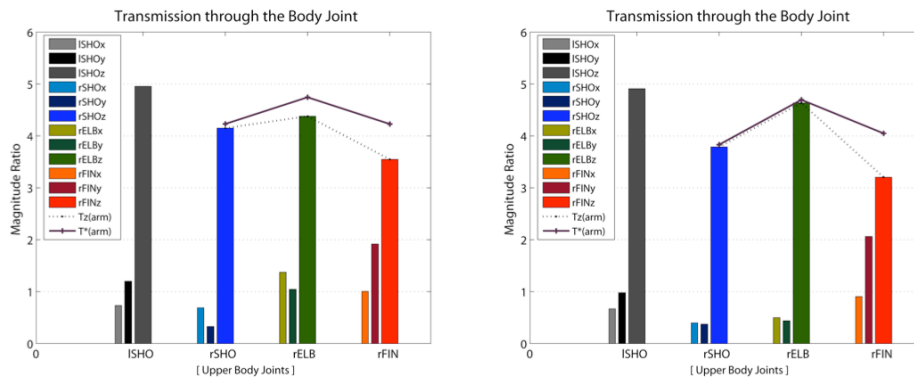
Table 5.10: 3-way ANOVA for Vision, Target location, and Vibration Frequency

	Transmission (ISHO)				
	DoF	p (T _X)	p (T _Y)	p (T _Z)	p (T _{TOTAL})
Vision	1	0.0356	0.1936	0.0397	0.5175
Target-L	5	0.0210	0.0641	0.0009	0.0055
Vib-Freq	2	0	0	0	0
Vision × Target-L	5	0.0500	0.0148	0.7925	0.2509
Vision × Vib-Freq	2	0.4029	0.0581	0.4308	0.2167
Target-L × Vib-Freq	10	0.1358	0.0322	0.0037	0.0101
	Transmission (rSHO)				
	DoF	p (T _X)	p (T _Y)	p (T _Z)	p (T _{TOTAL})
Vision	1	0.9389	0.1267	0.5286	0.2755
Target-L	5	0	0.0001	0	0
Vib-Freq	2	0	0	0	0
Vision × Target-L	5	0.8022	0.8421	0.6457	0.5877
Vision × Vib-Freq	2	0.0824	0.7329	0.3782	0.2947
Target-L × Vib-Freq	10	0.0001	0.0012	0	0
	Transmission (rELB)				
	DoF	p (T _X)	p (T _Y)	p (T _Z)	p (T _{TOTAL})
Vision	1	0.7607	0.9832	0.0007	0.0011
Target-L	5	0	0	0	0
Vib-Freq	2	0	0	0	0
Vision × Target-L	5	0.1597	0.7170	0.2396	0.4117
Vision × Vib-Freq	2	0.3622	0.3204	0.0060	0.0056
Target-L × Vib-Freq	10	0	0	0	0
	Transmission (rFIN)				
	DoF	p (T _X)	p (T _Y)	p (T _Z)	p (T _{TOTAL})
Vision	1	0.0599	0.0228	0.0096	0.0027
Target-L	5	0.0241	0.0001	0	0.0002
Vib-Freq	2	0	0	0	0
Vision × Target-L	5	0.3038	0.1754	0.6322	0.7170
Vision × Vib-Freq	2	0.6992	0.4488	0.0088	0.0666
Target-L × Vib-Freq	10	0.0140	0.0039	0.0039	0.0615



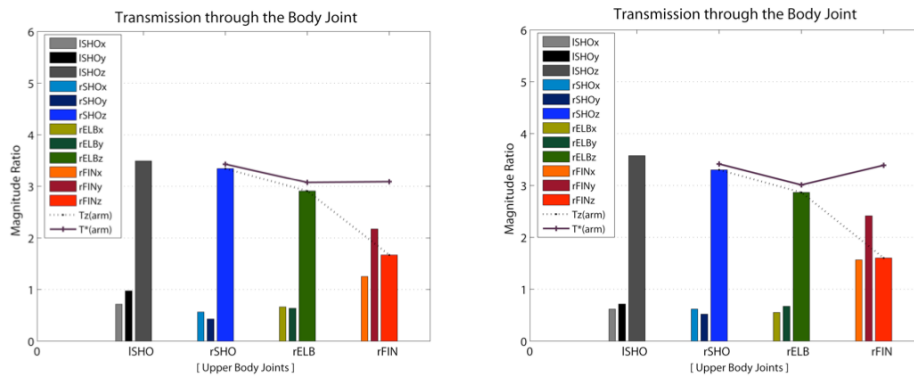
(a) without visual compensation (b) with compensation

Figure 5.25: Vibration transmission through upper body segments for diagonal-upward reach [TG5] under the 2Hz vertical WBV



(a) without visual compensation (b) with compensation

Figure 5.26: Peak of vibration transmission through upper body segments for diagonal-upward reach [TG5] under the 4Hz vertical WBV



(a) without visual compensation (b) with compensation

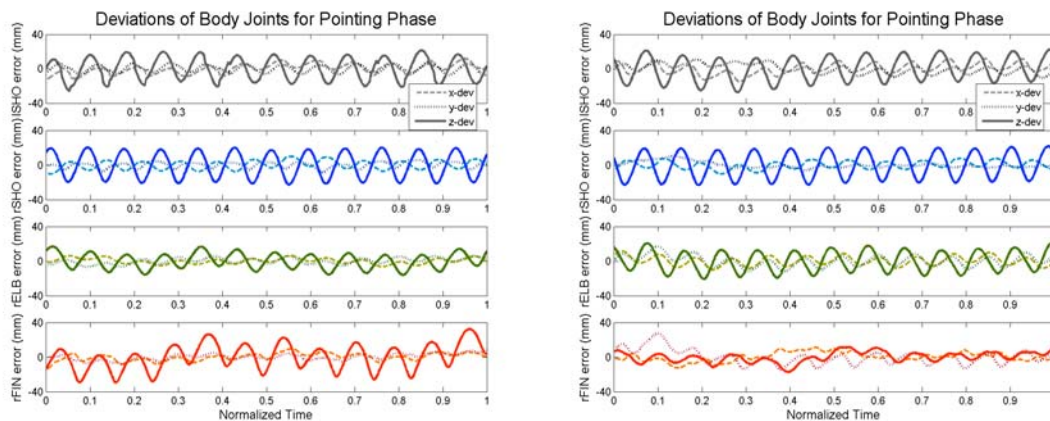
Figure 5.27: Peak of vibration transmission through upper body segments for diagonal-upward reach [TG5] under the 6Hz vertical WBV

5.3.3 Effects of Elbow Extension or Flexion on Vibration Transmission

Based on their similarity in transmission trend (see appendix A), two reach groups were distinguished: 1) horizontal reaches (diagonal [TG4] and lateral near [TG6]) and 2) upward reaches requiring shoulder flexion (upward [TG1], forward-upward [TG2], and diagonal-upward [TG5]). Diagonal reach [TG4] and diagonal-upward reach [TG5] are selected for representing each reach group, respectively.

5.3.3.1. Joint Displacements and Angles with Elbow Extended or Flexed

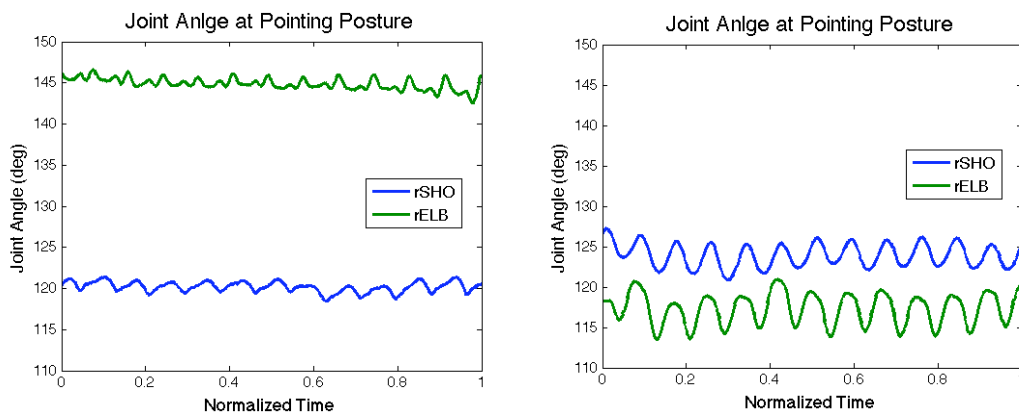
Posture



(a) Elbow extended posture

(b) Elbow flexed posture

Figure 5.28 3-dimensional displacements of upper limbs in diagonal reach [TG4] for the 4 Hz vertical vibration

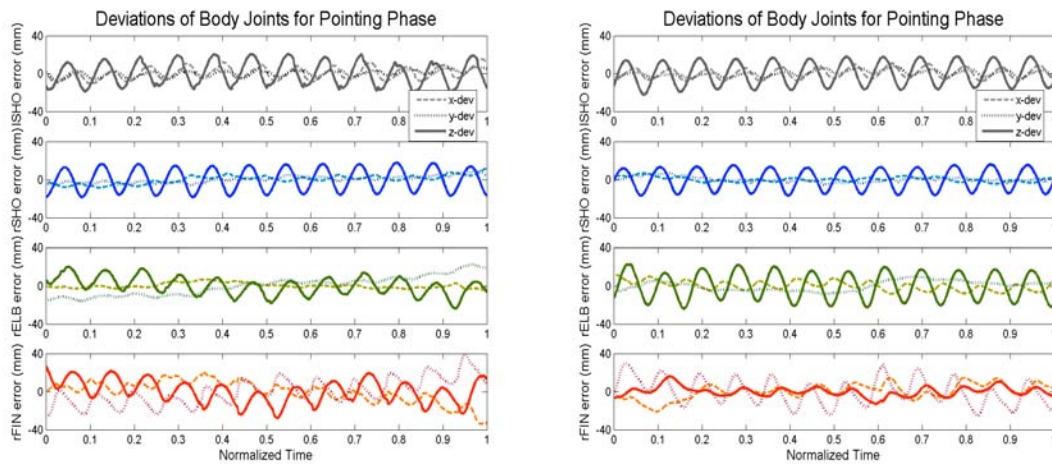


(a) Elbow extended posture

(b) Elbow flexed posture

Figure 5.29 Joint angles of the right shoulder and elbow in diagonal reach [TG4] for the 4 Hz vertical vibration

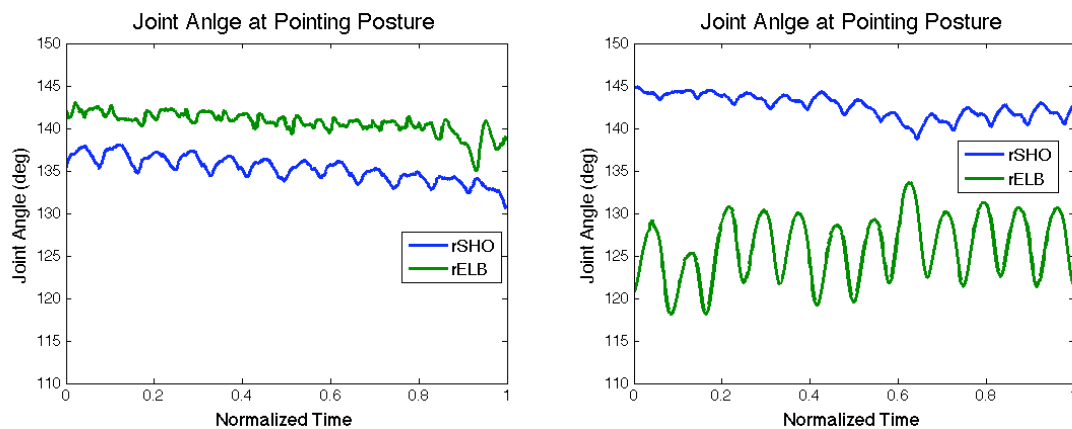
Displacements of the upper limbs when performing reaches to [TG4] and [TG5] with elbow constraint of extension/flexion are illustrated in Figure 5.28 and 5.30. The magnitude of elbow perturbation is smaller and the perturbation of the finger is larger for the elbow extended than for the elbow flexed posture. Figure 5.29 and 5.31 indicate that perturbations of all joint angles are smaller for the elbow extended than for the elbow flexed posture.



(a) Elbow extended posture

(b) Elbow flexed posture

Figure 5.30 3-dimensional displacements of upper limbs in diagonal-upward reach [TG5] for the 4 Hz vertical vibration



(a) Elbow extended posture

(b) Elbow flexed posture

Figure 5.31 Joint angles of the right shoulder and elbow in diagonal and upward reach [TG5] for the 4 Hz vertical vibration

5.3.3.2. Frequency Response and Vibration Transmission through Body Segments

Figure 5.32 and 5.33 illustrates the frequency responses of upper body joints for the lateral reach [TG4] and diagonal-upward reach [TG5] under the 4 Hz vertical vibration. The remarkable distinctions between elbow extended and flexed postures are that all three-directional responses of the elbow are larger and that the y-component of response at the finger is larger and z-component of response is smaller, for the flexed posture.

The 3-way ANOVA including elbow flexion, target location, and vibration frequency as main effects (Table 5.11), indicates that transmission through all upper body segments is affected by elbow posture as well as target location and vibration frequency. Especially, transmission of the elbow joint is significantly affected by the interaction between elbow posture and vibration frequency.

Three-dimensional transmission and total transmission through upper body segments when pointing to [TG4, diagonal reach] and [TG5, diagonal-upward] are illustrated in Figure 5.34 and 5.35. When the elbow is fully extended, the trend of transmission through the upper limbs is not altered by target location (see appendix A). Under the 2 Hz vibration, the magnitude of elbow extension does not affect transmission. Under the 4 Hz vibration, transmission through the elbow is larger with the elbow flexed than the elbow extended posture while transmission through the fingertip is smaller. Under the 6 Hz vibration, there is no significant difference in transmission through the shoulders and the elbow between two postures. Meanwhile, elbow flexed posture leads to a decrease in the z-component of transmission through the fingertip and an increase in cross-axis transmission through the fingertip; hence no significant difference in total transmission through the finger was observed.

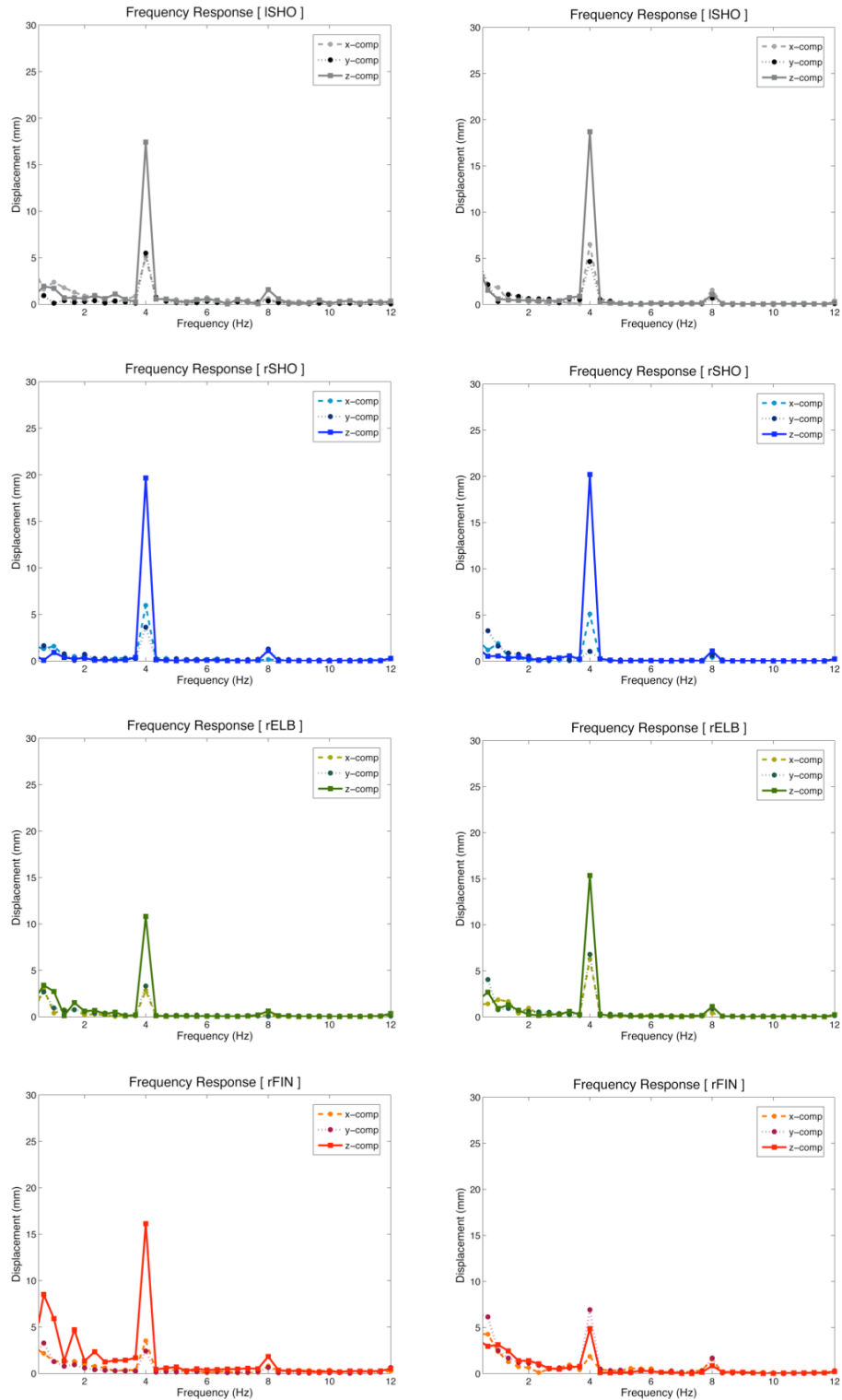


Figure 5.32: Frequency responses of upper limbs in diagonal reach [TG4] for the 4 Hz vertical vibration: ISHO (1st row), rSHO (2nd row), rELB (3rd row), and rFIN (4th row) & elbow extended posture (left) and elbow flexed posture (right)

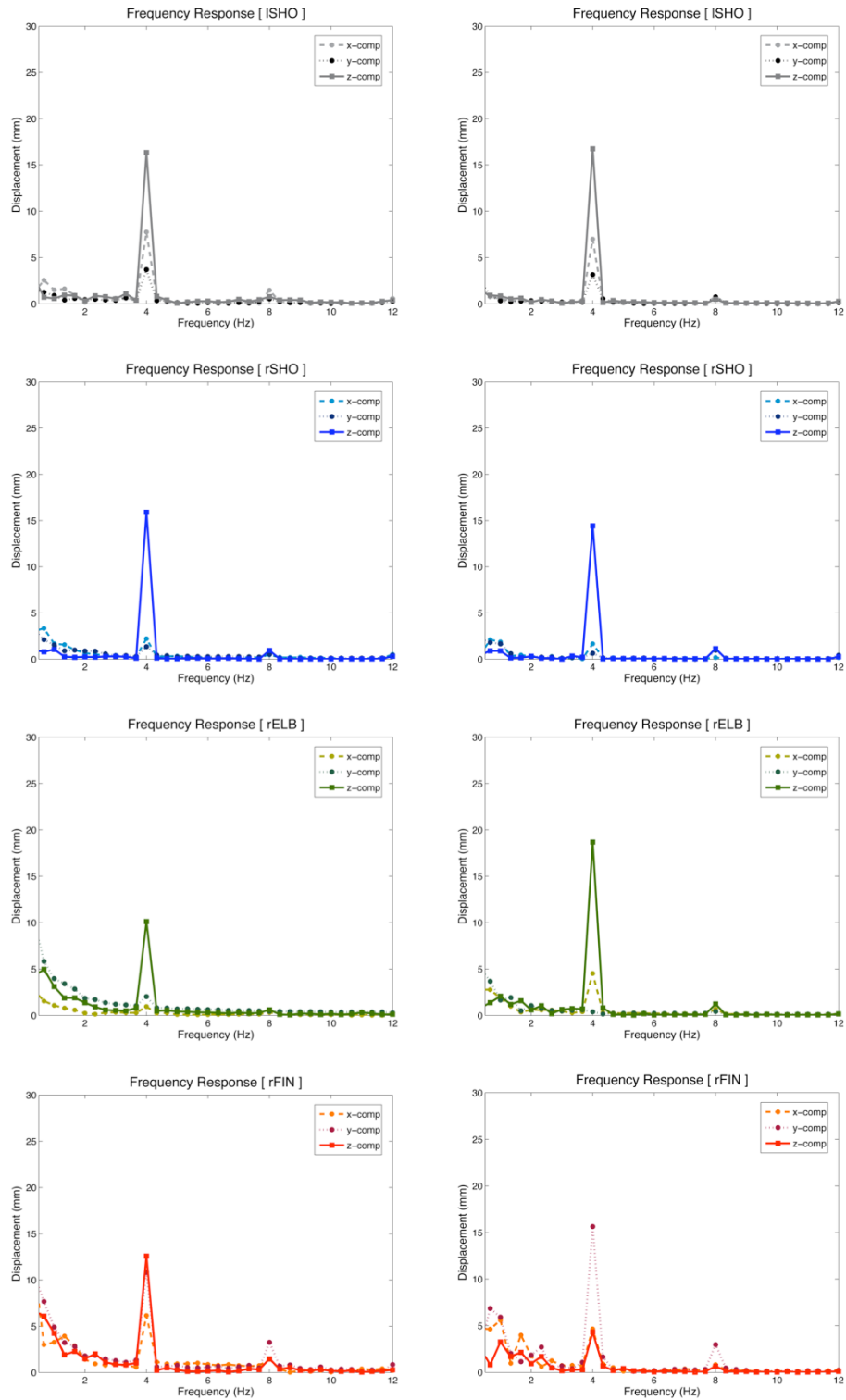


Figure 5.33: Frequency responses of upper limbs in diagonal-upward reach [TG5] for the 4 Hz vertical vibration: ISHO (1st row), rSHO (2nd row), rELB (3rd row), and rFIN (4th row) & elbow extended posture (left) and elbow flexed posture (right)

Table 5.11: 3-way ANOVA for Elbow, Target location, and Vibration Frequency

	Transmission (ISHO)				
	DoF	p (T _X)	p (T _Y)	p (T _Z)	p (T _{TOTAL})
Elbow-F	1	0.0378	0.0002	0	0.0001
Target-L	5	0.0151	0.0076	0.0095	0.0120
Vib-Freq	2	0	0	0	0
Elbow-F × Target-L	5	0.6689	0.1549	0.4304	0.8255
Elbow-F × Vib-Freq	2	0.4084	0.0007	0.0053	0.0234
Target-L × Vib-Freq	10	0.0587	0.0128	0.4503	0.5465
	Transmission (rSHO)				
	DoF	p (T _X)	p (T _Y)	p (T _Z)	p (T _{TOTAL})
Elbow-F	1	0.5546	0.0003	0.0057	0.0243
Target-L	5	0.0001	0.0032	0.0009	0.0005
Vib-Freq	2	0	0	0	0
Elbow-F × Target-L	5	0.0722	0.3814	0.1081	0.0811
Elbow-F × Vib-Freq	2	0.1311	0.0015	0.0954	0.2442
Target-L × Vib-Freq	10	0.0094	0.0764	0.0141	0.0134
	Transmission (rELB)				
	DoF	p (T _X)	p (T _Y)	p (T _Z)	p (T _{TOTAL})
Elbow-F	1	0.0074	0.0024	0.0003	0
Target-L	5	0.0016	0.0029	0.0052	0.0010
Vib-Freq	2	0	0	0	0
Elbow-F × Target-L	5	0.2694	0.3014	0.4974	0.5819
Elbow-F × Vib-Freq	2	0.0097	0.0312	0.0001	0
Target-L × Vib-Freq	10	0.0397	0.1353	0.0561	0.0395
	Transmission (rFIN)				
	DoF	p (T _X)	p (T _Y)	p (T _Z)	p (T _{TOTAL})
Elbow-F	1	0.6218	0.5277	0.0062	0.0013
Target-L	5	0.0371	0	0.6577	0.0009
Vib-Freq	2	0	0	0	0
Elbow-F × Target-L	5	0.1959	0.0162	0.0457	0.0312
Elbow-F × Vib-Freq	2	0.0435	0.6147	0.0307	0.0023
Target-L × Vib-Freq	10	0.2084	0.0001	0.7657	0.0314

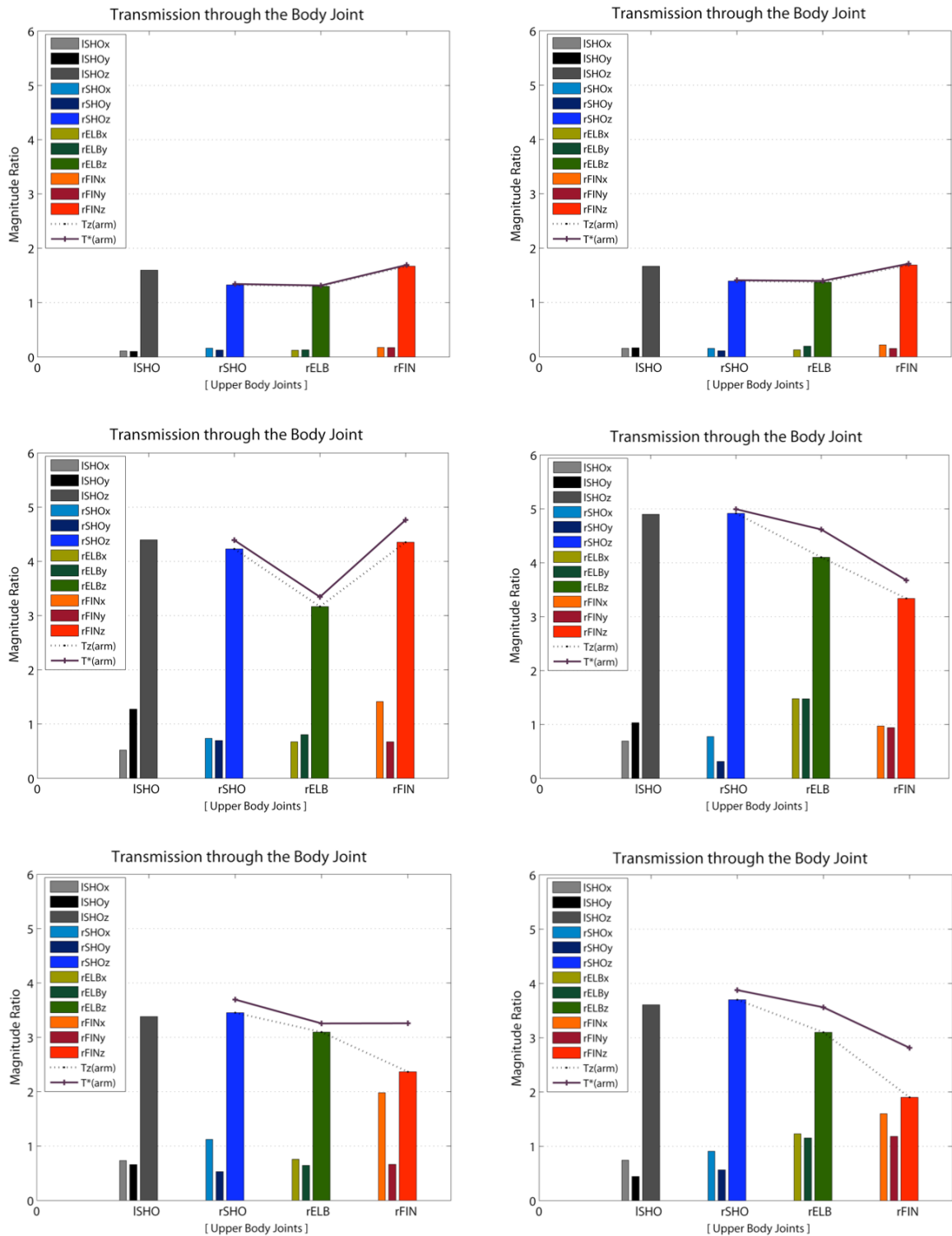


Figure 5.34: Vibration transmission of upper body segments in two pointing postures for lateral reach [TG4]: 2Hz (1st row), 4Hz (2nd row), and 6Hz (3rd row) & elbow extended posture (left) and elbow flexed posture (right)

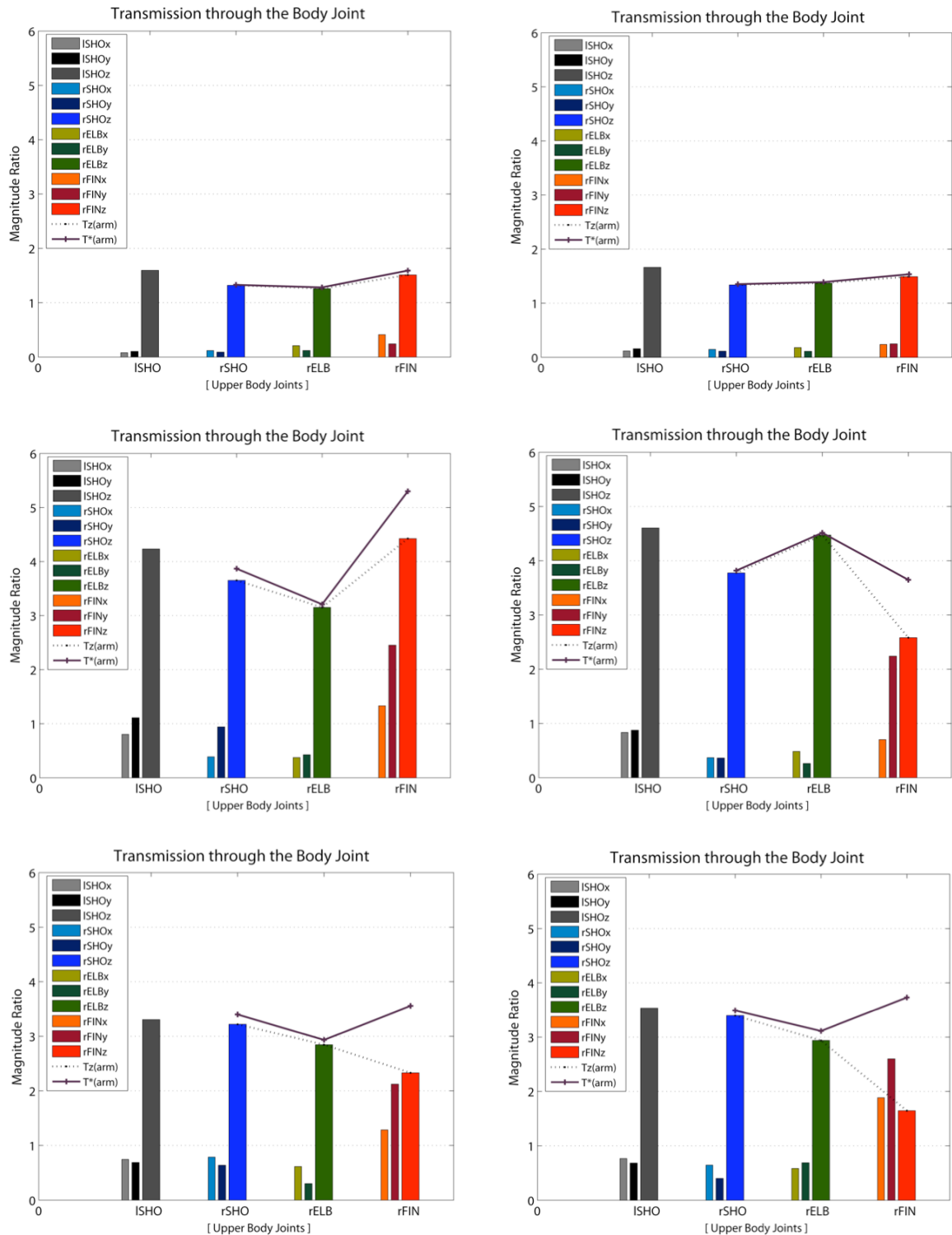


Figure 5.35: Vibration transmission of upper body segments in two pointing postures for diagonal and upward reach [TG5]: 2Hz (1st row), 4Hz (2nd row), and 6Hz (3rd row) & elbow extended posture (left) and elbow flexed posture (right)

5.4 Discussion

Vibration transmission through the upper body segment while performing a reach task is a function of posture and movement constraints as well as reach direction and vibration frequency. Vibration frequency is the dominant factor determining biodynamic responses and WBV transmission.

Specifically, posture change along the reach trajectories may affect vibration transmission through upper body segments, depending on movement direction and target distance. When a horizontal reach is required within the arm length distance, transmission is not significantly altered during the hand transition. However, when an upward reach is required, vibration transmission through the elbow increases largely. Elevation of the arm may lead to increase of muscle tension in a upper-arm and the higher center of mass of the arms may be much more difficult in maintaining stability, despite the fact that the upper-arm moment is smaller in this posture than in the arm extended forward posture. This phenomenon may be associated with the difference between the muscles to be controlled. In addition, when far reach beyond the arm length is required, torso leaning is necessary to complete a reaching task, thus producing the remarkable increase in vibration transmission through the fingertip. This instability may result from the large increase in the moment arm of the hand and the significant increase in torso instability associated with torso bending.

When visual feedback of the target location and hand position is allowed, vision-guided compensation can reduce slightly the peak values of transmission through all body segments, and reduce the contribution of a low frequency component in body perturbation. This stabilization may result from an improvement of body segment coordination to counteract the vibration-induced perturbation. However, visual compensation is not an active solution for improving

the task performance in vibratory environments, since vision compensation does not affect the trend of transmission along the path.

The posture fully extending the elbow influences WBV transmission for all reach directions, which suggests that stabilization of the arm is based primarily on elbow rather than shoulder muscle control. When the elbow is extended, the arm is likely to have to the same stiffness regardless of the azimuth or elevation; hence shoulder muscles may not be able to counteract the vibration-induced movement of the hand. The elbow constraint also interacts with vibration frequency. Under the 4Hz vibration exposure rather than under the 2 Hz and 6 Hz, effects of elbow constraint on WBV transmission along the path are more pronounced. The elbow extended posture contributes to a decrease in transmission through the elbow joint and an increase in transmission through the fingertip for all movement directions, except for overhead direction [TG1]. On the contrary, when the arm is elevated for upward reaches, the elbow flexed posture allows a large amount of vibration to be dissipated through the elbow and reduces the perturbation of the finger in the vertical direction. The elbow may play the role of a damping device that dissipates perturbation energy transmitted through the upper arm. However, since the hand is not anchored, cross-transmission increases along the transmission path from the shoulder to the fingertip, especially for the higher vibration frequency.

The interesting feature of WBV transmission through multi-body segments is that although auto-axial transmission through the upper limbs is small, the total transmission may be large due to an increase in large cross-transmission through the body segments and the orientation of the “elbow shock absorber” system relative to the direction of vibration. The cross-effects are more pronounced under 4 Hz and 6 Hz WBV than under 2 Hz vibration exposure. Therefore, for the proper assessment of the reach performance and the realistic prediction of WBV responses, cross-functional transmission must be also considered to provide a more complete

description of vertical vibration effects. Therefore, a biomechanical model must be developed on the basis of a multi-degrees-of-freedom system and not limited to the model simulating one directional motion.

5.5 Conclusions

These empirical analyses were performed to understand biodynamic characteristics of body segments during movements in vibratory environments. Vibration transmission through the upper limbs was determined as a function of vibration frequency, reaching movement direction and associated posture, postural variation along movement trajectory, visual compensation, and elbow extension/flexion. The present results constitute the empirical database that may be useful in the development of an active biodynamic model for the future work. The results also suggest that a model simplification may be derived from similarities in the propagated transmission through the upper limbs for movement direction zones.

CHAPTER 6

Empirical Support for a Model Representing the Biodynamic Response to Whole-Body Vibration during Upper Limb Movements in the Seated Posture

For the proper evaluation of WBV effects on reach performance and mechanical behavior of the seated operator in a dynamic environment, this work has investigated characteristics of WBV transmission as a function of vibration frequency, movement condition, and visual feedback. The integration of all results provide the groundwork for the development of a biomechanical model capable of simulating reach movements and performance of the upper limbs under WBV exposure. This model may also be used to evaluate the efficiency of suspension systems designed to reduce vibration transmission to vehicle operators.

6.1 Introduction

In order to effectively improve the designs of controls and workplaces for better performance of vehicle operators in vibratory environments, it is indispensable to understand the mechanism of upper body movements in the required task and the biodynamic responses of the upper body under WBV exposure.

Numerous studies have extensively analyzed kinematic features of arm movements and upper-body reach postures in static environments (Prablanc et al, 1979; Morrasso, 1981; Soechting and Lacquaniti, 1981; Atkeson and Hollerbach, 1985; Jeannerod and Marteniuk, 1992; Wang, 1991; Soechting et al, 1995; Haggard et al., 1995; Jung et al, 1995; Desmurget and Prablanc, 1997; Gielen et al, 1997; Gottlieb et al, 1997; Jeannerod et al, 1998; Wang, 1999; Zhang and Chaffin, 2000; Barreca and Guenther, 2001; Faraway, 2003; Kim, et al; 2004). They found invariant features in pointing and reaching movements concerning the hand trajectory and joint angular velocity profiles, In addition, several arm movement models based on an inverse kinematics approach or optimization methods have been derived from these studies (Rosenbaum et al, 1995; Jung et al, 1996; Zhang et al, 1998; Wang, 1999; Park et al, 2002; Jax et al, 2003; Kang et al, 2005). However, all these investigations were limited to small ranges of motion in static conditions. Therefore, these models may not be extended to the reach movements performed in vibratory environments.

To identify vibration responses of the human body, many studies have attempted to develop biomechanical models (Amirouche, 1987; Fritz, 1998; Wei and Griffin, 1998; Harrison et al, 2000; Hinz et al, 2001; Holmlund and Lundstrom, 2001; Griffin, 2001; Matsumoto and Griffin, 2001; Seidel and Griffin, 2001; Seidel et al, 2001; Paddan and Griffin, 2002; Rosen and Arcan, 2003; Kim et al, 2005; Yoshimura et al, 2005; Liang and Chiang, 2006; Mansfield et al, 2006; Mansfield et al, 2007; Okunribido et al, 2007; Oullier et al, 2009). The majority of these studies have

considered a multi degree-of-freedom system consisting of multiple mass-spring-damper system designed to estimate the effects of vibration on the spinal system of the seated human (Amirouche, 1987; Fritz, 1998; Wei and Griffin, 1998; Rosen and Arcan, 2003; Kim et al, 2005; Yoshimura et al, 2005; Stein et al, 2007). Limited to the upper torso in the static postures, their models did not include the arm movements. However, to represent and simulate the effects of vibration on manual performance, a model must consider vibration transmission through the arm-hand system in various configurations.

To overcome this limitation, the present work was initiated to establish the groundwork for the development of a biomechanical model. This chapter describes how future research for a model development may be expanded based on the estimation of WBV transmission through multi-body segments as a function of upper body posture and vibration characteristics.

6.2 Groundwork for a Biodynamic Response Model

For the development of manageable biomechanical model, it is necessary to limit the degrees-of-freedom of the model and thus find possible simplifications by exploring experimental data. The biomechanical or physiological properties dominantly affecting reach kinematics or dynamic characteristics of the upper body segments need to be defined as well, since they influence muscle/joint stiffness and damping.

The biomechanical response model derived from this work focuses on the responses at the right shoulder, the elbow, and fingertip along the transmission path to the hand in a reaching task (see Figure 6.1). A tensor of transmission including auto-axial and cross-axial transmission was considered to quantify WBV response (see Eq.5.1), since the vertical vibration input produces the relative motions of

upper body segments in the horizontal plane as well as the response in the vertical direction as reported in previous chapters.

Figure 6.2 illustrate a simple example model based on five-lumped-mass system representing the multi-segmental upper body. This model must be extended to 3-dimensional representation with at least eleven degrees-of-freedom (1-cab, 3-trunk, 3-upperarm, 3-forearm-hand, and 1-head) for realistic modeling and simulation of upper body movements under vibration exposure.

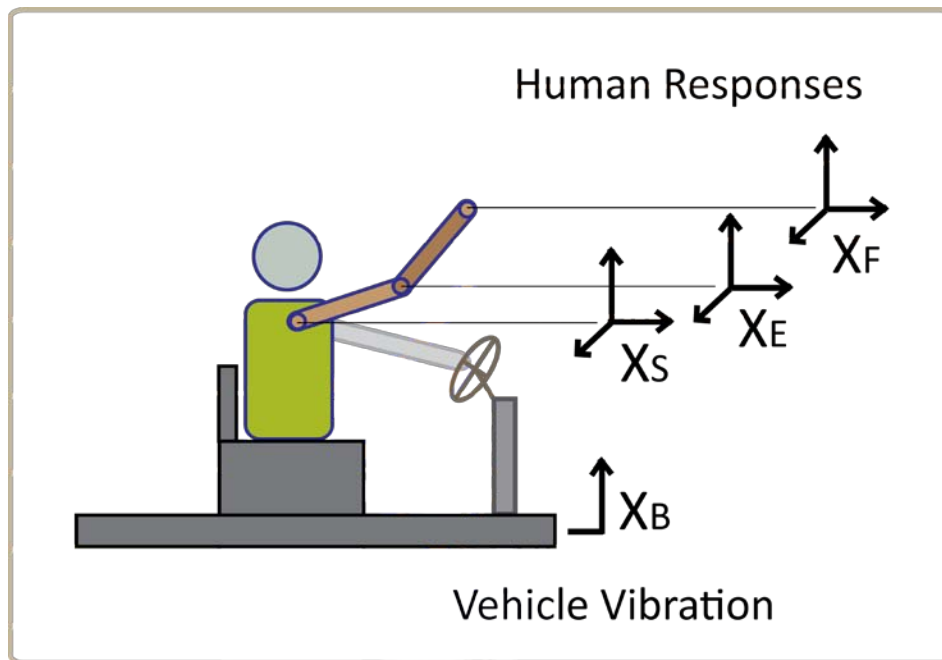


Figure 6.1: Vibration input and human body segment responses through the biodynamic system

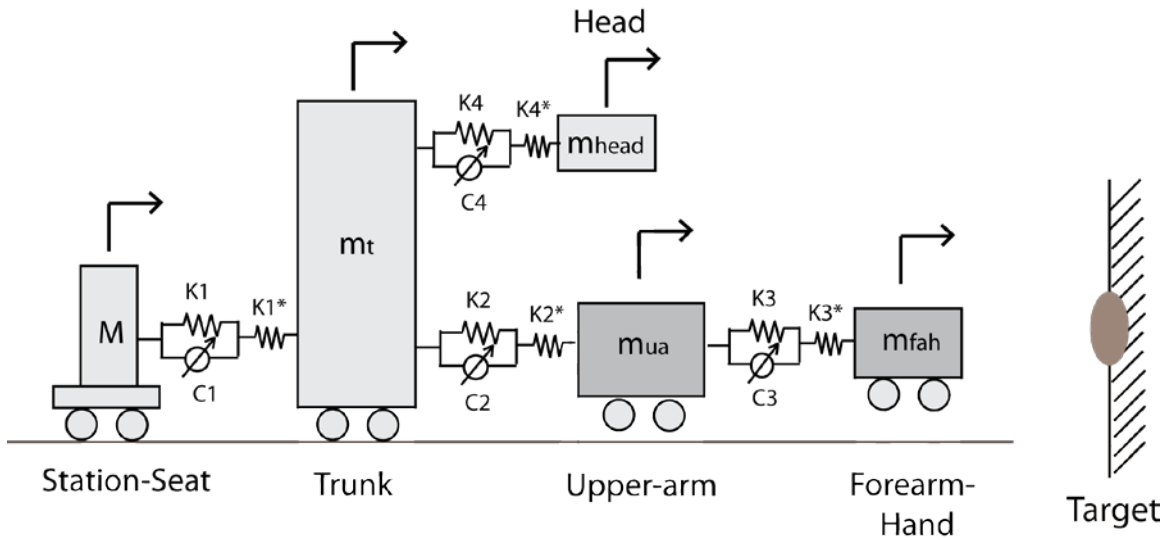


Figure 6.2: The simple biomechanical model to represent the upper body segments with equivalent parallel/series elements. The control of joints or segment stiffness is not represented.

The mass of body segments can be estimated by the percentage distribution of total body weight according to different segmentation plans (Chaffin, 1999; Table B.1). Joint stiffness can be derived from hand stiffness (Flash and Mussa-Ivaldi, 1990). Hand stiffness $[K]$ can be estimated by the relationship between force $[F]$ and displacement vectors $[dx]$ (Eq.6.1). The shape and orientation of the hand stiffness ellipse are highly dependent on arm configuration. Once the force and displacement vectors are measured for a given hand position, the matrix of hand stiffness can be obtained by a linear least squares regression algorithm.

$$\underline{F} = -\underline{K} \underline{dx} \quad \dots\dots\dots \text{(Eq. 6.1)}$$

The joint stiffness matrix $[\underline{R}]$ is relating joint torques $[\underline{T}]$ to joint angles $[d\theta]$ (Eq.6.2), R_{SS} and R_{EE} are the net shoulder and elbow stiffness, and R_{SE} and R_{ES} relate shoulder torque to elbow displacement, and R_{ES} relates elbow torque to shoulder displacement respectively (Eq.6.3). The joint stiffness matrix $[\underline{R}]$ can be

derived from hand stiffness matrix [\underline{K}] and the jacobian matrix [\underline{J}] relating hand velocity to joint angular velocity (Eq.6.4).

$$\underline{T} = \underline{R} d\underline{\theta} \quad \dots\dots\dots \text{(Eq. 6.2)}$$

$$\underline{R} = \begin{bmatrix} R_{SS} & R_{SE} \\ R_{ES} & R_{EE} \end{bmatrix} = \begin{bmatrix} R_S + R_T & R_T \\ R_T & R_E + R_T \end{bmatrix} \quad \dots\dots\dots \text{(Eq. 6.3)}$$

$$\underline{R} = \underline{J}^T \underline{K} \underline{J} \quad \dots\dots\dots \text{(Eq. 6.4)}$$

In addition, joint stiffness is dependent on muscle activity. For example, a relationship between the EMG signals from the biceps, long head of triceps, lateral head of triceps, anterior deltoid, lateral deltoid, posterior deltoid, and pectoralis muscles and joint stiffness has been proposed (Flash and Mussa-Ivaldi, 1990). Furthermore, these authors also indicated that joint stiffness and EMG amplitudes were functions of shoulder and elbow joint angles.

As presented in Chapter 5, three groups of reach direction were identified based on WBV transmission characteristics through the upper body segments. TG4 [diagonal reach], TG5 [diagonal-upward reach], and TG7 [lateral far reach] were selected as representative targets for each group. The shoulder and elbow angles while reaching the targets are listed in Table 6.2. Three-dimensional reach postures, joint trajectories in task space, frequency responses at selected landmarks, and peak transmission tensors are illustrated in Figure 6.3, 6.4 and 6.5 for the representative reaches respectively. WBV transmission through the right shoulder, elbow, and fingertip are listed in Table 6.2 – 6.9. These biomechanical responses associated with the estimation of the biomechanical properties of the multi-linkage system can

be used to develop a biomechanical model to simulate the seated reach movements under vibration exposure.

Table 6.1: Shoulder and elbow joint angles during reaching three representative target locations, [TG4], [TG5], and [TG7]

Joint Angle	TG4 (Diagonal)		TG5 (Diagonal-Upward)		TG7 (Lateral Far)	
	SHO (°)	ELB (°)	SHO (°)	ELB (°)	SHO (°)	ELB (°)
Min	125.88	113.70	136.31	108.54	150.88	141.62
Mean	128.49	118.98	139.87	116.15	153.54	149.15
Max	131.75	122.64	143.54	122.96	156.75	154.48

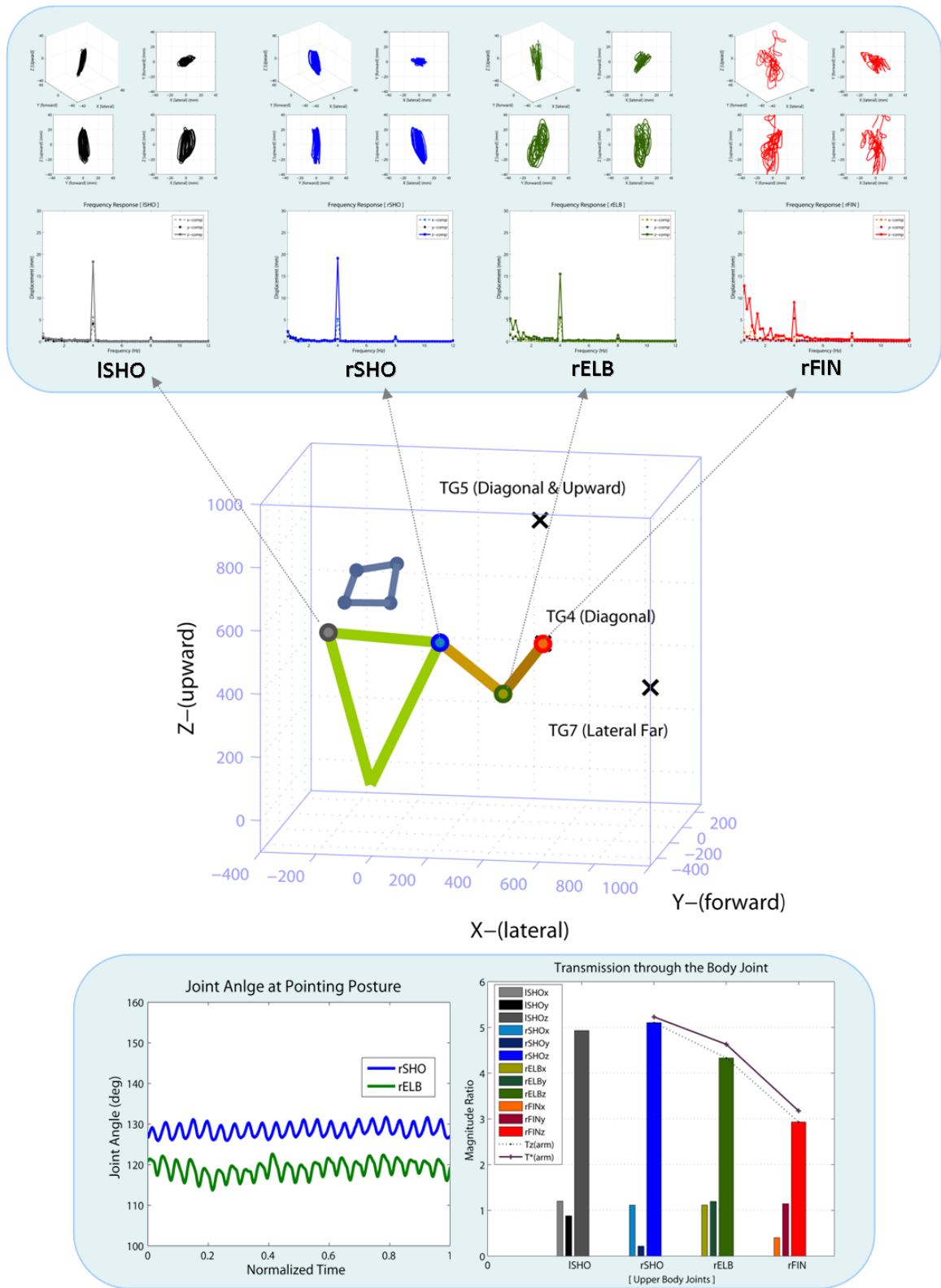


Figure 6.3: Reach posture, joint trajectories in task space, frequency responses, and transmission through upper right joints under 4 Hz vertical vibration exposure [TG4]

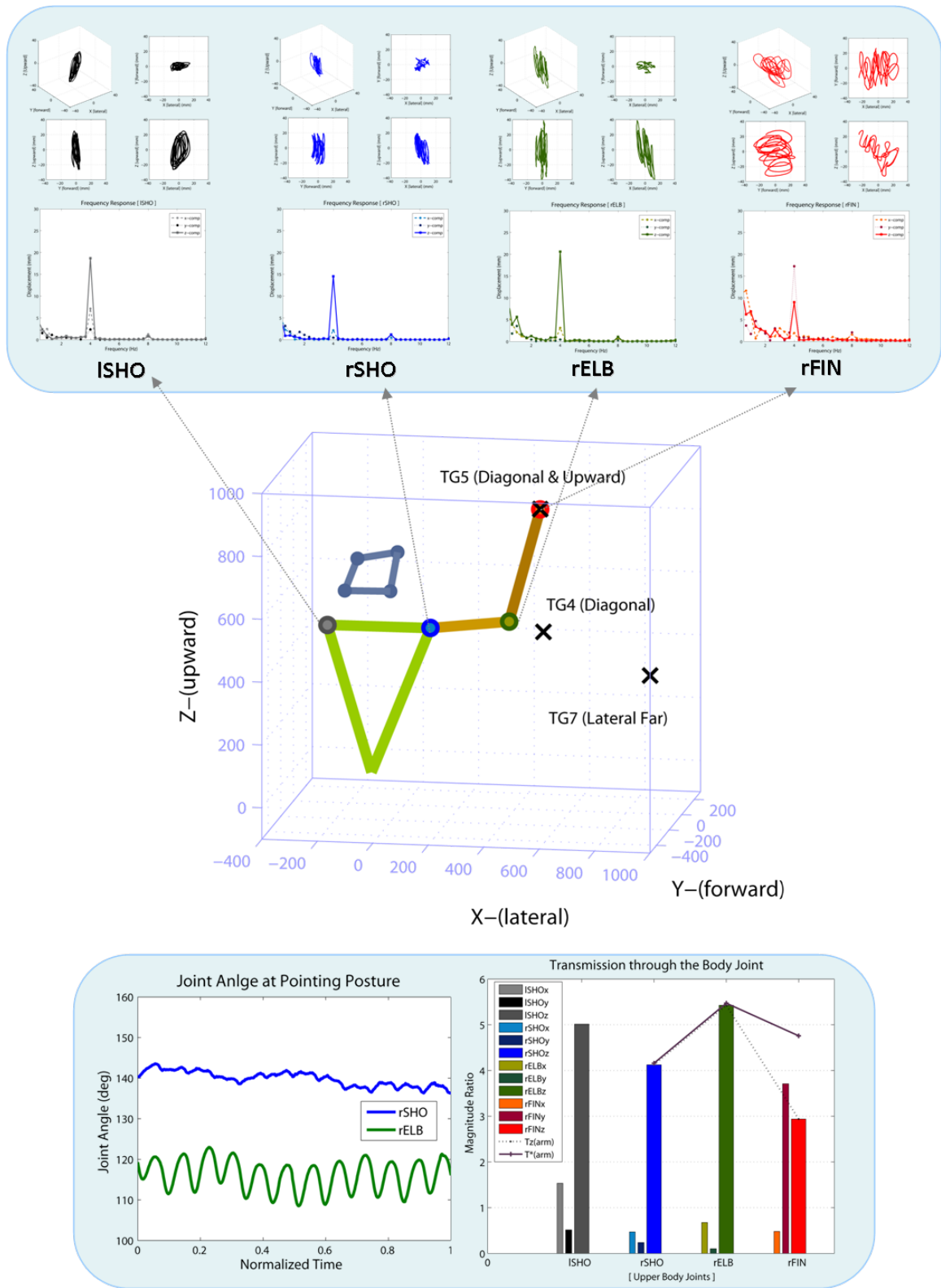


Figure 6.4: Reach posture, joint trajectories in task space, frequency responses, and transmission through upper right joints under 4 Hz vertical vibration exposure [TG5]

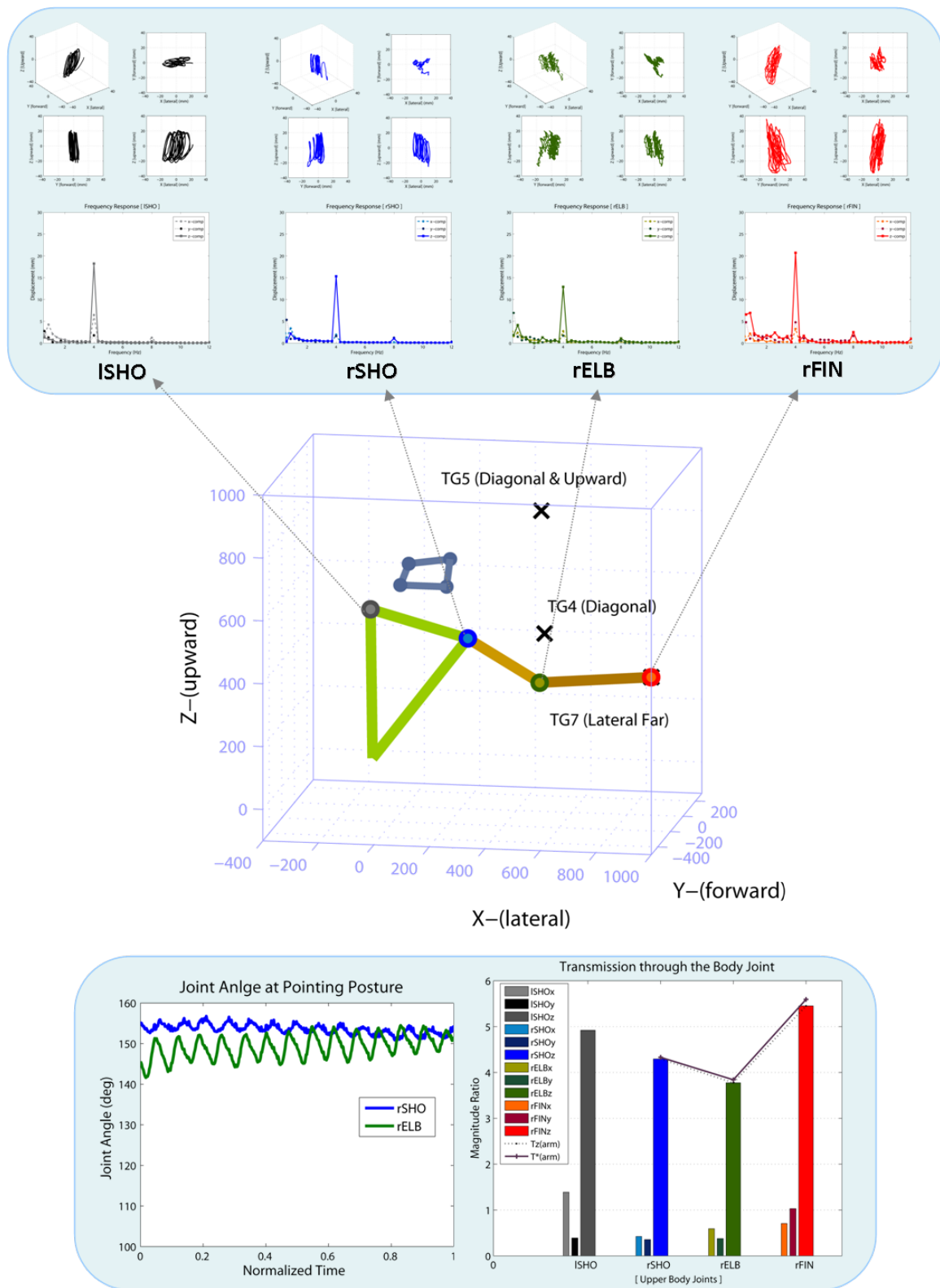


Figure 6.5: Reach posture, joint trajectories in task space, frequency responses, and transmission through upper right joints under 4 Hz vertical vibration exposure [TG7]

Table 6.2: Vibration transmission for each body segment (Mean \pm SD) [Session I – under the 2Hz vertical vibration exposure]

		No Visual Feedback											
		2Hz Vertical Vibration Exposure											
		Right Shoulder				Right Elbow				Right Fingertip			
		SHOx	SHOy	SHOz	SHOt	ELBx	ELBy	ELBz	ELBt	FINx	FINy	FINz	FINt
TG1	1-2	0.16 ± 0.03	0.20 ± 0.13	1.41 ± 0.07	1.44 ± 0.07	0.09 ± 0.03	0.25 ± 0.10	1.55 ± 0.19	1.58 ± 0.19	0.14 ± 0.05	0.34 ± 0.14	1.93 ± 0.38	1.97 ± 0.39
	1-3	0.17 ± 0.04	0.16 ± 0.13	1.36 ± 0.03	1.38 ± 0.05	0.17 ± 0.05	0.17 ± 0.07	1.63 ± 0.31	1.65 ± 0.31	0.14 ± 0.07	0.34 ± 0.17	1.74 ± 0.34	1.79 ± 0.35
	1-4	0.18 ± 0.01	0.12 ± 0.08	1.37 ± 0.04	1.38 ± 0.03	0.24 ± 0.06	0.20 ± 0.05	1.60 ± 0.17	1.63 ± 0.17	0.16 ± 0.04	0.34 ± 0.22	1.64 ± 0.17	1.70 ± 0.16
TG2	2-2	0.16 ± 0.03	0.20 ± 0.13	1.41 ± 0.07	1.44 ± 0.07	0.09 ± 0.03	0.25 ± 0.10	1.55 ± 0.19	1.58 ± 0.19	0.14 ± 0.05	0.34 ± 0.14	1.93 ± 0.38	1.97 ± 0.39
	2-3	0.17 ± 0.03	0.25 ± 0.18	1.40 ± 0.05	1.45 ± 0.06	0.14 ± 0.10	0.23 ± 0.12	1.61 ± 0.22	1.64 ± 0.23	0.17 ± 0.13	0.42 ± 0.16	1.83 ± 0.37	1.89 ± 0.39
	2-4	0.18 ± 0.02	0.19 ± 0.11	1.37 ± 0.04	1.40 ± 0.04	0.15 ± 0.06	0.16 ± 0.07	1.56 ± 0.25	1.58 ± 0.25	0.24 ± 0.12	0.44 ± 0.20	2.02 ± 0.45	2.09 ± 0.49
TG4	4-2	0.16 ± 0.03	0.20 ± 0.13	1.41 ± 0.07	1.44 ± 0.07	0.09 ± 0.03	0.25 ± 0.10	1.55 ± 0.19	1.58 ± 0.19	0.14 ± 0.05	0.34 ± 0.14	1.93 ± 0.38	1.97 ± 0.39
	4-3	0.16 ± 0.02	0.19 ± 0.12	1.40 ± 0.06	1.43 ± 0.07	0.16 ± 0.07	0.25 ± 0.09	1.49 ± 0.21	1.52 ± 0.20	0.24 ± 0.13	0.27 ± 0.10	1.77 ± 0.54	1.81 ± 0.55
	4-4	0.16 ± 0.04	0.23 ± 0.14	1.37 ± 0.05	1.41 ± 0.07	0.15 ± 0.08	0.24 ± 0.12	1.56 ± 0.29	1.59 ± 0.28	0.27 ± 0.17	0.24 ± 0.09	2.45 ± 0.82	2.49 ± 0.80
TG5	5-2	0.16 ± 0.02	0.21 ± 0.12	1.42 ± 0.05	1.45 ± 0.05	0.14 ± 0.07	0.24 ± 0.12	1.57 ± 0.22	1.60 ± 0.20	0.26 ± 0.15	0.30 ± 0.11	1.92 ± 0.43	1.97 ± 0.44
	5-3	0.17 ± 0.04	0.18 ± 0.11	1.39 ± 0.04	1.42 ± 0.05	0.17 ± 0.06	0.21 ± 0.06	1.72 ± 0.35	1.75 ± 0.33	0.34 ± 0.14	0.38 ± 0.20	2.06 ± 0.57	2.13 ± 0.58
	5-4	0.18 ± 0.05	0.20 ± 0.15	1.36 ± 0.04	1.39 ± 0.06	0.24 ± 0.11	0.21 ± 0.11	1.79 ± 0.46	1.82 ± 0.47	0.48 ± 0.34	0.63 ± 0.52	2.36 ± 1.01	2.51 ± 1.16
TG6	6-2	0.16 ± 0.02	0.19 ± 0.12	1.40 ± 0.06	1.43 ± 0.07	0.16 ± 0.07	0.25 ± 0.09	1.49 ± 0.21	1.52 ± 0.20	0.24 ± 0.13	0.27 ± 0.10	1.77 ± 0.54	1.81 ± 0.55
	6-3	0.17 ± 0.03	0.20 ± 0.09	1.40 ± 0.03	1.43 ± 0.05	0.20 ± 0.08	0.14 ± 0.05	1.62 ± 0.25	1.65 ± 0.25	0.22 ± 0.06	0.27 ± 0.07	2.39 ± 0.70	2.41 ± 0.70
	6-4	0.19 ± 0.05	0.19 ± 0.12	1.38 ± 0.05	1.41 ± 0.07	0.24 ± 0.15	0.14 ± 0.06	1.64 ± 0.34	1.67 ± 0.35	0.18 ± 0.06	0.29 ± 0.10	2.63 ± 0.95	2.66 ± 0.95
TG7	7-2	0.16 ± 0.02	0.19 ± 0.12	1.40 ± 0.06	1.43 ± 0.07	0.16 ± 0.07	0.25 ± 0.09	1.49 ± 0.21	1.52 ± 0.20	0.24 ± 0.13	0.27 ± 0.10	1.77 ± 0.54	1.81 ± 0.55
	7-3	0.16 ± 0.03	0.16 ± 0.13	1.38 ± 0.06	1.40 ± 0.08	0.20 ± 0.10	0.13 ± 0.04	1.53 ± 0.33	1.55 ± 0.34	0.19 ± 0.06	0.30 ± 0.15	2.11 ± 0.96	2.15 ± 0.97
	7-4	0.24 ± 0.04	0.13 ± 0.04	1.30 ± 0.07	1.33 ± 0.07	0.21 ± 0.10	0.23 ± 0.20	1.65 ± 0.36	1.69 ± 0.38	0.23 ± 0.11	0.29 ± 0.16	2.63 ± 1.06	2.66 ± 1.06

Table 6.3: Vibration transmission for each body segment (Mean \pm SD) [Session I – under the 4Hz vertical vibration exposure]

		No Visual Feedback											
		4Hz Vertical Vibration Exposure											
		Right Shoulder				Right Elbow				Right Fingertip			
		SHOx	SHOy	SHOz	SHOt	ELBx	ELBy	ELBz	ELBt	FINx	FINy	FINz	FINt
TG1	1-2	0.77 ± 0.39	0.53 ± 0.26	4.81 ± 0.64	4.92 ± 0.69	1.43 ± 0.51	1.96 ± 0.55	3.82 ± 0.33	4.58 ± 0.41	0.97 ± 0.34	1.42 ± 0.65	4.15 ± 0.66	4.54 ± 0.75
	1-3	0.50 ± 0.13	0.36 ± 0.13	3.83 ± 0.34	3.88 ± 0.35	0.43 ± 0.27	0.31 ± 0.13	4.53 ± 0.30	4.57 ± 0.30	0.97 ± 0.37	0.76 ± 0.69	3.54 ± 0.64	3.85 ± 0.51
	1-4	0.25 ± 0.13	0.36 ± 0.21	3.74 ± 0.31	3.77 ± 0.31	1.06 ± 0.37	0.74 ± 0.36	4.80 ± 0.29	4.99 ± 0.39	1.66 ± 0.70	1.35 ± 0.69	4.00 ± 0.50	4.65 ± 0.42
TG2	2-2	0.77 ± 0.39	0.53 ± 0.26	4.81 ± 0.64	4.92 ± 0.69	1.43 ± 0.51	1.96 ± 0.55	3.82 ± 0.33	4.58 ± 0.41	0.97 ± 0.34	1.42 ± 0.65	4.15 ± 0.66	4.54 ± 0.75
	2-3	0.78 ± 0.42	0.31 ± 0.04	4.32 ± 0.51	4.42 ± 0.57	1.12 ± 0.53	1.34 ± 0.39	4.19 ± 0.24	4.58 ± 0.34	0.99 ± 0.52	1.75 ± 0.60	3.50 ± 0.52	4.10 ± 0.62
	2-4	0.66 ± 0.39	0.37 ± 0.14	3.93 ± 0.43	4.01 ± 0.48	0.51 ± 0.11	0.47 ± 0.17	4.98 ± 0.27	5.03 ± 0.27	0.59 ± 0.26	2.31 ± 1.04	3.24 ± 0.81	4.10 ± 1.06
TG4	4-2	0.77 ± 0.39	0.53 ± 0.26	4.81 ± 0.64	4.92 ± 0.69	1.43 ± 0.51	1.96 ± 0.55	3.82 ± 0.33	4.58 ± 0.41	0.97 ± 0.34	1.42 ± 0.65	4.15 ± 0.66	4.54 ± 0.75
	4-3	0.74 ± 0.31	0.44 ± 0.27	4.94 ± 0.58	5.03 ± 0.62	1.89 ± 0.51	1.63 ± 0.39	4.13 ± 0.28	4.85 ± 0.46	1.53 ± 0.54	0.82 ± 0.25	4.06 ± 0.58	4.44 ± 0.69
	4-4	0.83 ± 0.31	0.40 ± 0.21	4.92 ± 0.52	5.01 ± 0.55	1.56 ± 0.48	1.35 ± 0.32	4.25 ± 0.24	4.75 ± 0.41	0.99 ± 0.56	0.88 ± 0.34	4.01 ± 0.56	4.27 ± 0.61
TG5	5-2	0.82 ± 0.35	0.35 ± 0.10	4.70 ± 0.56	4.79 ± 0.59	1.67 ± 0.53	1.63 ± 0.45	4.01 ± 0.21	4.68 ± 0.38	1.32 ± 0.54	1.44 ± 0.50	3.76 ± 0.56	4.27 ± 0.77
	5-3	0.69 ± 0.34	0.33 ± 0.11	4.15 ± 0.54	4.23 ± 0.58	1.37 ± 0.43	1.05 ± 0.34	4.38 ± 0.49	4.74 ± 0.44	1.01 ± 0.57	1.92 ± 0.64	3.55 ± 0.57	4.23 ± 0.69
	5-4	0.39 ± 0.22	0.31 ± 0.07	3.76 ± 0.35	3.80 ± 0.36	0.45 ± 0.21	0.47 ± 0.24	4.93 ± 0.41	4.98 ± 0.41	0.76 ± 0.26	2.56 ± 0.89	3.25 ± 0.68	4.30 ± 0.74
TG6	6-2	0.74 ± 0.31	0.44 ± 0.27	4.94 ± 0.58	5.03 ± 0.62	1.89 ± 0.51	1.63 ± 0.39	4.13 ± 0.28	4.85 ± 0.46	1.53 ± 0.54	0.82 ± 0.25	4.06 ± 0.58	4.44 ± 0.69
	6-3	0.56 ± 0.24	0.43 ± 0.25	4.77 ± 0.42	4.83 ± 0.45	1.81 ± 0.52	1.12 ± 0.18	4.08 ± 0.23	4.62 ± 0.38	0.90 ± 0.29	0.57 ± 0.35	3.98 ± 0.47	4.15 ± 0.51
	6-4	0.49 ± 0.21	0.53 ± 0.36	4.98 ± 0.42	5.05 ± 0.45	1.90 ± 0.27	0.72 ± 0.38	4.55 ± 0.43	5.00 ± 0.51	0.80 ± 0.22	0.83 ± 0.40	4.88 ± 0.59	5.03 ± 0.59
TG7	7-2	0.74 ± 0.31	0.44 ± 0.27	4.94 ± 0.58	5.03 ± 0.62	1.89 ± 0.51	1.63 ± 0.39	4.13 ± 0.28	4.85 ± 0.46	1.53 ± 0.54	0.82 ± 0.25	4.06 ± 0.58	4.44 ± 0.69
	7-3	0.56 ± 0.27	0.50 ± 0.10	4.62 ± 0.36	4.68 ± 0.38	1.86 ± 0.18	0.75 ± 0.21	3.88 ± 0.30	4.37 ± 0.35	0.89 ± 0.33	0.66 ± 0.33	4.10 ± 0.68	4.28 ± 0.65
	7-4	0.38 ± 0.15	0.44 ± 0.18	3.91 ± 0.20	3.96 ± 0.18	0.67 ± 0.10	0.56 ± 0.24	3.53 ± 0.34	3.65 ± 0.34	1.05 ± 0.39	1.67 ± 0.66	4.57 ± 0.65	5.03 ± 0.70

Table 6.4: Vibration transmission for each body segment (Mean \pm SD) [Session I – under the 6Hz vertical vibration exposure]

		No Visual Feedback											
		6Hz Vertical Vibration Exposure											
		Right Shoulder				Right Elbow				Right Fingertip			
		SHOx	SHOy	SHOz	SHOt	ELBx	ELBy	ELBz	ELBt	FINx	FINy	FINz	FINt
TG1	1-2	0.98 ± 0.29	0.38 ± 0.12	3.76 ± 0.39	3.91 ± 0.42	1.24 ± 0.32	1.31 ± 0.34	2.89 ± 0.27	3.43 ± 0.38	1.07 ± 0.44	1.64 ± 0.53	1.82 ± 0.32	2.71 ± 0.60
	1-3	0.89 ± 0.27	0.61 ± 0.21	3.46 ± 0.49	3.63 ± 0.54	0.48 ± 0.40	0.59 ± 0.24	2.56 ± 0.25	2.71 ± 0.30	0.84 ± 0.26	0.97 ± 0.25	1.87 ± 0.17	2.29 ± 0.17
	1-4	0.49 ± 0.18	0.31 ± 0.10	3.30 ± 0.43	3.36 ± 0.43	0.49 ± 0.37	0.65 ± 0.21	2.84 ± 0.26	2.99 ± 0.25	1.47 ± 0.41	1.29 ± 0.47	2.20 ± 0.28	3.01 ± 0.30
TG2	2-2	0.98 ± 0.29	0.38 ± 0.12	3.76 ± 0.39	3.91 ± 0.42	1.24 ± 0.32	1.31 ± 0.34	2.89 ± 0.27	3.43 ± 0.38	1.07 ± 0.44	1.64 ± 0.53	1.82 ± 0.32	2.71 ± 0.60
	2-3	0.90 ± 0.19	0.64 ± 0.22	3.38 ± 0.32	3.57 ± 0.32	1.01 ± 0.42	1.16 ± 0.19	2.35 ± 0.18	2.83 ± 0.32	1.07 ± 0.41	0.93 ± 0.40	1.40 ± 0.13	2.07 ± 0.17
	2-4	0.69 ± 0.15	0.42 ± 0.16	3.24 ± 0.35	3.34 ± 0.36	0.45 ± 0.31	0.64 ± 0.21	2.74 ± 0.36	2.87 ± 0.38	1.44 ± 0.44	1.13 ± 0.15	1.77 ± 0.45	2.60 ± 0.36
TG4	4-2	0.98 ± 0.29	0.38 ± 0.12	3.76 ± 0.39	3.91 ± 0.42	1.24 ± 0.32	1.31 ± 0.34	2.89 ± 0.27	3.43 ± 0.38	1.07 ± 0.44	1.64 ± 0.53	1.82 ± 0.32	2.71 ± 0.60
	4-3	0.82 ± 0.22	0.55 ± 0.15	3.64 ± 0.36	3.78 ± 0.37	1.39 ± 0.39	1.18 ± 0.24	2.92 ± 0.27	3.46 ± 0.35	1.19 ± 0.66	0.93 ± 0.43	1.97 ± 0.42	2.61 ± 0.38
	4-4	0.81 ± 0.18	0.70 ± 0.27	3.61 ± 0.28	3.78 ± 0.25	1.33 ± 0.39	1.18 ± 0.19	3.01 ± 0.24	3.52 ± 0.32	1.36 ± 0.69	0.91 ± 0.33	1.91 ± 0.44	2.66 ± 0.16
TG5	5-2	0.84 ± 0.24	0.72 ± 0.40	3.59 ± 0.36	3.78 ± 0.35	1.43 ± 0.45	1.19 ± 0.24	2.64 ± 0.24	3.25 ± 0.42	1.21 ± 0.62	1.16 ± 0.43	1.79 ± 0.24	2.54 ± 0.43
	5-3	0.75 ± 0.13	0.86 ± 0.52	3.49 ± 0.32	3.70 ± 0.36	1.40 ± 0.39	1.03 ± 0.16	2.36 ± 0.12	2.95 ± 0.32	0.67 ± 0.25	1.20 ± 0.23	1.72 ± 0.23	2.23 ± 0.20
	5-4	0.57 ± 0.18	0.43 ± 0.21	3.35 ± 0.34	3.43 ± 0.35	0.66 ± 0.17	0.64 ± 0.34	2.91 ± 0.32	3.08 ± 0.32	1.25 ± 0.54	2.18 ± 0.42	1.67 ± 0.31	3.09 ± 0.34
TG6	6-2	0.82 ± 0.22	0.55 ± 0.15	3.64 ± 0.36	3.78 ± 0.37	1.39 ± 0.39	1.18 ± 0.24	2.92 ± 0.27	3.46 ± 0.35	1.19 ± 0.66	0.93 ± 0.43	1.97 ± 0.42	2.61 ± 0.38
	6-3	0.76 ± 0.18	0.88 ± 0.40	3.66 ± 0.23	3.86 ± 0.28	1.40 ± 0.31	0.72 ± 0.19	3.24 ± 0.28	3.63 ± 0.17	1.18 ± 0.44	0.98 ± 0.39	2.37 ± 0.70	2.90 ± 0.66
	6-4	0.72 ± 0.13	1.13 ± 0.54	3.75 ± 0.20	4.02 ± 0.27	0.96 ± 0.32	0.48 ± 0.30	3.81 ± 0.11	3.98 ± 0.16	1.30 ± 0.42	1.52 ± 0.41	2.82 ± 0.65	3.52 ± 0.58
TG7	7-2	0.82 ± 0.22	0.55 ± 0.15	3.64 ± 0.36	3.78 ± 0.37	1.39 ± 0.39	1.18 ± 0.24	2.92 ± 0.27	3.46 ± 0.35	1.19 ± 0.66	0.93 ± 0.43	1.97 ± 0.42	2.61 ± 0.38
	7-3	0.75 ± 0.17	0.92 ± 0.47	3.55 ± 0.21	3.77 ± 0.30	1.40 ± 0.23	0.52 ± 0.19	3.14 ± 0.16	3.50 ± 0.12	1.08 ± 0.32	1.03 ± 0.22	2.16 ± 0.41	2.65 ± 0.40
	7-4	0.60 ± 0.18	0.70 ± 0.38	3.20 ± 0.22	3.36 ± 0.18	0.76 ± 0.16	0.67 ± 0.13	2.82 ± 0.58	3.01 ± 0.51	1.73 ± 0.36	2.43 ± 0.51	2.44 ± 0.78	3.93 ± 0.68

Table 6.5 Vibration transmission for each body segment (Mean \pm SD) [Session II – under the 2Hz vertical vibration exposure]

		Visual Compensation											
		2Hz Vertical Vibration Exposure											
		Right Shoulder				Right Elbow				Right Fingertip			
		SHOx	SHOy	SHOz	SHOt	ELBx	ELBy	ELBz	ELBt	FINx	FINy	FINz	FINt
TG1	1-2	0.15 ± 0.04	0.12 ± 0.04	1.41 ± 0.08	1.43 ± 0.08	0.09 ± 0.02	0.27 ± 0.09	1.47 ± 0.15	1.5 ± 0.15	0.15 ± 0.05	0.23 ± 0.07	1.76 ± 0.32	1.78 ± 0.32
	1-3	0.16 ± 0.05	0.13 ± 0.05	1.37 ± 0.05	1.39 ± 0.05	0.15 ± 0.05	0.14 ± 0.07	1.63 ± 0.30	1.64 ± 0.30	0.17 ± 0.05	0.25 ± 0.20	1.68 ± 0.37	1.72 ± 0.40
	1-4	0.18 ± 0.03	0.14 ± 0.02	1.34 ± 0.03	1.36 ± 0.03	0.3 ± 0.07	0.29 ± 0.07	1.58 ± 0.07	1.64 ± 0.06	0.21 ± 0.07	0.44 ± 0.29	1.67 ± 0.11	1.76 ± 0.17
TG2	2-2	0.15 ± 0.04	0.12 ± 0.04	1.41 ± 0.08	1.43 ± 0.08	0.09 ± 0.02	0.27 ± 0.09	1.47 ± 0.15	1.5 ± 0.15	0.15 ± 0.05	0.23 ± 0.07	1.76 ± 0.32	1.78 ± 0.32
	2-3	0.15 ± 0.03	0.14 ± 0.05	1.39 ± 0.06	1.41 ± 0.06	0.10 ± 0.02	0.13 ± 0.08	1.46 ± 0.16	1.47 ± 0.15	0.25 ± 0.05	0.22 ± 0.07	1.56 ± 0.22	1.59 ± 0.23
	2-4	0.15 ± 0.02	0.13 ± 0.04	1.38 ± 0.04	1.39 ± 0.04	0.14 ± 0.03	0.14 ± 0.02	1.48 ± 0.19	1.5 ± 0.19	0.21 ± 0.08	0.29 ± 0.06	1.74 ± 0.32	1.78 ± 0.33
TG4	4-2	0.15 ± 0.04	0.12 ± 0.04	1.41 ± 0.08	1.43 ± 0.08	0.09 ± 0.02	0.27 ± 0.09	1.47 ± 0.15	1.5 ± 0.15	0.15 ± 0.05	0.23 ± 0.07	1.76 ± 0.32	1.78 ± 0.32
	4-3	0.16 ± 0.03	0.12 ± 0.06	1.39 ± 0.07	1.40 ± 0.08	0.11 ± 0.04	0.21 ± 0.07	1.43 ± 0.10	1.45 ± 0.11	0.24 ± 0.08	0.18 ± 0.05	1.65 ± 0.28	1.68 ± 0.28
	4-4	0.14 ± 0.03	0.12 ± 0.05	1.40 ± 0.07	1.41 ± 0.07	0.09 ± 0.04	0.18 ± 0.05	1.47 ± 0.10	1.49 ± 0.10	0.22 ± 0.08	0.20 ± 0.08	1.79 ± 0.35	1.82 ± 0.34
TG5	5-2	0.17 ± 0.05	0.12 ± 0.04	1.40 ± 0.06	1.41 ± 0.06	0.12 ± 0.07	0.19 ± 0.10	1.45 ± 0.16	1.47 ± 0.15	0.23 ± 0.08	0.16 ± 0.05	1.62 ± 0.20	1.65 ± 0.20
	5-3	0.14 ± 0.04	0.12 ± 0.04	1.39 ± 0.09	1.41 ± 0.09	0.17 ± 0.11	0.13 ± 0.05	1.54 ± 0.16	1.56 ± 0.16	0.25 ± 0.10	0.22 ± 0.08	1.69 ± 0.18	1.72 ± 0.18
	5-4	0.15 ± 0.05	0.11 ± 0.03	1.35 ± 0.06	1.36 ± 0.06	0.19 ± 0.05	0.16 ± 0.12	1.46 ± 0.12	1.49 ± 0.12	0.30 ± 0.14	0.32 ± 0.10	1.65 ± 0.24	1.72 ± 0.23
TG6	6-2	0.16 ± 0.03	0.12 ± 0.06	1.39 ± 0.07	1.40 ± 0.08	0.11 ± 0.04	0.21 ± 0.07	1.43 ± 0.10	1.45 ± 0.11	0.24 ± 0.08	0.18 ± 0.05	1.65 ± 0.28	1.68 ± 0.28
	6-3	0.17 ± 0.02	0.10 ± 0.02	1.36 ± 0.05	1.38 ± 0.05	0.15 ± 0.08	0.19 ± 0.02	1.33 ± 0.09	1.36 ± 0.09	0.17 ± 0.05	0.19 ± 0.06	1.64 ± 0.13	1.66 ± 0.13
	6-4	0.14 ± 0.05	0.10 ± 0.02	1.35 ± 0.06	1.36 ± 0.06	0.21 ± 0.08	0.20 ± 0.04	1.32 ± 0.05	1.35 ± 0.05	0.18 ± 0.05	0.22 ± 0.07	1.68 ± 0.21	1.71 ± 0.20
TG7	7-2	0.16 ± 0.03	0.12 ± 0.06	1.39 ± 0.07	1.40 ± 0.08	0.11 ± 0.04	0.21 ± 0.07	1.43 ± 0.10	1.45 ± 0.11	0.24 ± 0.08	0.18 ± 0.05	1.65 ± 0.28	1.68 ± 0.28
	7-3	0.13 ± 0.04	0.11 ± 0.05	1.36 ± 0.06	1.38 ± 0.06	0.16 ± 0.09	0.18 ± 0.03	1.34 ± 0.07	1.36 ± 0.08	0.14 ± 0.05	0.19 ± 0.10	1.57 ± 0.18	1.59 ± 0.18
	7-4	0.22 ± 0.04	0.18 ± 0.05	1.26 ± 0.05	1.30 ± 0.05	0.08 ± 0.01	0.17 ± 0.05	1.43 ± 0.09	1.44 ± 0.08	0.16 ± 0.03	0.15 ± 0.04	2.16 ± 0.17	2.17 ± 0.16

Table 6.6 Vibration transmission for each body segment (Mean \pm SD) [Session II – under the 4Hz vertical vibration exposure]

		Visual Compensation											
		4Hz Vertical Vibration Exposure											
		Right Shoulder				Right Elbow				Right Fingertip			
		SHOx	SHOy	SHOz	SHOt	ELBx	ELBy	ELBz	ELBt	FINx	FINy	FINz	FINt
TG1	1-2	0.77 ± 0.29	0.48 ± 0.26	4.81 ± 0.64	4.90 ± 0.68	1.32 ± 0.26	1.91 ± 0.47	3.86 ± 0.29	4.53 ± 0.38	1.02 ± 0.53	1.34 ± 0.32	3.77 ± 0.61	4.17 ± 0.62
	1-3	0.48 ± 0.21	0.37 ± 0.11	3.84 ± 0.42	3.90 ± 0.43	0.54 ± 0.21	0.35 ± 0.07	4.09 ± 0.37	4.14 ± 0.34	0.79 ± 0.32	0.97 ± 0.48	3.38 ± 0.55	3.66 ± 0.50
	1-4	0.24 ± 0.14	0.30 ± 0.19	3.72 ± 0.40	3.75 ± 0.38	1.13 ± 0.26	0.73 ± 0.18	4.35 ± 0.37	4.56 ± 0.38	1.22 ± 0.39	1.61 ± 1.02	3.89 ± 0.38	4.51 ± 0.52
TG2	2-2	0.77 ± 0.29	0.48 ± 0.26	4.81 ± 0.64	4.90 ± 0.68	1.32 ± 0.26	1.91 ± 0.47	3.86 ± 0.29	4.53 ± 0.38	1.02 ± 0.53	1.34 ± 0.32	3.77 ± 0.61	4.17 ± 0.62
	2-3	0.83 ± 0.36	0.36 ± 0.15	4.36 ± 0.55	4.46 ± 0.61	1.14 ± 0.34	1.32 ± 0.34	3.94 ± 0.42	4.33 ± 0.41	1.01 ± 0.39	1.38 ± 0.20	3.23 ± 0.52	3.7 ± 0.38
	2-4	0.62 ± 0.27	0.32 ± 0.10	3.93 ± 0.43	4.00 ± 0.46	0.47 ± 0.15	0.43 ± 0.22	4.61 ± 0.47	4.66 ± 0.45	0.44 ± 0.27	1.43 ± 0.35	2.98 ± 0.61	3.37 ± 0.58
TG4	4-2	0.77 ± 0.29	0.48 ± 0.26	4.81 ± 0.64	4.90 ± 0.68	1.32 ± 0.26	1.91 ± 0.47	3.86 ± 0.29	4.53 ± 0.38	1.02 ± 0.53	1.34 ± 0.32	3.77 ± 0.61	4.17 ± 0.62
	4-3	0.68 ± 0.28	0.40 ± 0.20	5.01 ± 0.53	5.08 ± 0.56	1.69 ± 0.37	1.77 ± 0.29	4.09 ± 0.41	4.78 ± 0.47	1.35 ± 0.62	0.83 ± 0.08	3.77 ± 0.59	4.12 ± 0.70
	4-4	0.75 ± 0.32	0.35 ± 0.12	4.97 ± 0.53	5.04 ± 0.56	1.58 ± 0.36	1.45 ± 0.30	4.20 ± 0.32	4.73 ± 0.44	0.89 ± 0.52	0.86 ± 0.34	3.84 ± 0.40	4.07 ± 0.49
TG5	5-2	0.74 ± 0.26	0.35 ± 0.14	4.64 ± 0.58	4.72 ± 0.61	1.61 ± 0.42	1.53 ± 0.29	3.86 ± 0.17	4.47 ± 0.34	1.21 ± 0.38	1.23 ± 0.15	3.46 ± 0.84	3.90 ± 0.78
	5-3	0.67 ± 0.18	0.45 ± 0.15	4.14 ± 0.46	4.22 ± 0.49	1.36 ± 0.29	0.89 ± 0.28	4.16 ± 0.32	4.48 ± 0.35	1.09 ± 0.32	1.38 ± 0.36	3.43 ± 0.38	3.89 ± 0.36
	5-4	0.40 ± 0.17	0.37 ± 0.13	3.79 ± 0.43	3.83 ± 0.44	0.50 ± 0.31	0.44 ± 0.18	4.64 ± 0.33	4.70 ± 0.35	0.91 ± 0.33	2.06 ± 0.88	3.20 ± 0.58	4.05 ± 0.40
TG6	6-2	0.68 ± 0.28	0.40 ± 0.20	5.01 ± 0.53	5.08 ± 0.56	1.69 ± 0.37	1.77 ± 0.29	4.09 ± 0.41	4.78 ± 0.47	1.35 ± 0.62	0.83 ± 0.08	3.77 ± 0.59	4.12 ± 0.70
	6-3	0.59 ± 0.25	0.50 ± 0.30	4.88 ± 0.41	4.95 ± 0.45	1.99 ± 0.37	1.18 ± 0.17	4.14 ± 0.23	4.75 ± 0.34	0.98 ± 0.38	0.64 ± 0.22	4.01 ± 0.34	4.19 ± 0.43
	6-4	0.49 ± 0.21	0.63 ± 0.33	4.85 ± 0.38	4.93 ± 0.42	1.90 ± 0.26	0.60 ± 0.12	4.36 ± 0.33	4.79 ± 0.38	0.57 ± 0.24	0.77 ± 0.53	4.62 ± 0.50	4.75 ± 0.48
TG7	7-2	0.68 ± 0.28	0.40 ± 0.20	5.01 ± 0.53	5.08 ± 0.56	1.69 ± 0.37	1.77 ± 0.29	4.09 ± 0.41	4.78 ± 0.47	1.35 ± 0.62	0.83 ± 0.08	3.77 ± 0.59	4.12 ± 0.70
	7-3	0.69 ± 0.25	0.59 ± 0.20	4.48 ± 0.45	4.58 ± 0.47	1.87 ± 0.37	0.80 ± 0.15	4.02 ± 0.33	4.52 ± 0.36	0.97 ± 0.27	0.67 ± 0.44	4.30 ± 0.63	4.48 ± 0.68
	7-4	0.32 ± 0.21	0.38 ± 0.19	3.76 ± 0.22	3.80 ± 0.24	0.65 ± 0.08	0.49 ± 0.25	3.20 ± 0.35	3.31 ± 0.38	0.93 ± 0.31	0.99 ± 0.22	4.48 ± 0.96	4.69 ± 0.95

Table 6.7 Vibration transmission for each body segment (Mean \pm SD) [Session II – under the 6Hz vertical vibration exposure]

		Visual Compensation											
		6Hz Vertical Vibration Exposure											
		Right Shoulder				Right Elbow				Right Fingertip			
		SHOx	SHOy	SHOz	SHOt	ELBx	ELBy	ELBz	ELBt	FINx	FINy	FINz	FINt
TG1	1-2	1.05 ± 0.24	0.51 ± 0.25	3.77 ± 0.34	3.96 ± 0.38	1.29 ± 0.32	1.24 ± 0.19	3.01 ± 0.32	3.52 ± 0.37	1.07 ± 0.54	1.90 ± 0.64	1.77 ± 0.36	2.87 ± 0.73
	1-3	0.77 ± 0.27	0.51 ± 0.20	3.35 ± 0.35	3.48 ± 0.40	0.39 ± 0.27	0.50 ± 0.19	2.51 ± 0.45	2.62 ± 0.43	0.72 ± 0.26	0.99 ± 0.25	1.84 ± 0.19	2.25 ± 0.12
	1-4	0.37 ± 0.14	0.29 ± 0.16	3.22 ± 0.29	3.26 ± 0.27	0.85 ± 0.17	0.73 ± 0.31	2.69 ± 0.28	2.93 ± 0.33	0.95 ± 0.40	1.24 ± 0.62	2.34 ± 0.12	2.89 ± 0.32
TG2	2-2	1.05 ± 0.24	0.51 ± 0.25	3.77 ± 0.34	3.96 ± 0.38	1.29 ± 0.32	1.24 ± 0.19	3.01 ± 0.32	3.52 ± 0.37	1.07 ± 0.54	1.90 ± 0.64	1.77 ± 0.36	2.87 ± 0.73
	2-3	1.02 ± 0.21	0.45 ± 0.26	3.40 ± 0.32	3.60 ± 0.32	1.12 ± 0.35	1.18 ± 0.15	2.45 ± 0.27	2.95 ± 0.39	0.93 ± 0.50	1.02 ± 0.44	1.46 ± 0.21	2.12 ± 0.14
	2-4	0.78 ± 0.15	0.42 ± 0.22	3.28 ± 0.31	3.41 ± 0.31	0.41 ± 0.20	0.62 ± 0.18	2.67 ± 0.48	2.79 ± 0.44	1.11 ± 0.33	1.07 ± 0.17	1.55 ± 0.28	2.23 ± 0.21
TG4	4-2	1.05 ± 0.24	0.51 ± 0.25	3.77 ± 0.34	3.96 ± 0.38	1.29 ± 0.32	1.24 ± 0.19	3.01 ± 0.32	3.52 ± 0.37	1.07 ± 0.54	1.90 ± 0.64	1.77 ± 0.36	2.87 ± 0.73
	4-3	0.87 ± 0.23	0.32 ± 0.20	3.63 ± 0.33	3.76 ± 0.34	1.31 ± 0.29	1.06 ± 0.24	3.11 ± 0.45	3.55 ± 0.48	1.32 ± 0.66	1.18 ± 0.55	2.09 ± 0.44	2.85 ± 0.57
	4-4	0.88 ± 0.14	0.65 ± 0.15	3.65 ± 0.19	3.82 ± 0.17	1.26 ± 0.36	1.19 ± 0.22	3.22 ± 0.29	3.67 ± 0.36	1.55 ± 0.83	0.87 ± 0.28	1.88 ± 0.38	2.71 ± 0.51
TG5	5-2	0.91 ± 0.24	0.60 ± 0.25	3.53 ± 0.35	3.71 ± 0.35	1.37 ± 0.34	1.15 ± 0.23	2.67 ± 0.33	3.23 ± 0.42	1.10 ± 0.63	1.24 ± 0.52	1.66 ± 0.28	2.47 ± 0.39
	5-3	0.88 ± 0.19	0.96 ± 0.38	3.46 ± 0.29	3.71 ± 0.33	1.35 ± 0.41	1.05 ± 0.20	2.42 ± 0.22	2.98 ± 0.36	0.79 ± 0.39	1.40 ± 0.29	1.63 ± 0.22	2.35 ± 0.13
	5-4	0.62 ± 0.15	0.52 ± 0.27	3.3 ± 0.24	3.41 ± 0.23	0.55 ± 0.14	0.67 ± 0.23	2.87 ± 0.52	3.01 ± 0.50	1.57 ± 0.87	2.42 ± 0.81	1.60 ± 0.16	3.39 ± 0.90
TG6	6-2	0.87 ± 0.23	0.32 ± 0.20	3.63 ± 0.33	3.76 ± 0.34	1.31 ± 0.29	1.06 ± 0.24	3.11 ± 0.45	3.55 ± 0.48	1.32 ± 0.66	1.18 ± 0.55	2.09 ± 0.44	2.85 ± 0.57
	6-3	0.86 ± 0.20	0.67 ± 0.24	3.67 ± 0.14	3.84 ± 0.17	1.40 ± 0.33	0.69 ± 0.16	3.37 ± 0.32	3.74 ± 0.21	1.02 ± 0.56	0.95 ± 0.19	2.42 ± 0.56	2.85 ± 0.58
	6-4	0.83 ± 0.17	0.93 ± 0.45	3.81 ± 0.17	4.04 ± 0.20	0.96 ± 0.33	0.45 ± 0.20	3.96 ± 0.12	4.12 ± 0.11	1.15 ± 0.76	1.4 ± 0.34	3.22 ± 0.63	3.78 ± 0.71
TG7	7-2	0.87 ± 0.23	0.32 ± 0.20	3.63 ± 0.33	3.76 ± 0.34	1.31 ± 0.29	1.06 ± 0.24	3.11 ± 0.45	3.55 ± 0.48	1.32 ± 0.66	1.18 ± 0.55	2.09 ± 0.44	2.85 ± 0.57
	7-3	0.93 ± 0.20	1.00 ± 0.43	3.64 ± 0.12	3.91 ± 0.24	1.59 ± 0.23	0.50 ± 0.20	3.21 ± 0.19	3.63 ± 0.15	0.98 ± 0.40	0.97 ± 0.22	2.54 ± 0.60	2.91 ± 0.67
	7-4	0.70 ± 0.15	0.58 ± 0.41	3.3 ± 0.19	3.45 ± 0.19	0.89 ± 0.33	0.81 ± 0.17	2.86 ± 0.50	3.14 ± 0.35	1.58 ± 0.33	1.60 ± 0.45	2.72 ± 0.69	3.60 ± 0.49

Table 6.8 Vibration transmission for each body segment (Mean \pm SD) [Session III - elbow fully extended posture]

Elbow Fully Extended Posture												
2Hz Vertical Vibration Exposure												
Right Shoulder				Right Elbow				Right Fingertip				
	SHOx	SHOy	SHOz	SHOt	ELBx	ELBy	ELBz	ELBt	FINx	FINy	FINz	FINt
TG1	0.14 ± 0.01	0.18 ± 0.01	1.30 ± 0.00	1.32 ± 0.00	0.24 ± 0.02	0.34 ± 0.01	1.39 ± 0.01	1.45 ± 0.01	0.39 ± 0.03	0.97 ± 0.01	1.61 ± 0.01	1.92 ± 0.01
TG2	0.13 ± 0.03	0.12 ± 0.04	1.33 ± 0.04	1.34 ± 0.05	0.15 ± 0.06	0.19 ± 0.06	1.36 ± 0.16	1.39 ± 0.16	0.21 ± 0.11	0.29 ± 0.09	1.82 ± 0.28	1.86 ± 0.30
TG3	0.15 ± 0.04	0.11 ± 0.05	1.35 ± 0.05	1.37 ± 0.05	0.10 ± 0.03	0.16 ± 0.05	1.33 ± 0.17	1.34 ± 0.16	0.15 ± 0.04	0.22 ± 0.09	1.74 ± 0.37	1.76 ± 0.37
TG4	0.16 ± 0.04	0.13 ± 0.04	1.33 ± 0.06	1.34 ± 0.06	0.12 ± 0.03	0.13 ± 0.04	1.30 ± 0.13	1.31 ± 0.13	0.18 ± 0.05	0.17 ± 0.07	1.67 ± 0.28	1.69 ± 0.28
TG5	0.12 ± 0.03	0.09 ± 0.02	1.32 ± 0.03	1.33 ± 0.03	0.21 ± 0.03	0.12 ± 0.04	1.26 ± 0.12	1.28 ± 0.12	0.41 ± 0.10	0.24 ± 0.09	1.51 ± 0.21	1.59 ± 0.21
TG6	0.17 ± 0.04	0.11 ± 0.03	1.32 ± 0.04	1.34 ± 0.04	0.11 ± 0.04	0.16 ± 0.07	1.31 ± 0.06	1.32 ± 0.05	0.15 ± 0.05	0.23 ± 0.10	1.56 ± 0.15	1.59 ± 0.14
4Hz Vertical Vibration Exposure												
TG1	0.33 ± 0.08	0.24 ± 0.03	4.28 ± 0.00	4.30 ± 0.01	0.49 ± 0.31	0.27 ± 0.04	4.61 ± 0.22	4.65 ± 0.25	0.63 ± 0.11	5.38 ± 0.00	3.57 ± 0.31	6.49 ± 0.18
TG2	0.42 ± 0.19	0.84 ± 0.53	3.71 ± 0.56	3.88 ± 0.45	0.28 ± 0.17	0.63 ± 0.38	3.17 ± 0.20	3.27 ± 0.20	0.76 ± 0.48	1.41 ± 0.45	4.80 ± 0.67	5.12 ± 0.58
TG3	0.84 ± 0.45	0.62 ± 0.45	4.53 ± 0.72	4.69 ± 0.74	0.58 ± 0.17	0.92 ± 0.31	3.35 ± 0.25	3.54 ± 0.24	1.43 ± 0.47	1.45 ± 0.32	3.89 ± 0.41	4.43 ± 0.38
TG4	0.74 ± 0.39	0.70 ± 0.47	4.23 ± 0.60	4.39 ± 0.60	0.67 ± 0.15	0.80 ± 0.21	3.17 ± 0.15	3.34 ± 0.15	1.41 ± 0.99	0.67 ± 0.14	4.35 ± 0.87	4.76 ± 0.67
TG5	0.39 ± 0.10	0.94 ± 0.69	3.65 ± 0.47	3.87 ± 0.34	0.38 ± 0.19	0.43 ± 0.10	3.15 ± 0.17	3.21 ± 0.19	1.33 ± 0.46	2.45 ± 0.72	4.43 ± 0.76	5.30 ± 0.77
TG6	0.37 ± 0.12	0.84 ± 0.57	4.2 ± 0.32	4.33 ± 0.34	1.20 ± 0.21	0.50 ± 0.21	3.44 ± 0.34	3.68 ± 0.39	1.82 ± 0.88	0.68 ± 0.33	3.63 ± 0.95	4.18 ± 1.13
6Hz Vertical Vibration Exposure												
TG1	0.78 ± 0.02	0.33 ± 0.01	3.30 ± 0.08	3.41 ± 0.08	1.39 ± 0.27	0.48 ± 0.02	3.77 ± 0.02	4.06 ± 0.08	0.92 ± 0.55	4.23 ± 0.25	2.25 ± 0.01	4.92 ± 0.12
TG2	0.79 ± 0.35	0.67 ± 0.18	3.19 ± 0.44	3.37 ± 0.47	0.72 ± 0.23	0.29 ± 0.10	2.97 ± 0.23	3.08 ± 0.27	1.26 ± 0.64	1.74 ± 0.44	3.42 ± 1.15	4.09 ± 1.23
TG3	0.98 ± 0.34	0.64 ± 0.33	3.53 ± 0.46	3.74 ± 0.50	0.62 ± 0.11	0.79 ± 0.12	2.92 ± 0.39	3.09 ± 0.39	2.09 ± 0.77	0.97 ± 0.12	2.19 ± 0.71	3.20 ± 0.99
TG4	1.12 ± 0.37	0.53 ± 0.29	3.45 ± 0.36	3.69 ± 0.40	0.76 ± 0.15	0.64 ± 0.10	3.10 ± 0.53	3.26 ± 0.53	1.98 ± 0.79	0.66 ± 0.38	2.37 ± 0.81	3.26 ± 0.88
TG5	0.79 ± 0.34	0.64 ± 0.29	3.22 ± 0.46	3.40 ± 0.50	0.62 ± 0.20	0.30 ± 0.08	2.85 ± 0.16	2.93 ± 0.18	1.29 ± 0.62	2.12 ± 0.51	2.33 ± 0.79	3.56 ± 0.45
TG6	0.53 ± 0.13	0.65 ± 0.23	3.44 ± 0.29	3.55 ± 0.27	0.93 ± 0.12	0.36 ± 0.15	3.10 ± 0.21	3.27 ± 0.22	1.60 ± 0.52	0.80 ± 0.38	2.11 ± 0.59	2.83 ± 0.63

Table 6.9 Vibration transmission for each body segment (Mean \pm SD) [Session III - elbow flexed posture]

	Elbow Flexed Posture											
	2Hz Vertical Vibration Exposure											
	Right Shoulder				Right Elbow				Right Fingertip			
	SHOx	SHOy	SHOz	SHOt	ELBx	ELBy	ELBz	ELBt	FINx	FINy	FINz	FINt
TG1	0.14 ± 0.01	0.06 ± 0.01	1.32 ± 0.01	1.33 ± 0.01	0.28 ± 0.01	0.13 ± 0.00	1.42 ± 0.03	1.45 ± 0.03	0.16 ± 0.04	0.52 ± 0.02	1.48 ± 0.04	1.58 ± 0.03
TG2	0.12 ± 0.02	0.12 ± 0.04	1.36 ± 0.05	1.37 ± 0.04	0.13 ± 0.02	0.10 ± 0.03	1.39 ± 0.16	1.40 ± 0.16	0.16 ± 0.05	0.26 ± 0.06	1.65 ± 0.21	1.68 ± 0.21
TG3	0.15 ± 0.02	0.13 ± 0.04	1.40 ± 0.05	1.41 ± 0.05	0.09 ± 0.04	0.22 ± 0.07	1.34 ± 0.08	1.37 ± 0.09	0.15 ± 0.06	0.22 ± 0.08	1.74 ± 0.28	1.76 ± 0.28
TG4	0.16 ± 0.02	0.11 ± 0.05	1.40 ± 0.04	1.41 ± 0.04	0.13 ± 0.03	0.20 ± 0.10	1.37 ± 0.10	1.40 ± 0.10	0.22 ± 0.07	0.15 ± 0.07	1.69 ± 0.41	1.71 ± 0.41
TG5	0.15 ± 0.02	0.11 ± 0.03	1.34 ± 0.05	1.35 ± 0.05	0.18 ± 0.04	0.11 ± 0.04	1.37 ± 0.18	1.39 ± 0.17	0.24 ± 0.06	0.25 ± 0.11	1.49 ± 0.29	1.54 ± 0.30
TG6	0.16 ± 0.02	0.13 ± 0.06	1.35 ± 0.04	1.37 ± 0.04	0.19 ± 0.05	0.22 ± 0.05	1.34 ± 0.05	1.37 ± 0.06	0.19 ± 0.09	0.21 ± 0.04	1.65 ± 0.30	1.68 ± 0.30
	4Hz Vertical Vibration Exposure											
TG1	0.14 ± 0.02	0.09 ± 0.02	3.99 ± 0.01	3.99 ± 0.02	1.78 ± 0.08	1.02 ± 0.07	5.47 ± 0.25	5.85 ± 0.19	0.84 ± 0.42	4.03 ± 0.50	3.47 ± 0.09	5.41 ± 0.37
TG2	0.53 ± 0.16	0.34 ± 0.15	3.85 ± 0.27	3.91 ± 0.28	0.45 ± 0.25	0.38 ± 0.10	5.02 ± 0.42	5.06 ± 0.42	0.70 ± 0.32	1.78 ± 0.15	1.97 ± 0.47	2.80 ± 0.24
TG3	1.01 ± 0.25	0.29 ± 0.12	5.09 ± 0.35	5.2 ± 0.38	0.94 ± 0.20	1.54 ± 0.21	4.41 ± 0.25	4.77 ± 0.30	1.41 ± 0.61	1.33 ± 0.35	2.97 ± 0.66	3.60 ± 0.73
TG4	0.78 ± 0.22	0.32 ± 0.14	4.92 ± 0.35	4.99 ± 0.37	1.48 ± 0.34	1.48 ± 0.17	4.10 ± 0.15	4.62 ± 0.24	0.97 ± 0.49	0.94 ± 0.41	3.34 ± 1.00	3.67 ± 0.94
TG5	0.37 ± 0.21	0.36 ± 0.13	3.78 ± 0.31	3.82 ± 0.32	0.49 ± 0.23	0.26 ± 0.08	4.47 ± 0.47	4.51 ± 0.48	0.70 ± 0.28	2.24 ± 0.99	2.58 ± 0.52	3.65 ± 0.46
TG6	0.57 ± 0.17	0.46 ± 0.11	5.10 ± 0.30	5.16 ± 0.31	1.85 ± 0.25	0.74 ± 0.29	4.55 ± 0.26	4.98 ± 0.28	0.60 ± 0.35	0.88 ± 0.39	4.05 ± 0.72	4.21 ± 0.74
	6Hz Vertical Vibration Exposure											
TG1	0.35 ± 0.10	0.20 ± 0.04	3.16 ± 0.11	3.19 ± 0.12	1.31 ± 0.06	0.86 ± 0.08	3.24 ± 0.03	3.60 ± 0.02	1.63 ± 0.35	3.24 ± 0.14	2.00 ± 0.14	4.15 ± 0.31
TG2	0.72 ± 0.19	0.35 ± 0.14	3.41 ± 0.41	3.51 ± 0.41	0.49 ± 0.20	0.66 ± 0.30	2.73 ± 0.50	2.88 ± 0.49	1.68 ± 0.97	1.35 ± 0.32	2.25 ± 0.76	3.15 ± 1.19
TG3	0.99 ± 0.12	0.47 ± 0.17	3.66 ± 0.28	3.83 ± 0.26	0.78 ± 0.32	1.35 ± 0.47	2.98 ± 0.47	3.38 ± 0.66	2.75 ± 1.52	1.04 ± 0.38	1.97 ± 0.50	3.59 ± 1.52
TG4	0.91 ± 0.14	0.57 ± 0.38	3.70 ± 0.28	3.88 ± 0.24	1.23 ± 0.46	1.15 ± 0.29	3.10 ± 0.29	3.56 ± 0.40	1.60 ± 0.89	1.18 ± 0.36	1.90 ± 0.43	2.82 ± 0.88
TG5	0.65 ± 0.18	0.40 ± 0.19	3.40 ± 0.31	3.49 ± 0.31	0.58 ± 0.29	0.69 ± 0.30	2.94 ± 0.66	3.11 ± 0.62	1.88 ± 0.93	2.60 ± 1.02	1.65 ± 0.28	3.73 ± 1.04
TG6	0.76 ± 0.15	0.80 ± 0.32	3.83 ± 0.28	4.00 ± 0.27	1.01 ± 0.33	0.68 ± 0.24	3.86 ± 0.45	4.07 ± 0.43	1.27 ± 0.61	1.48 ± 0.66	2.89 ± 0.92	3.61 ± 0.88

CHAPTER 7

Conclusions

The development of an active biodynamic model must rely on the appropriate evaluation of WBV influence on human reach movements and performance. Hence, this work analyzed the influence of vibration characteristics, movement direction, and visual feedback on upper body segment transmission and joint movement trajectories while performing reaching movements. It was hypothesized that WBV responses may be derived from the vibration characteristics of body segments through the transmission path. These responses were used to propose the construct of a biomechanical model capable of predicting upper body movement behaviors under WBV exposure.

From 9,702 reach movements recorded in a series of experiments, this work investigated the mechanisms of WBV transmission from the vehicle cab to the hand, determined the kinematics of upper body joints under WBV exposure, and quantified vibration transmission through the upper limbs as a function of vibration frequency and direction, movement direction, and posture or movement constraints.

7.1 Summary of Findings

[1] WBV responses through the body segments can be derived from vibration characteristics of multi-body segments along the transmission path.

WBV transmission through the multi-linkage system of the upper body in the seated condition is significantly affected by vibration frequency and direction. Specifically, for the 2Hz excitation, the vibration motion is amplified through the upper limb from the shoulder to the fingertip, regardless of vibration direction and task condition. However, for the 6Hz excitation, the vibration motion is attenuated along the path for both the vertical and fore-and-aft vibration directions. Under the 4Hz excitation, transmission through the upper body segments is dependent on vibration direction and reaching direction. All participants stated that the 4Hz vertical vibration was the most uncomfortable environment and the most difficult condition in which to complete the reaching task. These perceptions are likely to result from torso resonance occurring around 4 to 5 Hz in the vertical vibration condition. Furthermore, for the 2Hz vibration, transmission through all body segments is higher under the fore-and-aft than under the vertical exposure, which may reflect the inverse pendulum motion of the upper body. These findings suggested that the vibration responses of the end-effector may be estimated and predicted by synthesizing the vibration characteristics of multi-body segments along the path.

[2] Elbow joint movement strongly contributes to the dynamic characteristics of upper body movements in reaching tasks.

The peaks of the angular velocity and acceleration are higher for the elbow joint than for the shoulder, regardless of the reach direction. In addition, the shoulder joint angular velocity profile is mono-phasic, while the elbow joint profile is multi-phasic. Interestingly, the elbow joint angles for all reaches show the “U-shaped” profiles that indicates a flexion followed by an extension. The initial elbow flexion may be to facilitate the release of the steering handle or be part of the reach

movement preparation to facilitate a rectilinear/planar hand trajectory. Alternatively, this flexion may help improve the controllability of movements by reducing the moment of inertia of the moving arm. Although joint trajectory and kinematics vary with reach direction, all joint tangential velocities present “bell-shaped” profiles corresponding to feed-forward and feedback control phases.

[3] In reaching tasks, movement initiation times are different for the shoulder and elbow, and any upper limb movement is not initiated before visual identification of the target location.

Head rotation always occurs first, and then the arm movement is initiated after target location is identified. In addition, body segment movements are not initiated simultaneously. Gaze remained on target during the whole movement, which suggests that vibration may disrupt the spatial representation of the target to be reached. Since proprioception is also disrupted by vibration-induced oscillations of the arm, guidance of the movement may be achieved by anchoring vision on the target while waiting for the hand to appear in the visual field of view. In addition, it may mean that the hand transition can be completed without visual information of the hand as long as visual information of the target location is allowed.

[4] One-dimensional vibrations influence reach movements significantly along the vibration axis, however a significant cross-talk occurs in other directions.

Under vertical vibration exposure, all three-dimensional joint trajectories and kinematics show periodic perturbations correlated with the vibration frequency. This cross-transmission may result from the eccentricity of the mass moment of

inertia for multi-body segment, the nonlinearity in biomechanical properties of the upper body segments as well as the non-alignment of the different joint axes with the direction of the vibration. Hence, the biomechanical properties of the multi-linkage system are likely to be the primary source of cross-talk. This effect also increases as the difficulty in balance maintenance increases.

[5] Vibration contributes to an increase in the peak velocity and acceleration for all joint movements. However, movement patterns of joint angular kinematics are not qualitatively altered.

WBV induces a periodic perturbation in the angular kinematics of the shoulder and elbow joint, which contribute to an increase in the peak values of joint angular velocity and acceleration. However, the desired reach trajectories and movement coordination planning are similar for static and vibratory conditions, since the filtered angular kinematics and movement patterns in vibratory conditions are qualitatively quite identical to those in a static condition. Hence, it appears that mechanical oscillations are only superimposed to the movement trajectory.

[6] Vibration transmission through the human body must be considered as a three-dimensional tensor including the auto-axis and cross-axis transmission.

Generally, vibration is predominantly transmitted through the body along the axis of the forcing direction. However, when performing far reaches under 4 and 6 Hz vibration conditions, the cross-axis transmission is not negligible. Estimation of the auto-axis transmission through body segment is essential to describe their vibration characteristics, while additional information of the cross-axis

transmission is also necessary to identify the degradation of the performance and to develop a multi-degrees-of-freedom model. It also implies that a biomechanical model must be capable of simulating multi-directional responses to WBV vibration.

[6] WBV transmission through the upper body segments while performing a reach task is a function of vibration frequency and direction, reach direction and target distance, posture or movement constraints (visual compensation and elbow flexion), and interactions between those factors.

Specific description for effects of each factor follows below.

[7] Vibration frequency is the dominant factor affecting WBV propagated transmission through upper-body segments.

Regardless of other factors, transmission through the upper body is predominantly affected by vibration frequency. It implies that WBV characteristics may be determined by the biomechanical properties of the human body and its mechanical configuration of the multi-linkage system.

[8] Reach direction also affects WBV transmission through the upper limbs. However, reach directions can be classified into three groups.

Posture varies with reach direction, which leads to changes in biomechanical properties such as muscle/joint stiffness and moment of inertia of each body segment, location of the mass center, and stability of the whole body. Reach directions can be divided into three groups corresponding to the propagated transmission. For horizontal reaches at arm length distance, transmission is not

significantly altered along reach direction. For upward reaches requiring arm elevation, auto-axis and total transmission to the elbow joint are the largest for the 4 Hz exposure and elbow transmission is larger than shoulder and finger transmission. The cross-axis transmission to the fingertip is larger than the auto-axis transmission under 6 Hz vibration, which means that fingertip oscillation is a three-dimensional motion, resulting from the position of the arm. Lateral far reach beyond the arm length results in large transmission to the finger, especially for the 4Hz and 6Hz vibration, as might be expected from a distant arm center of gravity. These differences reflect the changes in biomechanical properties associated with the configuration of the linkage system.

[9] Variation of WBV transmission during arm transition phase depends on reach direction as well as vibration frequency.

For the horizontal reach, there is no significant change in WBV transmission during the transition phase, regardless of vibration frequency. However, for the upward reach, WBV transmission changes depend on vibration frequency. Under the 2Hz vertical vibration, there is no significant change in the transmission trend through the upper body. Under 4Hz, the perturbation of the elbow significantly increases as the arm move closer to the final target and the trend of transmission through the upper limbs changes. Interestingly, under the 6Hz vibration exposure, the total transmission through the finger increases significantly when the hand arrives near the final target.

[10] Visual compensation can contribute to hand stabilization. However, it does not modify the trend of transmission through the arm and may not be sufficient to improve performance under WBV exposure.

Hand oscillation around the target is smaller when continuous visual feedback of target location is allowed. However, contribution of visual compensation to reduction the degradation of performance varies with vibration frequency. With visual compensation, the total transmissions at the finger decreases by 20.6 %, for the 2 Hz, 7.2 % for the 4 Hz, and 1.3 % for the 6 Hz WBV exposure, respectively. Therefore, movement adjustment by visual feedback may not be an effective way to improve task performance in all vibration environments.

[11] Elbow Flexion does contribute to the enhancement of hand stabilization for the upward reach requiring arm elevation.

The elbow flexed posture produces larger transmission to the elbow and smaller transmission to the finger than the elbow extended posture, which suggests that elbow flexion prevents large vibration transmission to the finger by dissipating energy at the elbow joint. This effect is more pronounced for the 4 Hz than for the 2 or 6 Hz WBV exposures. Especially when performing upward reach under the 4 Hz exposure, transmission to the elbow is larger than transmission to the shoulder and finger. Under the 4 Hz vibration, when compared to the extended posture, elbow flexion leads to 36.1 % increase in transmission through the elbow and 13.6 % decrease in transmission through the finger for the horizontal reach. For the upward reach, elbow flexion contributes to 40.4 % increase in elbow transmission and 31.0 % decrease in finger transmission. Under 2 Hz and 6 Hz WBV, the contribution of elbow flexion to the reduction of fingertip transmission is relatively smaller, nevertheless elbow flexion contributes to 10.2 % and 11.3 % decreases, respectively.

In conclusion, the characteristics of WBV transmission through multi-body segments along the upper body path provide valuable information that may be applied to the design of man-machine interfaces used in vibratory environments. These findings are also the basis of supporting the development of a biomechanical model representing and predicting human behavior under WBV.

7.2 Limitations and Future Research Opportunities

The biodynamic experiments and analyses in this work were performed with selected vibration conditions consisting of one-dimensional sinusoidal vibrations in order to explore the effects of the excitation frequency in the range of high sensitivity of human reach performance in vehicle operations. However, in order to provide a broader description of the frequency response of the human body, estimation of transfer functions would require exploring over a larger frequency range. It should be pointed out that simplifications in the design of experiment are necessary, since a change in biomechanical properties of body segments is expected to occur during movements.

This research was also limited by a simplified definition of the shoulder joint. However, since the shoulder is a multi-joint system activated by a large number of muscles, movements of the shoulder are too complex to be defined easily. Usually, movements of the shoulder are described by scapular retraction/protraction, scapular elevation/depression, arm abduction/ adduction, arm flexion/extension, medial/lateral rotation, and arm circumduction. All these movements may not be captured by an optical motion analysis system. In addition, due to difficulty in tracking the hip markers during arm movements with the limited number of cameras, the torso movements were not identified from motion capture data. For a more accurate and realistic model development, it may be critical to define how

many degrees-of-freedom must be considered for describing the torso and shoulder movements (Figure 7.1).

For the horizontal movements, three intermediate points associated with instantaneous postures may be sufficient to describe the variation of transmission along the movement trajectory. However, for the upward reaches, two additional intermediate postures may be necessary to obtain a complete description of transmission associated with changes in biomechanical properties of the upper limb along the movement trajectory. Indeed, upward reaches require a larger range of joint movements and more degrees of freedom for the shoulder than horizontal movements.

Two elbow flexions used to identify how elbow flexion/extension affects WBV-induced pointing error at the fingertip revealed an elbow anti-resonance phenomenon. This result may be expanded to construct a parametric model of the elbow joint by estimating posture-variant biomechanical properties with a few more flexion levels along specific movement direction.

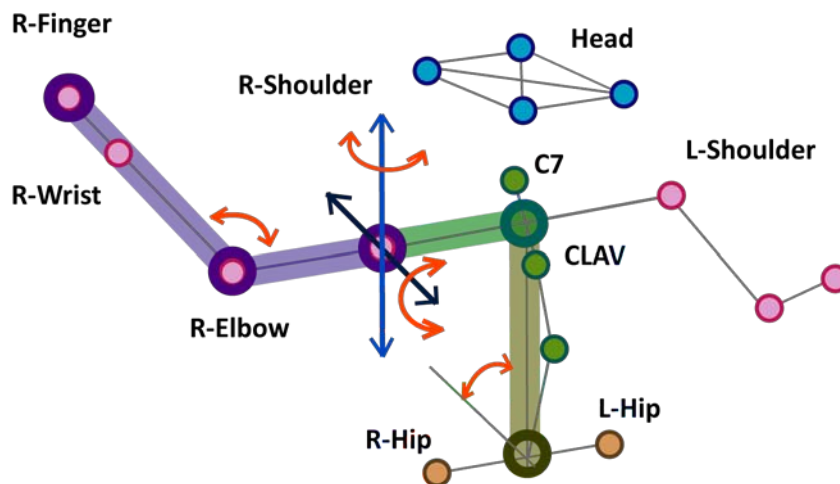


Figure 7.1: The example reach model of the seated human with six degrees-of-freedom

Estimation of the biomechanical properties is needed for the development of an active biomechanical model. As suggested in Chapter 6, the equilibrium point hypothesis and EMG measurement may be used for estimating the muscle and joint stiffness (Fledman, 1986; Flash and Mussa-Ivaldi, 1990; Gomi and Kawato, 1997). To model nonlinearities in the human system, the effects of the active voluntary and involuntary muscular control also need to be investigated to determine the contribution of their influence on stiffness estimations and the associated changes in responses to whole-body vibration. In addition, further investigation of the influence of vibration magnitude may also reveal more information about the nonlinear characteristics of the human body.

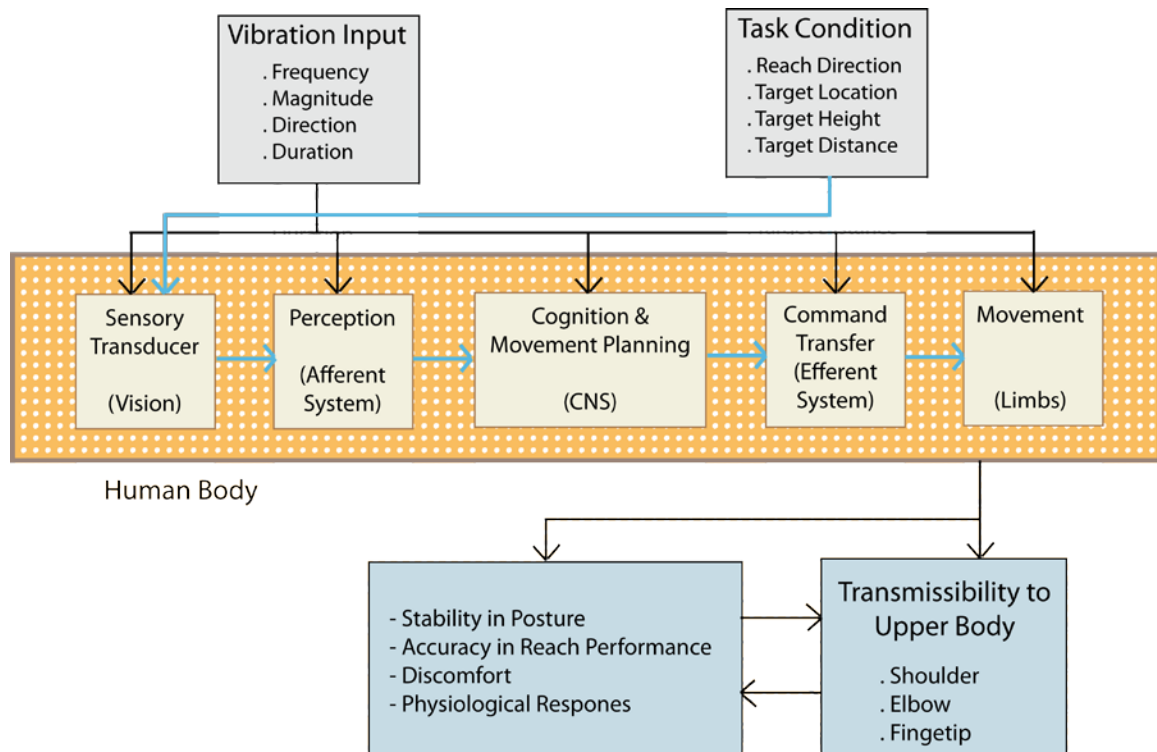


Figure 7.2: Information flow and vibration influence on human activity

Vibration transmission through body segments provides information about the amount of physical response of the body. However, vehicle vibration may

interfere with various functions in human body such as visual system, perception, and movement and posture control, as illustrated in Figure 7.2 (Martin et al, 1980a; Martin et al 1980b; Gauthier et al, 1981, Gauthier et al, 1984; Griffin, 1990). WBV exposure may also influence the central nervous system, but the effects on CNS have not been explicitly known. Therefore, for the realistic and synthetic evaluation of WBV effects on the human, overall human responses to vibration must be integrated with some weight factors.

The results of this work provide quantitative information about how mechanical vibration is transmitted to the upper body of the seated human. This physical stress is known to cause to health risks and safety issues that are more critical in evaluating operation environment and workplace. Thus, a relationship between WBV transmission and health issues or performance must be further investigated to improve the current exposure guidelines (ISO standard 2631) based arbitrary on discomfort. It should be noted that during our experiments some participants felt drowsiness under repetitive exposure of 2, 4, and 6 Hz. Furthermore, the present investigation, limited to a low frequency range, needs to be expanded to include higher frequencies also presented in the spectrum of vibrations generated by vehicles. For the synthetic analysis of WBV effects on the health and safety of the workers, physiological and psychological effects induced by WBV need to be investigated as well as physical response.

Discomfort induced by WBV is not easy and simple to evaluate, since it is a subjective perception based on the integration of sensory information partially distorted by the vibration-induced activation of the sensory mechano-receptors contributing to proprioception, exteroception, and exproprioception. Therefore, discomfort evaluation should be analyzed cautiously to avoid misinterpretation of the influence of vibration exposure.

This research did not explore effects of WBV on fatigue. However, muscle contractions required to counteract the mechanical perturbation or reflectively caused by vibration-induced muscle stretches and activation of mechanoreceptors may exacerbate fatigue, which in turn may modify vibration responses during exposure to WBV. Thus, effects resulting from long duration exposure, such as operating a vehicle for several hours, need to be investigated using electromyography (EMG) and other measures of muscle fatigue.

APPENDICES

Appendix A. Transmission propagated through the upper limbs in three-dimension

Vibration transmissions propagated through the upper limbs in three-dimension analyzed in Chapter 5 are presented in this appendix A. The results correspond to the experimental session I, II, and III associated with different movement constraints, respectively.

Figure A.1: Transmission propagated through the upper limbs [SS1 - 2 Hz Vertical WBV Exposure]

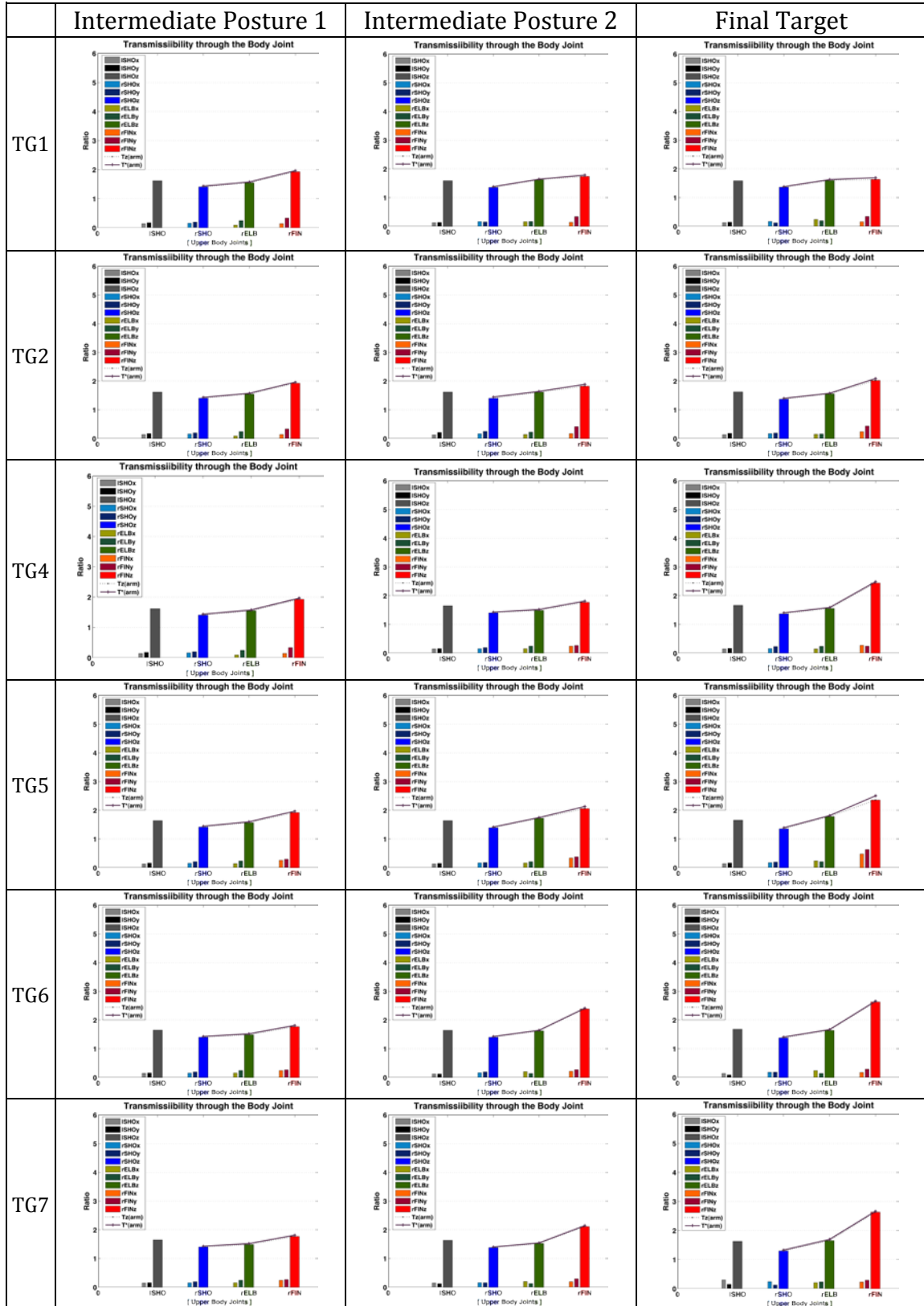


Figure A.2: Transmission propagated through the upper limbs[SS1 – 4 Hz Vertical WBV Exposure]

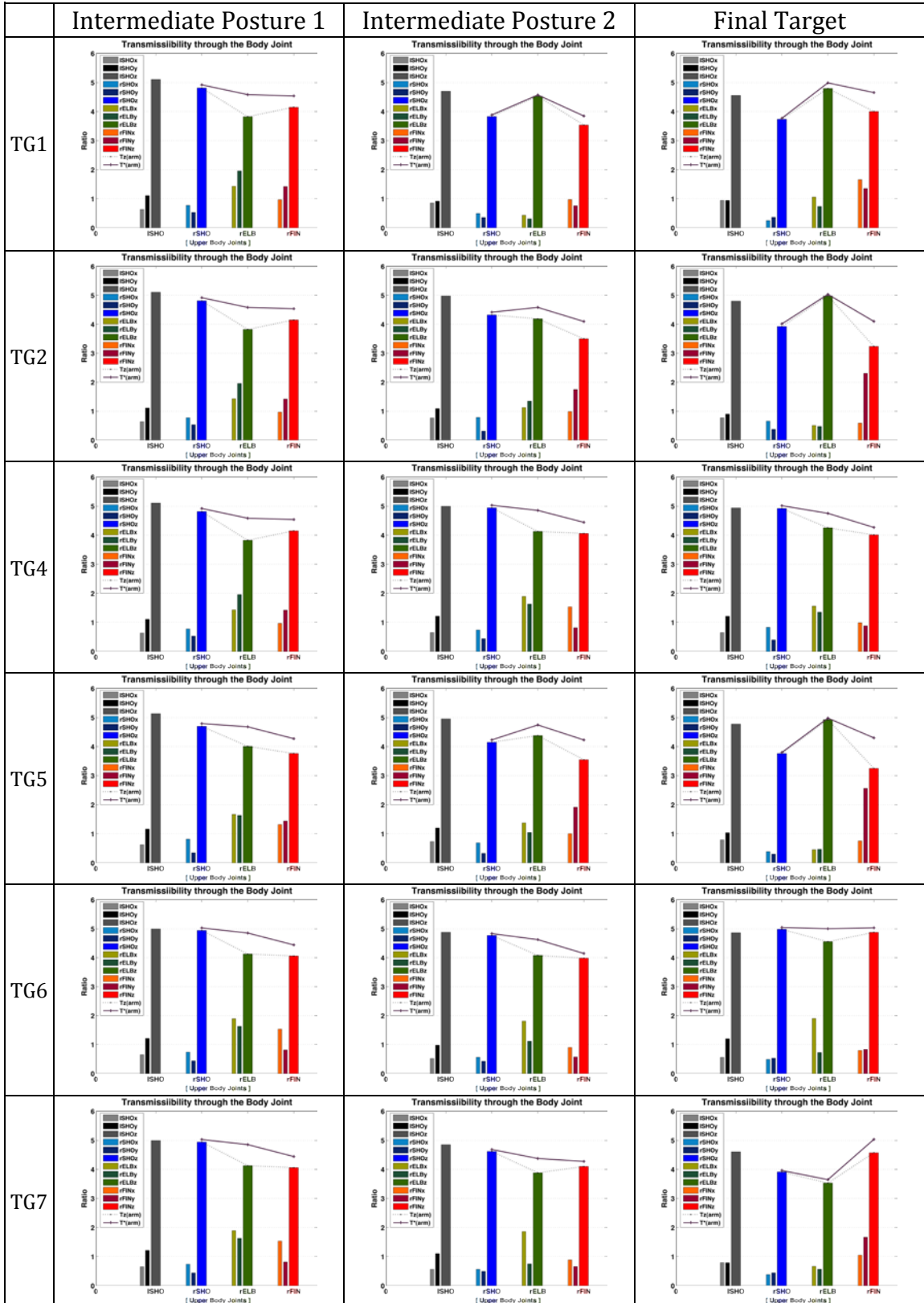


Figure A.3: Transmission propagated through the upper limbs[SS1 – 6 Hz Vertical WBV Exposure]

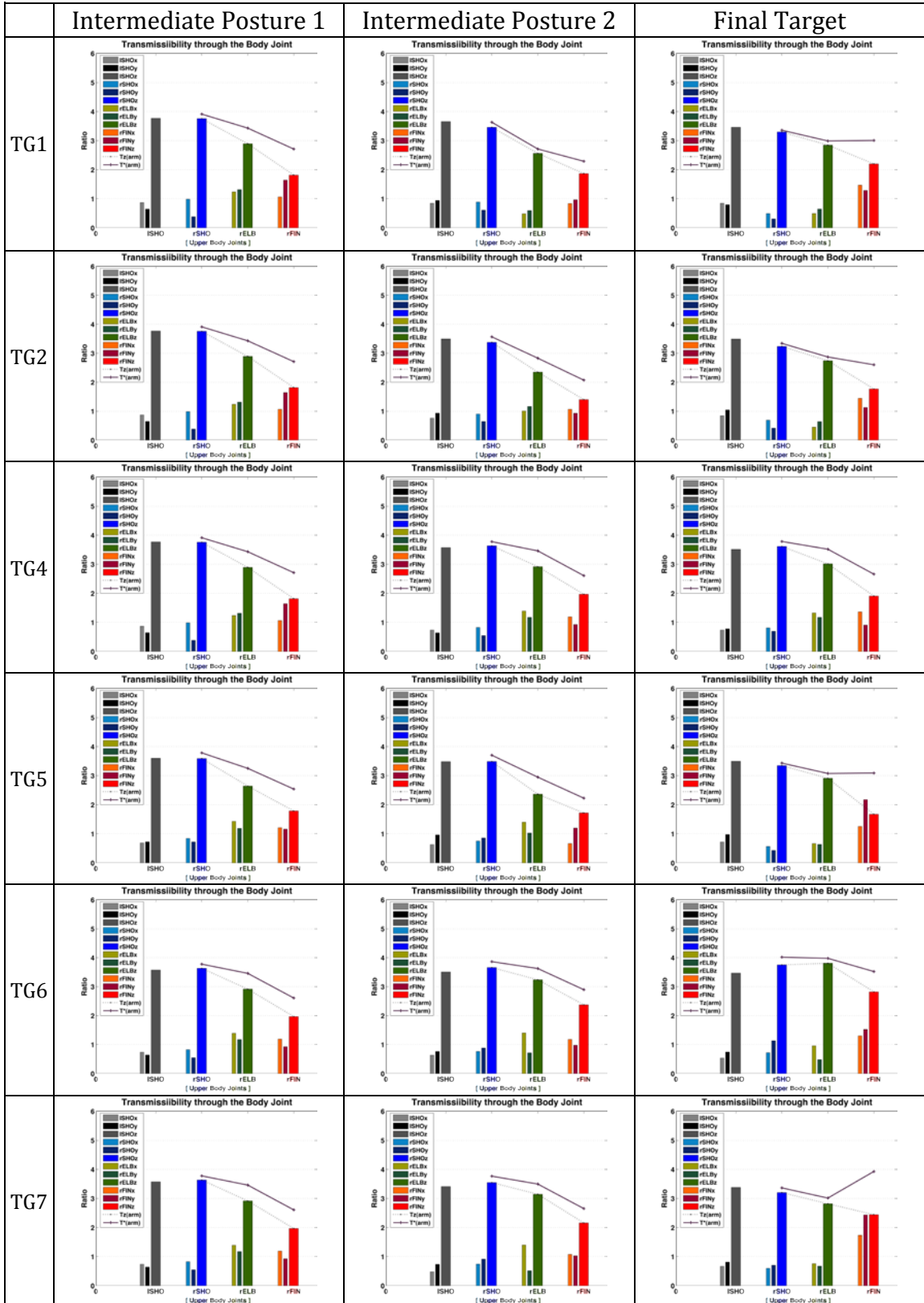


Figure A.4 Transmission propagated through the upper limbs [SS2 - 2 Hz Vertical WBV Exposure]

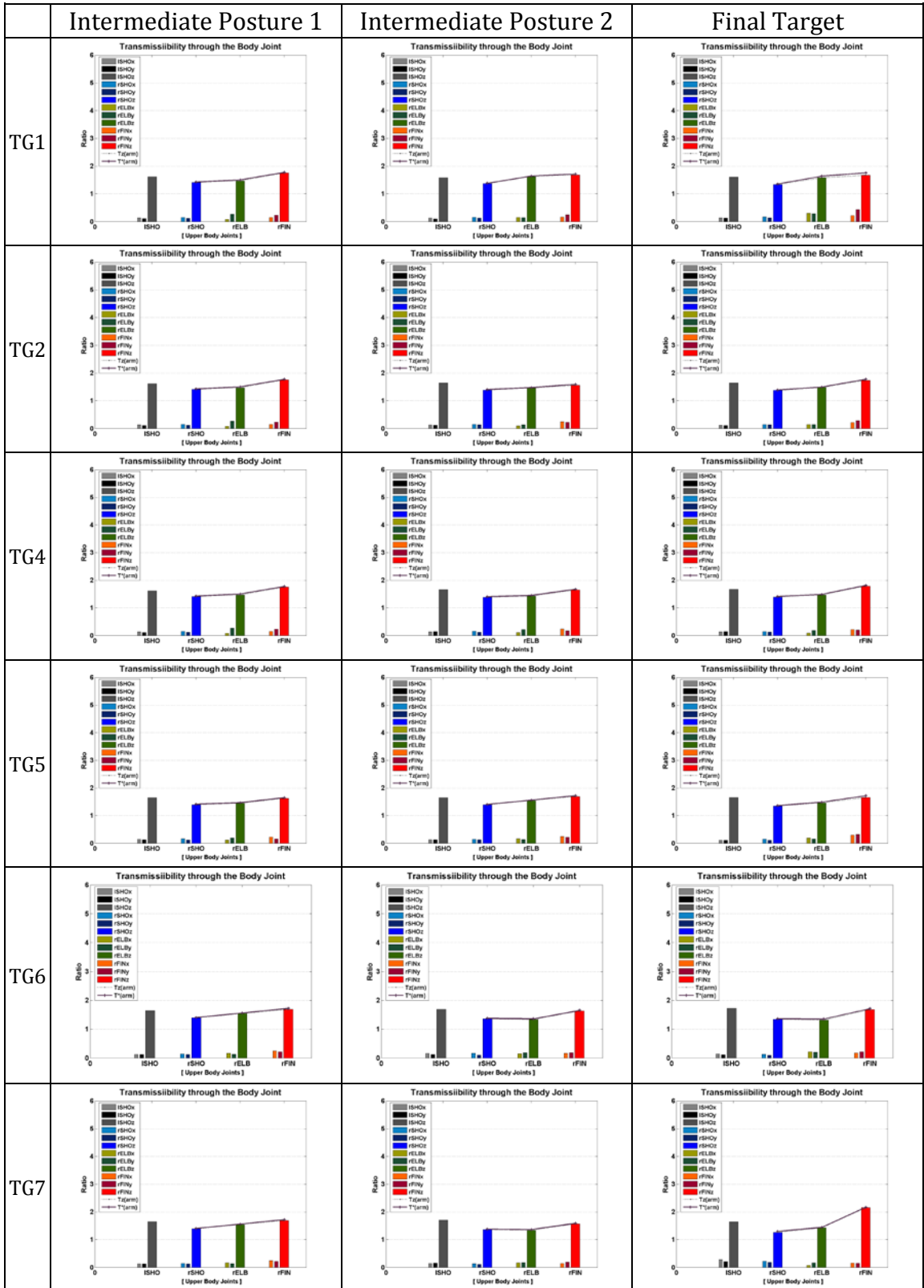


Figure A.5: Transmission propagated through the upper limbs [SS2 – 4 Hz Vertical WBV Exposure]

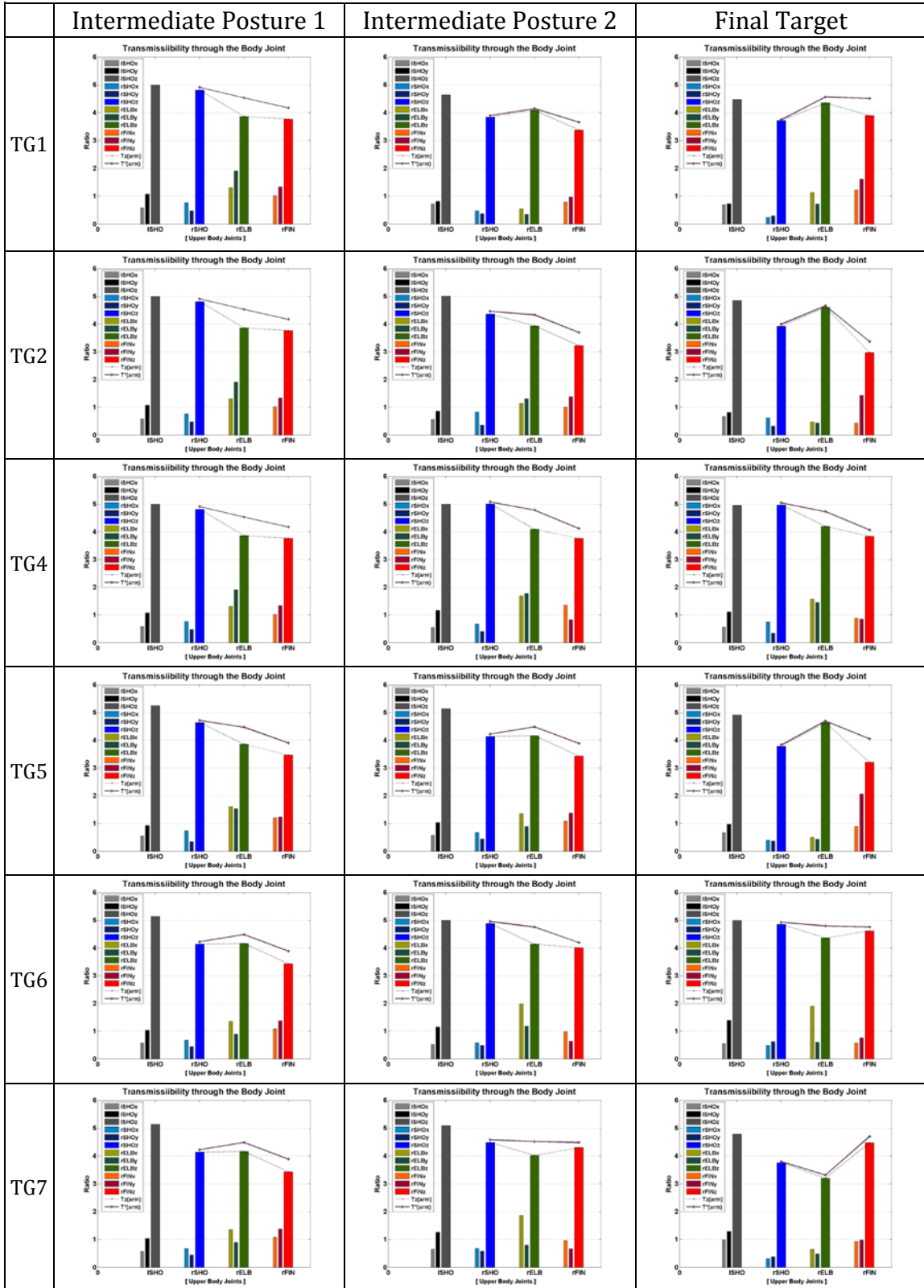


Figure A.6: Transmission propagated through the upper limbs [SS2 - 6 Hz Vertical WBV Exposure]

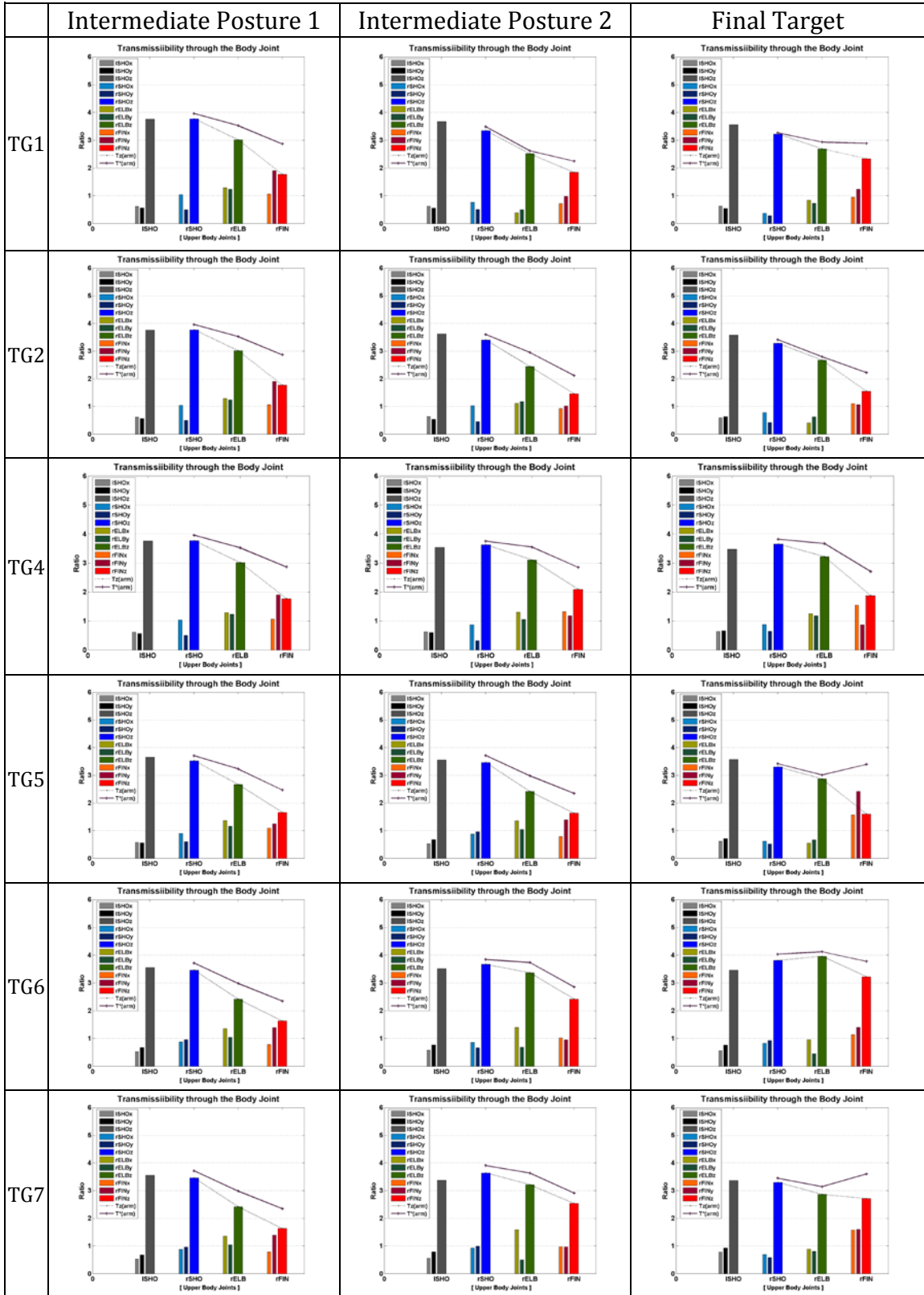


Figure A.7: Transmission propagated through the upper limbs [SS3 - 2 Hz Vertical WBV Exposure]

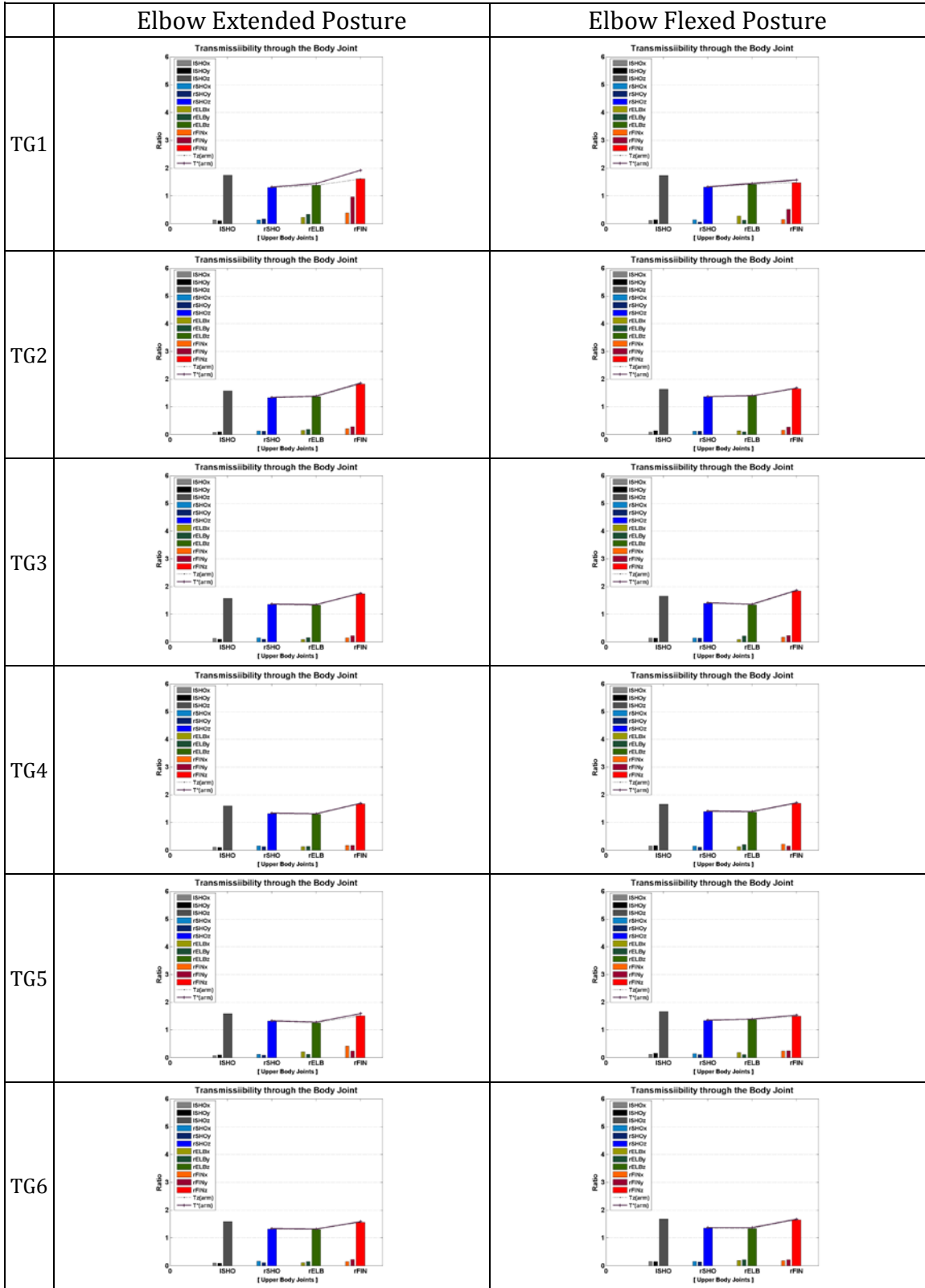


Figure A.8 Transmission propagated through the upper limbs [SS3 - 4 Hz Vertical WBV Exposure]

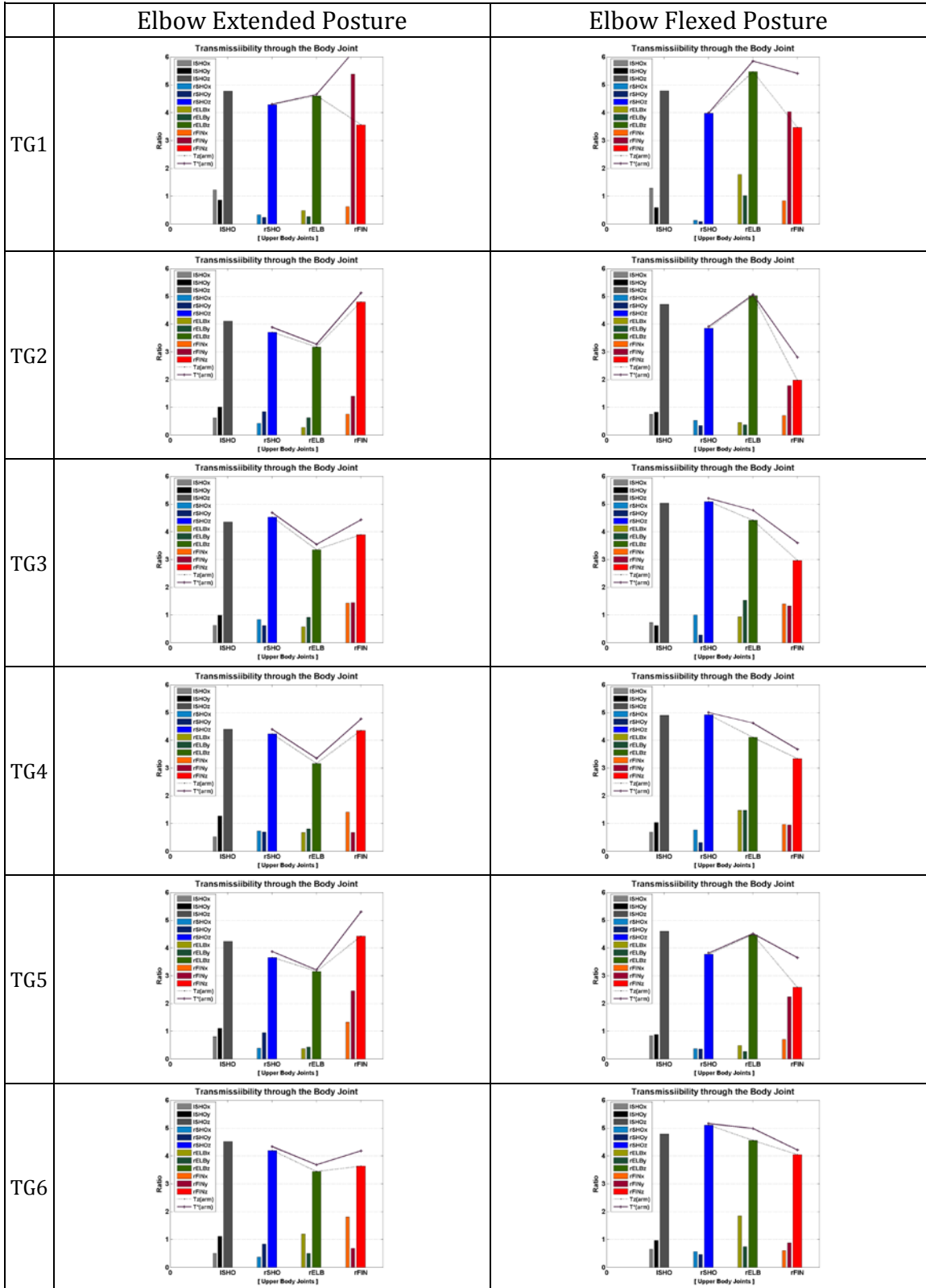
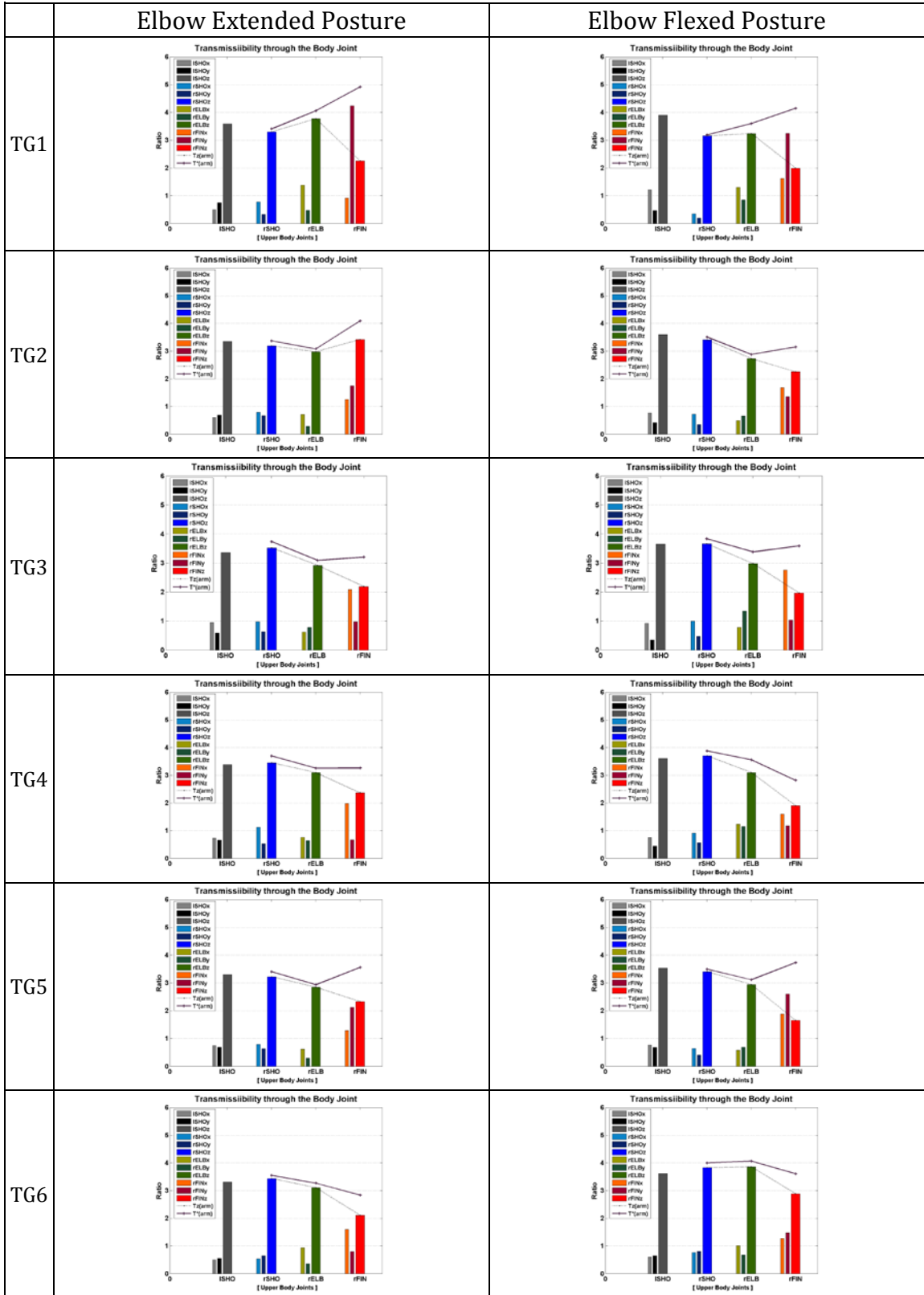


Figure A.9: Transmission propagated through the upper limbs [SS3 - 6 Hz Vertical WBV Exposure]



Appendix B. The Percentage Distribution of Total Body Weight

Table B.1: The Percentage Distribution of Total Body Weight According to Different Segmentation Plans (Chaffin, 1999, from Webb Associates, 1978)

Grouped Segments, % of Total Body Weight	Individual Segments, % of Grouped-Segments Weight	
Head and neck = 8.4 %	Head	73.8 %
	Neck	26.2 %
Torso = 50.0 %	Thorax	43.8 %
	Lumbar	29.4 %
	Pelvis	26.8 %
	Upper arm	54.9 %
Total arm = 5.1 %	Forearm	33.3 %
	Hand	11.8 %
	Thigh	63.7 %
Total leg = 15.7 %	Shank	27.4 %
	Foot	8.9%

Appendix C. The Effect of Total Body Weight on Fingertip Transmission

Table C.1: 3-way ANOVA for Subject Weight, Target Location, and Vibration Frequency

	Transmission (rFIN)				
	DoF	F (T _Z)	p (T _Z)	F (T _{TOTAL})	p (T _{TOTAL})
Subject Weight	20	7.82	0.0005	13.93	0
Target-L	5	8.19	0.0001	5.42	0.0011
Vib-Freq	2	90.18	0	99.31	0
S-Weight × Target-L	100	1.41	0.2041	0.84	0.6307
S-Weight × Vib-Freq	40	5.6	0.0005	2.64	0.0352
Target-L × Vib-Freq	10	1.64	0.143	0.98	0.481

A 3-way ANOVA including subject weight, target location, and vibration frequency was performed to estimate the influence of body weight on finger tip transmission. This analysis indicates that subject weight significantly affects the z-component and total WBV transmission of the finger (Table C.1). However, the relationship between body weight and transmission is not a monotonous function, which suggests the possible interaction of other body characteristics such as segment length, inertia and muscle tension. Hence body weight alone may not be a good indicator of vibration transmission in the context of dynamic activities. The difficulty in finding a correlation between weight and transmission may result from the complexity and/or the nonlinearity of the human body. Therefore, further in-depth investigation is necessary for exploring the relationship between anthropometry and WBV transmissibility.

BIBLIOGRAPHY

- [1] Abend, W., Bizzi, E., Morraso, P., (1982). "Human arm trajectory formation." *Brain* 105: 331-348.
- [2] Abercromby, A.F., Amonetter, W.E, Layne, C.S., Mcfarlin, B.K., Hinman, M.R, Paloski, W.H. (2007). "Vibration exposure and biodynamic responses during whole-body vibration training." *Medicine and Science in Sports and Exercise*, 39(10): 1794-1800.
- [3] Admirral, M.A, Kusters, M.J., Gielen, S.C. (2004). "Modeling kinematics and dynamics of human arm movements." *Motor Control* 8(3): 312-338.
- [4] Amirouche, F.M. (1987a). "Biodynamic analysis of the human body subjected to vibration." *IEEE Engineering in Medicine and Biology Magazine* 6: 22-26.
- [5] Amirouche, F.M. (1987b). "Modeling of human reactions to whole-body vibration." *Journal of Biomechanical Engineering* 109(3): 210-217.
- [6] Arkeson, C.G., Hollerbach, J.M. (1985). "Kinematic features of unrestrained vertical arm movements" *Journal of Neuroscence* 5, 2318-2330.
- [7] Barreca, D.M., Guenther, F.H. (2001). "A modeling study of potential sources of curvature in human reaching movements." *Journal of Motor Behavior* 33(4): 387-400.
- [8] Boileau, P. (1990). "Evaluating the exposure of tanker truck drivers to whole-body vibration." IRSST R-047.
- [9] Boileau, P., Rakheja, S. (1990). "Vibration attenuation performance of suspension seats for off-road forestry vehicles." *International Journal of Industrial Ergonomics* 5: 275-291.
- [10] Bovenzi, M., Zadini, A. (1992). "Self-reported low back symptoms in urban bus drivers exposed to whole-body vibration." *Spine* 17(9): 1048-1059.
- [11] Bovenzi, M. (2006). "Health risks from occupational exposures to mechanical vibration." *La Medicina del lavoro* 97(3): 535-541.

- [12] Burdet, E., Osu, R., Franklin, D.W., Yoshioka, T., Milner, T.E., Kawato, M. (2000). "A method for measuring endpoint stiffness during multi-joint arm movements." *Journal of Biomechanics* 33: 1705-1709.
- [13] Burton, A.K., Balague, F., Cardon, G., Eriksen, H.R., Henrotin, Y., Lahad, A., Leclerc, A., Muller, G., van der Beek, A.J. (2006). "Chapter 2 European guidelines for prevention in low back pain." *European Spine Journal* 15(2): S136-S168.
- [14] Chaffin, D.B., Andersson, G., and Martin, B. J. (1999). Occupational Biomechanics. John Wiley & Sons.
- [15] Chaffin, D.B., Faraway, J., Zhang, X. (1999). "Simulating reach motions." 1999-01-1916, SAE International Human Modeling for Design and Engineering Conference, The Hague, The Netherlands.
- [16] Chaffin, D.B. (2002) "On simulating human reach motions for Ergonomics Analyses." *Human Factors and Ergonomics in Manufacturing* 12(3): 235-247.
- [17] Chaffin, D.B. (2005). "Improving digital human modeling for proactive ergonomics in design." *Ergonomics* 48(5): 478-491.
- [18] Charlton, L., Roren, L. (2004). "Model specification, calibration, and kinematic fitting in optical motion capture." Technical Paper 2001-01-2154, SAE International.
- [19] Darainy, M., Malfait, N., Towhidkhan, F., Ostry, D. (2006). "Transfer and durability of acquired patterns of human arm stiffness." *Experimental Brain Research* 170: 227-237.
- [20] Darainy, M., Towhidkhan, F., Ostry, D. (2007). "Control of hand impedance under static conditions and during reaching movement." *Journal of Neurophysiology* 97: 2676-2685.
- [21] Desmurget, M., Prablanc, C., Rossetti, Y., Arzi, M., Paulignan, Y., Urquizar, C., Mignot, J. (1995). "Postural and synergic control for three-dimensional movements of reaching and grasping." *Journal of Neurophysiology* 74(2):905-910.
- [22] Desmurget, M., Prablanc, C., Rossetti, Y., Arzi, M., Rossetti, Y., Paulignan, Y., Urquizar, C. (1996). "Integrated control of hand transport and orientation during prehension movements." *Journal of Neurophysiology* 74(2):905-910.
- [23] Desmurget, M., Prablanc, C. (1997). "Postural control of three-dimensional prehension movements." *Journal of Neurophysiology* 77: 452-464.

- [24] European Commission. (2002). Directive 2002/44/EC of the European Parliament and of the Council of 25 June 2002 on the minimum health and safety requirements regarding the exposure of workers to the risks arising from physical agents (vibration) (16th individual Directive within the meaning of Article 16(1) of Directive 89/391/EEC). *Official Journal of the European Communities* L177: 13–9.
- [25] Fairley, T.E., Griffin, M.J., (1989). “The apparent mass of the seated human body: vertical vibration.” *Journal of Biomechanics* 22(2): 81-94.
- [26] Fairley, T.E., Griffin, M.J., (1989). “The apparent mass of the seated human body in the fore-and-aft and lateral directions.” *Journal of Sound and Vibration* 139(2): 299-306.
- [27] Faraway, J. (2000). “Modeling reach motions using functional regression analysis.” Technical Paper 2000-01-2175, SAE International.
- [28] Faraway, J., Hu, J. (2001). “Modeling variability in reaching motions.” Technical Paper 2001-01-2094, SAE International.
- [29] Faraway, J. (2001). “Statistical modeling of reaching motions using functional regression with endpoint constraints.” Technical Report #384. Department of Statistics, University of Michigan.
- [30] Faraway, J. (2003). “Regression modeling of motion with endpoint constraints.” *Journal of Visualization and Computer Animation* 14:31-41.
- [31] Faraway, J. (2007). “Statistics for digital human motion modeling in ergonomics.” *Technometrics* 49(3): 277-290.
- [32] Feldman A.G. (1986). “Once more on the equilibrium-point hypothesis (lambda model) for motor control.” *Journal of Motor Behavior* 18(1): 17-54.
- [33] Fitts, P.M. (1954). “The Information capacity of the human motor system in controlling the amplitude of movement.” *Journal of Experimental Psychology* 47:381-391.
- [34] Fitts, P.M., Peterson, J.R., (1964). “Information capacity of discrete motor responses.” *Journal of Experimental Psychology* 67:103-112.
- [35] Flash, T., Hogan, N. (1985). “The coordination of arm movements: an experimentally confirmed mathematical model.” *Journal of Neuroscience*
- [36] Flash, T., Mussa-Ivaldi, F. (1990). “Human arm stiffness characteristics during the maintenance of posture.” *Experimental Brain Research* 82: 315-326.

- [37] Franklin, D.W., Burdet, E., Osu, R., Kawato, M., Milner, T.E. (2003). "Functional significance of stiffness in adaptation of multijoint arm movements to stable and unstable dynamics." *Experimental Brain Research* 151: 145-157.
- [38] Fritz, M. (1991). "A improved biomechanical model for simulating the strain for the head-arm system under vibration stress." *Journal of Biomechanics* 24(12): 1165-1171.
- [39] Fritz, M. (1997). "Estimation of spine forces under whole-body vibration by means of a biomechanical model and transfer function." *Aviation, Space, and Environmental Medicine* 68(6): 512-519.
- [40] Fritz, M. (1998). "Three-dimensional biomechanical model for simulating the response of the human body to vibration stress." *Medical and Biological Engineering and Computing* 36: 686-692.
- [41] Fritz, M. (2000). "Description of the relation between the forces acting in the lumbar spine and whole-body vibrations by means of transfer functions." *Clinical Biomechanics* 15: 234-240.
- [42] Fritz, M., Fischer, S., Bröde, P. (2005). "Vibration induced low back disorders – comparison of the vibration evaluation according to ISO 2631 with a force – related evaluation." *Applied Ergonomics* 36: 481-488.
- [43] Gauthier, G.M., Roll, J.P., Martin, B., Harlay, F. (1981). "Effects of whole-body vibrations on sensory motor system performance in man." *Aviation, Space, and Environmental Medicine* 52(8): 473-479.
- [44] Gauthier, G.M., Piron, J.P., Roll, J.P., Marchetti, E., Martin, B. (1984). "High frequency vestibule-ocular reflex activation through forced head rotation in man." *Aviation, Space, and Environmental Medicine* 55(1): 1-7.
- [45] Gielen, C.C., Vrijenhoek, E.J., Flash, T., Neggers, S.F.W. (1997). "Arm position constraints during pointing and reaching in 3-D space." *Journal of Neurophysiology* 78: 660-673.
- [46] Gillespie, R.B., Sövényi, S. (2006). "Model-based cancellation of biodynamic feedthrough using a force-reflecting joystick." *ASME Journal of Dynamic Systems, Measurement and Control* 128: 94-103.
- [47] Gomi, H., Kawato, M. (1996). "Equilibrium-point control hypothesis examined by measured arm stiffness during multijoint movement." *Science* 272: 117-120.
- [48] Gomi, H., Kawato, M. (1997). "Human arm stiffness and equilibrium-point trajectory during multi-joint movement." *Biological Cybernetics* 76: 163-171.

- [49] Gomi, H., Osu, R. (1998). "Task-dependent viscoelasticity of human multijoint arm and its spatial characteristics for interaction with environments." *Journal of Neuroscience* 18(21): 8965-8978.
- [50] Gottlieb, G.L., Song, Q., Almeida, G.L, Hong, D.A., Corcos, D. (1997). "Directional control of planar human arm movement." *Journal of Neurophysiology* 78: 2985-2998.
- [51] Griffin, M.J. (1978). "The evaluation of vehicle vibration and seats." *Applied Ergonomics* 9(1): 15-21.
- [52] Griffin, M.J. (1990). Handbook of human vibration (ISBN: 0-12-303040-4). San Diego: Academic Press.
- [53] Griffin, M.J. (2001). "The validation of biodynamic models." *Clinical Biomechanics* 16(1): S81-S92.
- [54] Gurdjian, E.S., Hodgson, V.R., Thomas, L.M. (1970). "Studies on mechanical impedance of the human skull: preliminary report." *Journal of Biomechanics* 3: 239-247.
- [55] Haggard, P., Hutchinson, K., Stein, J. (1995). "Patterns of coordinated multi-joint movement." *Experimental Brain Research* 107: 254-266.
- [56] Haken, H., Kelso, J.A.S., Bunz, H. (1985). "A theoretical model of phase transitions in human hand movements." *Biological Cybernetics* 51: 347-356.
- [57] Harrison, D.D., Harrison S.O., Croft, A.C., Harrison, D.E., Troyanovich, S.J. (2000). "Sitting biomechanics, part II: optimal car driver's seat and optimal driver's spinal model." *Journal of Manipulative and Physiological Therapeutics* 23(1): 37-47.
- [58] Hinz, B., Menzel, G., Bluthner, R., Seidel, H. (2001). "Transfer functions as a basis for the verification of models – variability and restraints." *Clinical Biomechanics* 16(1): S93-S100.
- [59] Hoff, B., Arbib, M.A. (1993). "Models of trajectory formation and temporal interaction of reach and grasp." *Journal of Motor Behavior* 25(3): 175-192.
- [60] Hogan, N. (1985). "The mechanics of multi-joint posture and movement control." *Biological Cybernetics* 52: 315-331.
- [61] Holmlund, P., Lundström, R. (2001). "Mechanical impedance of the sitting human body in single-axis compared to multi-axis whole-body vibration exposure." *Clinical Biomechanics* 16(1): S101-S110.

- [62] Hondzinski, J.M., Kwon, T. (2009). "Pointing control using a moving base of support." *Experimental Brain Research* 197: 81-90.
- [63] Hongwei, H. (1990). "Posture preferences and postural behavior during static, seated, visual and manual tasks (seated work, musculoskeletal disorders)." Dissertation (Ph.D) – *The University of Michigan*.
- [64] Huang, Y., Griffin, M.J. (2006). "Effect of voluntary periodic muscular activity on nonlinearity in the apparent mass of the seated human body during vertical random whole-body vibration." *Journal of Sound and Vibration* 298: 824-840.
- [65] ISO 2631-5:2003(E) 2003-10-16: "Mechanical vibration and shock – evaluation of human exposure to whole-body vibration – Part 5: method for evaluation of vibration containing multiple shocks." International Standards Organization.
- [66] Jax, S.A., Rosenbaum, D.A., Vaughan, J., Meulenbroek, R.G. (2003). "Computational motor control and human factors: modeling movements in real and possible environments." *Human Factors* 45(1): 5-27.
- [67] Jeannerod, M. (1988). *The neural and behavioural organization of goal-directed movements*. Oxford psychology series, 15. Clarendon Press/Oxford University Press.
- [68] Jung, E.S., Choe, J., Kim, S.H. (1994). "Psychophysical cost function of joint movement for arm reach posture prediction." *Proceedings of the Human Factors and Ergonomics Society 38th Annual Meeting*, 636-640
- [69] Jung, E.S., Kee, D., Chung, M.K. (1995). "Upper body reach posture prediction for ergonomic evaluation models." *International Journal of Industrial Ergonomics* 16, 95-107.
- [70] Jung, E.S., Choe, J. (1996). "Human reach posture prediction based on psychophysical discomfort." *International Journal of Industrial Ergonomics* 18, 173-179.
- [71] Kaminski, T.G., Gentile, A.M. (1986). "Joint control strategies and hand trajectories in multijoint pointing movements." *Journal of Motor Behavior* 18(3): 261-278.
- [72] Kaminski, T.G., Bock, C., Gentile, A.M. (1995). "The coordination between trunk and arm motion during pointing movements." *Experimental Brain Research* 106(3): 457-466.
- [73] Kang, T., He, J., Tillery, S.I.H. (2005). "Determining natural arm configuration along a reaching trajectory." *Experimental Brain Research* 167: 352-361.

- [74] Karst, G.M., Hasan, Z., (1991). "Timing and magnitude of electromyographic activity for two-joint arm movements in different directions." *Journal of Neurophysiology* 66: 1594-1604.
- [75] Kim, HJ, Chang, KJ, and Park, YP. (1997). "Improved experimental component mode synthesis based purely on experimental results." *Proceedings of Asia-Pacific Vibration Conference*, 1349-1354.
- [76] Kim, H.J., Martin, B.J. (2007). "Estimation of body link transfer functions in vehicle vibration environment." *Digital Human Modeling for Design and Engineering Conference*, Technical Paper 2007-01-2484, SAE International.
- [77] Kim, H.J., Martin, B.J. (2008). "Three-dimensional reach kinematics of the upper extremity in a dynamic vehicle environment." *Digital Human Modeling for Design and Engineering Conference*, Technical Paper 2008-01-1886, SAE International.
- [78] Kim, H.J., Martin, B.J. (2008). "Three-dimensional joint kinematics of the upper extremity in reach movements under whole-body vibration exposure." *Human Factors and Ergonomics Society 52nd Annual Meeting*. 52(15): 1000-1004.
- [79] Kim, H.J., Martin, B.J. (2009). "Effects of posture and movement on vibration transmissibility affecting human reach performance under vehicle vibration." *Human Factors and Ergonomics Society 53rd Annual Meeting*.
- [80] Kim, K.H, Gillespie, R.B., Martin, B.J., (2004). "Modeling the coordinated movements of the head and hand using differential inverse kinematics." *Digital Human Modeling for Design and Engineering Conference*, Technical Paper 2004-01-2178, SAE International.
- [81] Kim, T.H., Kim, Y.T., Yoon, Y.S. (2005). "Development of a biomechanical model of the human body in a sitting posture with vibration transmissibility in the vertical direction." *International Journal of Industrial Ergonomics* 35: 817-829.
- [82] Kim, W.S., Ellis, S.R., Tyler, M.E., Hannaford, B., Stark, L.W. (1987). "Quantitative evaluation of perspective and stereoscopic displays in three-axis manual tasking tasks." *IEEE Transactions on Systems, Man, and Cybernetics* 17(1): 61-72.
- [83] Kistemaker, D.A., Van Soest, A.K., Bobbert, M. (2007). "A model of open-loop control of equilibrium position and stiffness of the human elbow joint" *Biological Cybernetics* 96: 341-350.

- [84] Kitrazaki, S., Griffin, M.J. (1995). "A data correction method for surface measurement of vibration on the human body." *Journal of Biomechanics* 28(7): 885-890.
- [85] Kitrazaki S., Griffin M.J. (1997). "A modal analysis of whole-body vertical vibration, using a finite element model of the human body." *Journal of Sound and Vibration* 200(1): 83-103.
- [86] Kitrazaki, S., Griffin, M.J. (1998). "Resonance behavior of the seated human body and effects of posture." *Journal of Biomechanics* 31: 143-149.
- [87] Liang, C.C., Chiang, C.F. (2006). "A study on biodynamic models of seated human subjects exposed to vertical vibration." *International Journal of Industrial Ergonomics* 26: 869-890.
- [88] Ljungberg, J., Neely, G., Lundström, R. (2004). "Cognitive performance and subjective experience during combined exposures to whole-body vibration and noise." *International Archives of Occupational and Environmental Health* 77: 217-221.
- [89] Lee, R.A., Pradko, F. (1968). "Analytical analysis of human vibration." Society of Automotive Engineers, Automotive Engineering Congress, Detroit, Michigan, January 8-12, 680091.
- [90] Lewis, C.H., Griffin, M.J. (2002). "Evaluating the vibration isolation of soft seat cushions using an active anthropodynamic dummy." *Journal of Sound and Vibration* 253(1): 295-311.
- [91] Li, S., Patwardhan, A.G., Amirouche, F.M., Havey, R., Meade K.P. (1995). "Limitations of the standard linear solid model of intervertebral discs subject to prolonged loading and low-frequency vibration in axial compression." *Journal of Biomechanics* 28: 779-790.
- [92] Liang, C.Y., Magdaleno, R., Lee, D.C., Kylde, D.H., Allen, R.W., Rider, K., Overmeyer, K. (2005). "A biodynamic model for the assessment of human operator performance under vibration environment." Technical Paper 2005-01-2742. SAE International, Warrendale, PA
- [93] Lim S.H., Martin, B.J., Chung, M.K. (2004). "The effects of target location on temporal coordination of the upper body during 3D seated reaches considering the range of motion." *International Journal of Industrial Ergonomics* 34,395-405.
- [94] Linder, G.S. (2004). "Mechanical vibration – critical human effects." *Health and Science Series* 3.

- [95] Mansfield, N.J., Griffin, M.J. (1998). "Effect of magnitude of vertical whole-body vibration on absorbed power for the seated human body." *Journal of Sound and Vibration* 215(4): 813-825.
- [96] Mansfield, N. J. (2000). "Difference thresholds for automobile seat vibration." *Applied Ergonomics* 31: 255-261.
- [97] Mansfield, N. J. (2004). *Human Response to Vibration* (ISBN: 0-415-28239-X). CRC Press.
- [98] Mansfield, N. J. (2005). "Impedance methods (apparent mass, driving point mechanical impedance and absorbed power) for assessment of the biomechanical response of the seated person to whole-body vibration." *Industrial Health* 43: 378-389.
- [99] Mansfield, N.J., Maeda, S. (2006). "Comparison of the apparent masses and cross-axis apparent masses of seated humans exposed to single- and dual-axis whole-body vibration." *Journal of Sound and Vibration* 298: 841-853.
- [100] Mansfield, N. J., Holmlund, P., Lundstöm, R., Lenzuni, P., Nataletti, P. (2006). "Effect of vibration magnitude, vibration spectrum and muscle tension on apparent mass and cross axis transfer functions during whole-body vibration exposure." *Journal of Biomechanics* 39: 3062-3070.
- [101] Mansfield, N. J., Maeda, S. (2007). "The apparent mass of the seated humans exposed to single-axis and multi-axis whole-body vibration." *Journal of Biomechanics* 40: 2543-2551.
- [102] Martin, B., Guathier, G.M., Mussa-Ivadi, F. (1980a). "Effects of whole-body vibrations on spinal reflexes in man." *Aviation, Space, and Environmental Medicine* 51(11): 1227-1233.
- [103] Martin, B., Guathier, G.M., Roll, J.P., Hugon, M., Harlay, F. (1980b). "Effects of whole-body vibrations on standing posture in man." *Aviation, Space, and Environmental Medicine* 51(8): 778-787.
- [104] Martin, B.J., Roll, J.P., Renzo, N.D. (1991). "The interaction of hand vibration with oculomanual coordination in pursuit tracking."
- [105] Matsumoto, Y., Griffin, M.J. (2001). "Modelling the dynamic mechanisms associated with the principal resonance of the seated human body." *Clinical Biomechanics* 16(1): S31-S44.
- [106] Matsumoto, Y., Griffin, M.J. (2002). "Effect of phase on human responses to vertical whole-body vibration and shock – analytical investigation." *Journal of Sound and Vibration* 250(5): 813-834.

- [107] Matsumoto, Y., Griffin, M.J. (2002). "Effect of muscle tension on nonlinearities in the apparent masses of seated subjects exposed to vertical whole-body vibration." *Journal of Sound and Vibration* 253(1): 77-92..
- [108] Matsumoto, Y., Griffin, M.J. (2005). "Nonlinear subjective and biodynamic responses to continuous and transient whole-body vibration in the vertical direction." *Journal of Sound and Vibration* 287: 919-937.
- [109] Matsumoto, Y., Ohdo, K., Saito, T. (2006). "Dynamic and subjective responses of seated subjects exposed to simultaneous vertical and fore-and-aft whole-body vibration: The effect of the phase between the two single-axis components." *Journal of Sound and Vibration* 298: 773-787.
- [110] McLeod, R.W. and Griffin, M. J. (1989). "A review of the effects of translational whole-body vibration on continuous manual control performance." *Journal of Sound and Vibration*, 133(1): 55-115.
- [111] Morraso, P. (1981). "Spatial control of arm movements." *Experimental Brain Research* 42(2): 223-227.
- [112] Morraso, P. (1983). "Three dimensional arm trajectory." *Biological Cybernetics* 48: 187-194.
- [113] Moussa-Hamouda, E., Mourant, R.R. (1981). "Vehicle fingertip reach controls – human factors recommendation." *Applied Ergonomics* 12(2): 66-70.
- [114] National Research Council and the Institute of Medicine. (2001). *Musculoskeletal disorders and the workplace: low back and upper extremities*. National Academy Press, Washington, D.C., 219-286.
- [115] Nawayseh, N., Griffin, M.J. (2004). "Tri-axial forces at the seat and backrest during whole-body vertical vibration." *Journal of Sound and Vibration* 277: 309-326.
- [116] Osu, R., Gomi, H. (1999). "Multijoint muscle regulation mechanisms examined by measured human arm stiffness and EMG signals." *Journal of Neurophysiology* 81: 1458-1468.
- [117] Okunribido, O.O., Shimbles, S.J., Magnusson, M., Pope, M. (2007). "City bus driving and low back pain: A study of the exposure to posture demands, manual materials handling and whole-body vibration." *Applied Ergonomics* 38:29-38.
- [118] Oullier, O., Kavounoudias, A., Duclos, C., Albert, F., Roll, J.P., Roll, R. (2009). "Countering postural posteffects following prolonged exposure to whole-body vibration: a sensorimotor treatment." *European Journal Applied Physiology* 105: 235-245.

- [119] Paddan, G.S., Griffin, M.J. (2002). "Evaluation of whole-body vibration in vehicles." *Journal of Sound and Vibration* 253(1): 195-213.
- [120] Paddan, G.S., Griffin, M.J. (2002). "Effect of seating on exposures to whole-body vibration in vehicles." *Journal of Sound and Vibration* 253(1): 215-241.
- [121] Palmer, K.T., Griffin, M.J., Bendall, H., Pannett, B., Coggon, D. (2000). "Prevalence and pattern of occupational exposure to whole body vibration in Great Britain: findings from a national survey." *Occupational and Environmental Medicine* 57Z: 229-236.
- [122] Park, W.J., Chaffin, D.B, Martin, B.J. (2002). "A motion modification algorithm for memory-based human motion simulation." *Proceedings of Human Factors and Ergonomics Society* 46, 1172-1175.
- [123] Park, W.J., Martin, B.J., Choe, S., Chaffin, D.B., Reed, M.P. (2005). "Representing and identifying alternative movement techniques for goal-directed manual tasks." *Journal of Biomechanics* 38: 519-527.
- [124] Park, W.J., Singh, D., Martin, B.J. (2006). "A memory-based model for planning target` reach postures in the presence of obstructions." *Ergonomics* 49(15): 1565-1580.
- [125] Park, W.J., Chaffin, D.B., Martin, B.J., Yoon, J. (2008). "Memory-based human motion simulation for computer-aided ergonomic design." *IEEE Transactions on Systems Man and Cybernetics* 38(3): 513-527.
- [126] Péllisson, D., Prablanc, D., Goodale, M.A., Jeannerod, M. (1986). "Visual control of reaching movements without vision of the limb – II. Evidence of fast unconscious processes correcting the trajectory of the hand to the final position of a double-step stimulus." *Experimental Brain Research* 62: 303-311.
- [127] Pope, M.H., Wilder, D.G., Magnusson, M.L. (1999). "A review of studies on seated whole body vibration and low back pain." Proceedings of the Institution of Mechanical Engineers, Part H: *Journal of Engineering in Medicine* 213(6): 435-446.
- [128] Prablanc, C. Echallier, J.F., Komilis, E., Jeannerod, M. (1979a). "Optimal response of eye and hand motor systems in pointing at a visual target. – I. Spatio-temporal characteristics of eye and hand movements and their relationships when varying the amount of visual information." *Biological Cybernetics* 35: 113-124.
- [129] Prablanc, C. Echallier, J.F., Jeannerod, M., Komilis, E. (1979b). "Optimal response of eye and hand motor systems in pointing at a visual target. – II.

Static and dynamic visual cues in the control of hand movement." *Biological Cybernetics* 35: 183-187.

- [130] Prablanc, D., Péllisson, D., Goodale, M.A. (1986). "Visual control of reaching movements without vision of the limb – I. Role of retinal feedback of target position in guiding the hand." *Experimental Brain Research* 62: 293-302.
- [131] Rahmatalla, S., Xia, T., Contratto, M., Wilder, D., Frey-Law, L., Kopp, G., Grosland, N. (2006). "3D displacement, velocity, and acceleration of seated operators in whole-body vibration environment using optical motion capture systems." *The 9th International Symposium on the 3-D Analysis of Human Movement, Valenciennes, France, June 28-30*.
- [132] Rahmatalla, S., Xia, T., Ankrum, J., Wilder, D., Law, L.F., Abdel-malek, K., Contratto, M., Kopp, G. (2007). "A framework to study human response to whole body vibration." Technical Paper 2007-01-2474, SAE International.
- [133] Rakheja, S. Stiharu, I., Boileau, P.E. (2002). "Seated occupant apparent mass characteristics under automotive postures and vertical vibration." *Journal of Sound and Vibration*, 253(1): 57-75.
- [134] Reed, M.P., Parkinson, M.B., Klinkenberger, A.L. (2003). "Assessing the validity of kinematically generated reach envelopes for simulations of vehicle operators." Technical Paper 2003-01-2216, SAE International.
- [135] Reed, M.P., Parkinson, M.B., Wagner, D.W. (2004). "Torso kinematics in seated reaches." Technical Paper 2004-01-2176, SAE International.
- [136] Ribot, E., Roll, J.P., Gauthier, G.M. (1986). "Comparative effects of whole-body vibration on sensorimotor performance achieved with a mini-stick and a macro-stick in force and position control modes." *Aviation, Space, and Environmental Medicine* 57: 792-799.
- [137] Rider, K., Chaffin, D., Nebel, K., Mikol, K., and Reed, M. (2003). "A pilot study of the effects of vertical ride motion on reach kinematics." Technical Paper 2003-01-0589. SAE International, Warrendale, PA.
- [138] Rider, K., Chaffin, D., Nebel, K., Mikol, K., and Reed, M. (2004). "Modeling in-vehicle reaches perturbed by ride motion." Technical Paper 2004-01-2180. SAE International, Warrendale, PA
- [139] Rider, K., Chaffin, D., Martin, B.J. (2006). "Development of active human response model to ride motion." Technical Paper 2006-01-2363. SAE International, Warrendale, PA

- [140] Rosen, Jacob and Arcan, Mircea (2003). "Modeling the human body/seat system in a vibration environment." *Journal of Biomechanical Engineering*, 125: 223-231.
- [141] Roesenbaum, D.A., Loukopoulos, L.D., Meulenbroek, R.G.J., Vaughan, J., Engelbrecht, S.E. (1995). "Planning reaches by evaluating stored postures." *Psychological Review*, 102: 28-67.
- [142] Schoner, G., Haken, H., Kelso, J.A.S. (1986). "A stochastic theory of phase transitions in human hand movement." *Biological Cybernetics* 53: 247-257.
- [143] Scott, P.A., Candler, P.D., Li, J.-C. (1996). "Stature and seat position as factors affecting fractionated response time in motor vehicle driver." *Applied Ergonomics* 27(6): 411-416.
- [144] Seidel, H., Griffin, M.J. (2001). "Modeling the response of the spinal system to whole-body vibration and repeated shock." *Clinical Biomechanics* 16(1): S3-S7.
- [145] Seidel, H., Bluthner, R., Hinz, B. (2001). "Application of finite-element models to predict forces acting on the lumbar spine during whole-body vibration." *Clinical Biomechanics* 16(1): S57-S63.
- [146] Seidel, H., Hinz, B., Hofmann, J., Menzel, G. (2008). "Intraspinal forces and health risk caused by whole-body vibration – Predictions for European drivers and different field conditions." *International Journal of Industrial Ergonomics* 38: 856-867.
- [147] Soechting, J.F., Lacquaniti, F. (1981). "Invariant characteristics of a pointing movement in man." *Journal of Neuroscience* 1(7): 710-720.
- [148] Soechting, J.F., Buneo, C.A., Herrmann, U., Flanders, M., (1995). "Moving effortless in three dimensions: does Donders' law apply to arm movement?" *Journal of Neuroscience* 15(9): 6271-6280.
- [149] Sövényi, S., Gillespie, R.B. (2007). "Cancellation of biodynamic feedthrough in vehicle control tasks." *IEEE Transactions on Control System Technology* 15(6): 1018-1029.
- [150] Stein, G.J., Múčka, P., Chmúrny, R., Hinz, B., Blüthner, R. (2007). "Measurement and modelling of x-direction apparent mass of the seated human body-cushioned seat system." *Journal of Biomechanics*, 40(7):1493-1503.
- [151] Wadman, W.J., Denier, van der Gon, J.J., Derksen, R.J.A. (1980). "Muscle activation patterns for fast goal-directed arm movements." *Journal of Human Movement Study* 6:19-37.

- [152] Wallis, G., Chatzistros, A., Bühlhoff, H. (2002). "An unexpected role for visual feedback in vehicle steering control." *Current Biology* 12: 295-299.
- [153] Wang, W., Rakheja, S., Boileau, P.-E. (2004). "Effects of sitting postures on biodynamic response of seated occupants under vertical vibration." *International Journal of Industrial Ergonomics*, 34: 289-306.
- [154] Wang, X., Verriest, J.P. (1998a). "A geometric algorithm to predict the arm reach posture for computer-aided ergonomic evaluation." *Journal of visualization and computer animation* 9: 33-47.
- [155] Wang, X. (1999a). "Three-dimensional Kinematic Analysis of Influence of Hand Orientation and Joint Limits on the Control of Arm Postures and Movements." *Biological Cybernetics* 80: 449-463.
- [156] Wang, X. (1999) "A behavior-based inverse kinematics algorithm to predict arm prehension postures for computer-aided ergonomic evaluation." *Journal of Biomechanics* 32: 453-460.
- [157] Wei L., Griffin, M.J. (1998). "Mathematical models for the apparent mass of the seated human body exposed to vertical vibration." *Journal of Sound and Vibration* 212(5):855-874.
- [158] Wierwille, E.M., Tijerina, L., (1996). "An analysis of driving accident narratives as a means of determining problems caused by in-vehicle visual allocation and visual workload." In: *Vision in Vehicles* (Gale AG et al., eds). Amsterdam: North-Holland.
- [159] Wilder, D.G., Pope, M.H. (1996). "Epidemiological and etiological aspects of low back pain in vibration environments – an update." *Clinical Biomechanics* 11(2): 61-73.
- [160] Winter, D.A., (2005). *Biomechanics and Motor Control of Human Movement*. John Wiley & Sons, Inc.
- [161] Yang, Z., Rahmatalla, S., Marler, T., Abdel-Malek, K., Harrison, C. (2007). "Validation of predicted posture for the virtual human santos™." *12th International Conference on Human-Computer Interaction*, July, Beijing, China, Springer, London, England. 500-510.
- [162] Yoshimura, T., Nakai, K., Tamaok, G. (2005). "Multi-body dynamics modelling of seated human body under exposure of whole-body vibration." *Industrial Health* 43: 441-447.
- [163] Yu, K., Luo, A.C.J. (2004). "The periodic impact responses and stability of a human body in a vehicle traveling on rough terrain." *Journal of Sound and Vibration* 272: 267-286.

- [164] Zehr, E.P., Collins, D.F, Frigon, A., Hoogenboom, N. (2003). "Neural control of rhythmic human arm movement: phase dependence and task modulation of Hoffman reflexes in forearm muscles." *Journal of Neurophysiology* 89: 12-21.
- [165] Zhang, X., Chaffin, D.B., (1996). "Task effects on three-dimensional dynamic postures during seated reaching movements: an investigative scheme and illustration." *Proceedings of the 40th Annual Meeting of the Human Factors and Ergonomics Society* 1(1), Philadelphia, PA, 594-598.
- [166] Zhang, X., Kuo, A.D., Chaffin, D.B., (2000). "Optimization-based differential kinematic modeling exhibits a velocity-control strategy for dynamic posture determination in seated reaching movements." *Journal of Biomechanics* 31, 1035-1042.
- [167] Zhang, X., Chaffin, D.B., (2000). "A three-dimensional dynamic posture prediction model for simulating in-vehicle seated reaching movements: development and validation." *Ergonomics* 43(9), 1314-1330.